BIOACTIVE COMPOUNDS FROM *PTEROSPERMUM GRANDE* CRAIB AND *MITREPHORA WANGII* HU

By
Patcharawan Tanamatayarat

A Thesis Submitted in Partial Fulfillment of the Requirements for the Degree
DOCTOR OF PHILOSOPHY
Program of Pharmaceutical Chemistry and Natural Products
Graduate School
SILPAKORN UNIVERSITY
2011

BIOACTIVE COMPOUNDS FROM *PTEROSPERMUM GRANDE* CRAIB AND *MITREPHORA WANGII* HU

By
Patcharawan Tanamatayarat

A Thesis Submitted in Partial Fulfillment of the Requirements for the Degree
DOCTOR OF PHILOSOPHY
Program of Pharmaceutical Chemistry and Natural Products
Graduate School
SILPAKORN UNIVERSITY
2011

สารประกอบที่มีฤทธิ์ทางชีวภาพจากสามเต้าและลำดวนดอย

โดย

นางสาวพัชรวรรณ ตันอมาตยรัตน์

วิทยานิพนธ์นี้เป็นส่วนหนึ่งของการศึกษาตามหลักสูตรปริญญาเภสัชศาสตรดุษฎีบัณฑิต

สาขาวิชาเภสัชเคมีและผลิตภัณฑ์ธรรมชาติ

บัณฑิตวิทยาลัย มหาวิทยาลัยศิลปากร

ปีการศึกษา 2554

The Graduate School, Silpakorn University has approved and accredited the Thesis title of "Bioactive Compounds from *Pterospermum grande* Craib and *Mitrephora wangii* Hu" submitted by Miss Patcharawan Tanamatayarat as a partial fulfillment of the requirements for the degree of Doctor of Philosophy in Pharmaceutical Chemistry and Natural Products.

…….....
(Assistant Professor Panjai Tantatsanawong, Ph.D.)
Dean of Graduate School
...../...../.....

The Thesis Advisors

1. Assoc. Prof. Onoomar Toyama, Ph.D.
2. Assoc. Prof. Uthai Sotanaphun, Ph.D.

The Thesis Examination Committee

..... Chairman
(Asst. Prof. Kanawan Pochanakom, Ph.D.)
...../...../.....

..... Member
(Assoc. Prof. Rutt Suttisri, Ph.D.)
...../...../.....

..... Member
(Assoc. Prof. Panadda Phattanawasin, Ph.D.)
...../...../.....

..... Member
(Assoc. Prof. Onoomar Toyama, Ph.D.)
...../...../.....

..... Member
(Assoc. Prof. Uthai Sotanaphun, Ph.D.)
...../...../.....

49356803 : MAJOR : PHARMACEUTICAL CHEMISTRY AND NATURAL PRODUCTS
KEY WORDS : *PTEROSPERMUM GRANDE* / *MITREPHORA WANGII* / DPPH / BRINE SHRIMP LETHALITY / HYPHAE FORMATION ASSAY / CYTOTOXICITY / NEOLIGNAN
PATCHARAWAN TANAMATAYARAT : BIOACTIVE COMPOUNDS FROM *PTEROSPERMUM GRANDE* CRAIB AND *MITREPHORA WANGII* HU. THESIS ADVISORS : ASSOC.PROF.ONOOMAR TOYAMA, Ph.D. AND ASSOC.PROF.UTHAI SOTANAPHUN, Ph.D. 310 pp.

Pterospermum grande Craib (Sterculiaceae) and *Mitrephora wangii* Hu (Annonaceae) are found on Doi Tung. In the preliminary testing, these two methanol plant extracts exhibited antioxidative activity against DPPH and toxicity against brine shrimp.

The structure determination of isolated compounds from both plants was accomplished by spectroscopic methods, namely UV, IR, MS, and NMR and compared with published reports. The chemical investigation of the leaves of *P. grande* yielded seven compounds, including three triterpenes, i.e. taraxerol, taraxerol acetate, and simiarenol, one steroid, i.e. *β*-sitosterol, three flavonoids, i.e. kaempferol-*O*-*β*-D-galactopyranoside, kaempferol-3-*O*-*β*-D-6''(4-hydroxy-*E*-cinnamoyl)-*β*-glucopyranoside, and (-)-epicatechin. Investigation of the leaves and the twigs of *Mitrephora wangii* led to the isolation of eleven compounds including three dihydrobenzofuran neolignans, i.e. (2*R*,3*R*)-2,3-dihydro-2-(4'-methoxyphenyl)-3-methyl-5-[1-(*E*)-propenyl]benzofuran or methyl conocarpan, (2*R*,3*R*)-2,3-dihydro-2-(4'-hydroxy-3'-methoxyphenyl)-3-methyl-5-[1-(*E*)-propenyl]benzofuran or 3'-methoxy conocarpan, and (2*R*,3*R*)-2,3-dihydro-2-(4'-hydroxyphenyl)-3-methyl-5-[1-(*E*)-propenyl]benzofuran or conocarpan, two aporphine alkaloids, i.e. magnoflorine and corytuberine, two phenolic amides, i.e. *N*-*p*-coumaroyltyramine and *N*-caffeoyltyramine, quebrachitol, linoleic acid, sitosterol-3-*O*-*β*-glucoside, and allantoin. This is the first time of the isolation of methyl conocarpan from nature.

Only the neolignans from *M. wangii* were studied for their biological activities. Conocarpan displayed the strongest toxicity in BSL with LC_{50} value of 6.21 µg/ml. In hyphae formation inhibition assay, conocarpan exhibited significant activity against *Streptomyces* 85E with diameter of clear zone inhibition of 21 mm and 3'-methoxy conocarpan with that of bald zone inhibition of 11 mm, respectively. Moreover, conocarpan and 3'-methoxy conocarpan were active against HepG2 cell with IC_{50} values of 6.3 and 5.9 µg/ml, respectively.

Program of Pharmaceutical Chemistry and Natural Products Graduate School, Silpakorn University Academic Year 2011
Student's signature .....
Thesis Advisors' signature 1.……..……..……..……2. ……..……..……..……..

49356803 : สาขาวิชาเภสัชเคมีและผลิตภัณฑ์ธรรมชาติ
คำสำคัญ : สามเต้า / ลำดวนดอย / สารต้านอนุมูลอิสระ / ความเป็นพิษต่อไรทะเล / การยับยั้งการสร้างไฮฟา / ความเป็นพิษต่อเซลล์มะเร็ง / นีโอลิกแนน

พัชรวรรณ ตันอมาตยรัตน์ : สารประกอบที่มีฤทธิ์ทางชีวภาพจากสามเต้า และลำดวนดอย. อาจารย์ที่ปรึกษาวิทยานิพนธ์ : ภญ.รศ.ดร.อรอุมา โต๊ะยามา และ ภก.รศ.ดร.อุทัย โสธนะพันธุ์. 310 หน้า.

สามเต้า (*Pterospermum grande* Craib, Sterculiaceae) และลำดวนดอย (*Mitrephora wangii* Hu, Annonaceae) เป็นพืชที่พบบนดอยตุง เมื่อนำมาทดสอบเบื้องต้นพบว่าสารสกัดเมทานอลจากพืช 2 ชนิดให้ฤทธิ์ต้านอนุมูลอิสระ DPPH และความเป็นพิษต่อไรทะเล

การพิสูจน์โครงสร้างทางเคมีของสารประกอบที่แยกได้จากพืชทั้งสองชนิดอาศัยวิธีวิเคราะห์ทางสเปกโตรสโกปี ได้แก่ UV, IR, MS และ NMR ร่วมกับการเปรียบเทียบข้อมูลของสารเคมีที่เคยมีรายงานมาแล้ว การศึกษาองค์ประกอบทางเคมีจากใบของสามเต้าสามารถแยกสารได้ 7 ชนิด คือ ไตรเทอร์พีน จำนวน 3 ชนิด ได้แก่ taraxerol acetate, taraxerol และ simiarenol สารกลุ่มสเตอรอยด์ จำนวน 1 ชนิด ได้แก่ β-sitosterol สารกลุ่มฟลาโวนอยด์ จำนวน 3 ชนิด ได้แก่ keampferol-3-*O*-β-D-galactopyranoside, keampferol-3-*O*-β-D-6" (4-hydroxy-*E*-cinnamoyl)-β-glucopyranoside และ (-)-epicatechin สำหรับการศึกษาองค์ประกอบทางเคมีจากใบและกิ่งของลำดวนดอยสามารถแยกสารได้จำนวน 11 ชนิด คือ สารกลุ่มนีโอลิกแนน แบบไดไฮโดรเบนโซฟิวแรน จำนวน 3 ชนิด ได้แก่ (*2R,3R*)-2,3-dihydro-2-(4'-methoxyphenyl)-3-methyl-5-[1-(*E*)-propenyl]benzofuran หรือ methyl conocarpan, (*2R,3R*)-2,3-dihydro-2-(4'-hydroxy-3'-methoxyphenyl)-3-methyl-5-[1-(*E*)-propenyl]benzofuran หรือ 3'-methoxy conocarpan และ (*2R,3R*)-2,3-dihydro-2-(4'-hydroxyphenyl)-3-methyl-5-[1-(*E*)-propenyl]benzofuran หรือ conocarpan สารกลุ่มอะพอร์ฟีนอัลคาลอยด์ จำนวน 2 ชนิด ได้แก่ magnoflorine และ corytuberine สารกลุ่มฟีนอลิก เอไมด์ จำนวน 2 ชนิด ได้แก่ *N-p*-coumaryltyramine และ *N*-caffeoyltyramine นอกจากนี้พบสารอื่นๆ ได้แก่ quebrachitol, linoleic acid, sitosterol-3-*O*-β-glucopyranoside และ allantoin และพบว่า สาร methyl conocarpan พบในธรรมชาติเป็นครั้งแรก

สารกลุ่มนีโอลิกแนนจากลำดวนดอยแสดงฤทธิ์ทางชีวภาพ โดย conocarpan แสดงความเป็นพิษต่อไรทะเลสูงที่สุดโดยให้ค่า LC_{50} เท่ากับ 6.21 ไมโครกรัมต่อมิลลิลิตร สำหรับวิธีทดสอบการยับยั้งการสร้างไฮฟา พบว่าสาร conocarpan ให้ค่าการยับยั้งเชื้อ *Streptomyces* 85E โดยแสดงเส้นผ่านศูนย์กลางของ clear zone เท่ากับ 21 มิลลิเมตร และ 3'-methoxy conocarpan แสดงด้วยเส้นผ่านศูนย์กลางของ bald zone เท่ากับ 11 มิลลิเมตร ตามลำดับ นอกจากนี้ conocarpan และ 3'-methoxy conocarpan แสดงความเป็นพิษต่อเซลล์มะเร็ง HepG2 ด้วยค่า IC_{50} เท่ากับ 6.3 และ 5.9 ไมโครกรัมต่อมิลลิลิตร ตามลำดับ

ลายมือชื่อนักศึกษา.....

ลายมือชื่ออาจารย์ที่ปรึกษาวิทยานิพนธ์1.....2. .....

ACKNOWLEDGMENTS

I would like to express my sincere thanks to the people who have given me support from the beginning of my study, along the way till the completion of my thesis.

First and foremost, I would like to gratefully and sincerely thank my thesis supervisor Assoc. Prof. Dr. Onoomar Toyama for her guidance, understanding, patience, and kindness during my study at Silpakorn University. I would like to acknowledge Assoc. Prof. Dr. Uthai Sotanaphun as my co-advisor who helped me develop ideas and experiments.

I would also like to thank the members of my thesis examination committee, Asst. Prof. Dr. Kanawan Pochanakom, Assoc. Prof. Dr. Panadda Phattanawasin, and Assoc. Prof. Dr. Rutt Suttisri for their comments.

I would like to express my appreciation to Asst. Prof. Dr. Siripan Limsirichaikul for her assistance in MTT assay.

I would like to express my sincere gratitude to Asst. Prof. Dr. Leng Chee Chang for her help in HFI assay and Dr. Ghee Teng Tan for cytotoxicity test at the University of Hawaii at Hilo.

I would like to thank, environmental authorities of Doi Tung Project, Mr. Thawatchai Katphab and Mr. Jatupong Apipongpisarn.

I would like to thank scientists at the Faculty of Pharmacy and Scientific and Technological Research Equipment Center, Silpakorn University for their kindness and helpful assistances in several experiments. A special ackowledgment is extended to the Department of Pharmaceutical Chemistry and Department of Pharmacognosy, Faculty of Pharmacy, Silpakorn University for providing research facilities.

I would like to thank the Commission on Higher Education, Thailand, for financial support in this study.

I am also grateful to Faculty of Pharmacy and the Graduate School of Silpakorn Research Grant, Silpakorn University for partial financial support, and University of Phayao for giving me the opportunity to enter on Ph.D. program.

I also wish to thank all teachers who have taught me all of my life.

I would like to thank my brothers, sisters, and friends, P´Pam, P´Tum, P´Kuad, P´Am, P´Ni, Toey, Aon, Nummon, Aae, Aew, N´Tan, N´Ple, N´Nui, N´Jew, N´Yim, Samour group, and Kawin group for encouragement.

I would also like to thank my best friends, Nok and Dek (Secret Heart College, 1995), for encourangement, support, and stimulation during my thesis.

Finally, my special thanks to my parents for their financial support, encourangment, and love.

TABLE OF CONTENTS

Page

Chapter Page

Chapter Page

LIST OF TABLES

LIST OF FIGURES

Figure **Page**

Figure **Page**

Figure **Page**

Figure **Page**

LIST OF SCHEMES

CHAPTER 1
INTRODUCTION

Human have used natural products as the sources of foods, medicines, habitats, and clothing (Kong et al., 2003). One of the important sources for natural products is plant which has been used in healthcare both for the prevention and treatment of diseases. Evidences have shown that men used plants as medicines as far back as 60,000 years ago (Fabricant and Farnsworth, 2001). Four-thousand year-old Sumerian clay tablets recorded pharmacological recipes for various diseases (Kong et al., 2003). Moreover, medicinal uses of plants have been recorded in both western and eastern countries such as Greek, China, and India. From World Health Organization (WHO) report, 80% of the world's population have relied on herbal medicines for primary health care (Gossell-Williams et al., 2006). It is well known that plants consist of secondary metabolites which possess several biological activities. As a result, many active compounds have been derived from plants during the drug discovery processes. Plant compounds that enter clinical trials are, for example, Phenserine (Phase III) from *Physostigma venenosum* Balf. for mild-to-moderate Alzheimer´s disease, and *PMI-5011* (Phase II) from *Artemisia dracunculus* L. for type II diabetic treatment (Saklani and Kutty, 2008). Recently, Grazax® from the pollen of *Phleum pratense* L. was launched for hay fever treatment (Dahl et al., 2006). Crofelemer from the latex of *Croton lecheri* L. was launched for the treatment of diarrhea in AIDS (Saklani and Kutty, 2008). Moreover, examples of natural products that have been approved by U.S. Food and Drug Administration (FDA) are paclitaxel from *Taxus brevifolia* Nutt., teniposide from *Podophyllum peltatum* L., arteether from *Artemisia annua* L., galantamine from *Galanthus woronowii* Losinsk., nitisinone from *Callistemon citrinus* Stapf., and tiotropium from *Atropa belladonna* L. (Balunas and Kinghorn, 2005).

Currently, the world has changed in geography and global climate. Not only do older diseases such as tuberculosis relapses, but also new pathogens establish in human. Several medicines from other ways, including synthesis, and semi-synthesis have been studied, but plant-derived drugs have shown efficacy to pathogens with novel ways (Dobson, 1995). Furthermore, data have shown that an estimate of 250,000 to 350,000 species of plants were identified worldwide, but only about 35,000 species were used in medicine (Jachak and Saklani, 2007). These information indicated that enormous plant sources are still available for investigation.

Doi Tung belongs to Mae Fa Luang district in the mountainous Chiang Rai Province in the north of Thailand (The Mae Fahluang Foundation under Royal Patronage, 2008). The area surrounding Doi Tung covers 150 km^2 and goes from 350 to 1,525 meters elevation. Doi Tung has three distinctive seasons: hot (March-May), rainy (June-October), and cool (November-February). In 2007, Maxwell thoroughly examined the entire area of Doi Tung and recorded about 1,013 plant species from 170 families. Among these plants, a new species, *Sauropus poomae* Welz. & Chay. (Euphorbiaceae) was discovered. Additionally, some species such as *Eriobotrya salwinensis* Hand-Mazz. (Rosaceae), *Trisepalum prazeri* Burtt (Gesneriaceae), *Garcinia propinqua* Craib (Clusiaceae), and *Premna subcapitata* Rehd (Verbenaceae) were described as new records of Thai flora. Moreover, *Sageretia cordifolia* Tard. (Rhamnaceae), first reported in Laos, was also located here (Maxwell, 2007). The high biodiversity of tropical forests in Doi Tung makes this area a suitable source for phytochemical studies and drug discovery project.

Eighteen plants from 15 families, including herbs, trees, and treelets, were collected from Doi Tung. Extracts were made from these plants and then tested for toxicity using brine shrimp and for antioxidative activity using 1,1-Diphenyl-2-picrylhydrazyl (DPPH) assay. It is well known that drug combination is used to achieve better therapeutic efficacy (Chou, 2006; Asbagh et al., 2008) and some antioxidants have been proven for this effectiveness. For example, the combination of Pycnogenol® with trolox was able to significantly obstruct lipid oxidation better than individual antioxidant (Sivonova et al., 2006). Rosemary extract has displayed different synergistic effects with various antioxidants (Hras et al., 2000). Therefore,

synergistic effect of these 18 plant extracts with *L*-ascorbic acid on antioxidative activity was included in the screening part of this study.

From the brine shrimp lethality and antioxidative activity, two plants with moderate to high activity, i.e. *Pterospermum grande* Craib (Sterculiaceae) and *Mitrephora wangii* Hu (Annonaceae) were chosen for further phytochemical studies. There have been several phytochemical and biological activity researches on Sterculiaceae. For example, chemical compounds from dried roots of *Glossostemon bruguieri* Desf. (Moghat) were moghatin, 3′′′-hydroxycupressuflavone, 4′-methoxyisoscutellargin, sesamin, chrysophanol, emodin, and physcion (Meselhy, 2003). Friedelin, betulinic acid, sitost-4-en-3-one, (24*R*),6*β*-hydroxy-24-ethyl-cholesterol-4-en-3-one, and physcion were separated from the hexane extract of *Heritiera littoralis* Dryand. (Daengrot et al., 2005). Cyclopeptide alkaloids, including chamaedrine, adouetine X, frangulaline, scutianine B, and scutianine C were identified from the methanol extract of *Melochia chamaedrys* f. *typica* Ekman, which was used for hypertension and cancer in ethnomedicine (Dias et al., 2007). The 50% ethanol extract from *Helicteres isora* Linn. roots was able to decreased blood sugar in rats when given at doses of 100 and 250 mg/kg and has shown an increase in superoxide dismutase and catalase (Sharma et al., 2009). The methanol extract from *Scaphium scaphigerum* reduced lipid peroxidation (Sudjaroen, 2008).

Both chemical compounds and biological activities are well studied in the annonaceous family. Ten compounds were isolated from the twigs of *Miliusa mollis* Pierre such as (2*S*,3*S*)-2,3-dihydro-2-(4-methoxyphenyl)-3-methyl-5-[1(*E*)-propenyl] benzofuran, (7*S*,8*S*)-*threo*-$\Delta^{8'}$-4-methoxyneolignan, and tyrosol-1-*O*-*β*-xylopyranosyl-(1→6)-*O*-*β*-glucopyranoside (Sawasdee et al., 2010). Four isoquinoline alkaloids, (-)-asimilobine, atherospermidine, (-)-anonaine, and (-)-norsterphalagine, were isolated from the bark of *Popowia perakensis* King. The crude extract containing these alkaloids showed activity against *Plasmodium falciparum* in the lactate dehydrogenase (LDH) assay with an IC_{50} of 6.85 µg/ml (Saripah et al., 2009). Annomuricin F and muricapentocin were isolated from the leaf extract of *Annona muricata* L. Annomuricin F exhibited cytotoxicity against the pancreatic carcinoma (PACA-2) and colon adenocarcinoma (HT-29) with an IC_{50} of 6.68 x 10^2 and 2.42 x 10^2 µg/ml, respectively. Muricapentocin showed cytotoxicity against the same cell

lines with IC_{50} values of 7.10 x 10^2 and 5.03 x 10^2 μg/ml, respectively (Kim et al., 1998). Five aporphine alkaloids such as artabotrysine, bidebiline, and artacinatine and polycarpol were isolated from the roots of *Artabotrys spinosus* Craib. Artabotrysine, a novel compound, showed cytotoxicity against KB and HeLa cell lines with IC_{50} values of 25.8, and 32.3 μg/ml, respectively (Sichaem et al., 2011).

The above data exhibited the biological activities of isolated compounds from plants in Sterculiaceae and Annonaceae. However, there has been no scientific report on *P. grande* (Sterculiaceae) and *M. wangii* (Annonaceae). Therefore, the aims of this research were the isolation, structure elucidation, and biological activity evaluation of chemical constituents from *P. grande* and *M. wangii*. The crude extracts from these plants were fractionated using chromatographic methods until pure compounds were isolated. The structures of pure compounds obtained were identified using spectroscopic methods such as infared spectroscopy (IR), mass spectroscopy (MS), and nuclear magnetic resonance spectroscopy (NMR). Compounds obtained in adequate amount were determined for biological activities such as cytotoxicity using brine shrimp lethality (BSL) assay, hyphae formation inhibition (HFI) assay, 3-(4,5-dimethylthiazol-2-yl)-2,5-diphenyl tetrazolium bromide (MTT) assay, and antioxidative activity using DPPH assay.

CHAPTER 2
LITERATURE REVIEW

1. Family Sterculiaceae

The sterculiaceous family consists of trees and shrubs, but rarely herbs. Leaves are stellately hairy and alternate. Leaf blade is simple. The stipules generally are present, caduceus. Bark contains mucilage and plenty of fibers. Flowers generally are unisexual, bisexual or polygamous. A number of flowers are axillary inflorescences, paniculate, corymbose, racemose or cymose. Sepals are 3 to 5, connate and petals are 5. Fruit usually is a capsule or follicle, but rarely berry or nut. The habitats of this family are in tropical areas. About 68 genera and 1,000 species are found on the global. China is the largest habitat which comprises of approximately 90 species (Carr, 2006; Ya et al., 2010).

1.1 Genus *Pterospermum*

Plants in the genus *Pterospermum* usually are trees or shrubs. The characteristic of plants in this genus was velutinous, stellate, and scurfy. Leaves are simple. The stipules are linear to palmately fimbriate. Leaf blade is lobed. The base is often oblique and margin is entire or serrate. Flowers are axillary inflorescence. Flowers are bisexual. The epicalyx lobes are usually 3 and distant from calyx. Calyx has 5 or 6 lobes. It has flowers with 5 white or yellow petals. There are 15 stamens. Ovary has 5 locules. Fruit is a cylindrical or ovoid schizocarp. Each locule has at least 2 seeds (Ya et al., 2010). In Thailand, there are nine species of *Pterospermum* i.e. *P. acerifolium* Willd. (กะหนานปลิง, Kanan pling), *P. cinnamomeum* Kruz (ตองเต้า, Tong tao), *P. diversifolium* Blume (ลำป้าง, Lam pang), *P. grande* Craib (สามเต้า, Sam tao), *P. grandiflorum* Craib (สะเต้า, Sa tao), *P. lanceaefolium* Roxb. (พลากวาง, Phla kwang), *P. littorale* Craib var. *litorale* var. *venustrun* (กะหนาย, Kanai), *P. pecteniforme* Kostem (ยู, Yu), *P. semisagittatum* (ขามคัวะ, Kham khua) (เต็ม สมิตตินันทน์, 2544)

1.2 Phytochemistry and Biological Activities of Genus *Pterospermum*

Several isolated compounds and biological activities were presented in earlier reports (Figures 1-9, Table 1). The 50% methanol extract from all parts excluding root of *Pterospermum heyneanum* Wall. was screened for tannin content and insecticidal activity (Atal et al., 1978). The methanol extract from *P. suberifolium* L., which was used in ethnomedicine for smallpox and hemicranias, exhibited significant toxicity on brine shrimp with LC_{50} of 2.48±0.88 μg/ml (Rahman et al., 2008). The methanol extract from *P. suberifolium* leaves was screened for anti-proliferative activity against the pancreatic adenocarcinoma cell line (Panc-1). This plant showed the activity against Panc-1 cell line with an IC_{50} of 0.59±0.06 μg/ml (Sherine et al., 2010).

In phytochemical study, isolation from the light petroleum extract of *P. acerifolium* Willd. flowers yielded several compounds such as 24*β*-ethylcholest-5-*en*-3*β*-*O*-*α*-cellobioside,3,7-diethyl-7-methyl-1:5-pentacosanolide, *n*-hexacosane-1-dilignocerate,26-diol, friedelan-3*α*-ol, friedelan-3*β*-ol, arachidic acids and lignoceric (Rizvi and Sultana, 1972). Isolation of the *n*-hexane, chloroform, and methanol extracts from *P. heyneanum* Wall. or *P. xylocarpum* Santapau & Wagh heartwood yielded cyclotriterpene compounds, e.g., cyclopterospermol (Figure 8 (1.21)), 30-norcyclopterospermol (Figure 8 (1.22)), 30-norcyclopterospermone (Figure 8 (1.23)), 30-nor-22-methylene-9-cyclolanostan-3-one, 22-methylene-9,19-cyclolanostan-3*β*-ol, 30-nor-22-methylene-9,9-cyclolanostan-3*β*-ol, *n*-octacosanol, 3-hydroxy-5-methoxy-2-methylbenzoquinone, and *β*-sitosterol (Figure 8 (1.24)) (Anjaneyulu and Raju, 1987b). Neolignans and megastigmane glycosides such as (7*S*,8*R*)-dihydrodehydro-diconiferyl alcohol-9′-*O*-*β*-*D*-glucopyranoside (Figure 5 (1.18)), 10-*O*-acetyl-4,7-megastigmadien-3-one-9-*O*-(2′,3',4',6′-tetra-*O*-acetyl)-*β*-*D*-glucopyranoside (Figure 9 (1.27)), 10-hydroxy-4,7-megastigmadien-3-one-9-*O*-*β*-*D*-glucopyranoside (Figure 9 (1.28)), 9-*O*-acetyl-4,7-megastigmadien-3-one-10-*O*-(2′,3′, 4′,6′-tetra-*O*-acetyl)-*β*- *D*-glucopyranoside (Figure 9 (1.29)), and 9-hydroxy-4,7 megastigmadien-3-one-10-*O*-*β*-*D*-glucopyranoside (Figure 9 (1.30)) were isolated from the *n*-butanol extract of *P. semisegittatum* Buch-Ham. leaves (Khan et al., 2005). Several extracts of *P. acerifolium* Willd. bark were tested for antimicrobial and antioxidative activities. The

dichloromethane and carbon tetrachloride extracts at the concentration of 400 μg/disc exhibited the average inhibition zone of 13-16 mm against *Bacillus cereus* and 12-13 mm against *Sarcina lutea*. The dichloromethane extract showed IC_{50} of 26.50 μg/ml for DPPH radical. IC_{50} values of the petroleum ether and dichloromethane extracts for brine shrimp lethality assay were 1.362 and 1.867 μg/ml, respectively. Three compounds, pentadec-11-enoic acid methyl ester, oleanolic acid, and *β*-sitosterol, were isolated from the petroleum extract of this plant (Muhit et al., 2010). In addition, the ethyl acetate, *n*-butanol and chloroform extracts from its leaves were tested for antioxidative and anti-inflammatory activity. The ethyl acetate extract exhibited the highest antioxidative activity in all models. For example, its IC_{50} for DPPH radicals and superoxide anion scavenging were 26.2 and 51.8 μg/ml. For anti-inflammatory activity, the ethyl acetate extract at a concentration of 150 mg/kg reduced paw edema induced by carrageenan in rats in 3 hours (Sannigrahi et al., 2010). Several extracts of *P. acerifolium* bark were also examined for antimicrobial and anthelmintic activities. The ethyl acetate extract was more active than the methanol extract against both gram negative and gram positive bacteria with the inhibition zone of 16-25 mm. For anthelmintic activity, the petroleum ether extract displayed stronger activity against *Pheretima posthuma* than piperazine citrate. The petroleum ether extract at a concentration of 1.0 gm% paralyzed the worm in 17 min, compared with 25 min for piperazine (Pattanaik and Parida, 2010). The extract from *P. acerifolium* barks were investigated in ethanol induced gastric ulceration in rats. The result showed that the extract at 300 mg/kg inhibited 61.65% of the ulceration in albino rats, while omeprazole at 10 mg/kg gave 82.15% inhibition. The extract at this same dose reduced lipid peroxidation with less activity than omeprazole (Manna et al., 2009).

The acetone, ethanol, and water extracts from *P. acerifolium* leaves were tested for free radical scavenging activity against DPPH and nitric oxide compared with ascorbic acid. The ethanol extract was the most active. Their IC_{50} were 27.88 and 44 μg/ml for DPPH and nitric oxide assays, respectively (Saboo et al., 2010).

Information of chemical constituents of the genus *Pterospermum* was acquired from NAPRALERT database and are shown in Table 1.

Table 1 Chemical constituents of the genus *Pterospermum*.

Chemical compound	No.	species	part	Referenece
Alkane				
triacontan-1-ol	1.1	*P. heyneanum*	barks	Anjaneyulu and Raju, 1988
		P.xylocarpum	barks	Anjaneyulu and Raju, 1988
Octacosan-1-ol	1.2	*P. xylocarpum*	heartwood	Anjaneyulu and Raju, 1987a
Coumarin				
scopolein	1.3	*P. lanceaefolium*	leaves	Dan and Dan, 1988
		P. semisagittatum	leaves	Dan and Dan, 1988
Fatty acid				
malvalic acid	1.4	*P. acerifolium*	seeds	Bohannon and Kleiman, 1978
sterculic acid	1.5	*P. acerifolium*	seeds	Bohannon and Kleiman, 1978
Flavonoids				
kaempferol	1.6	*P. heyneanum*	leaves	Anjaneyulu and Raju, 1988
		P. lanceaefolium	leaves	Dan and Dan, 1988
		P. semisaggittatum	leaves	Dan and Dan, 1988
		P. suberifolium	leaves	Dan and Dan, 1988
		P. xylocarpum	stem	Tiwari et al., 1977
kaempferol-3-*O*-*α*-L	1.7	*P. acerifolium*	leaves	Dan and Dan, 1988
-galactoside		*P. suberifolium*	leaves	Dan and Dan, 1988
		P. xylocarpum	leaves	Dan and Dan, 1988
kaempferol-7-*O*-*β*-D -glucoside; populnin	1.8	*P. xylocarpum*	stems	Tiwari et al., 1977

Table 1 Chemical constituents of the genus *Pterospermum* (Continued).

Chemical compound	No.	species	part	Referenece
kaempferol-3-*O*-*β*-*D*-rutinoside	1.9	*P. suberifolium*	flowers	Gunasegaran and Subramanian, 1979
luteolin	1.10	*P. acerifolium*	leaves	Dan and Dan, 1988
		P. semisagittatum	flowers	Dan and Dan, 1988
		P. xylocarpum	flowers	Gunasegaran and Subramanian, 1979
luteolin-7-*O*-*α*-glucoside, cynaroside	1.11	*P. acerifolium*	leaves, flowers	Gunasegaran and Subramanian, 1979; Dan and Dan, 1988
luteolin-7-*β*-*O*-*D*-glucuronide	1.12	*P. acerifolium*	leaves	Gunasegaran and Subramanian, 1979; Dan and Dan, 1988
quercetin	1.13	*P. lanceaefolium*	leaves	Dan and Dan, 1988
		P. semisaggittatum	leaves	Dan and Dan, 1988
		P. suberifolium	leaves	Gunasegaran and Subramanian, 1979
quercetin-3-*O*-*β*-*D*-galactoside; hyperoside	1.14	*P. acerifolium*	flowers	Gunasegaran and Subramanian, 1979
		P. xylocarpum	leaves	Dan and Dan, 1988

Table 1 Chemical constituents of the genus *Pterospermum* (Continued).

Chemical compound	No.	species	part	Referenece
quercetin-3-α-*L*-arabinoside; avicularin	1.15	*P. suberifolium*	leaves	Gunasegaran and Subramanian, 1979
quercetin-3-α-*L*-arabinopyranoside; foeniculin; guaijaverin	1.16	*P. suberifolium*	leaves	Gunasegaran and Subramanian, 1979; Dan and Dan, 1988
quercetin-3-α-*L*-rhamnoside; quercitrin	1.17	*P. suberifolium*	leaves	Dan and Dan, 1988
Neolignans				
(7*S*,8*R*)-dihydrodehydrodiconiferyl alcohol-9′-*O*-*β*-D-glucopyranoside	1.18	*P. semisegittatum*	leaves	Khan et al., 2005
Phenolic amides				
aurantiamide acetate	1.19	*P. heyneanum*	barks	Anjaneyulu and Raju, 1988
		P. xylocarpum	leaves	Anjaneyulu and Raju, 1988
Quinone				
3-hydroxy-5-methoxy-2-methyl benzoquinone	1.20	*P. xylocarpum*	heartwood	Anjaneyulu and Raju, 1987a

Table 1 Chemical constituents of the genus *Pterospermum* (Continued).

Chemical compound	No.	species	part	Referenece
Steroids				
cyclopterospermol	1.21	*P. xylocarpum*	heartwood	Anjaneyulu and Raju, 1987a
30-norcyclopterospermol	1.22	*P. xylocarpum*	heartwood	Anjaneyulu and Raju, 1987a
30-norcyclopterospermone	1.23	*P. xylocarpum*	heartwood	Anjaneyulu and Raju, 1987a
β-sitosterol	1.24	*P. acerifolium*	leaves	Dan and Dan, 1988
		P. heyneanum	barks	Anjaneyulu and Raju, 1988
		P.lanceafolium	leaves	Zhong et al., 1993
		P. semisagittatum	leaves	Dan and Dan, 1988
		P. suberifolium	leaves	Dan and Dan, 1988
		P. xylocarpum	stems	Tiwari et al., 1977
β-sitosterol-3-*O*-*D*-gluco-pyranoside, daucosterol	1.25	*P. heyneanum*	barks	Anjaneyulu and Raju, 1988
		P. xylocarpum	heartwood	Anjaneyulu and Raju, 1987a
sterculin A	1.26	*P. acerifolium*	leaves	Zhong et al., 1993

Table 1 Chemical constituents of the genus *Pterospermum* (Continued).

Chemical compound	No.	species	part	Referenece
Terpenes				
sesquiterpenes				
10-*O*-acetyl-4,7-megastigmadien-3-one 9-*O*-(2',3',4',6'-tetra-*O*-acetyl)-*β*-D-glucopyranoside	1.27	*P. semisegittatum*	leaves	Khan et al., 2005
10-hydroxy-4, 7-megastigmadien-3-one-9-*O*-*β*-D-glucopyranoside	1.28	*P. semisegittatum*	leaves	Khan et al., 2005
9-*O*-acetyl-4,7-megastigmadien-3-one 10-*O*-(2',3',4',6'-tetra-*O*-acetyl)-*β*-D-glucopyranoside	1.29	*P. semisegittatum*	leaves	Khan et al., 2005
9-hydroxy-4,7–megastigmadien-3-one-10-*O*-*β*-D-glucopyranoside	1.30	*P. semisegittatum*	leaves	Khan et al., 2005

Table 1 Chemical constituents of the genus *Pterospermum* (Continued).

Chemical compound	No.	species	part	Referenece
triterpenes				
α-amyrin	1.31	*P. lanceaefolium*	flowers	Dan and Dan, 1988
		P. semisagittatum	leaves	Dan and Dan, 1988
		P. suberifolium	seeds	Dan and Dan, 1988
		P. xylocarpum	leaves	Dan and Dan, 1988
β-amyrin	1.32	*P. semisagittatum*	leaves	Dan and Dan, 1988
		P. suberifolium	seeds	Dan and Dan, 1988
bauerenol	1.33	*P. acerifolium*	leaves	Dan and Dan, 1988
		P. semisagittatum	flowers	Dan and Dan, 1988
		P. suberifolium	seeds	Dan and Dan, 1988
		P. xylocarpum	leaves	Dan and Dan, 1988
bauerenol acetate	1.34	*P. lanceaefolium*	flowers	Dan and Dan, 1988
		P. semisagittatum	leaves	Dan and Dan, 1988
		P. suberifolium	seeds	Dan and Dan, 1988
betulin	1.35	*P. acerifolium*	leaves,	Dan and Dan, 1988
		P. suberifolium	flowers,	Dan and Dan, 1988
		P. xylocarpum	seeds	Dan and Dan, 1988

Table 1 Chemical constituents of the genus *Pterospermum* (Continued).

Chemical compound	No.	species	part	Referenece
epi-friedelinol	1.36	*P. acerifolium*	flowers	Dan and Dan, 1988
friedelin	1.37	*P. acerifolium*	leaves	Dan and Dan, 1988
		P. heyneanum	flowers	Anjaneyulu and Raju, 1988
		P. suberifolium	barks	Dan and Dan, 1988
		P. xylocarpum	leaves	Dan and Dan, 1988
lupanone	1.38	*P. heyneanum*	barks	Anjaneyulu and Raju, 1988
		P. xylocarpum	leaves	Anjaneyulu and Raju, 1988
lupeol	1.39	*P. acerifolium*	leaves	Dan and Dan, 1988
		P. suberifolium	flowers	Dan and Dan, 1988
lupeol acetate	1.40	*P. heyneanum*	barks	Anjaneyulu and Raju, 1988
		P. xylocarpum	leaves	Anjaneyulu and Raju, 1988
taraxerol	1.41	*P. heyneanum*	barks	Anjaneyulu and Raju, 1988
		P. xylocarpum	leaves	Anjaneyulu and Raju, 1988
taraxerone	1.42	*P. heyneanum*	barks	Anjaneyulu and Raju, 1988
		P. semisagittatum	leaves	Dan and Dan, 1988
		P. suberifolium	leaves	Dan and Dan, 1988
		P. xylocarpum	leaves	Dan and Dan, 1988
Carbohydrates				
polysaccharide	-	*P. acerifolium*	barks	Bishnoi and Gupta, 1979

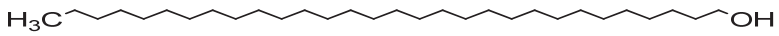

(1.1) Triacontan-1-ol

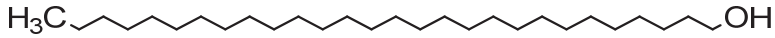

(1.2) Octacosan-1-ol

Figure 1 Alkanes isolated from *Pterospermum* species.

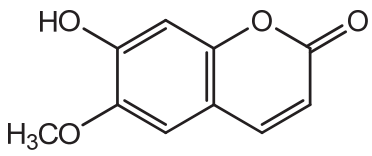

(1.3) Scopoletin

Figure 2 Coumarin isolated from *Pterospermum* species.

(1.4) Malvalic acid

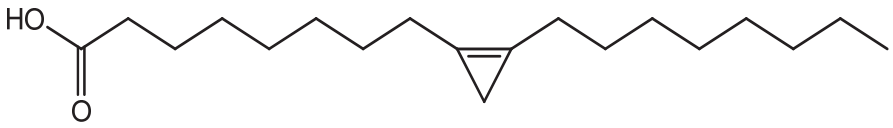

(1.5) Sterculic acid

Figure 3 Fatty acids and ester derivative isolated from *Pterospermum* species.

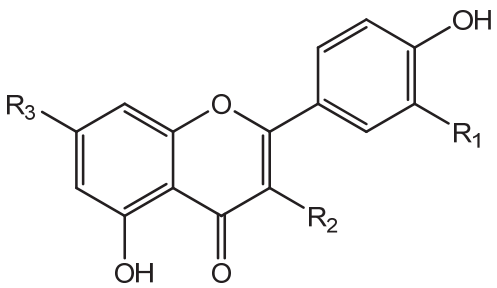

		R_1	R_2	R_3
(1.6)	Kaempferol		H	OH
(1.7)	Kaempferol-3-*O*-*L*-galactoside		galactose	OH
(1.8)	Kaempferol-7-*O*-*D*-glucoside		glucose	OH
(1.9)	Kaempferol-3- *O*-*D*-galactoside		galactose	OH
(1.10)	Luteolin	OH	OH	H
(1.11)	Luteolin-7-*O*-*α*- glucose	OH	OH	*α*-glucose
(1.12)	Luteolin-7-*O*-*β*-glucuronide	OH	OH	glucuronic acid
(1.13)	Quercetin	OH	OH	OH
(1.14)	Quercetin-3-*O*-*D*-galactoside	OH	galactose	OH
(1.15)	Quercetin-3-*α*-*L*-arabinoside	OH	arabinose	OH
(1.16)	Quercetin-3-*α*-*L*-arabinopyranoside	OH	arabiono-pyranose	OH
(1.17)	Quercetin-3-*α*-*L*-rhamnoside	OH	rhamnose	OH

Figure 4 Flavonoids isolated from *Pterospermum* species.

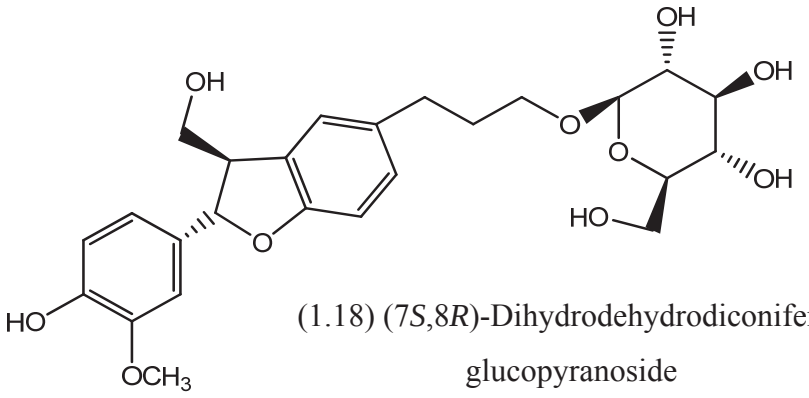

(1.18) (7*S*,8*R*)-Dihydrodehydrodiconiferylalcohol-9'-*O*-*β*-*D*-glucopyranoside

Figure 5 Neolignan isolated from *Pterospermum* species.

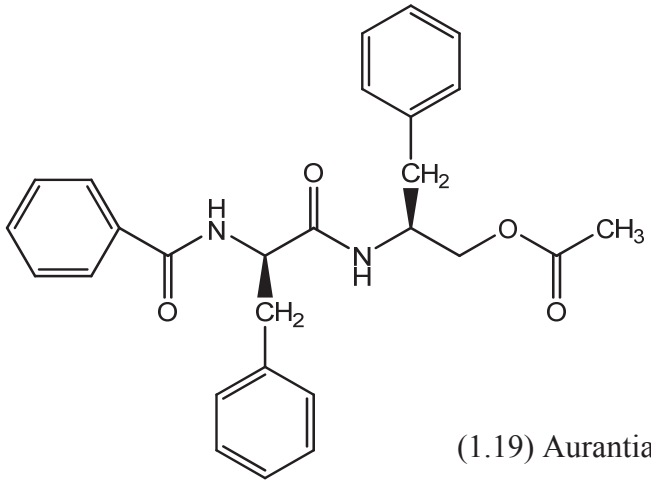

(1.19) Aurantiamide acetate

Figure 6 Phenolic amide isolated from *Pterospermum* species.

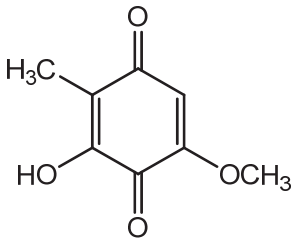

(1.20) 3-Hydroxy-5-methoxy-2-methyl benzoquinone

Figure 7 Quinone isolated from *Pterospermum* species.

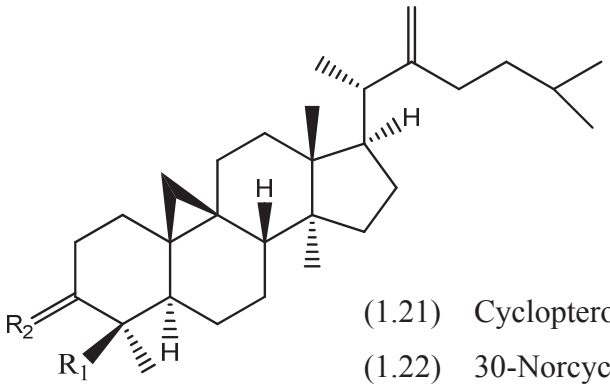

		R_1	R_1
(1.21)	Cyclopterospermol	CH_3	OH
(1.22)	30-Norcyclopterospermol	H	OH
(1.23)	30-Norcyclopterospermone	H	O

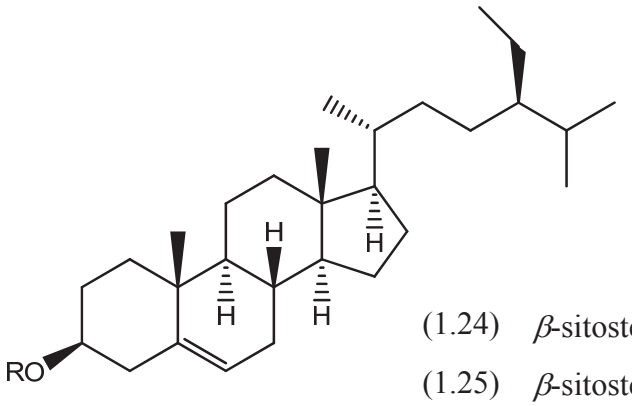

		R
(1.24)	*β*-sitosterol	H
(1.25)	*β*-sitosterol glucoside	glucose

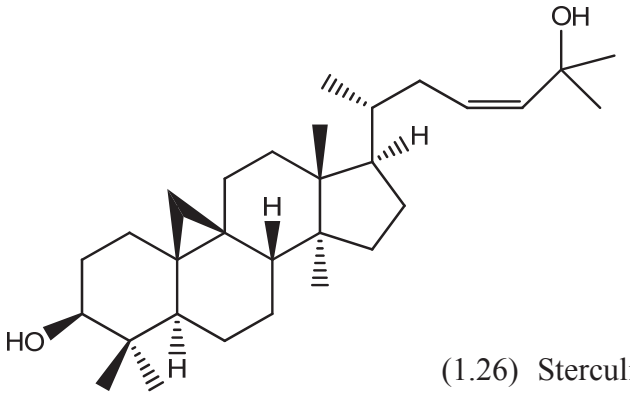

(1.26) Sterculin A

Figure 8 Saponins and steroids isolated from *Pterospermum* species.

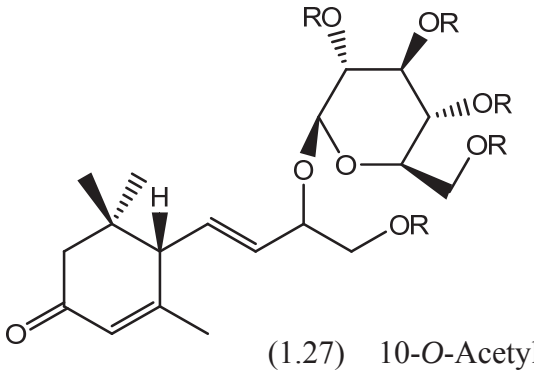

		R
(1.27)	10-*O*-Acetyl-4,7-megastigmadien-3-one-9-*O*-(2',3',4',6'-tetra-*O*-acetyl)-*β*-*D*-glucopyranoside	$COCH_3$
(1.28)	10-Hydroxy-4,7-megastigmadien-3-one-9-*O*-*β*-*D*-glucopyranoside	H

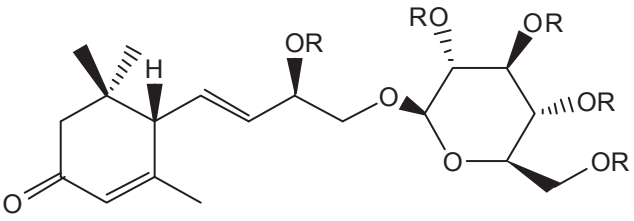

		R
(1.29)	9-*O*-Acetyl-4,7-megastigmadien-3-one-10-*O*-(2',3',4',6'-tetra-O-acetyl)-*β*-*D*-glucopyranoside	$COCH_3$
(1.30)	9-Hydroxy-4,7-megastigmadien-3-one-10-*O*-*β*-*D*-glucopyranoside	H

Figure 9 Terpenes isolated from *Pterospermum* species.

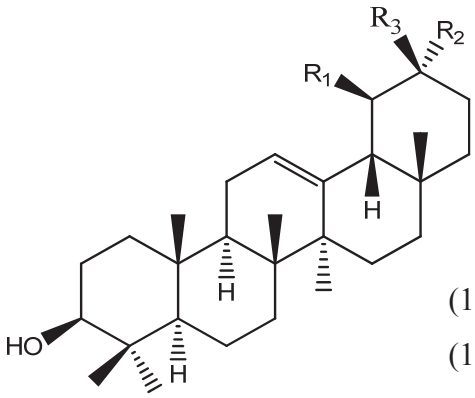

		R_1	R_2	R_3
(1.31)	α-Amyrin	CH_3	CH_3	
(1.32)	β-Amyrin		CH_3	CH_3

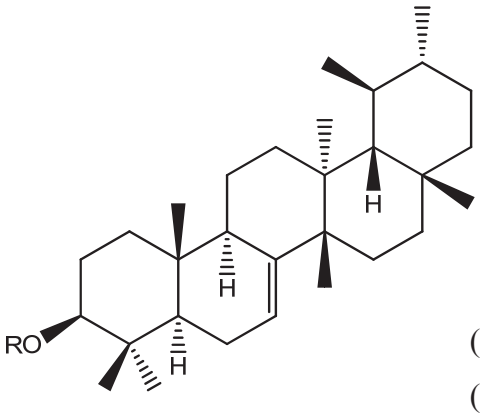

		R
(1.33)	Bauerenol	H
(1.34)	Bauerenol acetate	$COCH_3$

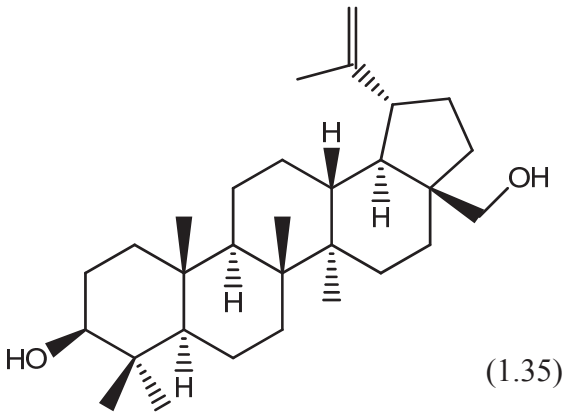

(1.35) Betulin

Figure 9 Terpenes isolated from *Pterospermum* species.

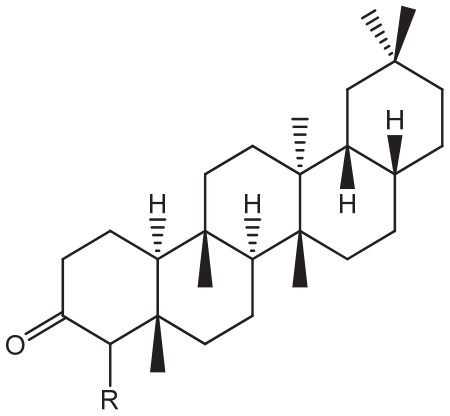

		R
(1.36)	*Epi*-friedelin	····H
(1.37)	Friedelin	H

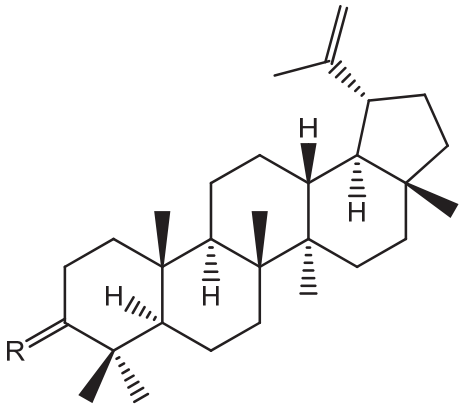

		R
(1.38)	Lupanone	O
(1.39)	Lupeol	OH
(1.40)	Lupeol acetate	$COCH_3$

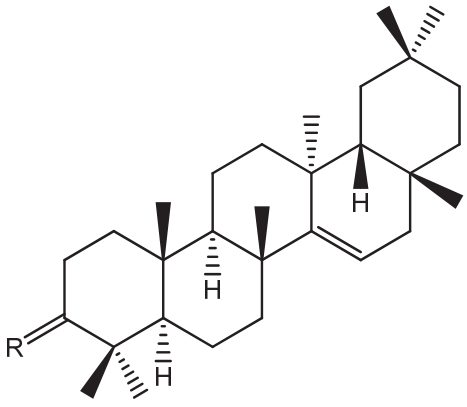

		R
(1.41)	Taraxerol	OH
(1.42)	Taraxerone	O

Figure 9 (Continued) Terpenes isolated from *Pterospermum* species.

1.3 *Pterospermum grande* Craib (Figure 10)

This plant has common name as Tong mom (Mae Hong Son Province), Sam Tao (Chiang Mai Province), and Hae Bass (Chiang Mai Province) (เต็ม สมิตตินันทน์, 2544). The plant is an evergreen tree of 16 m height and 36 cm dbh. External barks are thick, rough, gray-brownish. Inner barks seem pale light yellow. Branch and plumule have dense brownish hairs. Stipules are linear with 1.5 cm long. Petiole is robust and striate. Leaves are basal, simple, alternate, petiolate, and reticulate in venation. Leaf blades are nearly orbicular or oblong with 11-28 cm width, 15-45 cm long which dark green above and pale light greenish-grayish below. Flowers are axillary inflorescences and densely brown hairy. Epicalyx lobes are fimbriate and palmately divided. Sepals are linear-oblong, densely brownish. Fruits are woody capsule, cylindrical, reddish brown velutinous, glabrescent, tapering base, round apex, and without groove with 5-7 cm width, 8-15 cm long. There are many seeds, obliquely ovate, flat, large thin brown wing with 1.5 cm width and 4 cm long. The plant is found at 1,375 m elevation in evergreen forest near limestone terrain of Doi Tung. In addition, Laos and China (Yunnan) are also the habitats of this plant (สุธรรม อารีกุล, 2552; Maxwell, 2007; Ya et al., 2010).

In Yunnan, *P. grande* is prescribed as internal medication for its antipyretic, antitussive, anti-inflammatory activities. Externally, smashed fresh stem is spread on troubled parts of the body as a treatment (Traditional Chineses Medicine Daynetwork, 2010).

(1)

(2)

Figure 10 *Pterospermum grande* Craib (Sterculiaceae)

(1) Leaves of *P. grande*

(2) Flower of *P. grande*

2. Family Annonaceae

The Annonaceae family comprises of 130 genera and 2300 species. In Thailand, there are 41 genera and 195 species of this plant family including, *Artabotrys*, *Goniothalamus*, *Polyalthia*, *Desmos*, and *Mitrephora* (ปิยะ เฉลิมกลิ่น, 2544). They are mostly tree, shrub, and climbers. The characteristic are those of tropical trees and shrubs. They are usually with resin canals and septate pith; while many species produce aromatic oils. Barks and twigs are typically striated and fibrous. Leaves are simple, entire, alternate, typically distichous, no stipules and with a glaucous or metallic sheen. Buds are naked. Flowers are in solitary or in cymose inflorescences. Flowers are fragrant. They have 3 sepals and 6 petals. They have many stamens and pistils. Fruits consist of an aggregate of berries (Hutchinson, 1959). In addition to edible fruits such as sugar apple (*Annona squamosa* L.), soursop (*A. muricata* L.), custard apple (*A. reticulata* L.), and cherimoya (*A. cherimola* Mill.) (Heywood, 1985), a large number of species in Annonaceae are used in ethnomedicine. For example, *A. muricata* L. is used for its anti-inflammatory and antispasmodic effects in Thailand, *Orophea enterocarpa* Maingay ex. Hook. f. & Thomson. for nausea and vertigo in Thailand, and *Enantia chlorantha* Oliv or Awogba, for antipyretic effect in West Africa, and (Chuakul and Sornthornchareonon, 2003).

2.1 Genus *Mitrephora*

One of the largest genera in Annonaceae is the genus *Mitrephora* that comprises 48 species worldwide. In Southeast Asia, it distributes in the Philippines, Indonesia, Malaysia, Thailand, China (Yunnan, Hainan), southern India (Karnatako, Kerala, and Tamil Nadu), and North West Australia (Queenland) (Weerasooriya et al., 2006). To date, nine species of *Mitrephora* have been found in Thailand, including *M. alba* Ridl. (พรหมขาว; Phrom khao), *M. keithii* Ridl. (กลาย; Klai), *M. maingayi* Hook. f. & Thomson (นางแดง; Nang dang) or *M. teysmannii* Scheff., *M. tomentosa* Hook. f. & Thomson (มะป่วน; Ma puan) or *M. bousigoniana* Pierre (Bingtao et al., 2011) or *M. collinsae* Craib (กิ่งขื้น; King khuen) or *M. edwardsii* Pierre or *M. thorelii* Pierre, *M.*

vulpina C.E.C. Fischer (มะป่วนใต้; Ma puan tai), *M. wangii* Hu (ลำดวนดอย; Lamduan doi), *M. winitii* Craib (มหาพรหม; Maha phrom), *M. marginalis* (Scheff.) J. Sinclair (มะแฟด; Ma faed), and *M. sirikitiae* Weerasooriya, Chalermglin & R.M.K. Saunders (Weerasooriya et al., 2006) or *M. macclurei* Weerasooriya & R.M.K. Saunders (Bingtao et al., 2011) (มหาพรหมราชินี; Maha phrom rachinee). Some species such as *M. alba*, *M. winitii*, and *M. sirikitiae* are endemic and endangered plants since they are rare and found only in specific area (เต็ม สมิตินันทน์, 2544; ปิยะ เฉลิมกลิ่น, 2544).

In general, characteristics of the *Mitrephora* are small to large trees, 2 to 30 meters in height, occurring in tropical rain forest or hilly evergreen forest and go from more than 1,000 meters in elevation. The petiole is short. Leaves are elliptical or ovate. The leaf blade has arculately looped venation nearly margin, each side of mid vein contains 4-24 of secondary veins. Barks appear thin or thick dark, brownish. Flowers oppose leaves and are bisexual. Pedicel with basal bracts is short or long. They have three sepals and two whorls of three petals. The outer petals are large, spreading and the inner petals are small, rhombic, and clawed. Fruits are multiple which are obvoid or cyclindrical (Heywood, 1985; Bingtao et al., 2011).

2.2 Phytochemistry and Biological Activities of Genus *Mitrephora*

Several isolated compounds and biological activities were reported for *Mitrephora* (Table 2 and Figures 11-22). Four diterpenes were isolated from the stem bark of *M. celebica* Scheff. These diterpenes are, *ent*-kaur-16-en-19-oic acid (Figure 22 (2.55)), *ent*-trachyloban-19-oic acid (Figure 22 (2.66)), 8(14), 15-pimaradien-18-oic acid, and 7,15-pimaradien-18-oic acid. *Ent*-trachyloban-19-oic acid exhibited antimicrobial activity against *Mycobacterium smegmatis* and *Staphylococcus aureus* with equal MIC of 6.25 µg/ml (Zgoda-Pols et al., 2002). Polyacetylene carboxylic acids from the dichloromethane and methanol (1:1) extract of the dried bark of this plant were isolated and evaluated for antimicrobial activity. It was found that 13(*E*),17-octadecadiene-9,11-diynoic acid (13,14-dihydrooropheic acid) and 17-octadecene-9,11,13-triynoic acid (oropheic acid) exhibited antimicrobial activity against methicillin-resistant *Staphylococcus aureus* (MRSA) with MICs of 25 and

12.5 μg/ml, respectively, and *M. smegmatis* with equal MIC of 12.5 μg/ml (Zgoda et al., 2001).

Dimeric sesquiterpenoids such as meiogynin A and 1-*epi*-meiogynin A were isolated from the ethyl acetate extract of *M. cylindrocarpa* Burck bark. These compounds were investigated in Bcl-xL (fluorescent-tagged BH3 domain of the protein Bak) and showed Ki values of 10.8±3.1 and > 100 μM, respectively. Meiogynin A also exhibited cytotoxicity against KB cell line with IC_{50} of 4.0 μM (Litaudon et al., 2009).

Two azaflurenone alkaloids were isolated from the dichloromethane and methanol extracts of *M. diversifolia* (Span.) Miq. and evaluated for antimalarial activity against *Plasmodium falciparum* 3D7 and Dd2 strains and cytotoxicity against human embryonic kidney cell line, HEK193. 5-Hydroxy-6-methoxyonychine (Figure 11 (2.9)) exhibited more antimalarial and cytotoxic activity than 5,8-dihydroxy-6-methoxyonychine (Figure 11 (2.8)) with IC_{50} of 9.9 -11.4 μM, and 96% at 120 μM, respectively (Mueller et al., 2009).

M. maingayi Hook. f. & Thomson has been investigated for chemical compounds and biological activities. 5-Oxonoraporphine alkaloids and aromatic hydrocarbons such as 1,2-dimethoxy-3-hydroxy-5-oxonoraprophine (Figure 11 (2.6)), 1,2,3,-trimethoxy-5-oxonoraporphine (Figure 11 (2.7)), ouregidione, 3-methoxycepharadione B, and *trans*-isoelemicin were isolated from the *n*-hexane and chloroform extracts of its dried bark and evaluated for cytotoxicity against P-388 cell lines (Lee et al., 1999). In addition, several alkaloids were found in ethanol extract of the twigs of this plant, including dicentrinine, dicentrinone (Figure 11 (2.2)), and maingayinine (Figure 11 (2.10)) (Yu et al., 2005), whereas (+)-*epi*eudesmin (Figure 14 (2.13)), eudesmin (Figure 14 (2.15)), magnone A (Figure 14 (2.16)), (-)-kaur-16-en-19-oic acid (Figure 22 (2.55)), and didymooblongin were found in the hexane and chloroform extracts of its leaves. Liriodenine (Figure 11 (2.3)), oxostephanine (Figure 11 (2.5)), (+)-pimaric acid (Figure 22 (2.60)), and pinocembrin were obtained from the hexane and chloroform extracts of its stem (Deepralard et al., 2007).

M. tomentosa Hook. f. & Thomson (synonym: *Pseuduvaria rugosa* (Blume) Merr) contains two diterpenoid compounds, i.e., (-)-kaur-16-en-19-oic acid (Figure 22 (2.55)) and (-)-8β-hydroxypimar-15-en-18-oic acid (Figure 22 (2.59))

which were isolated from the methanol extract of its stem bark (Supudompol et al., 2004).

Three *ent*-trachylobane diterpenoids, mitrephorones A, B, and C were found in *M. glabra* and evaluated for antimicrobial and cytotoxic activities. Mitrephorone A displayed broad activities against four cell lines, i.e., KB, MCF-7, H460, and SF-268 with IC_{50} values of 8.0, 15.7, 23.3, and 30.9, respectively. Mitrephorone C revealed the strongest antimicrobial activity. However, activities of all compounds were less than positive controls (Li et al., 2005). Nine compounds of terpenoids, alkaloids, and polyacetylenic acids such as liriodenine (Figure 11 (2.3)), octadeca-9,11,13-triynoic acid (Figure 19 (2.31)), oropheolide (Figure 19 (2.32)), and 4-*epi*-kaurenic acid, mitrekaurenone (Figure 22 (2.57)) were isolated from the stem bark extract. All compounds were examined for cytotoxic and antimicrobial activities. The results showed that liriodenine, octadeca-9,11,13-triynoic acid, and oropheolide were active against KB, MCF-7, and NCI-H460 with IC_{50} values ranging from 5 to 40 μM. MICs for antimicrobial activity of these compounds ranged from 6.3 to 250 μg/ml (Li et al., 2009).

The methanol extract of the twigs of *M. vandaeflora* Kurz (synonym: *M. vulpina* C.E.C. Fischer or *M. javanica* Backer) contained oxoputerin (Figure 11 (2.4)), liriodenine, quebrachitol (Figure 12 (2.11)), and phylligenin (Figure 14 (2.14)). All compounds were investigated in a test for antiplatelet aggregation. Phylligenin and quebrachitol showed inhibitory activity on platelet activating factors with ICs_{50} of 13.1 and 42.2 μM, respectively (Moharam et al., 2010).

The chloroform extract from air-dried aerial part of *M. thorelii* Pierre gave two clerodane-type diterpenes, 6*α*,16,18-trihydroxycleroda-3(4),13(14)-dien-15,16-olide (Figure 22 (2.53)), 13(14)-dien-15,16-olide (Figure 22 (2.54)), and 16-hydroxycleroda-3(4). These compounds inhibited proliferation of BEL-7402 cell line with ICs_{50} of 44.6 and 20.1 μM, respectively. 16-Hydroxycleroda-3(4),13(14)-dien-15,16-olide also inhibited the growth of murine hepatoma H22 cell line (Meng et al., 2007). Lignanamides, such as cannabisin G (Figure 15 (2.18)), thoreliamides A-C (Figure 15 (2.19-2.21)), *N-trans*-sinapolytyramine (Figure 18 (2.29)), and a sesquiterpenoid, thorelinin, were also isolated from the ethyl acetate extract of the stem of this plant from southwest China (Ge et al., 2008).

Chemical constituents of the genus *Mitrephora,* collected from previous reports and NAPRALERT database, are present in Table 2.

Table 2 Chemical constituents of the genus *Mitrephora*.

Chemical compound	No.	species	part	Reference
Alkaloids				
dicentrine	2.1	*M. vulpina*	twigs	Moharam et al., 2010
dicentrinone	2.2	*M. vulpina*	twigs	Moharam et al., 2010
liriodenine	2.3	*M. glabra,*	barks	Li et al., 2009
		M. maingayi	dried stems	Deepralard et al., 2007
		M. vulpina	twigs	Moharam et al., 2010
oxoputerine	2.4	*M. vulpina*	twigs	Moharam et al., 2010
oxostephanine	2.5	*M. maingayi*	dried stems	Deepralard et al., 2007
1,2,3-trimethoxy-5-oxonoraporphine	2.6	*M. maingayi*	barks	Lee et al., 1999
1,2-dimethoxy-3-hydroxy-5-oxonoraporphine	2.7	*M. maingayi*	barks	Lee et al., 1999
5,8-dihydroxy-6-methoxyonychine	2.8	*M. diversifolia*	root	Mueller et al., 2009
5-hydroxy-6-methoxyonychine	2.9			
maingayinine	2.10	*M. maingayi*	twigs	Yu et al., 2005
Cyclitols				
quebrachitol	2.11	*M.vulpina*	twigs	Moharam et al., 2010

Table 2 Chemical constituents of the genus *Mitrephora* (Continued).

Chemical compound	No.	species	part	Reference
Flavonoids				
pinocembrin	2.12	*M. maingayi*	dried stems	Deepralard et al., 2007
Lignans				
(+)-*epi*eudesmin	2.13	*M. maingayi*	leaves	Deepralard et al., 2007
phylligenin	2.14	*M. vulpina*	twigs	Moharam et al., 2010
eudesmin	2.15	*M. maingayi*	leaves	Deepralard et al., 2007
magnone A	2.16	*M. maingayi*	leaves	Deepralard et al., 2007
Lignanamides				
cannabisin F	2.17	*M. thorelii*	stems	Ge et al., 2008
cannabisin G	2.18	*M. thorelii*	stems	Ge et al., 2008
thoreliamide A	2.19	*M. thorelii*	stems	Ge et al., 2008
thoreliamide B	2.20	*M. thorelii*	stems	Ge et al., 2008
thoreliamide C	2.21	*M. thorelii*	stems	Ge et al., 2008
Napthylamine derivatives				
N-phenyl-2-napthylamine	2.22	*M. maingayi*	twigs	Yu et al., 2005
Phenolic acid derivatives				
terephthalic acid	2.23	*M. maingayi*	twigs	Yu et al., 2005
Phenolic amides				
N-trans-caffeoyltyramine	2.24	*M. thorelii*	stems	Ge et al., 2008
N- trans -coumaroyltyramine	2.25	*M. thorelii*	stems	Ge et al., 2008
N-trans-feruloyldopamine	2.26	*M. thorelii*	stems	Ge et al., 2008
N-trans-feruloyl-3-methyldopamine	2.27	*M. thorelii*	stems	Ge et al., 2008
N-trans-feruloyltyramine	2.28	*M. thorelii*	stems	Ge et al., 2008
N-trans-sinapoyltyramine	2.29	*M. thorelii*	stems	Ge et al., 2008

Table 2 Chemical constituents of the genus *Mitrephora* (Continued).

Chemical compound	No.	species	part	Reference
Polyacetylene compounds				
methyloropheate	2.30	*M. glabra*	stem bark	Li et al., 2009
octadeca-9, 11,13-triynoic acid	2.31	*M. glabra*	stem bark	Li et al., 2009
oropheolide	2.32	*M. glabra*	stem bark	Li et al., 2009
9,10-dihydrooropheolide	2.33	*M. glabra*	stem bark	Li et al., 2009
13(*E*),17-octadecadiene-9,11-diynoic acid or (13,14-dihydrooropheic acid)	2.34	*M. celebica*	bark	Zgoda et al., 2001
		M. tomentosa	stem bark	Supudompol et al., 2004
17-octadecene-9,11,13-triynoic acid (orophenic acid)	2.35	*M. celebica*	bark	Zgoda et al., 2001
Purine derivatives				
allantoin	2.36	*M. maingayi*	twigs	Yu et al., 2005
Saponins and Steroids				
β-sitosterol	2.37	*M. tomentosa*	stem bark	Supudompol et al., 2004
stigmasterol	2.38	*M. vulpina*	twigs	Moharam et al., 2010
Terpernoids & Steroids				
Monoterpenes				
limonene	2.39	*M. zippeliana*	leaves	Brophy et al., 2004
α-pinene	2.40	*M. zippeliana*	leaves	Brophy et al., 2004
β-pinene	2.41	*M. zippeliana*	leaves	Brophy et al., 2004

Table 2 Chemical constituents of the genus *Mitrephora* (Continued).

Chemical compound	No.	species	part	Reference
Sesquiterpenes				
aromadendrene	2.42	*M. zippeliana*	leaves	Brophy et al., 2004
spathulenol	2.43	*M. zippelian,*	leaves	Brophy et al., 2004
α-caryophyllene or *α*-humulene	2.44	*M. zippeliana*	leaves	Brophy et al., 2004
β-caryophyllene	2.45	*M. zippeliana*	leaves	Brophy et al., 2004
caryophylene oxide	2.46	*M. zippeliana*	leaves	Brophy et al., 2004
bicyclogermacrene	2.47	*M. zippeliana*	leaves	Brophy et al., 2004
α-copaene	2.48	*M. zippeliana*	leaves	Brophy et al., 2004
ar-curcumene	2.49	*M. zippeliana*	leaves	Brophy et al., 2004
meiogynin A	2.50	*M. cylindrocarpa*	bark	Litaudon et al., 2009
1-*epi*-meiogynin A	2.51	*M. cylindrocarpa*	bark	Litaudon et al., 2009
thorelinin	2.52	*M. thorelii*	stems	Ge et al., 2008
Diterpenes				
Clerodanes				
6α-16,18-trihydroxycleroda-3(4),13(14)-dien-15,16-olide	2.53	*M. thorelii*	aerial	Meng et al., 2007
16-hydroxycleroda-3(4),13(14)-dien-15-16-olide	2.54	*M. thorelii*	aerial	Meng et al., 2007

Table 2 Chemical constituents of the genus *Mitrephora* (Continued).

Chemical compound	No.	species	part	Reference
Kauranes				
ent-kaur-16-en-19-oic acid,13,14-dihydrooropheic acid	2.55	*M. tomentosa*	bark	Supudompol et al., 2004
		M. maingayi,	leaves, dried stems	Deepralard et al., 2007
		M. celebica	Stem barks	Zgoda-Pols et al., 2002
4-*epi*-kaurenic acid	2.56	*M. glabra*	bark	Li et al., 2009
mitrekaurenone	2.57	*M. glabra*	bark	Li et al., 2009
methylmitrekaurenate	2.58	*M. glabra*	bark	Li et al., 2009
Pimaranes				
(-)-8*β*-hydroxypimar-15-en-18-oic acid	2.59	*M. tomentosa*	barks	Supudompol et al., 2004
(+)-pimaric acid	2.60	*M. maingayi*	dried stem	Deepralard et al., 2007
8(14),15-pimaradien-18-oic acid	2.61	*M. celebica*	stem bark	Zgoda-Pols et al., 2002
7,15-pimaradien-18-oic acid	2.62	*M. celebica*	stem bark	Zgoda-Pols et al., 2002
mitrephorone A	2.63	*M. glabra*		Li et al., 2005
mitrephorone B	2.64	*M. glabra*		Li et al., 2005
mitrephorone C	2.65	*M. glabra*		Li et al., 2005
Trachylodanes				
ent-trachyloban-19-oic acid	2.66	*M. celebica*	stem bark, leaves, twigs	Zgoda-Pols et al., 2002

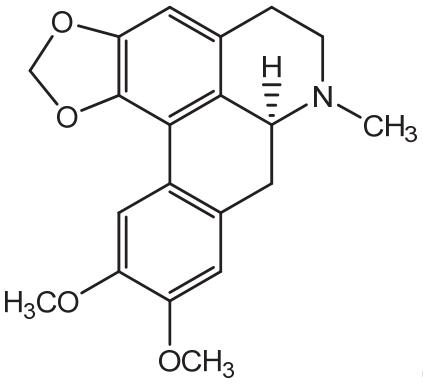

(2.1) Dicentrine

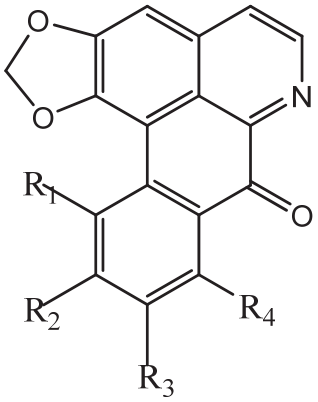

		R_1	R_2	R_3	R_4
(2.2)	Dicentrinone		OCH_3	OCH_3	
(2.3)	Liriodenine				
(2.4)	Oxoouterine	OCH_3			
(2.5)	Oxostephanine				OCH_3

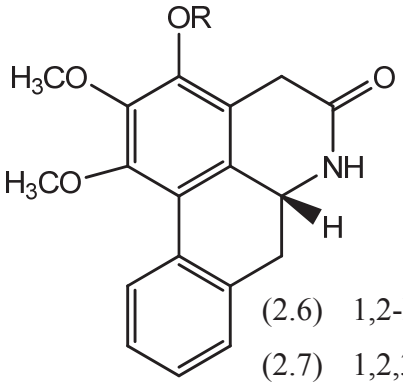

		R
(2.6)	1,2-Dimethoxy-3-hydroxy-5 -oxonoraporphine	OH
(2.7)	1,2,3,-Trimethoxy-5-oxonoraporphine	OCH_3

Figure 11 Alkaloids isolated from *Mitrephora* species.

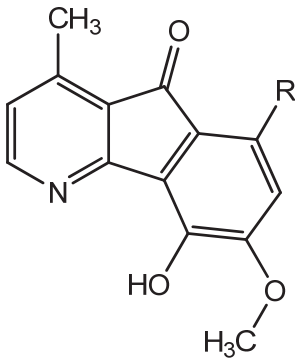

		R
(2.8)	5,8-Dihydroxy-6-methoxyonychine	OH
(2.9)	5-Hydroxy-6-methoxyonychine	H

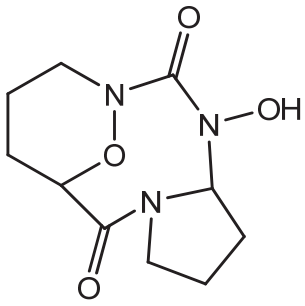

(2.10) Maingayinine

Figure 11 (Continued) Alkaloids isolated from *Mitrephora* species.

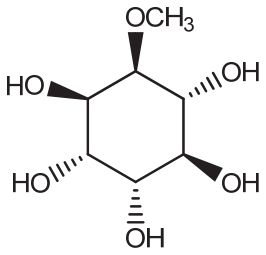

(2.11) Quebrachitol

Figure 12 Cyclitol isolated from *Mitrephora* species.

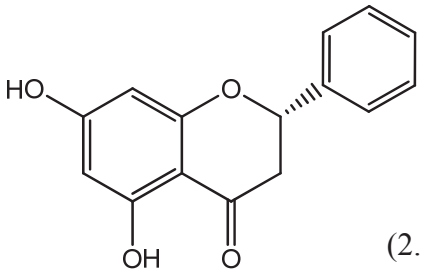

(2.12) Dihydrochrysine; pinocembrin

Figure 13 Flavonoid isolated from *Mitrephor* species.

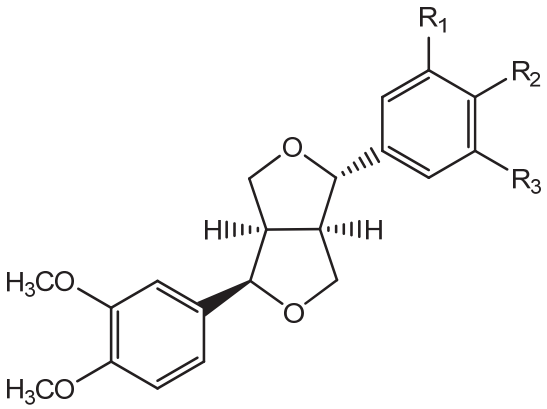

		R_1	R_2	R_3
(2.13)	(+)-Epieudesmin	OCH_3	OCH_3	
(2.14)	Phyllignin		OH	OCH_3

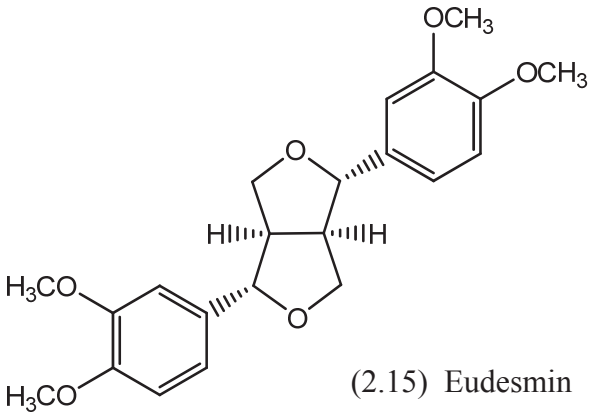

(2.15) Eudesmin

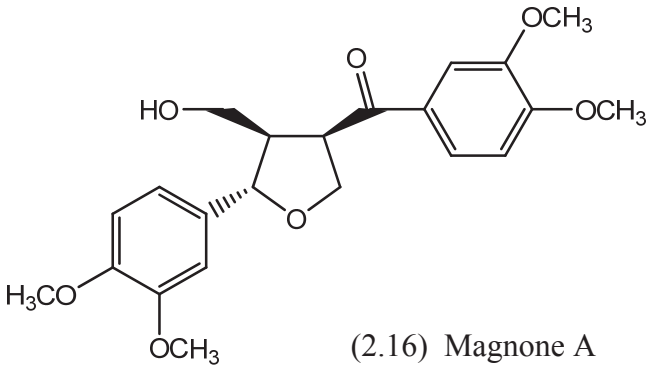

(2.16) Magnone A

Figure 14 Lignans isolated from *Mitrephora* species.

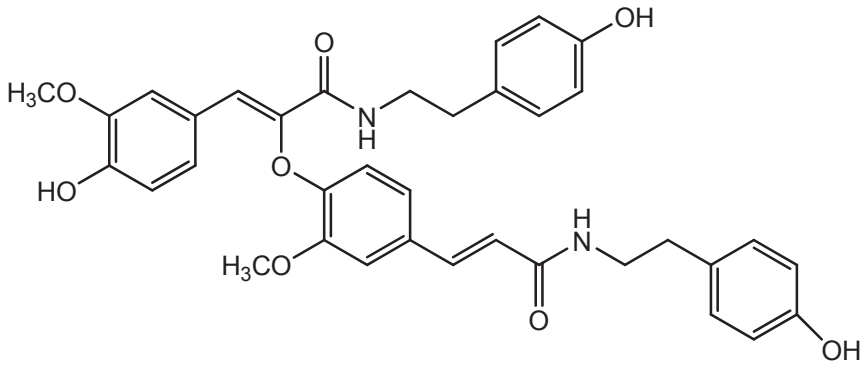

(2.17) Cannabisin F

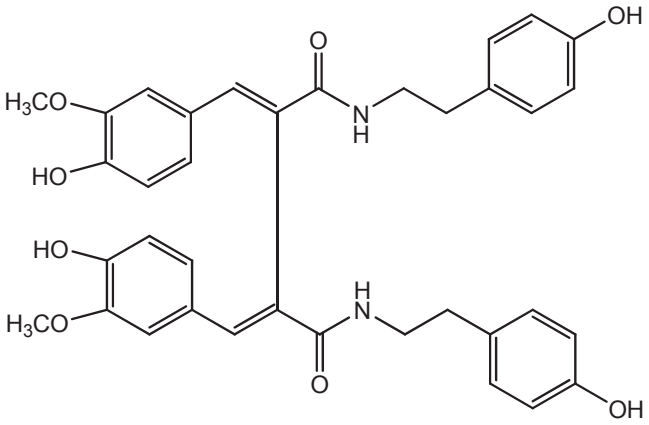

(2.18) Cannabisin G

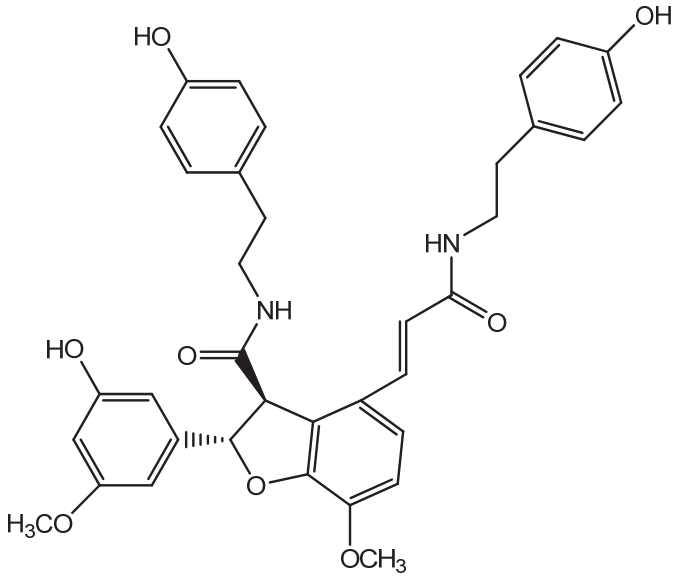

(2.19) Thoreliamide A

Figure 15 Lignanamides isolated from *Mitrephora* species.

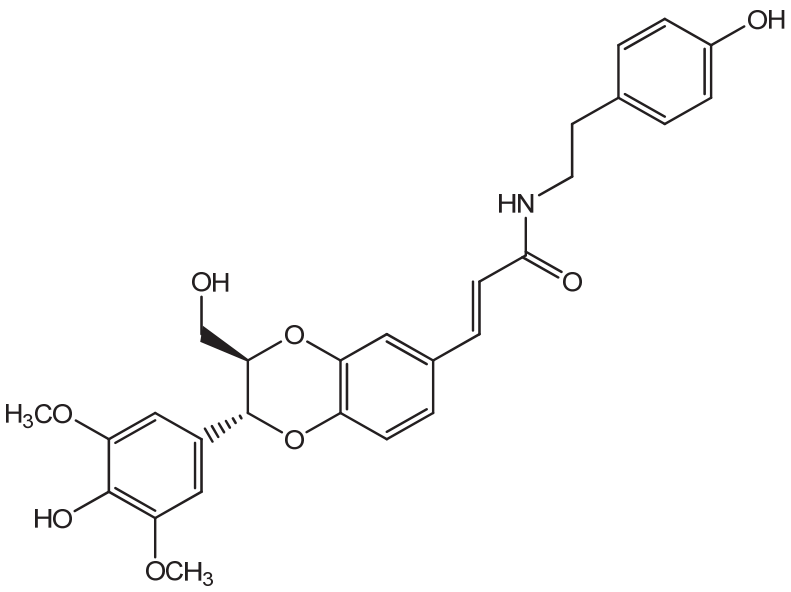

(2.20) Thoreliamide B

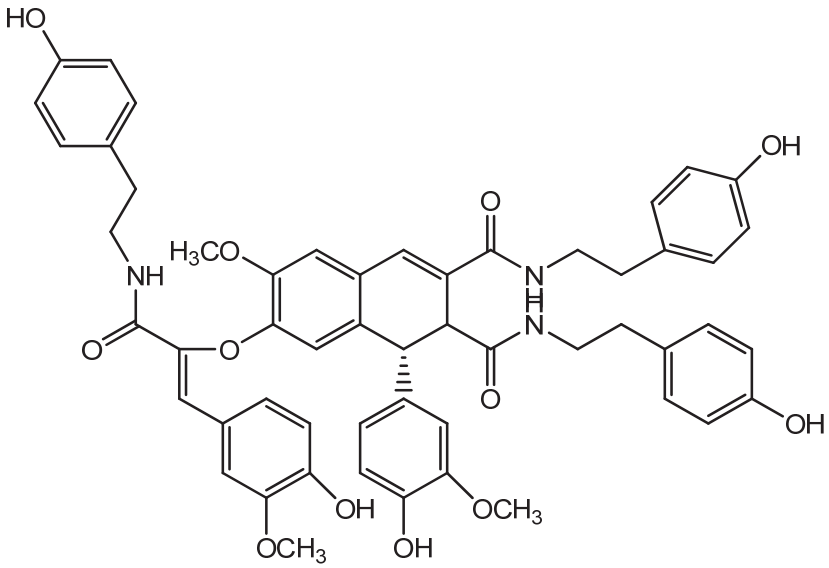

(2.21) Thoreliamide C

Figure 15 (Continued) Lignanamides isolated from *Mitrephora* species.

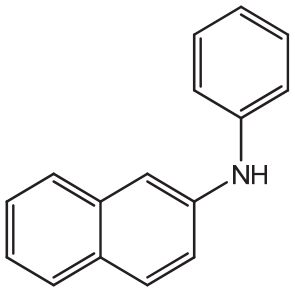

(2.22) *N*-Phenyl-2-napthylamine

Figure 16 Napthylamine compound isolated from *Mitrephora* species.

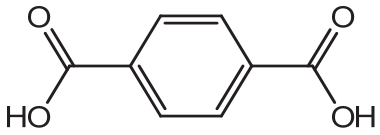

(2.23) Terephthalic acid

Figure 17 Phenolic acid isolated from *Mitrephora* species.

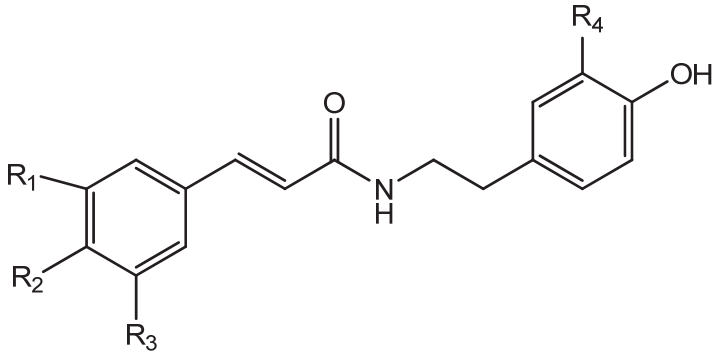

		R_1	R_2	R_3	R_4
(2.24)	*N-trans*-Caffeoyltyramine	OH	OH	OH	H
(2.25)	*N-trans*-Coumaroyltyramine		OH		H
(2.26)	*N-trans*-Feruloyldopamine		OH	OCH_3	OH
(2.27)	*N-trans*-Feruloyl-3-methyldopamine		OH	OCH_3	OCH_3
(2.28)	*N-trans*-Feruloyltyramine		OH	OCH_3	H
(2.29)	*N-trans*-Sinapoyltyramine	OCH_3	OH	OCH_3	H

Figure 18 Phenolic amides isolated from *Mitrephora* species.

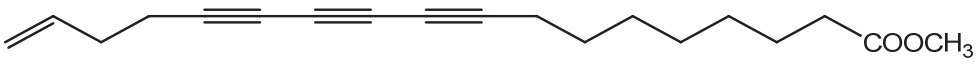

(2.30) Methyloropheate

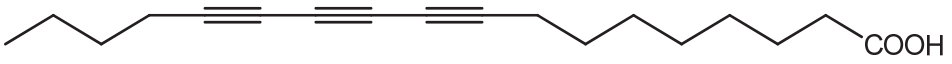

(2.31) Octadeca-9, 11, 13-triynoic acid

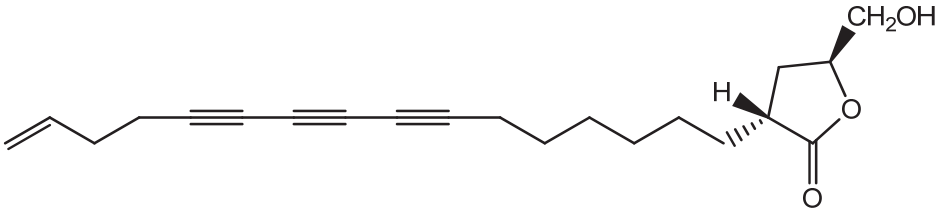

(2.32) Oropheolide

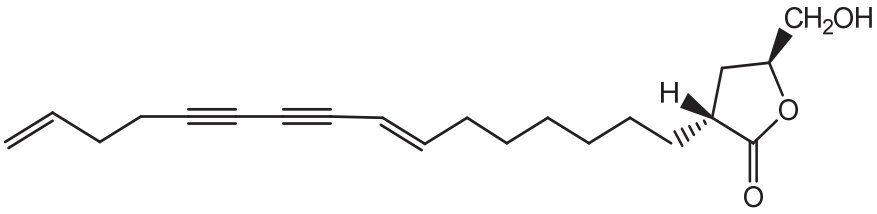

(2.33) 9, 10-Dihydroorpheolide

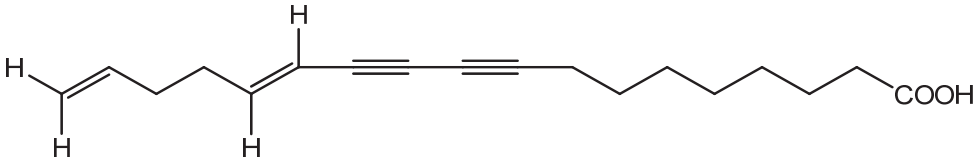

(2.34) 13(*E*), 17-Octadecadiene-9, 11-diynoic acid (13, 14-dihydrooropheic acid)

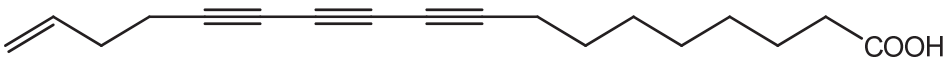

(2.35) 17-Octadecene-9, 11, 13-trinoic acid; oropheic acid

Figure 19 Polyacetylene compounds isolated from *Mitrephora* species.

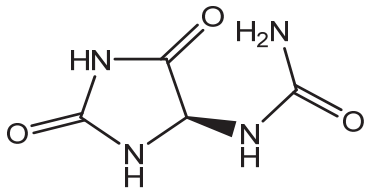

(2.36) Allantoin

Figure 20 Purine derivative isolated from *Mitrephora* species.

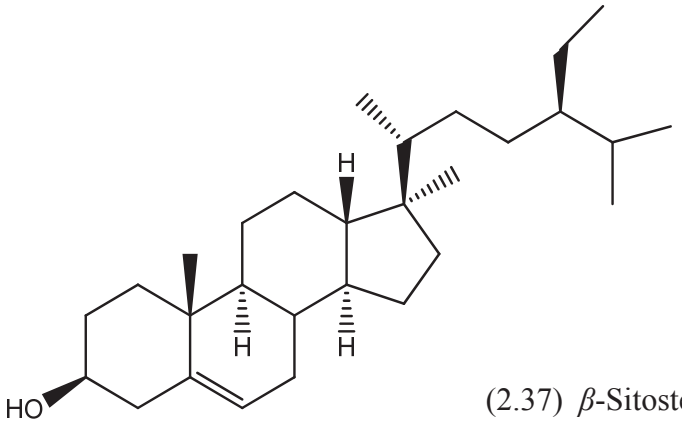

(2.37) *β*-Sitosterol

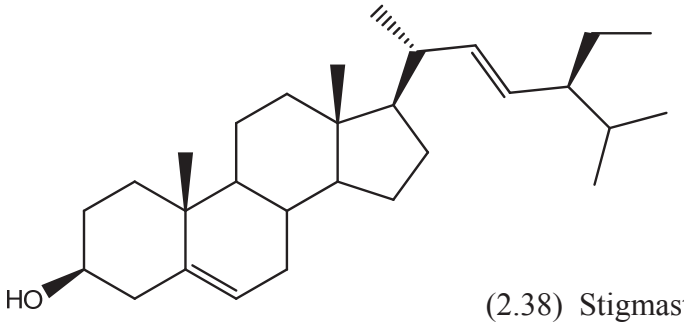

(2.38) Stigmasterol

Figure 21 Steroids isolated from *Mitrephora* species.

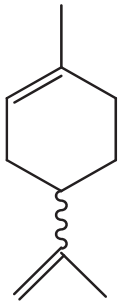

(2.39) Limonene

(2.40) α-Pinene

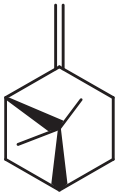

(2.41) β-Pinene

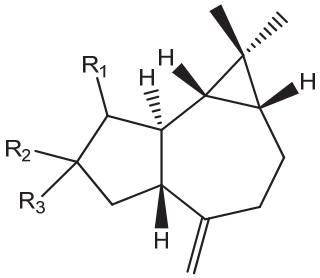

		R_1	R_2	R_3
(2.42)	Aromadendrene	⋯		
(2.43)	Spathylenol		⋯	OH

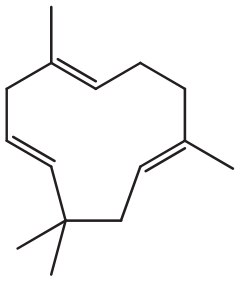

(2.44) *α*-Caryophyllene

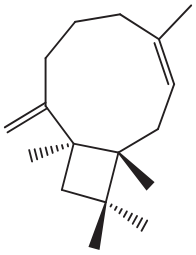

(2.45) *β*-Caryophyllene

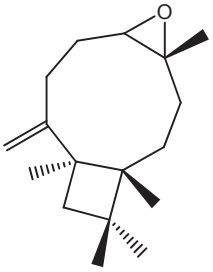

(2.46) Caryophyllene oxide

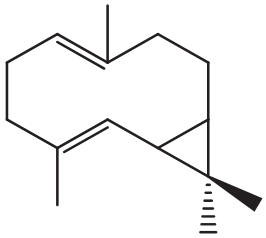

(2.47) Bicyclogermacrene

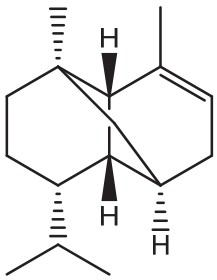

(2.48) *α*-Copaene

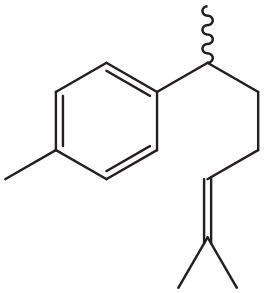

(2.49) ar-Curcumene

Figure 22 Terpenes isolated from *Mitrephora* species.

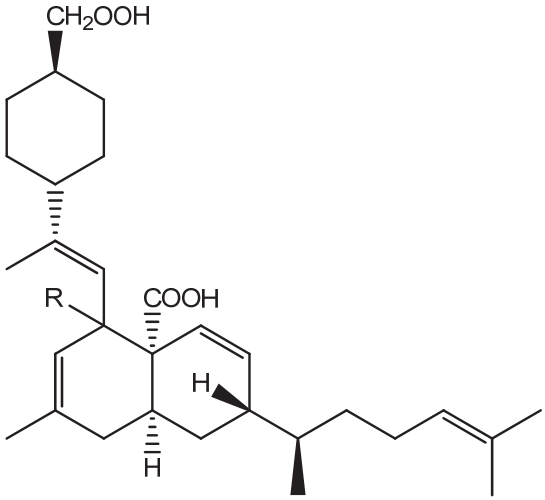

R

(2.50) Meiogynin A

(2.51) 1-*Epi*-meiogynin A

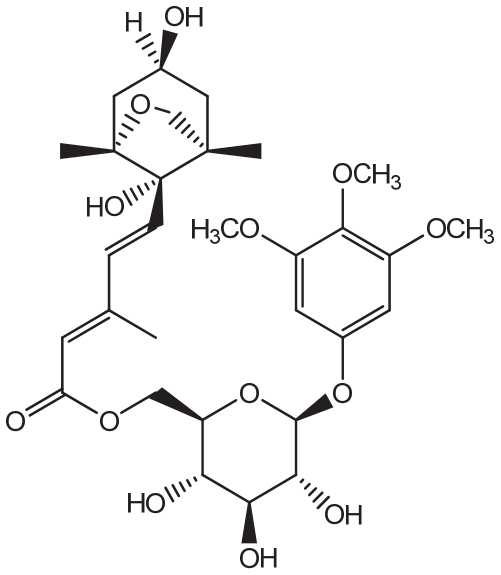

(2.52) Thorelinin

Figure 22 (Continued) Terpenes isolated from *Mitrephora* species.

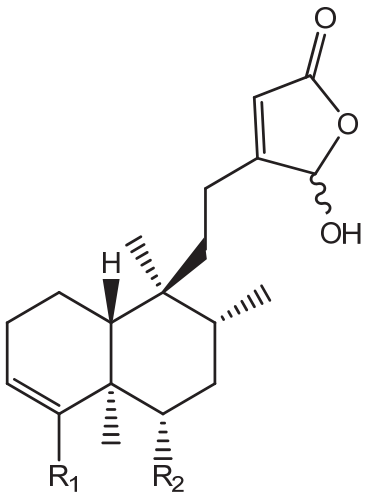

		R_1	R_2
(2.53)	6a,16,18-Trihydroxycleroda-3(4),13(14)-dien-15,16-olide	CH_2OH	OH
(2.54)	16-Hydroxycleroda-3(4),13(14)-dien-15,16-olide	CH_3	H

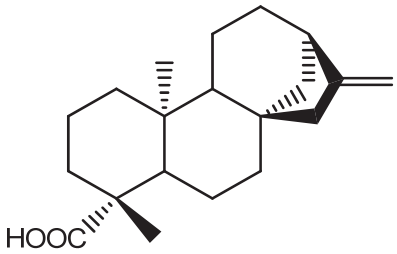

(2.55) *Ent*-kaur-16-en-19-oic acid

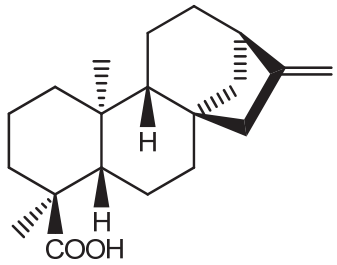

(2.56) 4-*Epi*-kaurenic acid

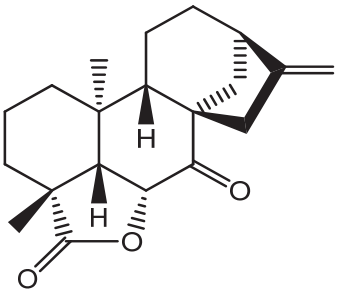

(2.57) Mitrekaurenone

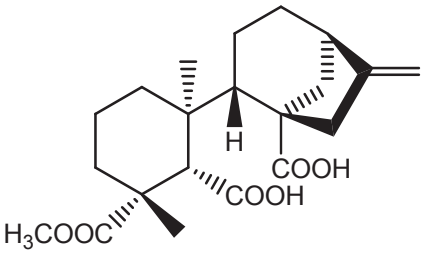

(2.58) Methylmitrekaurenate

Figure 22 (Continued) Terpenes isolated from *Mitrephora* species.

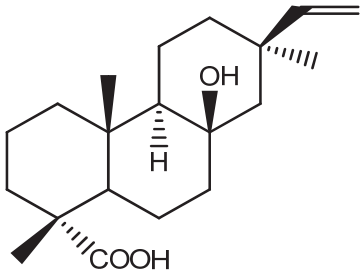

(2.59) (-)-8*β*-Hydroxypimar-15-en-18-oic acid

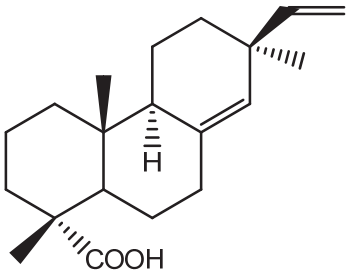

(2.60) (+)-Pimaric acid

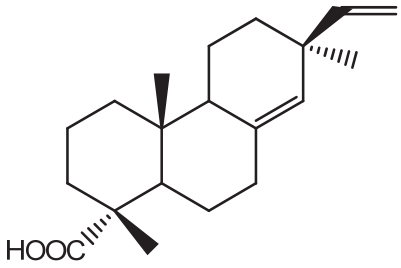

(2.61) 8(14), 15-Pimaradien-18-oic acid

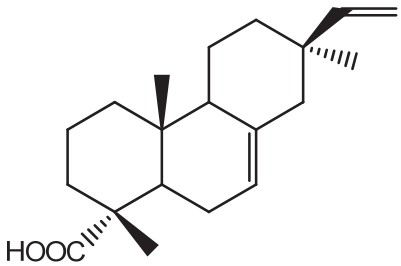

(2.62) 7,15-Pimaradien-18-oic acid

Figure 22 (Continued) Terpenes isolated from *Mitrephora* species.

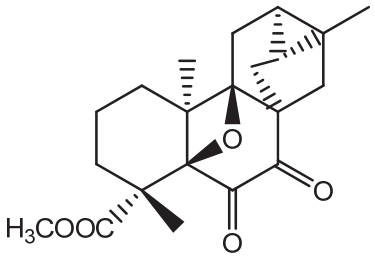

(2.63) Mitrephorone A

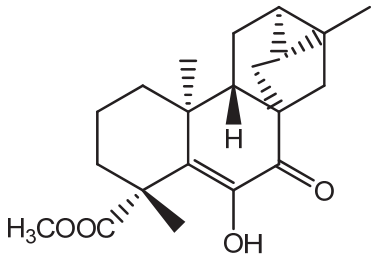

(2.64) Mitrephorone B

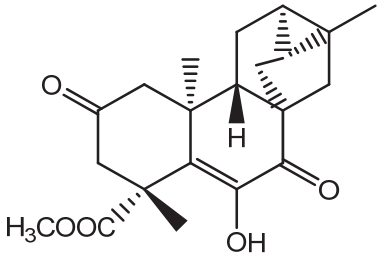

(2.65) Mitrephorone C

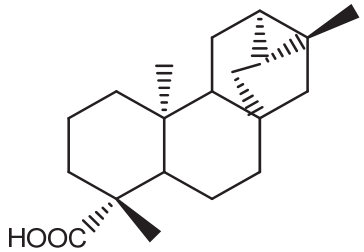

(2.66) *Ent*-trachyloban-19-oic acid

Figure 22 (Continued) Terpenes isolated from *Mitrephora* species.

2.3 *Mitrephora wangii* Hu (Figure 23)

Mitrephora wangii Hu, common names as Lamduan doi (ลำดวนดอย), Ma puan yai (มะป่วนใหญ่), and Ma puan doi (มะป่วนดอย) (ปิยะ เฉลิมกลิ่น, 2544), is a large evergreen tree of 14 m in height and 68 cm dbh. Barks are thin, dark gray, very finely roughened, and sparsely cracked. Branchlets are dark gray. Leaf blades are dark green above and light green below. Leaves have an elliptic shape with 5-7 cm width and 13-20 cm long, acuminate apex. Leaves are laminable, coriaceous, and subglabrous to hairy abaxially. The petiole is hairy. Flowers are short inflorescences opposite to leaves. Flower peduncles are dull light green. Sepals are light green. Both sides of outer 3 petals are white, rapidly becoming yellow and that of inner 3 petals which are connate, dull light purples are vaulted. Claws of outer petals are cream and turning light yellow. Connectives are light pale yellow. Stigmas are light yellow. Flowers are fragrant and blossom in February to March. Fruits contain pedicel woody 2-3 cm long. Cylindrical fruits with shiny peel, aggregate fruits, have 5-7 monocarps, 1.5-2.5 cm width, 4-6 cm long. Seeds are compressed and horizontal oriented (ปิยะ เฉลิมกลิ่น, 2544; Heywood, 1985; Maxwell, 2007).

The plants distributed at Doi Tung, the north of Thailand and Yunnan, China. There are no ethnomedical information about this plant.

(1) (2)

(3) (4)

Figure 23 *Mitrephora wangii* Hu (Annonaceae)

(1) Flower of *M. wangii*

(2) Flower of *M. wangii*

(3) Leaves and Twigs of *M. wangii*

(4) Fruits of *M. wangii*

CHAPTER 3

MATERIALS AND METHODS

1. Sources of Plant Materials

The leaves and whole plants of eighteen plants (Table 3) were collected from Doi Tung, Chiang Rai, Thailand in November, 2006. The leaves of *Pterospermum grande* Craib and the leaves and twigs of *Mitrephora wangii* Hu were collected from Doi Tung in December, 2007. Botanical identification was performed by J. F. Maxwell (a botanist at the herbarium of the Department of Biology, Faculty of Science, Chiang Mai University). The voucher specimen number of *P. grande* was 06-378, and that of *M. wangii* was 05-152. Voucher specimens of all plants were deposited at the herbarium of the Department of Biology, Faculty of Science, Chiang Mai University, Chiang Mai, Thailand.

2. Biological Activities of the Methanol Extracts from 18 Plants

Dried leaves and dried whole plants (5.0 g) were extracted with methanol (3 x 20 ml). The methanol extracts were filtered and were evaporated under vacuum using rotary evaporator. The methanol extracts from plants were investigated for toxicity using brine shrimp, antioxidative activity using DPPH assay, and the combination index with *L*-ascorbic acid. Extracts with good biological activities were selected for the further study.

Table 3 Eighteen plants for screening processes.

Family	Scientific name	Local name	Voucher specimen no.
Acanthaceae	*Strobilanthes erectus* Cl. ex Hoss.		04-673
Aceraceae	*Acer chiangdaoense* Santi.	ก่วมเชียงดาว	05-149
Annonaceae	*Mitrephora wangii* Hu	ลำดวนดอย	05-152
Apiaceae	*Hydrocotyle javanica* Pont. ex Thumb.		04-652
Begoniaceae	*Begonia* sp.		05-610
Clusiaceae	*Garcinia propingua* Craib		06-312
Ebenaceae	*Diospyros martabanica* Cl.	ไข่เต่า	05-122
Euphobiaceae	*Trigonostemon thyrsoideus* Stapf	โลดทะนงเหลือง	06-258
Fabaceae	*Lespedeza parviflora* Kurz	เลือดใน	06-95
	Lespedeza sulcata (Schindl.) Craib	วนารมย์	649
Lamiaceae	*Colebrookia oppositifolia* Sm.		05-97
Rhamnaceae	*Sageretia cordifolia* Tard.		05-673
Rosaceae	*Eriobotrya salwinesis* Hand.-Mazz.		05-680
Sterculiaceae	*Heritiera macrophylla* Wall. ex Boj	หงอนไก่ฟ้า	06-275
	Pterospermum grande Craib	สามเต้า	06-378
	Pterospermum semisagittatum B.-H. ex Roxb.	ขามคัวะ	06-343
Ulmaceae	*Ulmus lancaefolia* Roxb. ex Wall.	ดู่ช้างย้อย	06-673
Verbenaceae	*Premna racemosa* Wall. ex Schauer		05-305

3. General Techniques

3.1 Solvents

All organic solvents were commercial grade and were redistilled prior to use.

3.2 Analytical Thin-Layer Chromatography (TLC)

Technique:	one dimension, ascending
Adsorbent:	Silica gel 60 F_{254} (No. 105554, Merck) precoated on aluminium sheet
Layer thickness:	0.2 mm
Distance:	6.0 cm
Temperature:	Laboratory temperature (25-30 ^{o}C)
Detection:	1) Ultraviolet light (254 and 356 nm)
	2) Spraying with 1% vanillin-sulfuric acid solution and heating at 110 ^{o}C for 5 min
	3) Spraying with 10% sulfuric acid solution and heating at 110 ^{o}C for 5 min
	4) Spraying with Dragendroff's reagent

3.3 Column Chromatography

3.3.1 Open Column Chromatography

Column:	glass column (7.0, 4.5, 3.75, and 2.0 cm diameters, ratio 1:30)
Adsorbent:	Silica gel 60 particle size 0.063-0.200 (No. 7734, Merck)
Solvent:	various solvent systems depending on materials
Packing method:	adsorbent was wet-packed
Sample loading:	the sample extract was dissolved in a small amount of the organic solvent, mixed with a

small quantity of the adsorbent, dried and packed on the top of the column

Detection: fractions were examined by TLC technique in the same manner as described in section 3.2

3.3.2 Flash Column Chromatography

Column: glass column (1.5 and 1.0 cm diameter, ratio 1:30)

Adsorbent: Silica gel 60 particle size 0.040-0.063 (No. 9385, Merck)

Solvent: various solvent systems depending on materials

Packing method: adsorbent was wet-packed

Sample loading: the sample extract was dissolved in a small amount of the organic solvent, mixed with a small quantity of the adsorbent, dried and packed on the top of the column

Detection: fractions were examined by TLC technique in the same manner as described in section 3.2

3.3.3 Gel Filtration Chromatography

Column: glass column (2.5 cm diameter)

Gel Filter: Sephadex LH20

Solvent: methanol, dichloromethane:methanol

Packing method: gel filter was suspended in the eluent and left standing to swell for 24 hrs prior to use, then poured into the column and allowed to set tightly.

Sample loading: the sample was dissolved in a small amount of the eluent and then applied gently on the top of the column

Detection: fractions were examined by TLC technique in the same manner as described in section 3.2

3.3.4 RP18 Column Chromatography

Column:	glass column (1.0 cm diameter)
Adsorbent:	Silica gel RP-18, Cosmosil 140C_{18}-OPN (No. MOE5823, Nacalai)
Solvent:	various solvent systems depending on materials
Packing method:	adsorbent was wet-packed
Sample loading:	the sample extract was dissolved in a small amount of the organic solvent, mixed with a small quantity of the adsorbent, dried and packed on the top of the column
Detection:	fractions were examined by TLC technique in the same manner as described in section 3.2

3.4 Instruments for Determination of Physicochemical Properties

3.4.1 Ultraviolet (UV) Absorption Spectra

UV absorption was measured on a Hitachi UV-Vis U-2000 spectrophotometer (Faculty of Pharmacy, Silpakorn University).

3.4.2 Infrared (IR) Absorption Spectra

IR spectra (KBr disc) were obtained on a Nicolet 4700 FT-IR Spectrometer and a Magna-IR™ 750 Spectrometer, Nicolet® (Faculty of Pharmacy, Silpakorn University), a Perkin Elmer FT-IR1760X spectrometer (Scientific and Technological Research Equipment Center, Chulalongkorn University), or a Perkin Elmer FT-IR GX spectrometer (Department of Chemistry, Faculty of Science, Mahidol University).

3.4.3 Mass Spectra (MS)

Mass spectra were recorded on a microTOF 72, a positive mode, Bruker® (The Scientific and Technological Research Equipment Center, Mahidol University).

3.4.4 Nuclear Magnetic Resonance (NMR) Spectra

^{1}H (300 MHz) and ^{13}C NMR (75 MHz) spectra were recorded on an Ultrashild™ 300 Bruker® (The Scientific and Technological Research Equipment Center, Silpakorn University). Chemical shifts were recorded as parts per million (ppm) on the δ scale, using tetramethylsilane (TMS) as an internal standard.

3.4.5 Optical Rotation

The angle of rotation was measured on a Jasco P-1010 Polarimeter (Department of Chemistry, Faculty of Sciences, Silpakorn University).

3.4.6 Melting Point

The melting points were obtained on a Stuart® SMP10 Digital Melting Point Apparatus (Department of Pharmaceutical Science, Faculty of Pharmacy, Payap University).

4. Biological Assays

4.1 Brine Shrimp Lethality

The brine shrimp (*Artemia salina*) lethality assay was modified according to Meyer et al. (1982) and Sam (1993). Brine shrimp eggs (S.K. Trading, Thailand) were hatched in a rectangular tank which was filled with artificial sea water (38 g/L) (Jor Charoen Aquarium, Thailand). The tank was divided into 2 parts as hatching part and growing part where hatching part was covered with an aluminum foil. A lamp was arranged above the hatching side. After 48 hrs, shrimp larvae passed a small gap to the growing side.

Ten shrimp larvae were put in a vial containing 5 ml of extract solution and incubated for 24 hrs. After that, the number of shrimp larvae in each vial was counted. The concentration of the sample extract at 50% lethal dose (LC_{50}) was calculated using the probit analysis method described by Finney (1971) and SPSS.

Sample extracts were prepared by dissolving in artificial sea water of which dimethyl sulfoxide (DMSO) at less than 1% was a co-solvent. The concentrations of sample extracts were 2,000, 200, and 20 μg/ml. Each sample extract concentration (2.5 ml) was added to a vial and filled with 2.5 ml of artificial sea water containg ten shrimps, to make the final concentrations to 1,000, 100, and 10 μg/ml, respectively. The negative control was ten shrimps in artificial sea water or artificial sea water with less than 1% of DMSO. Each concentration was assayed in triplicate. Four criteria for the toxicity were: highly toxic (LC_{50} of less than 20.0 μg/ml), moderately toxic (LC_{50} of 20.1-100.0 μg/ml), weakly toxic (LC_{50} of 100.1-1,000 μg/ml), and inactive (LC_{50} of more than 1,000 μg/ml) (Meyer et al., 1982; Mclaughlin, 1991; Sam, 1993).

4.2 Hyphae Formation Inhibition (HFI) Assay

The protein kinase inhibitor and cytotoxicity of plant extracts or pure compounds were determined by HFI assay (Waters et al., 2002; Yao et al., 2011). The mycelium fragments of *Streptomyces* 85E were maintained on minimal medium ISP4 agar plates. Filter paper discs (ϕ 7 mm) were sterilized and dropped with the sample solution prepared in suitable solvents such as ethyl acetate or methanol. The dried discs were applied onto plates and incubated at 30 ^{o}C for 30 hrs. The sample extracts were prepared at the concentration of 80 μg/disc, whereas purified compounds were tested at the concentration of 20 μg/disc. The results were observed as clear zone or bald zone. Inhibition of the formation of *Streptomyces* 85E hyphae involves the activity of protein kinase. Clear zone indicates that the extract inhibits both growth and sporulation of *Streptomyces* 85E cells which implied the cytotoxicity. The bald zone indicates that the extract inhibits aerial hyphae formation, but no inhibition of cellular growth. Thus, the bald zone of the extract exhibits protein kinase inhibition. This test is used as an alternative to cytotoxicity and protein kinase inhibition

screening. Surfactin, the sporulation inhibitor, was a positive control and a solvent was a negative control. This test was done in duplicate. An inhibition zone of greater than 9 mm was considered active (Yao et al., 2011).

4.3 DPPH Assay

The antioxidative activity of sample extract was determined according to DPPH radical scavenging assay. This procedure was modified from the method of Hou et al. (2003) and Molyneux (2004). DPPH (Sigma, USA) solution was prepared at 75 µg/ml in methanol. Both sample extracts and a positive control (*L*-ascorbic acid, Fisher Scientifics, UK) were tested at the final concentration of 100, 50, 10, 5, and 1 µg/ml, respectively. Each concentration was assayed in triplicate. Equal amount of sample extracts and DPPH radical were mixed and incubated at room temperature for 60 min. After incubation, the decrease in absorbance of the combined solution was monitored at 517 nm by UV-Vis U-2000 spectrophotometer (Hitachi, Japan). The positive control, *L*-ascorbic acid, was prepared in the same way. The plant extract without DPPH solution was used as a negative control. The absorbance was calculated as % scavenging activity in order to analyze the inhibition concentration of samples that produced 50% reduction of the DPPH (IC_{50}) (Hou et al., 2003; Molyneux, 2004).

The percentage of scavenging activity of each plant extract was calculated according to the following formula:

$$\%\ \text{scavenging activity} = \frac{[\text{Abs(DPPH)} - (\text{Abs(sample} + \text{DPPH)} - \text{Abs(sample)})]\ x\ 100}{\text{Abs (DPPH)}}$$

Abs = Absorbance

Four criteria of antioxidative activity were: highly active (IC_{50} of less than 10.0 µg/ml), moderately active (IC_{50} of 10.1-50.0 µg/ml), weakly active (IC_{50} of 50.1-100.0 µg/ml), and inactive (IC_{50} of more than 100.0 µg/ml).

4.4 Combination Index with *L*-Ascorbic Acid of Methanol Plant Extracts

Currently, drug combination has been used to complete therapeutic efficacy (Asbagh et al., 2008) and some antioxidants have been proven for this effectiveness. The combination index (CI) using DPPH assay was established and modified according to Chou (2006). The mixtures of methanol plant extracts and *L*-ascorbic acid were prepared at various concentrations as described in 4.3. The ratio of the methanol extract and *L*-ascorbic acid at each concentration was 1:1. The percentage of scavenging activity and the IC_{50} of each mixture solution were calculated. The CI was obtained according to the following formula:

$$CI = 0.5 \text{ x } \frac{IC_{50\text{ (mixture)}}}{IC_{50\text{ (}L\text{−ascorbic acid)}}} + 0.5 \text{ x } \frac{IC_{50\text{ (mixture)}}}{IC_{50\text{ (plant extract)}}}$$

All experiments were performed in triplicate. Results were described as synergistic, additive, or antagonistic effect of the extracts with *L*-ascorbic acid. If the CI was less than, equal, or more than 1, the extract would be considered synergistic, additive, or antagonistic with *L*-ascorbic acid, respectively (Chou, 2006).

4.5 MTT Assay

The MTT assay bases on the ability of a mitochondrial dehydrogenase enzyme from viable cells to cleave the tetrazolium rings of the pale yellow MTT and form dark blue formazan crystals. The numbers of surviving cells are proportional to formazan product. The MTT assay is an advance *in vitro* cytotoxicity test. This method is rapid, sensitive, quantitative, and highly reproducible (Carmichael et al., 1987). The criteria for pure compounds for cytotoxicity was less than 4 μg/ml (Cordell et al., 1993).

The cytotoxic assay using MTT method was adapted from Mosmann (1983). The cell lines used in this study were human epithelial carcinoma (HeLa), human leukemic monocyte lymphoma (U937), and human hepatocellular liver carcinoma (HepG2). The cells were suspended in the growth medium with a final

concentration of 5 x 10^5 cells/well. A positive control, 5-fluorouracil (5-FU), was included in each experiment at appropriate concentrations. Three concentration levels of pure compounds in a cultured medium were prepared, of which DMSO concentration was less than 0.5% in each well. After a period of cell incubation, various dilutions of pure compounds were added to the prepared plate. The plate was further incubated for 24 hours. The cytotoxic activity of pure compounds was measured using MTT method. Absorbance was read at 540 nm and 630 nm (reference wavelength). Each concentration was assayed in triplicate. The 50% inhibition concentration (IC_{50}) of the active substances were determined as the concentration which reduced cell growth by 50% in treated compared to untreated culture (Mosmann, 1983). The compound which exhibited IC_{50} value of less than 4 μg/ml was considered to be active (Colegate and Molyneux, 1993).

5. Extraction, Fractionation, and Isolation

5.1 Extraction of *Pterospermum grande* Craib Leaves

The dried leaves of *P. grande* (1.5 kg.) were ground, and macerated with methanol (3x2.5 L). Crude extract solution was filtered and evaporated under reduced pressure to afford methanol extract (71.5 g, 4.76 % of dried weight). The methanol extract was partitioned with several solvents from lower to higer polarity to obtain hexane extract (6.85 g, 0.45 % of dried weight), dichloromethane extract (6.08 g, 0.40 % dried of weight), and ethyl acetate extract (8.85 g, 0.59 % dried of weight). Finally, the aqueous phase was evaporated to the residue water extract (14.88 g, 0.99 % of dried weight).

5.1.1 Separation of Hexane Extract

The hexane extract (6.85 g) was redissolved in a small amount of hexane, triturated with silica gel 60 (No. 7734, 4.0 g) and dried at room temperature. A silica gel column (ϕ 4.5 cm) was prepared and eluted with gradient hexane and ethyl acetate (100:0 to 1:99). The eluate was collected at 60 ml per fraction for 78 fractions. Fractions with similar chromatographic pattern on TLC (hexane:dichloromethane (50:50) as a mobile phase) were combined to yield 7 fractions, including H-1 (0.34 g),

H-2 (0.67 g), H-3 (0.73 g), H-4 (0.89 g), H-5 (1.36 g), H-6 (1.21 g), and H-7 (1.09 g) (Scheme 1).

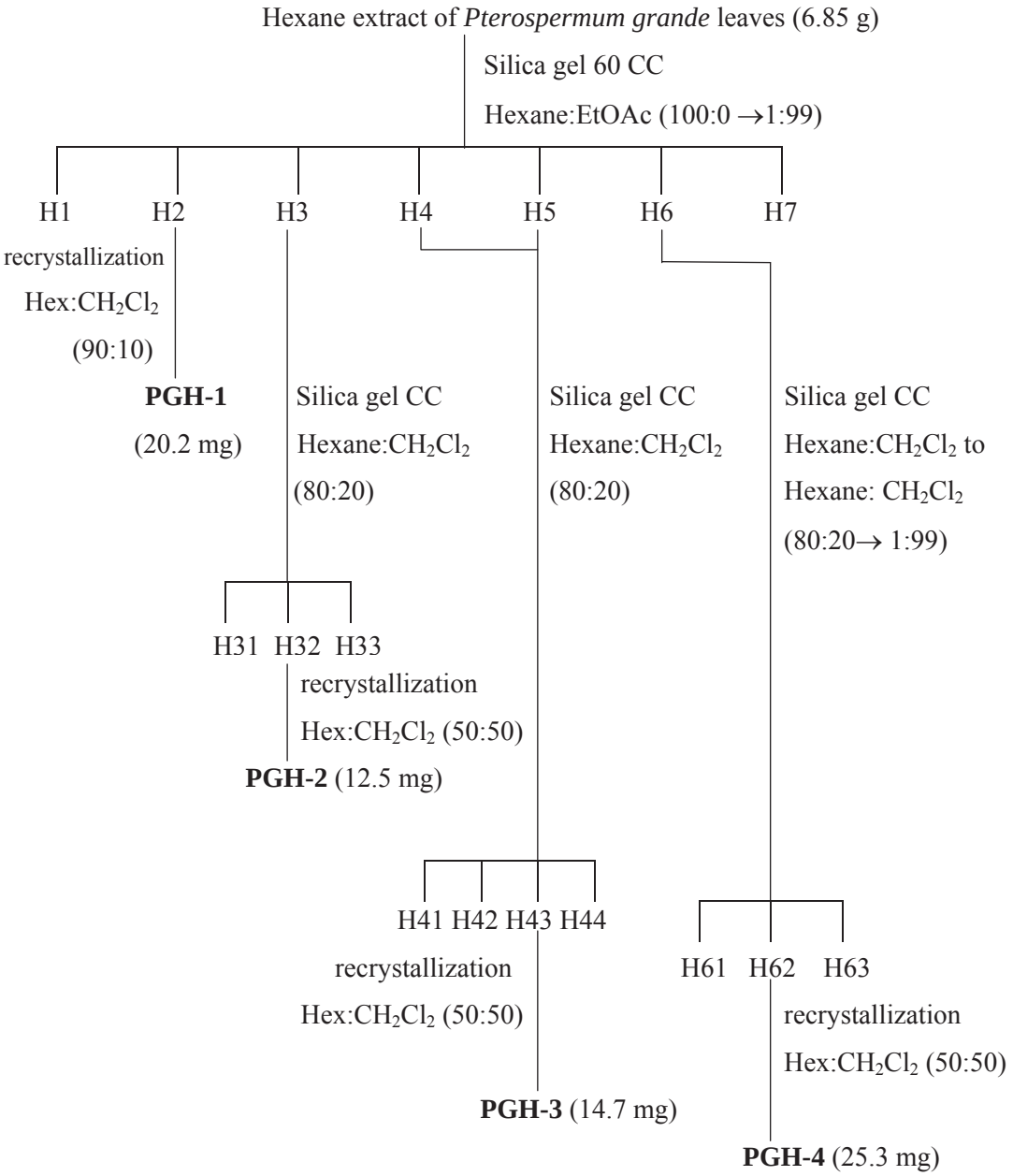

Scheme 1 Isolation of compounds from the hexane extract of *Pterospermum grande* leaves.

5.1.1.1 Isolation of PGH-1

Fraction H-2 (0.67 g) was purified by recrystallization in hexane:dichloromethane mixture (90:10) to afford a white powder of compound PGH-1 (20.2 mg, 0.29% yield). The compound gave a purple spot on TLC with 10% sulfuric acid spraying with the Rf value of 0.63 in hexane:dichloromethane (80:20). It was identified as taraxerol acetate (Scheme 1**)**.

5.1.1.2 Isolation of PGH-2

Fraction H-3 (0.73 g) was fractionated on a silica gel column (ϕ 1.5 cm) which was eluted with hexane:dichloromethane (80:20). The eluates were examined by TLC (4 x 6 cm) using hexane:dichloromethane (50:50) as a mobile phase. Fractions with similar chromatographic pattern were combined to yield 3 fractions (H31-H33). The compound PGH-2 (12.5 mg, 0.18% yield) was purified by recrytallization in hexane:dichloromethane (50:50) and obtained as a white powder from fraction H32(0.25 g). The compound gave a purple spot on TLC with 10% sulfuric acid spraying with the Rf value of 0.57 in hexane:dichloromethane (50:50). It was identified as simiarenol (Scheme 1**)**.

5.1.1.3 Isolation of PGH-3

Both fractions H-4 (1.06 g) and H-5 (1.36 g) were separated on a silica gel column (ϕ 2.0 cm) (hexane:dichloromethane (80:20)). The eluates were examined by TLC (4 x 6 cm) using hexane:dichloromethane (50:50) as a mobile phase. Fractions with similar chromatographic pattern were combined to yield 4 fractions (H41-H44). The compound PGH-3 (14.7 mg, 0.21% yield) was purified by recrytallization in hexane:dichloromethane (50:50) and obtained as a white powder in hexane:dichloromethane (60:40) mixture from fraction H43 (0.17 g). The compound gave a purple spot on TLC with 10% sulfuric acid spraying with the Rf value of 0.40 in hexane:dichloromethane (50:50). It was identified as taraxerol (Scheme 1**)**.

5.1.1.4 Isolation of PGH-4

Fraction H-6 (1.21 g) was chromatographed on a silica gel column (ϕ 2.0 cm) and eluted with gradient mixture solvents (hexane:dichloromethane (80:20) to hexane:dichloromethane (1:99)). The eluates were examined by TLC (4 x 6 cm) using hexane:dichloromethane (50:50) as a mobile phase. Fractions with similar chromatographic pattern were combined to yield 3 fractions (H61-H63). The compound PGH-4 (25.3 mg, 0.36% yield) was purified by recrytallization in hexane:dichloromethane (50:50) and obtained as a white powder from fraction H62 (0.31 g). The compound gave a purple spot on TLC with 10% sulfuric acid spraying with the Rf value of 0.37 in hexane:dichloromethane (40:60). It was identified as *β*-sitosterol (Scheme 1).

5.1.2 Separation of Ethyl Acetate Extract

The ethyl acetate extract (8.50 g) was dissolved in a small quantity of ethyl acetate, triturated with silica gel 60 (No. 7734, 6.0 g) and dried under room temperature, and futher fractionated on an open silica gel column (ϕ 4.5 cm). Elution was performed in a polarity gradient manner with dichloromethane:ethyl acetate to ethyl acetate:methanol (10:90→20:80), and washed out with 100% methanol. Fractions with same chromatographic pattern were combined to yield 9 fractions: E1 (0.10 g), E2 (0.07 g), E3 (0.45 g), E4 (0.66 g), E5 (0.93 g), E6 (0.65 g), E7 (3.31 g), E8 (0.68 g), and E9 (1.54 g) (Scheme 2).

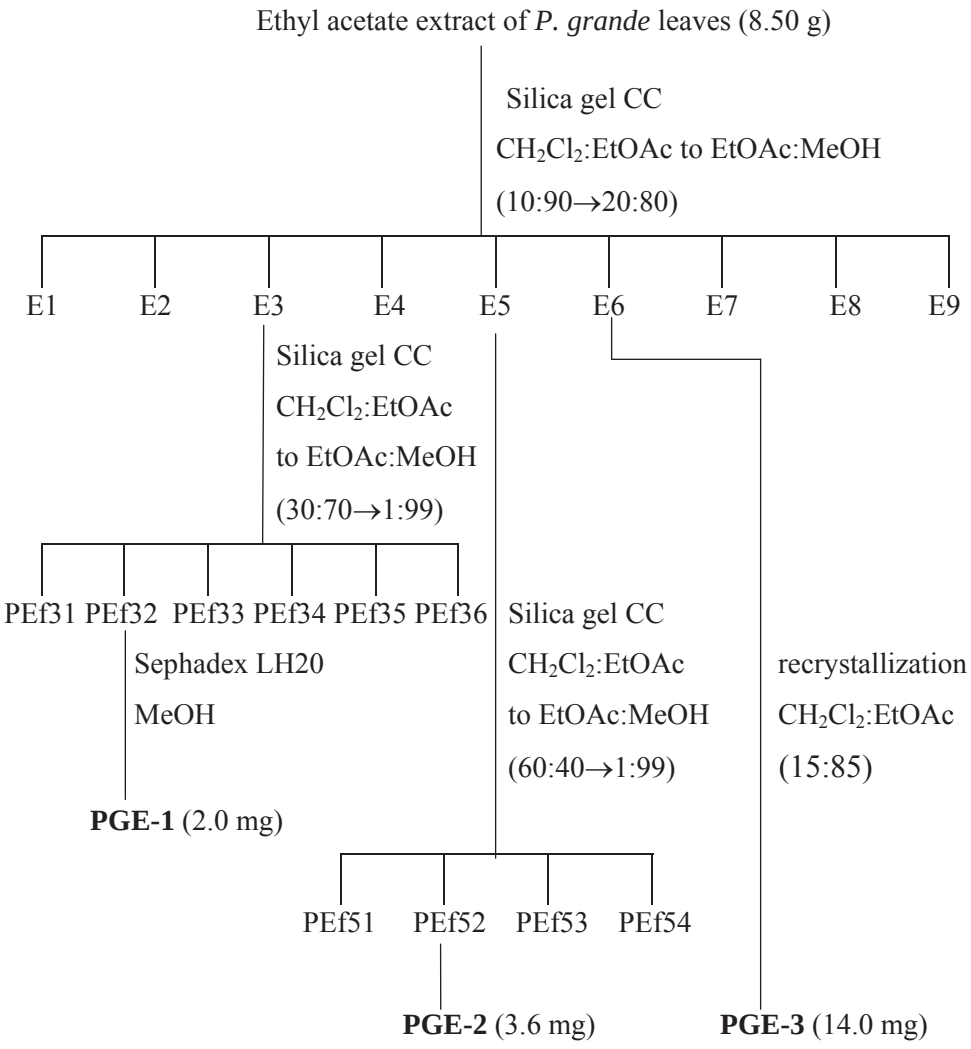

Scheme 2 Isolation of compounds from the ethyl acetate extract of *P. grande* leaves.

5.1.2.1 Isolation of PGE-1

Fraction E3 (0.45 g) was purified on a silica gel column (ϕ 1.0 cm) with a gradient of dichloromethane:ethyl acetate to ethyl acetate:methanol (30:70→1:99). The eluates were examined on TLC using ethyl acetate:methanol (70:30) as a mobile phase. Fractions with similar chromatographic pattern were combined to yield 6 fractions (PEf31-PEf36). Fraction PEf32 (0.18 g) was purified on a Sephadex LH20 (ϕ 2.5 cm) and eluted with methanol to give compound PGE-1 (2.0 mg, 0.02% yield) which was crystallized in ethyl acetate:methanol (70:30). This compound gave an orange-yellow spot with 10% sulfuric acid spraying with an Rf value of 0.62 in ethyl acetate:acetone (80:20). It was identified as tiliroside (Scheme 2).

5.1.2.2 Isolation of PGE-2

Fraction E5 (0.93 g) was chromatographed on a silica gel column chromatography (ϕ 1.5 cm) with a gradient elution from dichloromethane:ethyl acetate to ethyl acetate:methanol (60:40→1:99). The eluates were examined on TLC using ethyl acetate:methanol (90:10) as a mobile phase. Fractions with similar chromatographic pattern were combined to yield 4 fractions (PEf51-PEf54). A pure compound PGE-2 (3.6 mg, 0.04% yield) was purified by recrystallization in dichloromethane:ethyl acetate (40:60) and methanol and obtained from Fraction PEf52 (0.24 g). This compound gave an orange spot with 10% sulfuric acid spraying with Rf values of 0.55 in dichloromethane:ethyl acetate (40:60) and 0.72 in ethyl acetate:acetone (80:20). It was identified as trifolin (Scheme 2).

5.1.2.3 Isolation of PGE-3

PGE-3 was crystallized in dichloromethane:ethyl acetate (15:85) from fraction E6 (0.65 g) as a light yellow powder (14.0 mg, 0.16% yield) which gave a yellow spot on TLC with 10% sulfuric acid spraying. An Rf value of PGE-2 was 0.48 in ethyl acetate:methanol (9:1). This compound was identified as (-)-epicatechin (Scheme 2).

5.2 Extraction of *Mitrephora wangii* Hu Leaves

The dried leaves of *Mitrephora wangii* (505.0 g) were ground and macerated with methanol (3 x 2L). Crude extract solution was filtered and evaporated under reduced pressure to give methanol extract (40.94 g, 8.1% dried weight). The methanol extract was partitioned with several solvents from lower to higher polarity to obtain hexane extract (8.28 g, 1.6% dried weight), dichloromethane extract (11.11 g, 2.2% dried weight), and ethyl acetate extract (5.31 g, 1.0% dried weight). Finally, the residue aqueous phase was evaporated to water extract (3.92 g, 0.7% dried weight).

5.2.1 Separation of Hexane Extract

The hexane extract (8.28 g) was dissolved in a small amount of hexane, triturated with silica gel 60 (No. 7734, 6.0 g) and dried under room temperature. It was fractionated on an open column chromatography (ϕ 4.5 cm). Elution was completed in a polarity gradient manner with a mixture of hexane: ethyl acetate and ethyl acetate:methanol (95:5$\rightarrow$30:70). The eluate was collected at 60 ml per fraction and examined by TLC (hexane:ethyl acetate (50:50). Fractions with similar chromatographic pattern were combined to yield 9 fractions, including HL1 (0.35 g), HL2 (0.78 g), HL3 (0.68 g), HL4 (0.56 g), HL5 (0.91 g), HL6 (0.83 g), HL7 (1.14 g), HL8 (1.02 g), and HL9 (0.62 g) (Scheme 3).

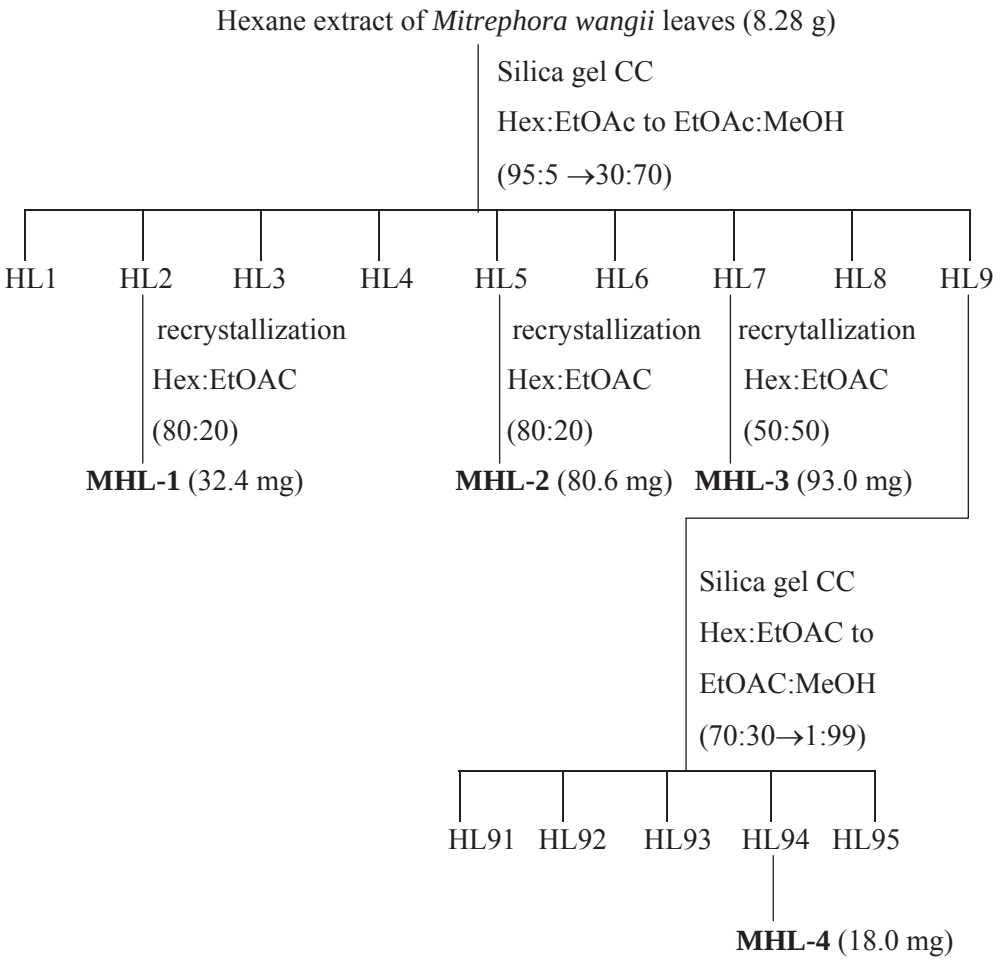

Scheme 3 Isolation of compounds from the hexane extract of *M. wangii* leaves.

5.2.1.1 Isolation of MHL-1

Fraction HL-2 (0.78 g) was purified by recrystallization in hexane:ethyl acetate mixture (80:20) to afford compound MHL-1 (32.4 mg, 0.39 % yield). This compound gave a magenta spot on TLC with 1% vanillin-sulfuric acid spraying reagent with an Rf value of 0.48 in hexane:dichloromethane (50:50). It was identified as methyl conocarpan (Scheme 3).

5.2.1.2 Isolation of MHL-2

Fraction HL-5 (0.91 g) was purified by recrystallization in hexane-ethyl acetate mixture (80:20) to obtain a compound MHL-2 (80.6 mg, 0.97% yield). This compound gave a magenta spot on TLC with 1% vanillin-sulfuric acid spraying with the Rf value of 0.46 in hexane:ethyl acetate (70:30) (Scheme 3). The MHL-2 was identified as 3'-methoxy conocarpan.

5.2.1.3 Isolation of MHL-3

Fraction HL-7 (1.14 g) was purified and recrystallization in hexane-ethyl acetate mixture (50:50) to obtain a compound MHL-3 (93.0 mg, 1.12% yield). This compound gave an orange spot on TLC with 1% vanillin-sulfuric acid spraying reagent with the Rf value of 0.42 in hexane:ethyl acetate (70:30) (Scheme 3). It was identified as conocarpan.

5.2.1.4 Isolation of MHL-4

Fraction HL-9 (0.62 g) was purified on a silica gel column (ϕ 1.5 cm) and eluted with a gradient mixture of hexane:ethyl acetate to ethyl acetate:methanol (70:30$\rightarrow$1:99). The eluates were examined on TLC (4 x 6 cm) using hexane:ethyl acetate (70:30) as a mobile phase. Fractions with similar chromatographic pattern were combined to yield 5 fractions (HL91-HL95). The compound MHL-4 (18.0 mg, 0.21% yield) was obtained from fraction HL94 (150.0 mg) and gave a gray spot on TLC with 1% vanillin-sulfuric acid spraying reagent with an Rf value of 0.33 in hexane:ethyl acetate (60:40). This compound was identified as linoleic acid (Scheme 3).

5.2.2 Separation of Dichloromethane Extract

The dichloromethane extract (8.5 g) was dissolved in a small amount of a mixture of dichloromethane and methanol, triturated with silica gel 60 (No. 7734, 6.0 g) and dried under room temperature. It was fractionated on an open column (ϕ 4.5). Elution was performed in a polarity gradient manner with hexane: ethyl acetate to ethyl acetate:methanol mixture (99:1$\rightarrow$1:99). The eluate was collected

at 60 ml per fraction and examined by TLC. Fractions with similar chromatographic pattern were combined to yield 9 fractions**,** including DL1 (0.57 g), DL2 (0.49 g), DL3 (1.40 g), DL4 (0.92 g), DL5 (0.48 g), DL6 (1.74 g), DL7 (0.85 g), DL8 (0.91 d), and DL9 (0.44 g).

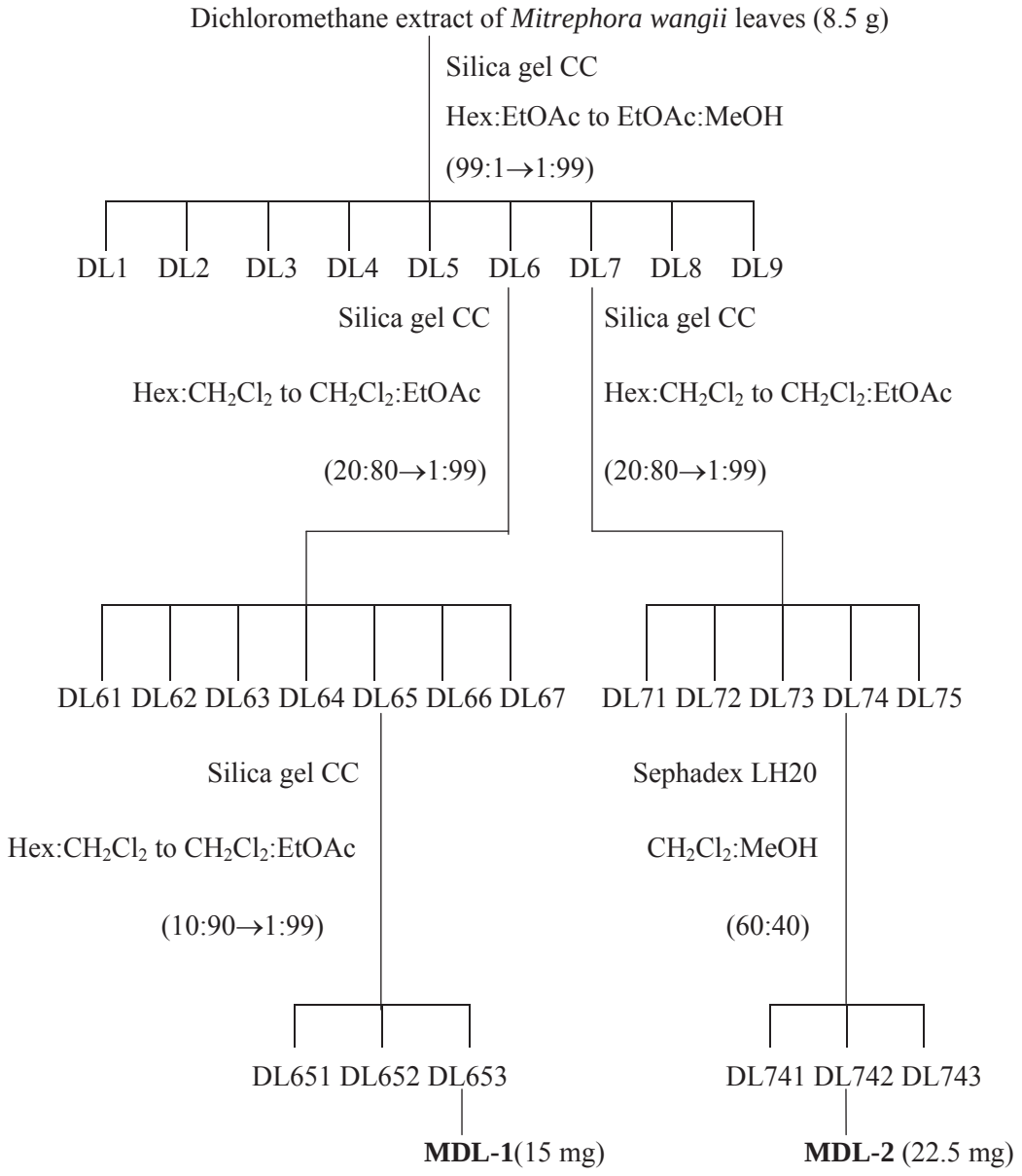

Scheme 4 Isolation of compounds from the dichloromethane extract of *M. wangii* leaves.

5.2.2.1 Isolation of MDL-1

Fraction DL6 (1.74 g) was purified on a silica gel column (ϕ 2.5 cm) and eluted with a gradient mixture of hexane:dichloromethane to dichloromethane:ethyl acetate (20:80→1:99). The eluates were examined on TLC (4 x 6 cm) using hexane:ethyl acetate (60:40) as a mobile phase. Fractions with similar chromatographic pattern were combined to yield 7 fractions (DL61-DL67). Fraction DL65 (0.52 g) was further purified on a silica gel column (ϕ 1.5 cm) and eluted with a gradient mixture of hexane:dichloromethane and dichloromethane:ethyl acetate (10:90→1:99). The eluates were examined by TLC (4 x 6 cm) using hexane:ethyl acetate (60:40) as a mobile phase. Fractions with similar chromatographic pattern were combined to yield 3 fractions (DL651-DL653). The compound MDL-1 (15.0 mg, 0.17% yield) was obtained from fraction DL653 (125 mg) and gave a magenta spot on TLC with 1% vanillin-sulfuric acid spraying with the Rf value of 0.46 in hexane:ethyl acetate (70:30) (Scheme 4). It was identified as 3'-methoxy conocarpan.

5.2.2.2 Isolation of MDL-2

Fraction DL7 (0.85 g) was purified on a silica gel column (ϕ 1.5 cm) and eluted with a gradient mixture of hexane:dichloromethane to dichloromethane:ethyl acetate (20:80→1:99). The eluates were examined on TLC using hexane:ethyl acetate (60:40) as a mobile phase. Fractions with similar chromatographic pattern were combined to yield 5 fractions (DL71-DL75). Fraction DL74 (0.35 g) was purified on a Sephadex LH20 (ϕ 2.5 cm) and eluted with dichloromethane:mehthanol (60:40). Fractions with similar chromatographic pattern were combined to yield 3 fractions (DL741-DL743). The compound MDL-2 (22.5 mg, 0.26% yield) was obtained from fraction DL742 (125.0 mg) and gave an orange spot on TLC with 1% vanillin-sulfuric acid spraying. The Rf value of this compound was 0.46 in hexane:ethyl acetate (70:30) (Scheme 4). It was identified as conocarpan.

5.2.3 Separation of Ethyl Acetate Extract

The ethyl acetate extract (5.0 g) was dissolved in a small amount of methanol, triturated with silica gel 60 (No. 7734, 3.0 g) and dried under room temperature. It was fractionated on a silica gel column (ϕ 3.75). The eluate was collected at 60 ml per fraction and examined by TLC using dichloromethane:methanol (70:30) as a mobile phase. Fractions with similar chromatographic pattern were combined to yield 11 fractions, including EL1 (1.4 mg), EL2 (13.9 mg), EL3 (129.4 mg), EL4 (0.15 g), EL5 (0.20 g), EL6 (0.25 g), EL7 (1.05 g), EL8 (0.70 g), EL9 (0.80 g), EL10 (0.32 g), and EL11 (1.33 g) (Scheme 5).

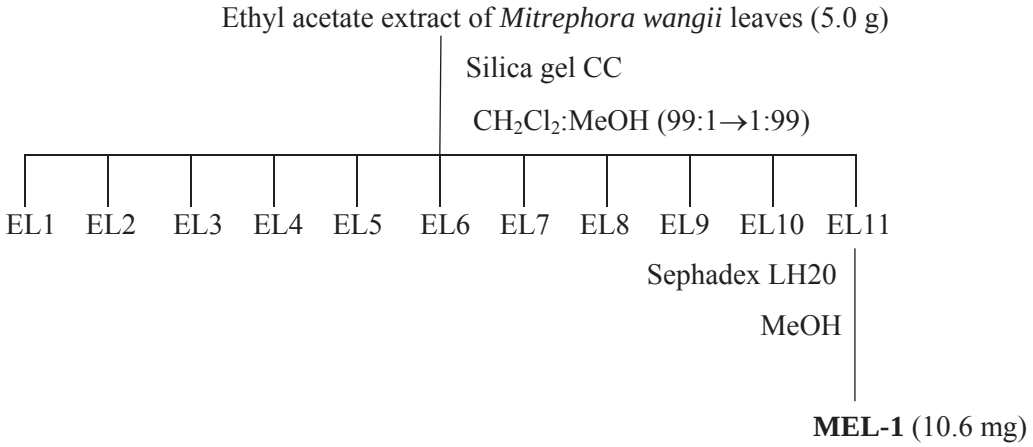

Scheme 5 Isolation of a compound from the ethyl acetate extract of *M. wangii* leaves.

5.2.3.1 Isolation of MEL-1

Fraction EL11 (1.33 g) was separated on a Sephadex LH20 (ϕ 2.5 cm) and eluted with methanol to obtain compound MEL-1 (10.6 mg, 0.212) with the Rf value of 0.35 in dichloromethane:methanol (95:5). It was identified as *β*-sitosterol- *O*-*β*-*D*-glucoside (Scheme 5).

5.3 Extraction of *Mitrephora wangii* Hu Twigs

The dried twigs of *Mitrephora wangii* (3.5 kg) were ground and macerated successively with methanol (3x10 L). Crude extract was filtered and evaporated under reduced pressure to afford methanol extract (203.30 g). The methanol extract was partitioned with several solvents from lower to higher polarity to obtain hexane extract (8.54 g, 0.24 % dried weight), ethyl acetate extract (77.65 g, 2.21 % dried weight), and *n*-butanol extract (6.90 g, 0.19 % dried weight). Finally, the residue aqueous phase was evaporated to water extract (9.03 g, 0.25 % dried weight).

5.3.1 Separation of Hexane Extract

The hexane extract (8.54 g) was dissolved in a small quantity of hexane, triturated with silica gel (6.0 g), and dried at room temperature. The hexane extract was purified on a silica gel column chromatography (ϕ 4.5) with gradient mixture solvents (hexane:ethyl acetate (1:99) to ethyl acetate:methanol (50:50)). The eluates were examined by TLC using hexane:ethyl acetate (70:30) as a mobile phase. Fractions with similar chromatographic pattern were combined to yield 7 fractions, including HT1 (0.46 g), HT2 (0.36 g), HT3 (0.90 g), HT4 (1.92 g), HT5 (0.99 g), HT6 (0.55 g), and HT7 (0.18 g) (Scheme 6).

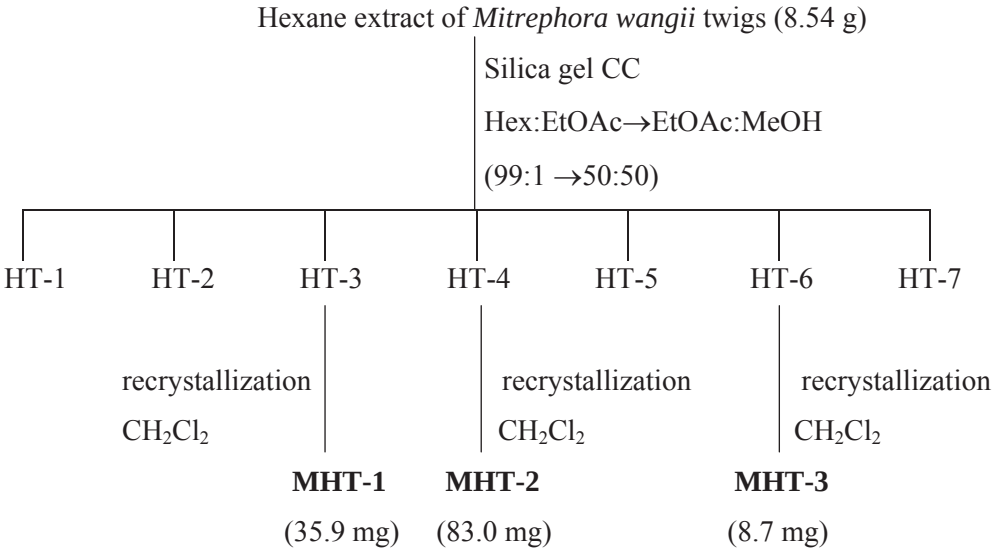

Scheme 6 Isolation of compounds from the hexane extract of *M. wangii* twigs.

5.3.1.1 Isolation of MHT-1

The compound MHT-1 (35.9 mg, 0.42% yield) was purified by recrystallization in dichloromethane and gave a magenta spot with 1% vanillin-sulfuric acid spraying with the Rf value of 0.33 in both hexane:dichloromethane (50:50) and hexane:ethyl acetate (70:30). It was identified as MHL-2 or 3'-methoxy conocarpan (Scheme 6).

5.3.1.2 Isolation of MHT-2

The compound MHT-2 (83.0 mg, 0.97% yield) was purified by recrystallization in dichloromethane and gave a magenta spot with 1% vanillin-sulfuric acid spraying with Rf value of 0.17 in hexane:dichloromethane (50:50). It was identified as MHL-3 or conocarpan (Scheme 6).

5.3.1.3 Isolation of MHT-3

The compound MHT-3 (8.7 mg, 0.10% yield) was purified by recrystallization in dichloromethane. It was identified as *β*-sitosterol (Scheme 6).

5.3.2 Separation of Ethyl acetate Extract

The ethyl acetate extract (50.0 g) was dissolved in a small amount of ethyl acetate, triturated with silica gel (25.0 g), and dried under room temperature. The extract was fractionated on a silica gel column (ϕ 7.0 cm) and eluted with a gradient of dichloromethane:methanol (99:1$\rightarrow$1:99). The eluate was collected at 60 ml per fraction and examined by TLC using dichloromethane:methanol (80:20) as a mobile phase. Fractions (111 fractions) with similar chromatographic pattern were combined to yield 8 fractions: ET-1 (0.02 g), ET-2 (0.61 g), ET-3 (2.32 g), ET-4 (2.14 g), ET-5 (10.56 g), ET-6 (11.97 g), ET-7 (9.18 g), and ET-8 (8.65 g) (Schemes 7a and 7b).

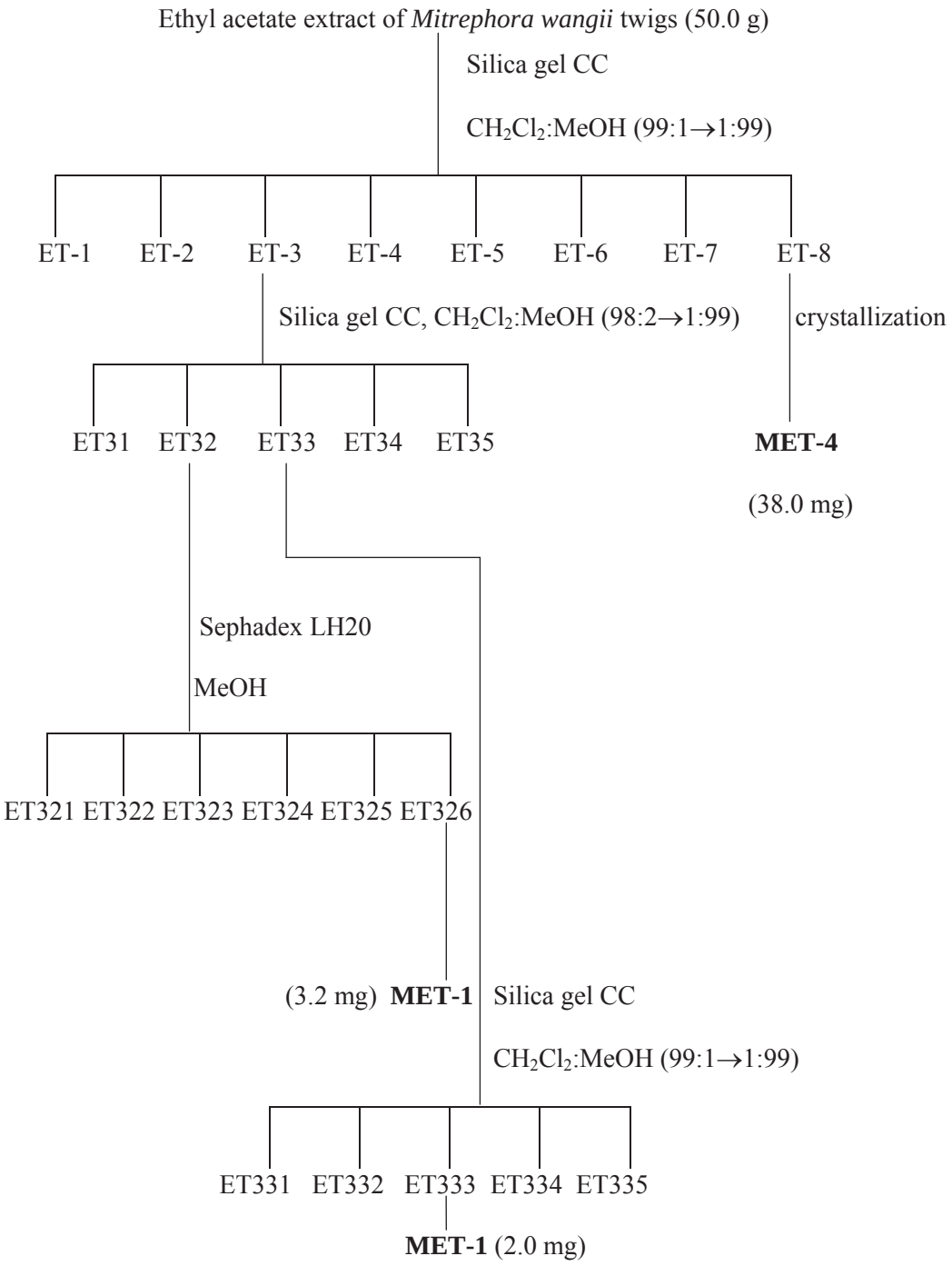

Scheme 7a Isolation of compounds from the ethyl acetate extract of *M. wangii* twigs.

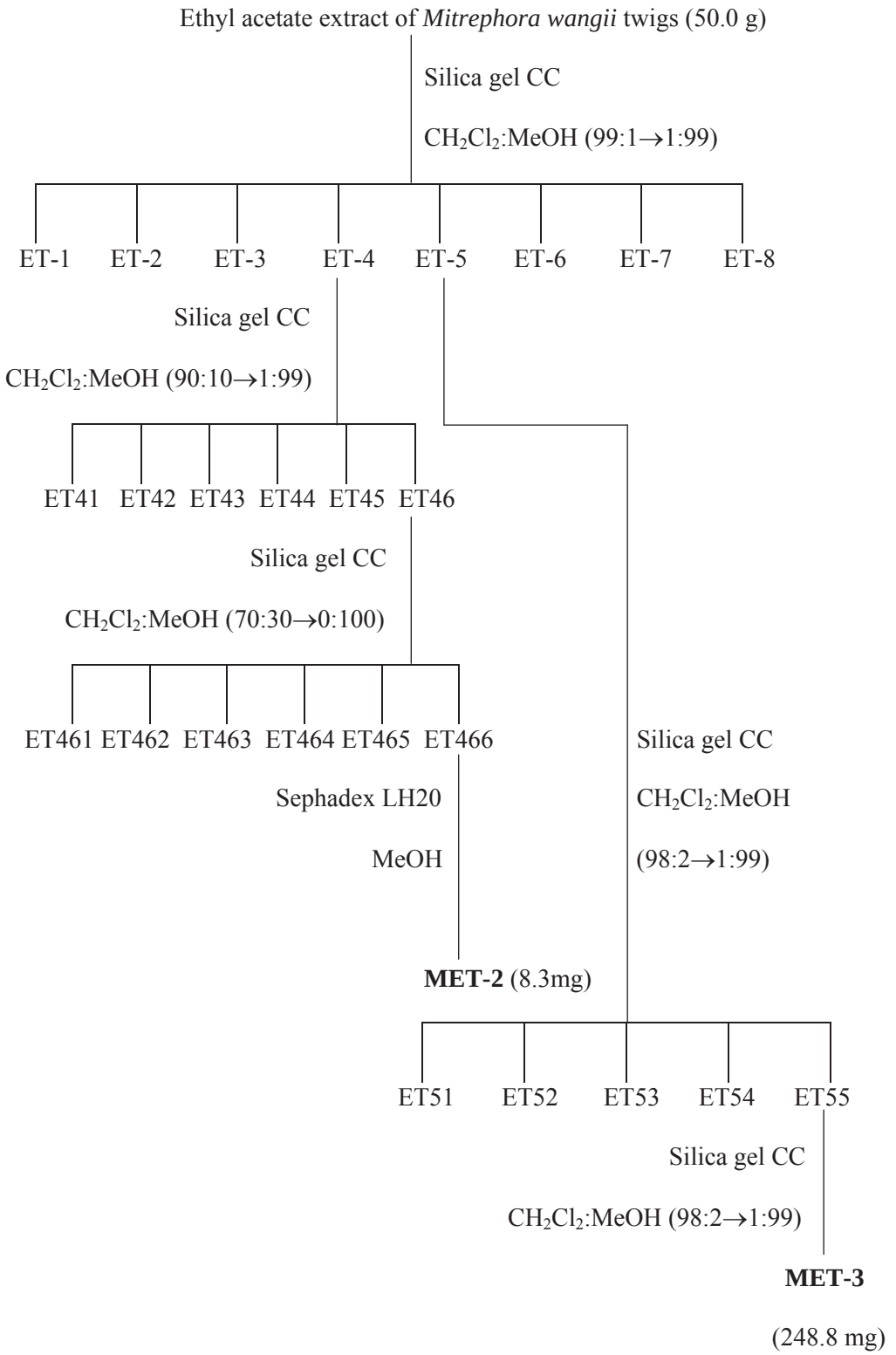

Scheme 7b Isolation of compounds from the ethyl acetate extract of *M. wangii* twigs (Continued).

5.3.2.1 Isolation of MET-1

Fraction ET-3 (2.32 g) was further separated on a silica gel column (ϕ 2.0 cm) using a gradient elution of dichloromethae:methanol (98:2→1:99). Fractions with similar chromatographic pattern were combined to yield 5 fractions (ET31-ET35) on TLC with dichloromethane:methanol (80:20) as a mobile phase. ET32 (0.43 g) was fractionated on a Sephadex LH20 (ϕ 2.5 cm) and eluted with methanol to obtain 6 fractions (ET321-ET326). Fraction ET326 (0.39 g) gave a white powder (MET-1) (3.2 mg, 0.006% yield).

Fraction ET33 (0.43 g) was purified on a silica gel 60 column using a gradient elution of dichloromethane:methanol (99:1→1:99). Fractions with similar chromatographic pattern were combined to yield 5 fractions (ET331-ET335) on TLC with dichloromethane:methanol (80:20). Fraction ET333 (0.15 g) gave a white powder of compound MET-1 (2.0 mg, 0.004% yield). The Rf value of MET-1 in hexane:ethyl acetate (30:70) was 0.32. It was identified as *N*-*p*-coumaroyltyramine (Scheme 7a).

5.3.2.2 Isolation of MET-2

Fraction ET-4 (2.14 g) was purified on a silica gel column (ϕ 2.0 cm) using a gradient elution of dichloromethane in methanol (90:10→1:99). The eluates were collected at 60 ml per fraction for 42 fractions. Fractions with similar chromatographic pattern were examined by TLC and combined to yield 6 fractions as ET41-ET46. Fraction ET46 (0.45 g) was purified on a silica gel using a gradient of dichloromethane:methanol (70:30→0:100) to yield another 6 fractions (ET461-ET466). Fraction ET466 (103 mg) was further purified on a Sephadex LH20 (methanol) column to give compound MET-2 (8.3 mg, 0.016% yield) as a light yellow powder with the Rf value of 0.22 in dichloromethane:methanol (90:10). It was identified as *N*-caffeoyltyramine (Scheme 7b).

5.3.2.3 Isolation of MET-3

Fraction ET-5 (10.56 g) was fractionated on a silica gel column chromatography (ϕ 4.5 cm) using a gradient elution of dichloromethane:methanol (98:2→1:99). The eluate was collected at 60 ml per fraction. Fractions with similar chromatographic pattern were examined by TLC and combined to yield 5 fractions as ET51-ET55. Fraction ET55 (5.62 g) was rechromatographed on silica gel column (ϕ 3.75 cm) to yield MET-3 as a white crystalline solid (248.8 mg, 0.49% yield). It was identified as quebrachitol (Scheme 7b).

5.3.2.4 Isolation of MET-4

MET-4 was obtained from fraction ET-8 as a white solid (38.0 mg, 0.07% yield) and was identified as allantoin (Scheme 7b).

5.3.3 Separation of *n*-Butanol Extract

The *n*-butanol extract (4.0 g) was fractionated on a Sephadex LH20 column using methanol as an eluent. The eluate was collected at 60 ml per fraction and examined by TLC using ethyl acetate:methanol (20:80) as a mobile phase. Fractions with similar chromatographic pattern were combined to yield 8 fractions, including BT1 (0.14 g), BT2 (0.35 g), BT3 (0.39 g), BT4 (0.36 g), BT5 (0.26 g), BT6 (0.67 g), BT7 (0.70 g), and BT8 (0.76 g) (Scheme 8).

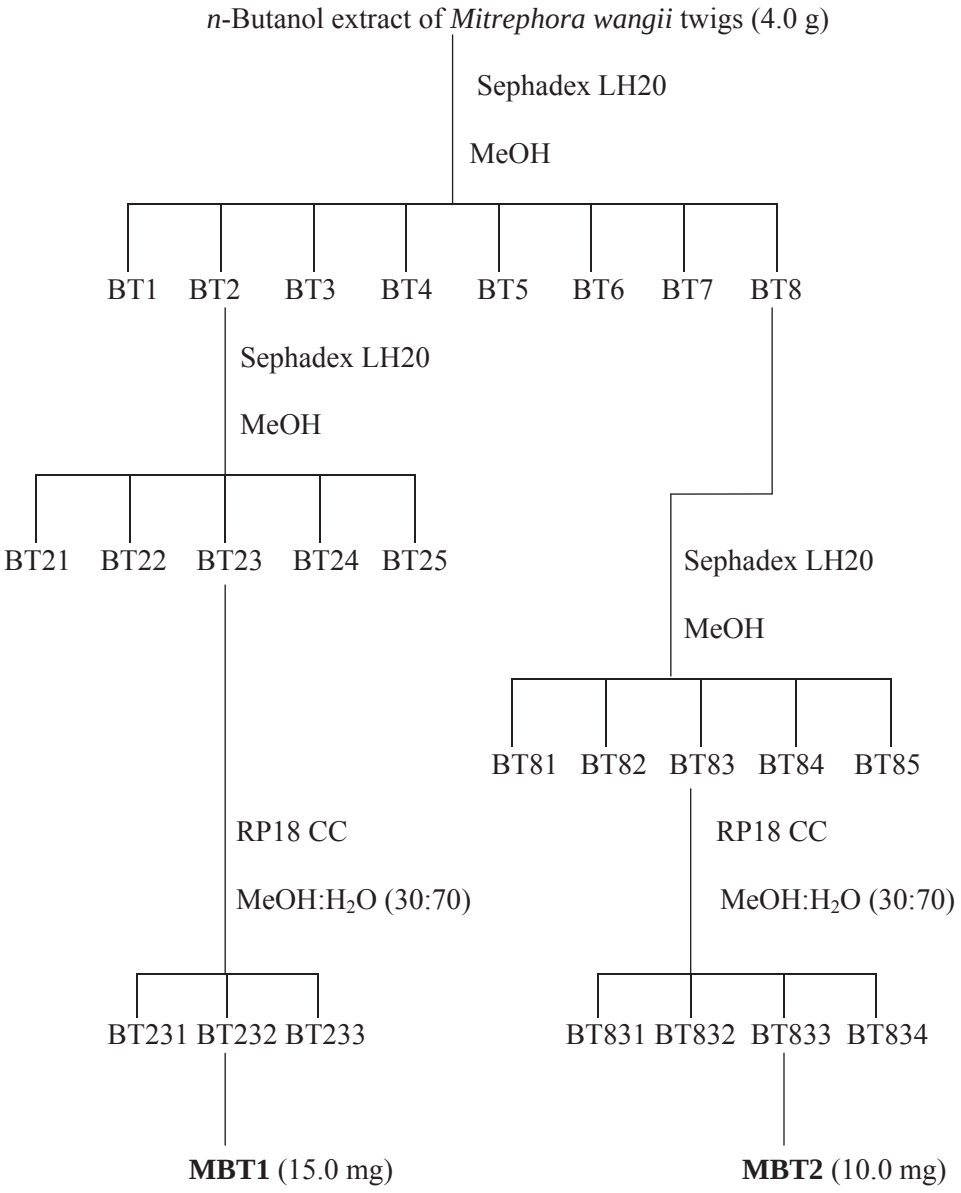

Scheme 8 Isolation of compounds from the *n*-butanol extract of *M. wangii* twigs.

5.3.3.1 Isolation of MBT-1

The fraction BT2 (0.35 g) was purified on a Sephadex LH20 using methanol as an eluent (Scheme 8). Fractions with similar chromatographic pattern were combined to yield 5 fractions (BT21-BT25) using ethyl acetate:methanol (10:90) as a mobile phase. Fraction BT23 (112.0 mg) was purified on RP-18 column chromatrography (ϕ 1 cm) using methanol:distillated water (30:70) as eluent. Fractions were combined by RP-18 TLC (Merck, HX085644) using methanol:distillated water (30:70) as a mobile phase to yield 3 fractions (BT231-BT233). Fraction BT232 (35.0 mg) yielded compound MBT-1. It was identified as corytuberine (15.0 mg, 0.37% yield) (Scheme 8).

5.3.3.2 Isolation of MBT-2

Fraction BT8 (0.76 g) was purified on a Sephadex LH20 using methanol as an eluent (Scheme 8). Fractions with similar chromatographic pattern were combined to yield 5 fractions (BT81-BT85) using ethyl acetate:methanol (20:80) as a mobile phase. Fraction BT83 (146 mg) was purified on RP-18 column chromatrography (ϕ 1 cm) using methanol:distillated water (30:70) as eluent. Fractions were combined by RP-18 TLC (Merck, HX085644) using methanol:distillated water (30:70) as a mobile phase to yield 4 fractions (BT831-BT834). Fraction BT833 (40.0 mg) yielded compound MBT-2. It was identified as magnoflorine (10.0 mg, 0.25% yield) (Scheme 8).

6. Physicochemical Properties of Isolated Compounds

6.1 Compound PGH-1 (taraxerol acetate)

Appearance:	white amorphous powder
Solubility:	soluble in chloroform
Melting point:	290-294 ^{o}C
Specific rotation:	$[\alpha]_{D}^{25}$ +2.97 ($CHCl_3$; *c* 0.19)
IR:	ν_{max}^{KBr} cm^{-1} (Figure 56); 3435, 2936, 1725
HRESI-MS:	491.3866 $[M+Na]^+$ (Figure 55)
^{1}H-NMR:	δ ppm, 300 MHz in $CDCl_3$ (Figure 57, Table 5); 5.53 (1H, *dd*, H-15), 4.46 (1H, *dd*, H-3), 2.04 (3H, *s*, 2'-C$\underline{H}_3$), 1.09 (3H, *s*, H-26), 0.95 (6H, *s*, H-25, 29), 0.91 (3H, *s*, H-24), 0.90 (3H, *s*, H-27), 0.88 (3H, *s*, H-30), 0.86 (3H, *s*, H-23), 0.82 (3H, *s*, H-28)
^{13}C-NMR:	δ ppm, 75 MHz in $CDCl_3$ (Figure 58, Table 5); 170.9 (C-1'), 157.9 (C-14), 116.9(C-15), 81.0 (C-3), 55.6(C-5), 49.1 (C-9), 48.7 (C-18), 41.3 (C-19), 38.9 (C-8), 37.8 (C-13), 37.7 (C-1), 37.6 (C-4), 37.5 (C-10), 37.3 (C-22), 36.6 (C-12), 35.7 (C-17), 35.1 (C-21), 33.6 (C-16), 33.3 (C-29), 33.0 (C-7), 27.9 (C-23), 29.9 (C-27), 29.6 (C-28), 28.8 (C-20), 27.9 (C-23), 25.9 (C-26), 23.4 (C-2), 21.3 (C-2'), 21.2 (C-30), 18.6 (C-6), 17.5 (C-11), 16.5 (C-24), 15.5 (C-32)

6.2 Compound PGH-2 (simiarenol)

Appearance:	white amorphous powder
Solubility:	soluble in chloroform
Melting point:	200-205 ^{o}C
Specific rotation:	$[\alpha]_{D}^{25}$ +26.06 ($CHCl_3$; *c* 0.10 g)
IR:	ν_{max}^{KBr} cm^{-1} (Figure 61); 3506, 3042-2867, 1470-1445, 1384
HRESI-MS:	449.3677 $[M+Na]^+$ (Figure 60)
^{1}H-NMR:	δ ppm, 300 MHz in $CDCl_3$ (Figure 62, Table 7); 5.61 (1H, *d*, H-6), 3.47 (1H, *dd*, H-3), 1.85 and 1.88 (2H, *m*, H-2), 1.82 and 1.19 (2H, *m*, H-20), 1.35 and 1.25 (2H, *m*, H-19), 1.14 (3H, *s*, H-24), 1.05 (3H, *s*, H-23), 1.01 (3H, *s*, H-26), 0.93 (3H, *s*, H-27), 0.90 (3H, *s*, H-25), 0.88 (3H, *d*, H-29), 0.83 (3H, *d*, H-30), 0.78 (3H, *s*, H-28
^{13}C-NMR:	δ ppm, 75 MHz in $CDCl_3$ (Figure 63, Table 7); 141.9 (C-5), 122.0 (C-6), 76.4 (C-3), 60.0 (C-21), 51.7(C-18), 50.2 (C-10), 44.3 (C-8), 42.7 (C-17), 40.8 (C-4), 39.3 (C-14), 38.6 (C-13), 35.4 (C-16), 34.8 (C-9), 34.2 (C-11), 30.7 (C-22), 29.1 (C-15), 29.1 (C-23), 28.9 (C-12), 28.3 (C-20), 27.7 (C-2), 25.5 (C-24), 24.1 (C-7), 22.9 (C-29), 21.9 (C-30), 19.9 (C-19), 18.1 (C-1), 17.8 (C-25), 16.1 (C-28), 15.7 (C-26), 15.0 (C-27)

6.3 Compound PGH-3 (taraxerol)

Appearance:	white amorphous powder
Solubility:	soluble in chloroform
Melting point:	270-275 ^{o}C
Specific rotation:	$[\alpha]_{D}^{25}$ +2.23 ($CHCl_3$; *c* 0.13 g)
IR:	ν_{max}^{KBr} cm^{-1} (Figure 69); 3447, 2934, 1597, 1384
HRESI-MS:	449.3785 $[M+Na]^+$ (Figure 68)
^{1}H-NMR:	δ ppm, 300 MHz in $CDCl_3$ (Figure 70, Table 6); 5.53 (1H, *dd*, H-15), 3.19 (1H, *dd*, H-3), 1.09 (3H, *s*, H-27), 0.98 (3H, *s*, H-23), 0.93 (3H, *s*, 25), 0.91 (6H, *s*, 28, 30), 0.82 (3H, *s*, H-26), 0.80 (3H, *s*, H-24)
^{13}C-NMR:	δ ppm, 75 MHz in $CDCl_3$ (Figure 71, Table 6); 158.0 (C-14), 116.9 (C-15), 79.0 (C-3), 55.5 (C-5), 49.3 (C-18), 48.7 (C-9), 41.3 (C-19), 38.9 (C-4), 38.7 (C-8), 37.9 (C-17), 37.7 (C-1), 37.6 (C-13), 36.7 (C-16), 35.8 (C-10), 35.1 (C-12), 35.1 (C-7), 33.7 (C-21), 33.4 (C-29), 33.1 (C-22), 29.9 (C-28), 29.8 (C-26), 28.8 (C-20), 28.0 (C-23), 27.2 (C-2), 25.9 (C-27), 21.3 (C-30), 18.8 (C-6), 17.5 (C-11), 15.4 (C-24)

6.4 Compound PGH-4 or MHT-3 (*β*-sitosterol)

Appearance:	white amorphous powder
Solubility:	soluble in chloroform
Melting point:	131-134 ^{o}C
IR:	ν_{max}^{KBr} cm^{-1} (Figure 73); 3433, 2936-2869
HRESI-MS:	413.2648 $[M-H]^{+}$ (Figure 72)
^{1}H-NMR:	δ ppm, 300 MHz in $CDCl_3$ (Figure 74, Table 8); 5.35 (1H, *d*, H-6), 5.16 (1H, *d*, H-22), 5.03 (1H, *m*, H-23), 3.52 (1H, *m*, H-3), 1.01 (3H, *s*, H-19), 0.92 (3H, *d*, H-21), 0.86 (3H, *d*, H-26), 0.83 (3H, *t*, H-29), 0.80 (3H, *d*, H-27), 0.68 (3H, *s*, H-18)
^{13}C-NMR:	δ ppm, 75 MHz in $CDCl_3$ (Figure 75, Table 8); 140.8 (C-5), 121.7(C-6), 71.8 (C-3), 56.7 (C-14), 56.0 (C-17), 50.1 (C-9), 45.8 (C-24), 42.3 (C-4, 13), 39.7 (C-12), 37.2 (C-1), 36.5 (C-10), 36.1 (C-20), 33.9 (C-22), 31.6 (C-7), 31.9 (C-2, 8), 29.1 (C-25), 28.2 (C-16), 26.1 (C-23), 24.3 (C-15), 23.1 (C-28), 18.7 (C-21), 21.1 (C-11), 19.4 (C-19), 19.8 (C-26), 19.0 (C-27), 18.7 (C-21), 11.9 (C-29), 11.8 (C-18)

6.5 Compound PGE-1 (kaempferol-3-*O*-*β*-D-6''(4-hydroxy-*E*-cinnamoyl)-(*β*)-glucopyranoside)

Appearance:	pale yellow powder
Solubility:	soluble in methanol, dimethyl sulfoxide
Melting point:	272-275 ^{o}C
IR:	ν_{max}^{KBr} cm^{-1} (Figure 77); 3455-3287, 1684, 1606
Specific rotation:	$[\alpha]_D^{25}$ -4.54 (CH_3OH; *c* 0.02)
HRESI-MS:	617.1126 $[M+Na]^+$ (Figure 76)
^{1}H-NMR:	δ ppm, 300 MHz in acetone-d_6 (Figure 78, Table 12); 8.12 (1H, *d*, H-2', H-6'), 7.49 (2H, *d*, H-2''', H-6'''), 7.43 (1H, *d*, H- 7'''), 6.94 (2H, *d*, H-3', H-5'), 6.89 (2H, *d*, H-3''', H-5'''), 6.49 (1H, *d*, H-8), 6.26 (1H, *d*, H-6), 6.17 (1H, *d*, H-8'''), 5.34 (1H, *d*, H-1''), 4.36 (1H, *dd*, H-6''A), 4.18 (1H, *d*, H-6''B), 3.44 (4H,*m*, H-2'', H-3'', H-4'', H-5'')
^{13}C-NMR:	δ ppm, 75 MHz in acetone-d_6 (Figure 79, Table 12); 172.4 (C-4), 166.3 (C-9'''), 160.0 (C-4', C-4'''), 148.7 (C-2),144.6 (C-6''', C-7'''), 134.0 (C-3), 131.2 (C-2'), 130.0 (C-2'''), 127.3 (C-6'), 126.0 (C-1'''), 123.0 (C-1'), 115.8 (C-3''', C-5'''), 114.9 (C-3', C-5'), 114.3 (C-8'''), 103.6 (C-1''), 99.0 (C-6), 93.8 (C-8), 77.2 (C-3''), 64.6 (C-5''), 74.5 (C-2''), 70.2 (C-4''), 63.1 (C-6'')

6.6 Compound PGE-2 (kaempferol-3-*O*-*β*-D-galactopyranoside)

Appearance:	pale orange powder
Solubility:	soluble in methanol, dimethyl sulfoxide
Melting point:	237-239 ^{o}C
Specific rotation:	$[\alpha]_{D}^{25}$ -63.12 (CH_3OH; *c* 0.03)
UV:	λ_{max} nm (log ε), in CH_3OH: 215.0 (3.86), 280.0 (3.19)
IR (KBr):	ν_{max}^{KBr} cm^{-1} (Figure 85); 3600-3000, 1900-1800, 1700-1600
HRESI-MS:	449.1196 $[M+Na]^+$ (Figure 84)
^{1}H-NMR:	δ ppm, 300 MHz in CD_3OD (Figure 86, Table 10); 8.01 (2H, *d*, H-2', H-6'), 6.85 (2H, *d*, H-3', H-5'), 6.54 (1H, *br s*, H-8), 6.17 (1H, *br s*, H-6), 4.60 (1H, *d*, H-1''), 3.73 (1H, *dd*, H-6A), 3.68 (1H, *dd*, H-6B), 3.49 (1H, *m*, H-2''), 3.37 (3H, *m*, H-3'', H-4'', H-5'')
^{13}C-NMR:	δ ppm, 75 MHz in CD_3OD (Figure 87, Table 10); 184.2 (C-4), 163.4 (C-2, C-7), 159.9 (C-4'),156.2 (C-5, C-8a), 127.3 (C-2', C-6'), 126.0 (C-3), 120.1 (C-1'), 114.0 (C-3', C-5'), 105.0 (C-1''), 103.0 (C-4a), 100.4 (C-8), 97.4 (C-6), 75.5 (C-5''), 74.8 (C-3''), 72.5 (C-2''), 67.7 (C-4''), 59.0 (C-6'')

6.7 Compound PGE-3 ((-)-epicatechin)

Appearance:	yellow amorphous powder
Solubility:	soluble in methanol
Melting point:	210-212 ^{o}C
Specific rotation:	$[\alpha]_{D}^{25}$ -3.62 (CH_3OH; *c* 0.14)
UV:	λ_{max} nm (log ε), in CH_3OH: 209.0 (3.54), 272.0 (3.38), 349.0.(3.33)
IR (KBr):	ν_{max}^{KBr} cm^{-1} (Figure 93); 3600-3000, 2100-1800, 1650
HRESI-MS:	291.0938 $[M+H]^+$ (Figure 92)
^{1}H-NMR:	δ ppm, 300 MHz in CD_3OD (Figure 94, Table 14); 6.87 (1H, *d*, H-2'), 6.77 (1H, *dd*, H-6'), 6.65 (1H, *d*, H-5'), 5.84 (1H, *d*, H-6), 5.81 (1H, *d*, H-8), 4.70 (1H, *br s*, H-2), 4.06 (1H, *ddd*, H-3), 2.75 (1H, *dd*, H-4α), 2.63 (1H, *dd*, H-4β)
^{13}C-NMR:	δ ppm, 75 MHz in CD_3OD (Figure 95, Table 14); 156.6 (C-5), 156.3 (C-7), 155.9 (C-8a), 144.5 (C-3'), 144.4 (C-4'), 130.8 (C-1'), 117.9 (C-6'), 114.5 (C-5'), 113.9 (C-2'), 98.6 (C-4a), 94.9 (C-6), 94.5 (C-8), 78.5 (C-2), 66.1 (C-3), 27.8 (C-4)

6.8 Compound MHL-1 ((2*R*, 3*R*)-2, 3-dihydro-2-(4'-methoxyphenyl)-3-methyl-5-[1-(*E*)-propenyl]benzofuran or methyl conocarpan)

Appearance:	colorless needles
Solubility:	soluble in dichloromethane, chloroform
Melting point:	80-82 ^{o}C
Specific rotation:	$[\alpha]_{D}^{25}$ +122.68 ($CHCl_3$; *c* 0.10,)
UV:	λ_{max} nm (log ε), in CH_3OH: 217 (3.94), 260 (3.88)
IR (KBr):	ν_{max}^{KBr} cm^{-1} (Figure 101); 2996-2839, 2025-1763, 1610, 1481
HRESI-MS:	303.1295 $[M+Na]^+$ (Figure 100)
^{1}H-NMR:	δ ppm, 300 MHz in $CDCl_3$ (Figure 102, Table 19); 7.34 (2H, *d*, H-2', H-6'), 7.12 (1H, *d*, H-6), 7.10 (1H, *s*, H-4), 6.90 (2H, *d*, H-3', H-5'), 6.76 (1H, *d*, H-7), 6.36 (1H, *dd*, H-8), 6.09 (1H, *dq*, H-9), 5.08 (1H, *d*, H-2), 3.80 (3H, *s*, 4'-OC$\underline{H}_3$), 3.39 (3H, *quintet*, H-3), 1.85 (3H, *dd*, H-10), 1.38 (3H, *d*, 3-C$\underline{H}_3$)
^{13}C-NMR:	δ ppm, 75 MHz in $CDCl_3$ (Figure 103, Table 19); 159.7 (C-7a), 158.3 (C-4'), 132.7 (C-3a), 132.4 (C-1'), 130.8 (C-8), 127.6 (C-2', C-6'), 126.3 (C-6), 122.9 (C-9), 120.7 (C-4), 114.0 (C-3', 5'), 109.3 (C-7), 92.7 (C-2), 55.3 (4'-O$\underline{C}H_3$), 45.2 (C-3), 18.4 (C-10), 17.8 (3-$\underline{C}H_3$)

6.9 Compound MHL-2 or MDL-1 ((2*R*,3*R*)-2,3-dihydro-2-(4'-hydroxy-3'-methoxyphenyl)-3-methyl-5-[1-(*E*)-propenyl] benzofuran or 3'-methoxy conocarpan)

Appearance:	white amorphous powders
Solubility:	soluble in dichloromethane, chloroform
Melting point:	102-106 ^{o}C
Specific rotation:	$[\alpha]_{D}^{25}$ +129.43 ($CHCl_3$; *c* 0.20,)
UV:	λ_{max} nm (log ε), CH_3OH: 220.0 (4.19), 260.0 (4.16)
IR (KBr):	ν_{max}^{KBr} cm^{-1} (Figure 105); 3382, 2963, 2058-1650, 1610, 1481
HRESI-MS:	319.1264 $[M+Na]^+$ (Figure 104)
^{1}H-NMR:	δ ppm, 300 MHz in $CDCl_3$ (Figure 106, Table 20); 7.14 (1H, *s*, H-4), 7.12 (1H, *d*, H-6), 6.95 (1H, *d*, H-6'), 6.92 (1H, *d*, H-5'), 6.90 (1H, *s*, H-2'), 6.77 (1H, *d*, H-7), 6.37 (1H, *dd*, H-8), 6.09 (1H, *dq*, H-9), 5.06 (1H, *d*, H-2), 3.40 (1H, *quintet*, H-3), 3.86 (3H, *s*, 3'-OC$\underline{H}_3$), 1.86 (3H, *dd*, H-10), 1.39 (3H, *d*, 3-C$\underline{H}_3$)
^{13}C-NMR:	δ ppm, 75 MHz in $CDCl_3$ (Figure 107, Table 20); 158.3 (C-7a), 146.8 (C-3'), 145.8 (C-4'), 132.4 (C-3a, C-1'), 131.3 (C-5), 130.8 (C-8), 126.3 (C-6), 123.1 (C-9), 120.7 (C-4), 119.7 (C-6'), 114.0 (C-5'), 109.3 (C-7), 108.6 (C-2'), 93.1 (C-2), 55.9 (3'-O$\underline{C}H_3$), 45.3 (C-3), 18.4 (C-10), 17.6 (3-$\underline{C}H_3$)

6.10 Compound MHL-3 or MDL-2 ((2*R*, 3*R*)-2, 3-dihydro-2-(4'-hydroxyphenyl)-3-methyl-5-[1-(*E*)-propenyl]benzofuran or conocarpan)

Appearance:	colorless plate crystals
Solubility:	soluble in chloroform, dichloromethane, methanol
Melting point:	140-142 ^{o}C
Specific rotation:	$[\alpha]_D^{25}$ +191.39 ($CHCl_3$; *c* 0.10,)
UV:	λ_{max} nm (log ε), in CH_3OH: 215.0 (3.37), 264.0 (3.79)
IR:	ν_{max}^{KBr} cm^{-1} (Figure 110); 3374, 2960, 1879-1770, 1614-1598
HRESI-MS:	289.1130 $[M+Na]^+$ (Figure 109)
^{1}H-NMR:	δ ppm, 300 MHz in $CDCl_3$ (Figure 111, Table 16); 7.25 (2H, *d*, H-2', H-6'), 7.11 (1H, *d*, H-6), 7.10 (1H, *br s*, H-4), 6.78 (1H, *d*, H-7), 6.75 (1H, *d*, H-3', H-5'), 6.36 (1H, *dd*, H-8), 6.08 (1H, *dq*, H-9), 5.07 (1H, *d*, H-2), 3.38 (1H, *quintet*, H-3), 1.85 (3H, *dd*, H-10), 1.37 (3H, *d*, 3-C$\underline{H}_3$)
^{13}C-NMR:	δ ppm, 75 MHz in $CDCl_3$ (Figure 112, Table 16); 158.1 (C-7a), 155.7 (C-4'),132.6 (C-1'), 132.4 (C-3a), 131.3 (C-5),130.7 (C-8), 127.9 (C-2', C-6'), 126.3 (C-6), 123.1 (C-9), 120.8 (C-4), 115.5 (C-3', C-5'), 109.3 (C-7), 92.7 (C-2), 45.1 (C-3), 18.4 (C-10), 17.8 (3-$\underline{C}H_3$)

6.11 Compound MHL-4 (linoleic acid)

Appearance:	pale yellow oil
Solubility:	soluble in dichloromethane and chloroform
Melting point:	50-55 ^{o}C
Specific rotation:	$[\alpha]_{D}^{25}$ +2.92 ($CHCl_3$; *c* 0.10)
UV:	λ_{max} nm (log ε), in CH_3OH: 220.0 nm (3.77)
IR:	ν_{max}^{KBr} cm^{-1} (Figure 118); 3422-2849, 1704
HRESI-MS:	279.2278 $[M-H]^+$ (Figure 117)
^{1}H-NMR:	δ ppm, 300 MHz in $CDCl_3$ (Figure 119, Table 32); 5.36 (4H, *br d*, H-9, H-10, H-12, H-13), 2.79 (2H, *t*, H-11), 2.34 (2H, *t*, H-2), 2.05 (4H, *m*, H-8, 14), 1.62 (2H, *quintet*, H-3), 1.28 (14H, *br s*, H-4 to H-7, H-15 to H-17), 0.88 (3H, *t*, H-18)
^{13}C-NMR:	δ ppm, 75 MHz in $CDCl_3$ (Figure 120, Table 32); 180.2 (C-1), 130.0 (C-9), 129.7 (C-13), 127.9 (C-10), 127.9 (C-12), 34.0 (C-2), 31.9 (C-16), 29.0-29.6 (C-4 to C-7, C-15), 27.2 (C-8, C-14), 24.6 (C-11), 24.4 (C-3), 22.7 (C-17), 14.1 (C-18)

6.12 Compound MEL-1 (*β*-sitosterol-3-*O*-glucopyranoside)

Appearance:	white amorphous powder
Solubility:	soluble in pyridine
Melting point:	295-298 ^{o}C
IR:	ν_{max}^{KBr} cm^{-} (Figure 121); 3434, 2933, 1384
^{1}H-NMR:	δ ppm, 300 MHz in pyridine-d_5 (Figure 122, Table 9); 5.37 (1H, *m*, H-6), 5.08 (1H, *d*, H-1'), 4.61 (1H, *br d*, H-6'A), 4.44 (1H, *dd*, H-6'B), 4.34 (2H, *m*, H-3', H-4'), 4.09 (1H, *t*, H-2'), 3.99 (1H, *m*, H-5'), 3.94 (1H, *m*, H-3), 1.00 (3H, *d*, H-21), 0.95 (3H, *s*, H-19), 0.91 (3H, *d*, H-26), 0.90 (3H, *t*, H-29), 0.88 (3H, *d*, H-27), 0.67 (3H, *s*, H-18)
^{13}C-NMR:	δ ppm, 75 MHz in pyridine-d_5 (Figure 123, Table 9); 141.4 (C-5), 122.4 (C-6), 103.1 (C-1'), 79.1 (C-3), 78.9 (C-3'), 78.6 (C-5'), 75.8 (C-2'), 72.2 (C-4'), 63.3 (C-6'), 57.3 (C-14), 56.7 (C-17), 50.8 (C-9), 46.5 (C-24), 42.8 (C-13), 39.5 (C-4), 39.8 (C-12), 38.0 (C-1), 37.4 (C-10), 36.9 (C-20), 34.7 (C-22), 32.6 (C-7), 32.5 (C-8), 30.0 (C-2), 29.8 (C-25), 29.0 (C-16), 26.9 (C-23), 25.0 (C-15), 23.9 (C-28), 19.9 (C-19), 19.7 (C-26), 19.7 (C-27), 19.5 (C-21), 21.8 (C-11), 12.4 (C-29), 12.4 (C-18)

6.13 Compound MET-1 (*N-p*-coumaroyltyramine)

Appearance:	white amorphous powder
Solubility:	soluble in methanol
Melting point:	256-258 ^{o}C
Specific rotation:	$[\alpha]_{D}^{25}$ +11.11 (CH_3OH; *c* 0.02)
UV:	λ_{max} nm (log ε), in CH_3OH: 224.0 (2.96), 290.0 (2.89)
IR:	ν_{max}^{KBr} cm^{-1} (Figure 125); 3433, 2080-1717, 1660, 1581, 1448, 1242
HRESI-MS:	306.1050 $[M+Na]^+$ (Figure 124)
^{1}H-NMR:	δ ppm, 300 MHz in CD_3OD (Figure 126, Table 22); 7.48 (1H, *d*, H-7), 7.41 (2H, *d*, H-2, H-6), 7.07 (2H, *d*, H-2', H-6'), 6.80 (2H, *d*, H-3, H-5), 6.73 (2H, *d*, H-3', H-5'), 6.39 (1H, *d*, H-8), 3.47 (1H, *t*, H-8'), 2.76 (1H, *t*, H-7')
^{13}C-NMR:	δ ppm, 75 MHz in CD_3OD (Figure 127, Table 22); 167.8 (C-9), 159.1 (C-4), 155.5 (C-4'), 140.5 (C-7), 129.9 (C-1'), 129.3 (C-2', C-6'), 129.1 (C-2, C-6), 126.3 (C-1), 117.0 (C-8), 115.3 (C-3, 5), 114.8 (C-3', C-5'), 41.2 (C-8'), 34.4 (C-7')

6.14 Compound MET-2 (*N*-caffeoyltyramine)

Appearance:	yellow amorphous powder
Solubility:	soluble in methanol
Melting point:	205-208 ^{o}C
Specific rotation:	$[\alpha]_{D}^{25}$ +2.79 (CH_3OH; *c* 0.08)
UV:	λ_{max} nm (log ε), in CH_3OH: 285.0 (3.53), 223.0 (3.74)
IR:	ν_{max}^{KBr} cm^{-1} (Figure 133); 3333, 1887, 1646, 1581, 1447, 1249
HRESI-MS:	322.1061 $[M+Na]^+$ (Figure 132)
^{1}H-NMR:	δ ppm, 300 MHz in CD_3OD (Figure 134, Table 24); 7.24 (1H, *d*, H-7), 6.92 (2H, *d*, H-2', H-6'), 6.86 (1H, *d*, H-2), 6.77 (1H, *dd*, H-6), 6.63 (1H, *d*, H-5), 6.58 (2H, *d*, H-3', H-5'), 6.20 (1H, *d*, H-8), 3.32 (2H, *t*, H-8'), 2.62 (2H, *t*, H-7')
^{13}C-NMR:	δ ppm, 75 MHz in CD_3OD (Figure 135, Table 24); 169.3 (C-9), 156.9 (C-4'), 148.7 (C-4), 146.7 (C-3), 142.2 (C-7), 131.3 (C-1'), 130.7 (C-2', C-6'), 128.3 (C-1), 122.1 (C-6), 118.4 (C-8), 116.5 (C-5), 116.3 (C-3', C-5'), 115.1 (C-2), 42.5 (C-8'), 35.8 (C-7')

6.15 Compound MET-3 (quebrachitol)

Appearance:	crystalline white powder
Solubility:	soluble in water, dimethylsulfoxide
Melting point:	194-196 ^{o}C
Specific rotation:	$[\alpha]_{D}^{25}$ -88.89 (distillation water; *c* 0.10)
IR:	ν_{max}^{KBr} cm^{-1} (Figure 141); 3500-3200, 2939-2836, 1200-1100
HRESI-MS:	217.0683 $[M+Na]^{+}$ (Figure 140)
^{1}H-NMR:	δ ppm, 300 MHz in DMSO-d_6 (Figure 142, Table 30); 3.86 (1H, *dd*, H-1), 3.67 (1H, *dd*, H-6), 3.44 (1H, *dd*, H-5), 3.39 (1H, *dd*, H-3), 3.31 (3H, *s*, 2-OC$\underline{H}_3$), 3.27 (1H, *dd*, H-3), 3.09 (1H, *dd*, H-2)
^{13}C-NMR:	δ ppm, 75 MHz in DMSO-d_6 (Figure 143, Table 30); 81.5 (C-2), 73.7 (C-3), 72.6 (C-4), 72.5 (C-6), 70.9 (C-5), 68.5 (C-1), 57.5 (2-O$\underline{C}$H$_3$)

6.16 Compound MET-4 (allantoin)

Appearance:	white crystal
Solubility:	soluble in DMSO
Melting point:	241-245 ^{o}C
IR:	ν_{max}^{KBr} cm^{-} (Figure 148); 3439-3062, 1781-1661, 1603, 1531
HRESI-MS:	399.0740 $[2M+Na]^{+}$ (Figure 147)
^{1}H-NMR:	δ ppm, 300 MHz in DMSO-*d*$_6$ (Figure 149, Table 33); 10.54 (1H, *br s*, 1-NH), 8.06 (1H, *s*, 3-NH), 6.86 (1H, *d*, 6-NH), 5.79 (2H, *s*, 8-NH), 5.24 (1H, *d*, H-4)
^{13}C-NMR:	δ ppm, 75 MHz in DMSO-*d*$_6$ (Figure 150, Table 33); 174.0 (C-5), 157.8 (C-7), 157.2 (C-2), 62.8 (C-4)

6.17 Compound MBT-1 (corytuberine)

Appearance:	dark orange oil
Solubility:	soluble in methanol
Melting point:	255-258 ^{o}C
Specific rotation:	$[\alpha]_{D}^{25}$ +11.01 (CH_3OH; *c* 0.10)
UV:	λ_{max} nm (log ε), in CH_3OH: 225.0 (3.93), 270.0 (3.51), 320.0 (3.21)
IR:	ν_{max}^{KBr} cm^{-1} (Figure 154); 3422, 2924, 1636, 1458-1384, 1252, 1065
HRESI-MS:	328.1792 $[M]^+$ (Figure 153)
^{1}H-NMR:	δ ppm, 300 MHz in CD_3OD (Figure 155, Table 28); 6.79 (1H, *d*, H-9), 6.65 (1H, *s*, H-3), 6.65 (1H, *d*, H-8), 4.29 (1H, *dd*, H-6a), 3.82 (6H, *s*, 2-OC$\underline{H}_3$, 10-OC$\underline{H}_3$), 3.19 (1H, *dd*, H-7A), 3.12 (3H, *t*, H-5A, H-5B), 2.75 (1H, *dd*, H-4B), 2.69 (3H, *s*, N-C$\underline{H}_3$), 2.47 (2H, *br d*, H-4A, H-4B)
^{13}C-NMR:	δ ppm, 75 MHz in CD_3OD (Figure 156, Table 28); 153.0 (C-2), 151.9 (C-10), 150.0 (C-1), 149.0 (C-11), 125.7 (C-7a), 123.2 (C-11a), 120.5 (C-1b), 116.9 (C-8), 110.3 (C-9), 109.2 (C-3), 71.1 (C-6a), 47.3 (C-5), 55.6 (2-O$\underline{C}H_3$), 55.9 (10-O$\underline{C}H_3$), 32.8 (N-$\underline{C}H_3$), 31.5 (C-7), 32.6 (C-4)

6.18 Compound MBT-2 (magnoflorine)

Appearance:	brownish yellow amorphous powder
Solubility:	soluble in methanol
Melting point:	226-230 ^{o}C
Specific rotation:	$[\alpha]_D^{25}$ +151.84 (CH_3OH; *c* 0.06)
UV:	λ_{max} nm (log ε), in CH_3OH: 229.0 (4.03), 271.0 (3.48), 313.0 (3.39)
IR:	ν_{max}^{KBr} cm^{-1} (Figure 163); 3424, 2934, 1602, 1458-1384, 1248, 1066
HRESI-MS:	364.1335 $[M-H+Na]^+$ (Figure 162)
^{1}H-NMR:	δ ppm, 300 MHz in CD_3OD (Figure 164, Table 26); 6.63 (1H, *d*, H-9), 6.49 (1H, *s*, H-3), 6.48 (1H, *d*, H-8), 4.04 (1H, *br d*, H-6a), 3.71 (3H, *s*, 10-C$\underline{H}_3$O), 3.70 (3H, *s*, 2-C$\underline{H}_3$O), 3.44 (3H, *m*, H-4β, H-5α, H-5β), 3.21 (3H, *s*, N-C$\underline{H}_{3\alpha}$), 2.99 (1H, *br d*, H-7α), 2.83 (3H, *s*, N-C$\underline{H}_{3\beta}$), 2.71 (1H, *br d*, H-4α), 2.56 (1H, *br t*, H-7β)
^{13}C-NMR:	δ ppm, 75 MHz in CD_3OD (Figure 165, Table 26); 153.4 (C-2), 151.9 (C-10),150.9 (C-1), 149.9 (C-11), 126.1 (C-7a), 123.8 (C-11a), 123.7 (C-1a), 121.0 (C-1b), 116.9 (C-8), 115.8 (C-3a), 110.6 (C-9), 109.5 (C-3), 71.5 (C-6a), 62.6 (C-5), 56.3 (2-O$\underline{C}H_3$), 56.0 (10-O$\underline{C}H_3$), 53.9 (N-$\underline{C}H_{3\alpha}$), 43.5 (N-$\underline{C}H_{3\beta}$), 31.9 (C-7), 24.8 (C-4)

CHAPTER 4
RESULTS AND DISCUSSIONS

1. Biological Activities of the Methanol Extracts from 18 Plants

Eighteen plants were collected and determined for biological activities using brine shrimp lethality and DPPH assay. For brine shrimp lethality, the LC_{50} of methanol extracts ranged from 13.3 to higher than 1,000 μg/ml. The active extracts of *Mitrephora wangii* and *Hydrocotyle javanica* were classified as highly toxic with LC_{50} of 14.8 and 13.3 μg/ml, respectively. For DPPH assay, the IC_{50} ranged from 6.7 to higher than 100 μg/ml. About 60% of the plant extracts possessed moderate activity. The highly antioxidative plants were *Sageretia cordifolia, Ulmus lancaefolia*, and *Acer chiangdaoense* with the IC_{50} of 6.7, 8.1, and 9.8 μg/ml. In addition to antioxidative assay, synergistic effect between the plant extract and *L*-ascorbic acid presented as combination index (CI). The plant extracts showed synergistic effect when CI value was less than 1. In this study, it was found that some plants exhibited slightly synergistic effect and may increase the antioxidative activity when co-administration with *L*-ascorbic acid. These plants were divided into nine groups according to their activities (Table 4) (Tanamatayarat et al., 2011). For example, the methanol extract of *M. wangii* in group I was highly toxic with LD_{50} of 14.8 μg/ml for BSL assay, and weak activity for DPPH assay. In group II, the methanol extract of *H. javantica* was highly toxic in BSL, but inactive in antioxidative activity. Due to the biological activities, *M. wangii* and *P. grande*, were chosen for further study.

Table 4 Brine shrimp lethalities and antioxidative activities of 18 methanol plant extracts

Group	Scientific name	BSL	Antioxidative activity	
		LC_{50} (μg/ ml)	IC_{50} (μg /ml)	CI
I[a]	*M. wangii*	14.8	96.3	1.2
II[b]	*H. javanica*	13.3	>100	1.2
III[c]	*P. grande*	98.5	13.6	1.0
IV[d]	*T. thyrsoideus*	41.3	>100	1.2
V[e]	*S. cordifolia*	191.6	6.7	0.8
	U. lancaefolia	866.9	8.1	0.9
VI[f]	*Begonia* sp.	140.0	32.4	1.3
	C. oppositifolia	233.3	16.9	1.2
	G. propingua	616.3	21.6	1.1
	H. macrophylla	139.7	12.5	1.1
	L. parviflora	519.7	29.2	1.2
	P. semisagittatum	700.6	10.7	1.4
	P. racemosa	610.4	14.1	1.1
VII[g]	*S. erectus*	136.8	>100	1.2
VIII[h]	*A. chiangdaoense*	>1000	9.8	0.9
IX[i]	*D. martabanica*	>1000	11.2	1.3
	E. salwinesis	>1000	14.6	1.0
	L. sulcata	>1000	15.7	1.3
	L-Ascorbic acid	-	3.4	-

Remarks: [a]highly toxic to brine shrimp; weakly antioxidative activity

[b]highly toxic to brine shrimp; inactive antioxidative activity

[c]moderate activity for both assays

[d]moderately toxic to brine shrimp; inactive antioxidative activity

[e]weakly toxic to brine shrimp; highly antioxidative activity

[f]weakly toxic to brine shrimp; moderately antioxidative activity

[g]weakly toxicity to brine shrimp; inactive antioxidative activity

[h]inactive to brine shrimp; highly antioxidative activity

[i]inactive to brine shrimp; moderately antioxidative activity

2. Isolation and Identification of Compounds from *Pterospermum grande* and *Mitrephora wangii*

From the biological activities of the methanol extracts from 18 plants, *Pterospermum grande* and *Mitrephora wangii* were selected for phytochemical and biological investigation. *P. grande* possessed moderate activities in both BSL assay with the LC_{50} of 98.5 μg/ml and DPPH with the IC_{50} of 13.6 μg/ml, whereas *M. wangii* showed strong toxicity in BSL assay with the LC_{50} of 14.8 μg/ml and weak antioxidative activity in DPPH assay with the IC_{50} of 96.3 μg/ml. The scientific studies of these two plants have never been reported.

Seven compounds were isolated from the leaves of *P. grande*. The hexane extract yielded compounds PGH-1, PGH-2, PGH-3, and PGH-4, while the ethyl acetate extract gave compounds PGE-1, PGE-2, and PGE-3. Seven compounds were isolated from the leaves of *M. wangii*. The hexane extract yielded compounds MHL-1, MHL-2, MHL-3, and MHL-4, the dichloromethane extract yielded compounds MDL-1 and MDL-2, and the ethyl acetate extract yielded compound MEL-1. Nine compounds were isolated from the twigs of *M. wangii*. The hexane extract gave compounds MHT-1, MHT-2 and MHT-3, the ethyl acetate extract yielded compounds MET-1, MET-2, MET-3, and MET-4, and the *n*-butanol extract afforded compounds MBT-1 and MBT-2. The structures of all isolated compounds were determined from their UV, IR, MS, and NMR spectral data, and compared with the literatures.

1.1 Identification of Triterpenoids

1.1.1 Compound PGH-1 (taraxerol acetate)

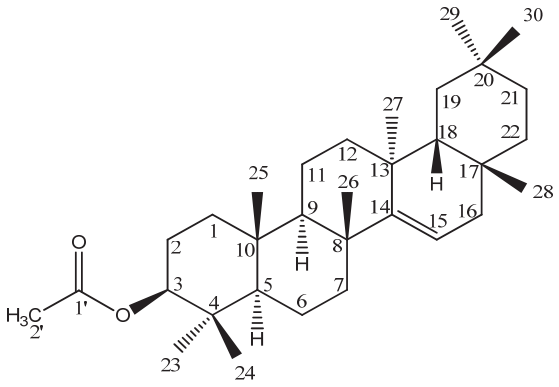

Figure 24 Structure of PGH-1

Compound PGH-1 was obtained as a white amorphous powder. Its was identified as taraxerol acetate. HRESI-MS of PGH-1 showed the $[M+Na]^+$ ion peak at *m/z* 491.3866 (Figure 55), corresponding to the molecular formula of $C_{32}H_{52}O_2$. From ^{13}C NMR and DEPT-135 spectra (Figures 58 and 59, Table 5), there were nine methyl, ten methylene, five methine, and eight quaternary carbons. ^1H-NMR (Figure 57, Table 5) signals of all nine methyl groups were singlets. An acetoxyl group at position 3 was observed by a carbonyl bond and an ester functions in IR at 1725 and 1251 cm^{-1}, respectively (Figure 56). The equatorial or β-orientation of this functional group was assigned based on axial-axial and axial-equatorial coupling constants between H-2 and H-3 of 11.6 and 6.5 Hz, respectively. An olefinic moiety was the other functional group of this compound. It was confirmed by two downfield ^{13}C signals at δ 157.9 (C-15) and 116.9 (C-16), and an olefinic proton at δ 5.53 (H-15) (Figure 58).

The NMR data of compound PGH-1 were compared with previous data of taraxerol acetate in Table 5 (Jin et al., 2007). Taraxerol acetate was obtained previously from several families such as *Laggera pterodonta* (DC.) Sch. Bip. Ex Oliv. (Asteraceae) (Kuljanabhagavad et al., 2009) and *Alnus hirsuta* Turcz. ex Rupr. (Betulaceae) (Jin et al., 2007). Taraxerol acetate has been found to exhibit antiviral activity against herpes simplex virus type II with ED_{50} value of 50

μg/ml (Kuljanabhagavad et al., 2009), but this compound had not inhibitory effect on the function of hypoxia-inducible factor-1 (Jin et al., 2007).

Table 5 ^{1}H and ^{13}C NMR chemical shift (in ppm) of taraxerol acetate (in $CDCl_3$) (Jin et al., 2007; Shu et al., 2008) and PGH-1 (in $CDCl_3$, 300 MHz).

Position	Taraxerol acetate		PGH-1	
	^{1}H (multiplicity, coupling constant (Hz))	^{13}C	^{1}H (multiplicity, coupling constant (Hz))	^{13}C
1		37.8	1.20-1.70 (*m*)	37.7
2		23.6	1.20-1.70 (*m*)	23.4
3	4.46 (*dd*, 10.5, 5.5)	81.2	4.46 (*dd*, 11.6, 6.5)	81.0
4		38.1		37.6
5		55.8	1.20-2.00 (*m*)	55.6
6		18.9	1.20-2.00 (*m*)	18.6
7		33.3	1.20-2.00 (*m*)	33.0
8		39.2		38.9
9		49.4	1.20-2.00 (*m*)	49.1
10		37.7		37.5
11		17.7	1.20-2.00 (*m*)	17.5
12		36.8	1.20-2.00 (*m*)	36.6
13		37.8		37.8
14		158.1		157.9
15	5.53(*dd*, 8.0, 3.5)	117.1	5.53 (*dd*, 11.3, 3.3)	116.9
16		33.8	A 1.94 (*dd*, 11.3, 3.3)	33.6
			B 1.20-2.00 (*m*)	
17		35.9	1.20-2.00 (*m*)	35.7
18		48.9	1.20-2.00 (*m*)	48.7
19		41.4	1.20-2.00 (*m*)	41.3
20		29.0		28.8
21		35.3	1.20-2.00 (*m*)	35.1
22		37.6	1.20-2.00 (*m*)	37.3
23	0.86 (*s*)	28.1	0.86 (*s*)	27.9
24	0.91 (*s*)	16.8	0.91 (*s*)	16.5
25	0.95 (*s*)	15.7	0.95 (*s*)	15.5
26	1.09 (*s*)	26.1	1.09 (*s*)	25.9
27	0.90 (*s*)	30.1	0.90 (*s*)	29.9
28	0.82 (*s*)	30.1	0.82 (*s*)	29.6
29	0.95 (*s*)	33.5	0.95 (*s*)	33.3
30	0.88 (*s*)	21.5	0.88 (*s*)	21.2
$\underline{C}OCH_3$		171.2		170.9
$CO\underline{CH_3}$	2.04 (*s*)	21.5	2.04 (*s*)	21.3

1.1.2 Compound PGH-3 (taraxerol)

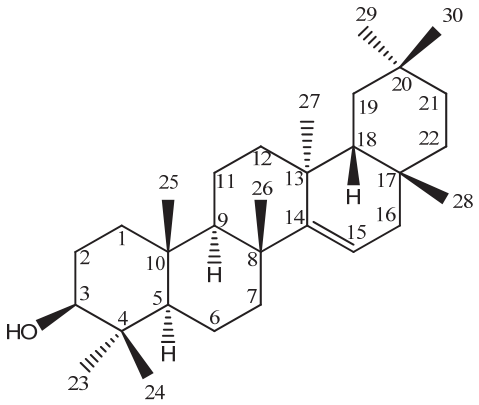

Figure 25 Structure of PGH-3

Compound PGH-3 was obtained as white amorphous powder. All of its spectral data were very close to PGH-1, except for the lack of data of an acetoxy group at position 3. IR absorption band at 3447 cm^{-1} (OH stretching) indicated the presence of a hydroxyl functional group for instead (Figure 69). Its $[M+Na]^+$ ion peak at m/z 449.3785 (Figure 68), which was 42 amu. less than that of PGH-1, also confirmed the absence of the acetyl group. The compound PGH-3 was identified as taraxerol.

NMR data (Figures 70 and 71, Table 6) of compound PGH-3 were compared with taraxerol (Kornwongwan and Luangkamin, 2011). Taraxerol was previously reported from other sterculiaceous plants such as *Pterospermum heyneanum* Wall. and *P. xylocarpum* Santapau & Wagh (Anjaneyulu and Raju, 1987b; Anjaneyulu and Raju, 1987a; Anjaneyulu and Raju, 1988). This compound displayed anti-inflammatory activity by reducing nitric oxide in murine microglial cells with an IC_{50} value of 24.2 ± 2.8 μM (Tsao et al., 2008).

Table 6 ^{1}H and ^{13}C NMR chemical shift (in ppm) of taraxerol (in $CDCl_3$) (Kornwongwan and Luangkamin, 2011) and PGH-3 (in $CDCl_3$, 300 MHz).

Position	Taraxerol		PGH-3	
	^{1}H (multiplicity, coupling constant (Hz))	^{13}C	^{1}H (multiplicity, coupling constant (Hz))	^{13}C
1	1.92 (*dd*, 14.7, 2.9)	37.7	1.92 (*dd*, 14.7, 3.0)	37.7
2		27.1	1.15-1.67 (*m*)	27.2
3	3.19 (*dd*, 11.2,4.8)	79.0	3.19 (*dd*, 10.3, 5.1)	79.0
4		38.9		38.9
5		55.5	1.15-1.67 (*m*)	55.5
6		18.8	1.15-1.67 (*m*)	18.8
7		35.1	1.15-1.67 (*m*)	35.1
8		38.7		38.7
9		48.7	1.15-1.67 (*m*)	48.7
10		35.8		35.8
11		17.5	1.15-1.67 (*m*)	17.5
12		35.1	1.15-1.67 (*m*)	35.1
13		37.5		37.6
14		158.0		158.0
15	5.53 (*dd*, 8.1, 3.2)	116.8	5.53 (*dd*, 8.1, 3.3)	116.9
16		36.6	1.15-1.67 (*m*)	36.7
17		37.9		37.9
18		49.2	1.15-1.67 (*m*)	49.3
19	2.04 (*dt*, 12.6, 3.0)	41.3	2.04 (*dt*, 12.6, 3.0)	41.3
20		28.8		28.8
21		33.7	1.15-1.67 (*m*)	33.7
22		33.0	1.15-1.67 (*m*)	33.1
23	0.97	28.0	0.98 (*s*)	28.0
24	0.80	15.4	0.80 (*s*)	15.5
25	0.92	15.4	0.93 (*s*)	15.4
26	0.82	29.8	0.91 (*s*)	29.8
27	1.09	25.9	1.09 (*s*)	25.9
28	0.90	29.9	0.82 (*s*)	29.9
29	0.94	33.3	0.95 (*s*)	33.4
30	0.90	21.3	0.91 (*s*)	21.3

1.1.3 Compound PGH-2 (simiarenol)

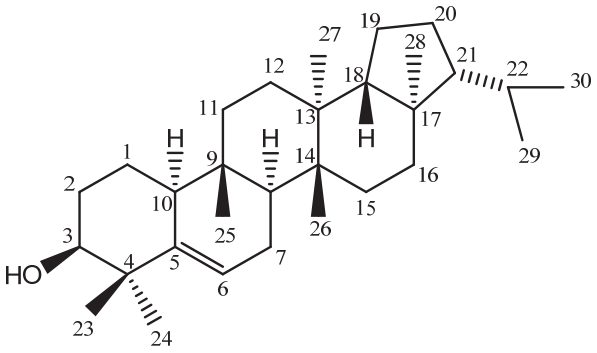

Figure 26 Structure of PGH-2

Compound PGH-2 was obtained as a white amorphous powder. The HRESI-MS showed the $[M+Na]^+$ ion-peak at *m/z* 449.3677 (Figure 60), implying its molecular formula to be $C_{30}H_{50}O$. IR bands at 3506 and at 1384 cm^{-1} suggested a hydroxyl group and a C-O group, respectively (Figure 61). By comparison its ^{1}H-NMR and ^{13}C NMR data (Figure 62 and 63) with the preceding literature, this compound was classified as a hopanoid pentacyclic triterpene (Mahato and Kundu, 1994).

The ^{13}C, DEPT-135 and HMQC spectra (Figures 63-65, Table 7) of this compound indicated a total of 30 carbons. These carbons were seven methine, nine methylene, six quaternary, and eight methyl carbons. The eight methyl groups were also confirmed by the ^{1}H-NMR data. Two doublet methyl signals of isopropyl chain were appeared at δ 0.82 (H-30, *J*= 5.8 Hz) and 0.88 (H-29, *J*= 5.8 Hz). Other methyl groups resonated as the singlets at δ 0.90 (H-25), 0.93 (H-27), 1.01 (H-26), 1.05 (H-23), and 1.14 (H-24).

A hydroxyl functional group was indicated by the signal of C-3 at 76.4 ppm and the oxy-methine proton (H-3) at δ 3.47 ppm. The doublet of doublet splitting pattern (*J*= 9.0, 3.0 Hz) of H-3 suggested the axia-axial and axial-equal coupling of H-3 to both methylene protons at position 2. This indicated that 3-OH was *β*-orientation or equatorial substitution. A double bond in the structure was revealed by NMR signals of two olefinic carbons (δ 141.9 and 122.0) and an

olefinic proton (δ 5.61). Long-range correlation from H-6 to C-10 and C-7 in HMBC experiment (Figure 67) concluded that this double bond was at position 5.

From the above data, the compound PGH-2 was identified as simiarenol. Its NMR data were comparable with that previously reported (Chakravarty, 1994) and showed in Table 7. Simiarenol was isolated from several plants species such as *Rhododendron simiarum* Hance (Ericaceae) (Arthur and Hui, 1965), *Erigeron annuus* (L.) Per. (Asteraceae) (Yoo et al., 2008), and *Trema orientalis* (L.) Bl. (Ulmaceae) (Panchal et al., 2010). This is the first isolation of this compound from *Pterospermum*. Simiarenol was inactive in multidrug resistance reversing or apoptosis induction activities on L5178 human MDR1 gene-transfected mouse lymphoma cells (Duarte et al., 2009).

Table 7 ^{1}H and ^{13}C NMR chemical shift (in ppm) of simiarenol (in $CDCl_3$) (Chakravarty, 1994) and PGH-2 (in $CDCl_3$, 300 MHz)

Position	Simiarenol		PGH-2	
	^{1}H (multiplicity, coupling constant (Hz))	^{13}C	^{1}H (multiplicity, coupling constant (Hz))	^{13}C
1		18.0	0.89 (*m*), 1.56 (*m*)	18.1
2	1.70, 1.86	27.7	A 1.85 (*m*), B 1.70 (*m*)	27.7
3	3.47 (*br s*)	76.3	3.47 (*dd*, 9.0, 3.0)	76.4
4		40.8		40.8
5		141.9		141.9
6		121.9	5.61 (*d*, 5.7)	122.0
7		24.0	1.86 (*m*)	24.1
8		44.2	A 1.53 (*m*), B 1.48 (*m*)	44.3
9		34.8		34.8
10		50.2	1.56 (*m*)	50.2
11		34.1	A 1.65 (*m*), B 1.48 (*m*)	34.2
12		29.0	A 1.50 (*m*), B 1.19 (*m*)	28.9
13		38.6		38.6
14		39.3		39.3
15		29.1	A 1.44 (*m*), B 1.37 (*m*)	29.1
16		35.4	A 1.65 (*m*), B 156 (*m*)	35.4
17		42.7		42.7
18		51.7	1.64 (*m*)	51.7
19	1.26, 1.36	19.9	A 1.35 (*m*), B 1.25 (*m*)	19.9
20	1.19, 1.82	28.3	A 1.82 (*m*), B 1.19 (*m*)	28.3
21		60.0	0.98 (*m*)	60.0
22		30.7	1.36 (*m*)	30.7
23	1.05 (*s*)	29.0	1.05 (*s*)	29.1
24	1.14 (*s*)	25.4	1.14 (*s*)	25.5
25	0.89 (*s*)	17.8	0.90 (*s*)	17.8
26	1.01 (*s*)	15.7	1.01 (*s*)	15.7
27	0.93 (*s*)	15.0	0.93 (*s*)	15.0
28	0.78 (*s*)	16.0	0.78 (*s*)	16.1
29	0.88 (*d*, 6.7)	22.9	0.88 (*d*, 5.8)	22.9
30	0.83 (*d*, 6.7)	21.9	0.82 (*d*, 5.8)	21.9

1.2 Identification of Steroids

1.2.1 Compound PGH-4 or MHT-3 (*β*-sitosterol)

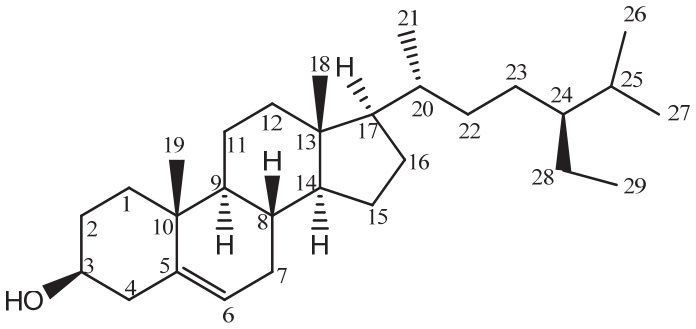

Figure 27 Structure of PGH-4 or MHT-3

Compound PGH-4 and MHT-3 were identified as the same compound, *β*-sitosterol. It was obtained as a white amorphous powder. HRESI-MS exhibited the $[M-H]^+$ ion peak at *m/z* 413.2648 (Figure 72), corresponding to the molecular formula of $C_{29}H_{50}O$. IR broad band at 3433 cm^{-1} indicated the hydroxyl functional group (Figure 73). ^1H and ^{13}C-NMR data (Figures 74 and 75, Table 8) were identifical with previous reported of *β*-sitosterol (Subhadhirasakul and Pechpongs, 2004). An oxy-methine proton (H-3) and a vinylic proton (H-6) signal were at δ 3.52 and 5.35 ppm, respectively. The olefinic carbon were at δ 140.8 (C-5) and 121.7 (C-6).

β-Sitosterol is a common phytochemical compound of plant families, including sterculiaceous and annonaceous families such as *Pterospermum acerifolium* (Dan and Dan, 1988), *Pterospermum heyneanum* (Anjaneyulu and Raju, 1988), *Pterospermum semisagittatum* (Anjaneyulu and Raju, 1988), *Mitrephora tomentosa* (Supudompol et al., 2004), and *Goniothalamus laotica* (Lekphrom et al., 2009). It has been shown to possess several activities such as gastroprotective, antibacterial, and anti-inflammatory activities (Martinez-Vazquez et al., 1999; Rachchh and Jain, 2008).

Table 8 ^{1}H and ^{13}C NMR chemical shift (in ppm) of *β*-sitosterol (in $CDCl_3$) (Patra et al., 2010) and PGH-4 or MHT-3 (in $CDCl_3$, 300 MHz)

Position	*β*-Sitosterol		PGH-4 or MHT-3	
	^{1}H (multiplicity, coupling constant (Hz))	^{13}C	^{1}H (multiplicity, coupling constant (Hz))	^{13}C
1	1.47	37.2	1.07-1.54 (*m*)	37.2
2	1.56	31.6	1.07-1.54 (*m*)	31.9
3	3.32 (*m*)	71.8	3.52 (*m*)	71.8
4	2.28	42.3	1.78-2.33 (*m*)	42.3
5		140.7		140.8
6	5.36	121.7	5.35 (*d*, 5.1)	121.7
7	2.03	31.6	1.78-2.33 (*m*)	31.6
8	1.67	31.9	1.58-1.72 (*m*)	31.9
9	1.48	50.1	1.07-1.54 (*m*)	50.1
10		36.5		36.5
11	1.52	21.1	1.07-1.54 (*m*)	21.1
12	1.49	39.8	1.07-1.54 (*m*)	39.7
13		42.3		42.3
14	1.50	56.7	1.07-1.54 (*m*)	56.7
15	1.60	24.3	1.58-1.72 (*m*)	24.3
16	1.84	28.2	1.78-2.33 (*m*)	28.2
17	1.49	56.0	1.07-1.54 (*m*)	56.0
18	0.68	11.8	0.68 (*s*)	11.8
19	1.02	19.4	1.01 (s)	19.4
20	1.64	36.5	1.58-1.72 (*m*)	36.1
21	0.94	18.7	0.92 (*d*, 6.3)	18.7
22	0.88	33.9	1.07-1.54 (*m*)	33.9
23	1.04	26.1	1.07-1.54 (*m*)	26.1
24	1.50	45.8	1.07-1.54 (*m*)	45.8
25	1.65	28.9	1.58-1.72 (*m*)	29.1
26	0.83	19.8	0.86 (*d*, 7.2)	19.8
27	0.85	18.7	0.80 (*d*, 6.6)	19.0
28	1.04	23.1	1.07-1.54 (*m*)	23.1
29	0.88	11.9	0.83 (*t*, 6.6)	11.9

1.2.2 Compound MEL-1 (*β*-sitosterol-3-*O*-glucopyranoside)

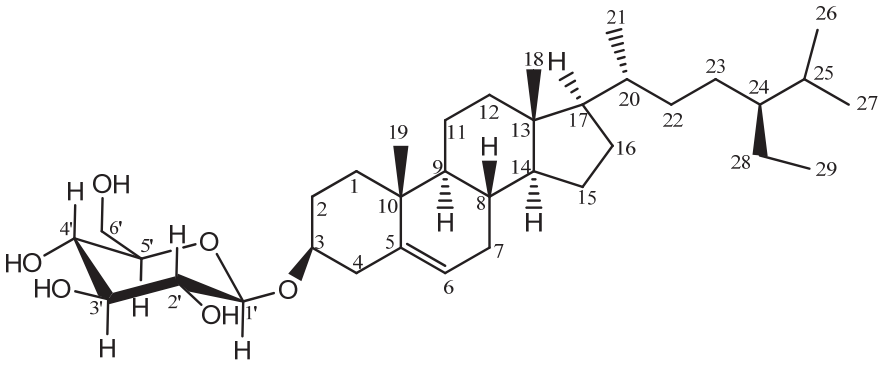

Figure 28 Structure of MEL-1

Compound MEL-1 was obtained as a white amorphous powder. Its NMR data (Figures 122-124) were typical for *β*-sitosterol-3-*O*-glucopyranoside (Moghaddam et al., 2006; Rai et al., 2006). The anomeric proton (H-1') was at δ 5.08 with the coupling constant of 7.5 Hz, which indicated that glucose moiety linked to the steroidal aglycone as *β*-linkage. The downfield signal of anomeric carbons at δ 103.1 (C-1') indicated that the sugar connected to the aglycone with an *O*-linkage. The sugar part was compared with previous data (Agrawal, 1992, Moghaddam et al., 2006, Rai et al., 2006) and identified as *β-D*-glucopyranose.

Comparison of its ^{13}C and ^{1}H NMR data (Figures 122-123, Table 9) with the previous report (Moghaddam et al., 2006; Rai et al., 2006), compound MEL-1was identified to be *β*-sitosterol-3-*O*-glucopyranoside which was found in several species, namely *Pergularia tomentosa* L. (Asclepiadaceae) (Gohar et al., 2000), *Ocimum sanctum* L. (Lamiaceae) (Rahman et al., 2009), *Erythrina vogelii* Hook. (Fabaceae) (Ali et al., 2011), *Pterospermum heyneanum* (Anjaneyulu and Raju, 1988), and *P. xylocarpum* (Sterculiaceae) (Anjaneyulu and Raju, 1987a). This compound exhibited antimicrobial activities against gram-positive and gram-negative bacteria (Madan et al., 2008) and cytotoxicity against colon cancer cell line (Jayaprakasha et al., 2009).

Table 9 ^{1}H and ^{13}C NMR chemical shift (in ppm) of *β*-sitosterol-3-*O*-*β*-D-glucopyranoside (in pyridine-d_5) (Moghaddam et al., 2006; Rai et al., 2006) and MEL-1 (in pyridine-d_5, 300 MHz)

Position	*β*-sitosterol-3-*O*-*β*-D-glucopyranoside		MEL-1	
	^{1}H (multiplicity, coupling constant (Hz))	^{13}C	^{1}H (multiplicity, coupling constant (Hz))	^{13}C
Aglycone				
1		37.4	1.10-1.55 (*m*)	38.0
2		30.2	1.10-1.55 (*m*)	30.0
3		78.5	3.94 (*m*)	79.1
4		39.9	1.67-2.17 (*m*)	39.5
5		140.8		141.4
6	5.31 (*m*)	121.9	5.37 (*m*)	122.4
7		32.1	1.67-2.17 (*m*)	32.6
8		32.0	1.67-1.88 (*m*)	32.5
9		50.3	1.10-1.55 (*m*)	50.8
10		36.9		37.4
11		21.2	1.10-1.55 (*m*)	21.8
12		39.3	1.10-1.55 (*m*)	39.8
13		42.4		42.8
14		56.8	1.10-1.55 (*m*)	57.3
15		24.5	1.67-1.88 (*m*)	25.0
16		28.5	1.67-2.17 (*m*)	29.0
17		56.2	1.10-1.55 (*m*)	56.7
18	0.67 (*s*)	11.9	0.67 (*s*)	12.4
19	0.93 (*s*)	19.4	0.95 (*s*)	19.9
20		36.3	1.67-2.17 (*m*)	36.9

Table 9 ^{1}H and ^{13}C NMR chemical shift (in ppm) of *β*-sitosterol-3-*O*-*β*-D-glucopyranoside (in pyridine-d_5) (Moghaddam et al., 2006; Rai et al., 2006) and MEL-1 (in pyridine-d_5, 300 MHz) (Continued)

Position	*β*-sitosterol-3-*O*-*β*-D-glucopyranoside		MEL-1	
	^{1}H (multiplicity, coupling constant (Hz))	^{13}C	^{1}H (multiplicity, coupling constant (Hz))	^{13}C
21	1.02 (*d*, 6.5)	19.0	1.00 (*d*, 6.3)	19.5
22		34.1	1.10-1.55 (*m*)	34.7
23		26.3	1.10-1.55 (*m*)	26.9
24		46.0	1.10-1.55 (*m*)	46.5
25		29.4	1.67-2.17 (*m*)	29.8
26		19.2	0.91 (*d*, 6.4)	19.7
27	0.86 (*d*, 7.7)	20.0	0.88 (*d*, 6.4)	19.7
28		23.3	1.10-1.55 (*m*)	23.9
29	0.90 (*t*, 7.0)	12.1	0.90 (*t*, 6.4)	12.4
Sugar				
1'		102.5	5.08 (*d*, 7.5)	103.1
2'		75.2	4.09 (*t*, 7.5)	75.8
3'		78.4	4.34 (*m*)	78.9
4'		71.6	4.34 (*m*)	72.2
5'		78.0	3.99 (*m*)	78.6
6'		62.8	A 4.60 (*br d*, 11.4)	63.3
			B 4.44 (*dd*, 11.4, 5.7)	

1.3 Identification of Flavonoids

1.3.1 Compound PGE-2 (kaempferol-3-*O*-*β*-D-galactopyranoside or trifolin)

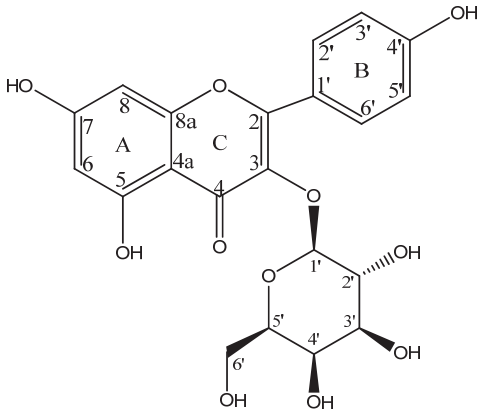

Figure 29 Structure of PGE-2

Compound PGE-2 was obtained as a pale orange powder. The HREIMS showed the $[M+Na]^+$ ion peak at *m/z* 449.1196 (Figure 84), corresponding to the molecular formula of $C_{21}H_{20}O_{11}$. The IR spectra showed OH stretching at 3600-3000 cm^{-1}, and C=O stretching at 1700-1600 cm^{-1} (Figure 85).

The ^{13}C-NMR, DEPT-135, and HMQC spectra (Figures 87, 88, and 90, Table 10) indicated twenty-one carbon atoms. There were one methylene, eleven methine, eight quaternary, and one carbonyl carbons. ^{1}H-NMR spectrum (Table 10, Figure 86) showed two protons of ring A at δ 6.17 and 6.54. Based on HMBC spectrum, their three bond correlations to carbon atoms of each other were observed (Figures 30 and 91, Table 11). Therefore, these protons were on *meta* position and they were assigned to H-6 and H-8, respectively. On ring B, symmetry aromatic protons which showed *ortho* coupling (*J*= 8.8 Hz.) were observed at δ 8.01(H-2' and H-6') and 6.85 (H-3' and H-5'). Then a hydroxyl functional group was substituted on C-4'. An anomeric proton appearing at δ 4.60 together with the signals in the range from δ 3.37 to 3.73, suggested the presence of a glycosyl moiety. Coupling constant of this proton (*J*=7.8 Hz) and its long-range correlation

with C-3 on ring C indicated the attachment of sugar moiety with *β*-orientation on this position (Agrawal, 1992). Identification of the sugar as galactose was based on ^{1}H NMR and COSY spectrum, compared to the preceding reports (Chen et al., 1991; Kim et al., 2002). ^{1}H and ^{13}C-NMR data of PGE-2 were compared with previous literature and assignments confirmed that this compound was trifolin or kaempferol-3-*O*-*β*-D-galactopyranoside (Chen et al., 1991; Kim et al., 2002) (Table 10). This compound has been previously isolated from *Pterospermum acerifolium* Willd., *P. suberifolium* L., *P. xylocarpum* (Gaertn.) Santapau & Wagh (Sterculiaceae) (Gunasegaran and Subramanian, 1979; Dan and Dan, 1988), *Cynanchum taiwanianum* T. Yamaza (Asclepiadaceae) (Chen et al., 1991), and *Prunus persica* Batsch (Rosaceae) (Kim et al., 2002). It has been reported that trifolin together with other flavonoid compounds, showed antioxidative activity on UVB-induced erythema formation in guinea pig skin with IC_{50} of 0.5 mg/cm^2 at 6 hr after UVB irradiation (Kim et al., 2002).

Table 10 ^{1}H and ^{13}C NMR chemical shift (in ppm) of trifolin (in DMSO-d_6) (Kim et al., 2002) and PGE-2 (in CD_3OD, 300 MHz)

Position	Trifolin		PGE-2	
	^{1}H (multiplicity, coupling constant (Hz))	^{13}C	^{1}H (multiplicity, coupling constant (Hz))	^{13}C
1				
2		156.4		163.4
3		133.2		126.0
4		177.5		184.2
4a		103.8		103.0
5		161.2		156.2
6	6.19 (*d*, 2.0)	98.8	6.17 (*br s*)	97.4
7		164.2		163.4
8	6.42 (*d*, 2.0)	93.7	6.54 (*br s*)	100.4
8a		156.3		156.2
1'		120.9		120.1
2'	8.06 (*d*, 8.0)	131.0	8.01 (*d*, 8.8)	127.3
3'	6.86 (*d*, 8.0)	115.0	6.85 (*d*, 8.8)	114.0
4'		159.9		159.9
5'	6.86 (*d*, 8.0)	115.0	6.85 (*d*, 8.8)	114.0
6'	8.06 (*d*, 8.0)	131.0	8.01 (*d*, 8.8)	127.3
Sugar	galactose			
1"	5.40 (*d*, 7.6)	101.7	4.60 (*d*, 7.8)	105.0
2"		71.2	3.49 (*m*)	72.5
3"		73.1	3.37 (*m*)	74.8
4"		67.9	3.37 (*m*)	67.7
5"		75.8	3.37 (*m*)	75.5
6"		60.2	A 3.73 (*dd*, 14.3, 3.1)	59.0
			B 3.68 (*dd*, 14.3, 3.1)	

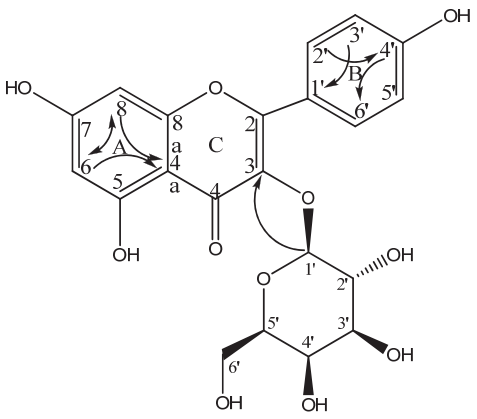

Figure 30 HMBC of PGE-2

Table 11 HMBC spectral data of PGE-2 (in CD_3OD, 300 MHz)

Position	^1H (multiplicity, coupling constant (Hz))	HMBC
6	6.17 (*s*)	C-4a, C-8
8	6.54 (*s*)	C-4a, C-6
2', 6'	8.01 (*d*, 8.8)	C-4'
3', 5'	6.85 (*d*, 8.8)	C-1'
1"	4.60 (*d*, 7.8)	C-3

1.3.2 Compound PGE-1 (kaempferol-3-*O*-*β*-D-6''(4-hydroxy-*E*-cinnamoyl)-glucopyranoside or tiliroside)

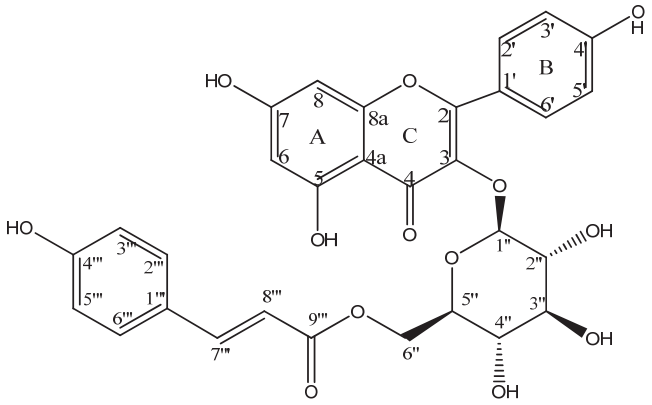

Figure 31 Structure of PGE-1

Compound PGE-1 was obtained as a pale yellow powder. The HRESI-MS spectrum showed the $[M+Na]^+$ ion peak at *m/z* 617.1126 (Figure 76), corresponding to the molecular formula of $C_{30}H_{26}O_{13}$. IR bands at 3455-3287, 1684, and 1606 cm^{-1} suggested a hydroxyl group, a carbonyl group, and an olefinic group, respectively (Figure 77).

The ^{13}C-NMR, DEPT-135, and HMQC spectra (Figures 79, 80, and 82, Table 12) of PGE-1 exhibited one methylene, seventeen methine, ten quaternary, and two carbonyl carbons. Spectroscopic data of this compound composed with the moieties kaempferol, glucose, and *p*-coumaroyl acid. The structure of kaempferol was identified in the same manner as compound PGE-2. The two *meta* protons on ring A were identified by signals in ^{1}H-NMR and COSY (Figures 78 and 81, Table 12) at δ 6.26 (*d*, *J*=2.1 Hz, H-6) and 6.49 (*d*, *J*=2.1 Hz, H-8). The two equivalent sets of *ortho*-coupling (*J*=10.5 Hz) protons on ring B was at δ 8.12 (H-2' and H-6') and δ 6.92 (H-3' and H-5'). The sugar part was identified as glucose based on its ^{1}H-NMR and COSY data. The coupling constant of its downfield anomeric proton (H-1") was 7.5 Hz. This proton displayed a long-range HMBC correlation (Figure 32, Table 13) to C-3. Then glucose was *β*-linkage to kaempferol at C-3 position.

The last part of the structure was *p*-coumaroyl acid. Its two pairs of *ortho* protons (*J*=8.9 Hz) were exhibited at δ 7.49 (H-2''' and H-5''') and 6.89 (H-3''' and H-6'''). A typical *trans*-configuration of the propenyl side chain was indicated by the coupling constant (*J*=15.9 Hz) between H-7''' and H-8'''. The carbonyl carbon signal at δ 166.3 displayed a long-range correlation, in HMBC experiment (Table 13), to H-6'' of glucose. Therefore, the *p*-coumaroyl moiety was connected to glucose at this position.

All data identified the compound PGE-1 as kaempferol-3-*O*-*β*-D-6''(4-hydroxy-*E*-cinnamoyl)-glucopyranoside or tiliroside. Its NMR data were comparable with those previously report (Adeloye et al., 2007) (Table 12). Tiliroside has been isolated from *Croton lobatus* Linn. (Euphorbiaceae) (Lagnika et al., 2009), *Potentilla chinensis* Ser. (Rosaceae) (Qiao et al., 2011), and *Waltheria indica* L. (Sterculiaceae) (Calderon-Montana et al., 2011). Tiliroside has been reported for antimalarial activity against *Plasmodium falciparum* with IC_{50} of 7.1 μM. This compound significantly decreased the level of blood sugar in alloxan-induced diabetic mice and streptozotocin-induced diabetic rat. It also exhibited increasing activity in HDL level and significant antioxidative activity (Lagnika et al., 2009)

Table 12 ^{1}H and ^{13}C NMR chemical shift (in ppm) of tiliroside (in DMSO-d_6) (Adeloye et al., 2007) and PGE-1 (in acetone-d_6, 300 MHz)

Position	Tiliroside		PGE-1	
	^{1}H (multiplicity, coupling constant (Hz))	^{13}C	^{1}H (multiplicity, coupling constant (Hz))	^{13}C
1				
2		156.7		148.7
3		133.4		134.0
4		177.7		172.4
4a		104.2		
5		161.2		
6	6.18 (*d*, 2.0)	99.1	6.26 (*d*, 2.1)	99.0
7		164.4		
8	6.38 (*d*, 2.0)	94.1	6.49 (*d*, 2.1)	93.8
8a		159.9		
1'		121.2		123.0
2'	7.98 (*d*, 8.8)	131.5	8.12 (*d*, 10.5)	131.2
3'	6.87 (*d*, 8.8)	115.0	6.94 (*d*, 10.5)	114.9
4'		159.8		160.0
5'	6.87 (*d*, 8.8)	115.0	6.94 (*d*, 10.5)	114.9
6'	7.98 (*d*, 8.8)	130.5	8.12 (*d*, 10.5)	127.3
sugar				
1"	5.48 (*d*, 7.8)	101.2	5.34 (*d*, 7.5)	103.6
2"		74.4	3.44 (*m*)	74.5
3"		76.4	3.44 (*m*)	77.2
4"		70.2	3.44 (*m*)	70.2
5"		74.5	3.44 (*m*)	74.6
6"		63.3	A 4.36 (*dd*, 11.7, 2.1) B 4.18 (*dd*,11.7, 6.0)	63.1
p-coumaryl				
1'''		125.7		126.0
2'''	7.37 (*d*, 8.6)	131.2	7.49 (*d*, 8.9)	130.0
3'''	6.70 (*d*, 8.6)	115.9	6.89 (*d*, 8.9)	115.8
4'''		160.2		160.0
5'''	6.58 (*d*, 8.9)	116.6	6.89 (*d*, 8.9)	115.8
6'''	7.55 (*d*, 8.7)	131.2	7.49 (*d*, 8.9)	144.6
7'''	7.34 (*d*, 15.9)	145.0	7.43(*d*, 15.9)	144.6
8'''	6.69 (*d*, 17.9)	113.9	6.17 (*d*, 15.9)	114.3
9'''		166.9		166.3

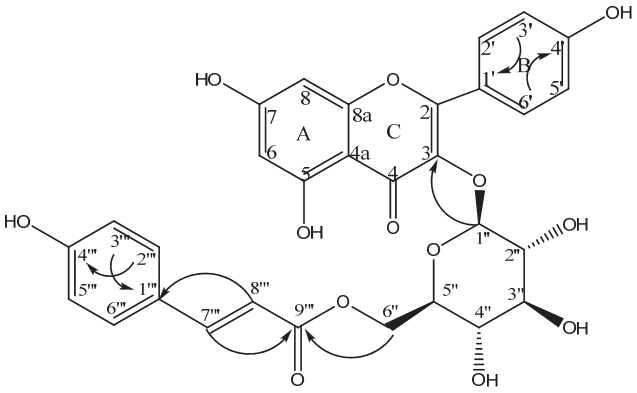

Figure 32 HMBC of PGE-1

Table 13 HMBC spectral data of PGE-1 (in acetone-d_6, 300 MHz)

Position	PGE-1	
	^{1}H (multiplicity, coupling constant (Hz))	HMBC
2', 6'	8.12 (*d*, 10.5)	C-4'
3', 5'	6.94 (*d*, 10.5)	C-1'
sugar		
1"	5.34 (*d*, 7.5)	C-3
6"	A 4.36 (*dd*, 11.7, 2.1), B 4.18 (*dd*, 11.7, 6.0)	C-9"'
p-coumaryl		
2"', 6"'	7.49 (*d*, 8.9)	C-4"',C-7"'
3"', 5"'	6.89 (*d*, 8.9)	C-1"'
7"'	7.43(*d*, 15.9)	C-9"'
8"'	6.17 (*d*, 15.9)	C-1"'

1.3.3 ompound PGE-3 ((-)-epicatechin)

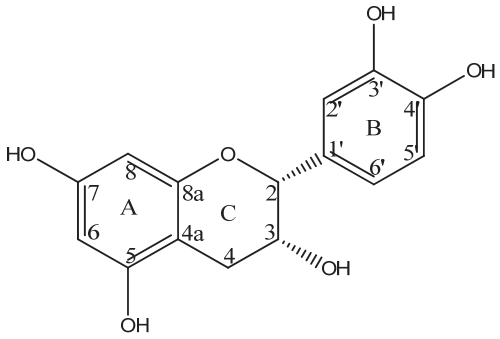

Figure 33 Structure of PGE-3

Compound PGE-3 was obtained as a light yellow amorphous powder. The HRESI-MS showed the $[M+H]^+$ ion peak at *m/z* 291.0938 (Figure 92), corresponding to the molecular formula of $C_{15}H_{14}O_6$. IR spectra presented absorption bands for broad OH stretching at 3600-3000 cm^{-1}, overtone of out of plane C-H bending at 2100-1800 cm^{-1}, and C=C stretching at 1650 cm^{-1} (Figure 93).

From ^{13}C-NMR, DEPT-135, and HMQC spectra (Figures 95, 96, and 98, Table 14), fifteen carbon atoms were classified into three groups. There were a methylene, seven methine, and seven quaternary carbons. In ^{1}H-NMR spectrum (Figure 94, Table 14), there were two methylene protons, two methine protons, and five aromatic protons. The small coupling constant (*J*=2.4 Hz) between two doublets at δ 5.84 and 5.81 revealed two *meta* coupling protons on ring A, corresponding to H-6 and H-8, respectively. Three protons on ring B were observed at δ 6.87 (*d*, *J*=1.7 Hz, H-2'), 6.65 (*d*, *J*=8.3 Hz, H-5'), and 6.77 (*dd*, *J*=8.3 and 1.7 Hz, H-6'), and their positiond were assigned based on their splitting patterns. Two methylene protons at δ 2.75 (H-4*α*, *dd*, *J*=16.0, 3.6 Hz) and 2.63 (H-4*β*, *dd*, *J*=16.0, 3.6 Hz) showed a geminal coupling between them and a vicinal coupling with the methine H-3 (δ 4.06, *ddd*). The other methine H-2 (δ 4.70, *br s*) also coupled with H-3 with a very small coupling constant of 1.5 Hz (Khallouki et al., 2007). This indicated that the dihedral angle between H-2 and H-3 was nearly

to 90^{o}. The connection of all parts of the structure was determined by HMBC experiment as shown in Figure 34 and Table 15. The optical rotation of this compound was levorotatory, then the compound PGE-3 was identified as (-)-epicatechin. Its NMR data were compared with previous reports (Cui et al., 1992; Khallouki et al., 2007), and shown in Table 14.

(-)-Epicatechin has been found in several plant families, such as Theaceae (Ogle, 2009) and Polygonaceae (Vrchotova et al., 2007). It has been isolated from *Theobroma cocoa* L. (Sterculiaceae) (Kofink et al., 2007) and *Guazuma ulmifolia* Lam (Sterculiaceae) (Lopes et al., 2009). For the family Sterculiaceae, this is the first report in genus *Pterospermum*. (-)-Epicatechin is a major polyphenolic compound of green tea. This compound showed antioxidative activities in LDL oxidation, ferric reducing antioxidant power (FRAP), but had less activity in DPPH assay (Xu et al., 2004).

Table 14 ^{1}H and ^{13}C chemical shift (in ppm) of (-)-epicatechin (in CD_3OD) (Cui et al., 1992; Khallouki et al., 2007) and PGE-3 (in CD_3OD, 300 MHz)

Position	(-)-epicatechin		PGE-3	
	^{1}H (multiplicity, coupling constant(Hz))	^{13}C	^{1}H (multiplicity, coupling constant (Hz))	^{13}C
1				
2	4.81 (*s*)	80.6	4.70 (*br s*)	78.5
3	4.18 (*ddd,* 4.6, 3.0, 1.5)	68.3	4.06 (*ddd*, 3.6, 3.6, 1.5)	66.1
4	2.85 (*dd*, 16.8, 3.0) 2.73 (*dd*, 16.8,4.6)	30.00	α 2.75 (*dd*, 16.0, 3.6) β 2.63 (*dd*, 16.0, 3.6)	27.8
4a		100.9		98.6
5		158.7		156.6
6	5.93 (*d*, 2.4)	97.2	5.84 (*d*, 2.4)	94.9
7		158.4		156.3
8	5.91 (*d*, 2.4)	96.7	5.81 (*d*, 2.4)	94.5
8a		158.1		155.9
1'		133.0		130.8
2'	6.97 (*d*, 1.8)	116.1	6.87 (*d*, 1.7)	113.9
3'		146. 7		144.5
4'		146.5		144.4
5'	6. 75 (*d*, 8.3)	116.7	6.65 (*d*, 8.3)	114.5
6'	6. 79 (*dd*, 8.2, 1.8)	120.2	6.77 (*dd*, 8.3, 1.7)	117.9

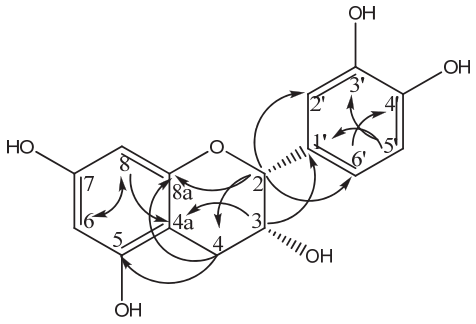

Figure 34 HMBC of PGE-3

Table 15 HMBC spectral data of PGE-3 (in methanol-d_4, 300 MHz)

Position	^{1}H (multiplicity, coupling constant (Hz))	HMBC
2	4.70 (*br s*)	C-4, C-8a, C-2', C-6'
3	4.06 (*br s*)	C-4a, C-1'
4	2.63 (*d*, 16.0, 4.0)	C-2, C-8a, C-5
	2.75 (*d*, 16.0, 4.0)	
6	5.84 (*d*, 2.4)	C-8
8	5.81 (*d*, 2.4)	C-4a, C-6
2'	6.87 (*d*, 1.7)	C-2, C-6', C-4'
5'	6.65 (*d*, 8.3)	C-1', C-3'
6'	6.77 (*d*, 8.3, 1.7)	C-2, C-2' ,C-4'

1.4 Identification of Neolignan derivatives

1.4.1 Compound MHL-3 or MDL-2 or MHT-2 ((2*R*,3*R*)-2,3-dihydro-2-(4'-hydroxyphenyl)-3-methyl-5-[1-(*E*)-propenyl] benzofuran or conocarpan)

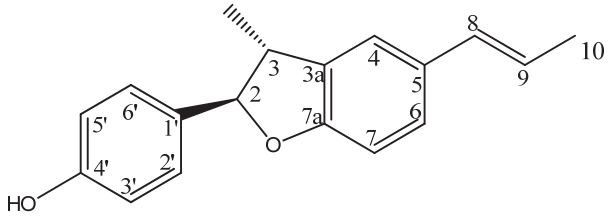

Figure 35 Structure of MHL-3 or MDL-2

Compound MHL-3 and MDL-2 and MHT-2 was obtained as a colorless plate crystal. There were identified as the same compound. The HRESI-MS displayed the $[M+Na]^+$ ion peak at *m/z* 289.1130 (Figure 110), representing the molecular formula of $C_{18}H_{18}O_2$. The IR spectra presented OH stretching at 3374 cm^{-1}, C-H stretching at 2960 cm^{-1}, overtone of out of plane C-H bending at 1879-1770 cm^{-1}, C-H stretching at 1614-1598 cm^{-1}, and C-O streching at 1239 cm^{-1} (Figure 111).

^{13}C NMR and DEPT-135 spectra (Figures 113 and 114, Table 16) indicated five quaternary, eleven methine, and two methyl carbons. ^1H NMR spectrum (Figures 112, Table 16) exhibited signals of seven aromatic, two methyl groups, two olefinic and two methine protons. The following signals were investigated from COSY spectra (Figure 115). The coupling of a *quintet* signal at δ 3.38 with oxymethine proton at δ 5.07 and methyl protons at δ 1.37 suggested a dihydrobenzofuran neolignan derivative, when comparison with the published data (Agrawal and Thakur, 1985; Achenbach et al., 1987). From ^1H NMR spectrum, signals of H-6 and H-7 on the dihydrobenzofuran ring based on their *ortho* coupling (*J*=7.9 Hz) were assigned to δ 7.11 and 6.78, respectively, whereas the singlet at δ 7.10 was assigned as H-4. The coupling pattern among H-8 (*dd*, *J*= 15.6, 1.5 Hz), H-9 (*dq*, *J*= 15.6, 6.6 Hz) and CH_3-10 (*dd*, *J*= 6.6, 1.5 Hz) suggested a vinyl side

chain. The coupling constant of 15.6 Hz between H-8 and H-9 implied the *trans* configuration. The three bond HMBC correlations (Figure 36, Table 17) from H-8 to C-4 and C-6, and from H-9 to C-5 confirmed that the substitution of this side chain was at C-5 position.

A para substituted phenyl group was the other substitution on the dihydrobenzofuran structure. Two pairs of symmetric *ortho* coupling (*J*=7.6 Hz) aromatic protons (H-2'/H-6' and H-3'/H-5') were shown on the ^{1}H NMR spectrum. HMBC correlation (Figure 36, Table 17) from both H-2' and H-6' to C-2 and from H-2 to C-2' and C-6' indicated that this phenyl group was at position 2. While at position 3, a methyl group was identified from its doublet signal coupling with H-3. Based on the coupling constant between H-2 and H-3 (*J*=8.1 Hz), orientation of this methyl group was in the opposite direction to a phenyl group. Dextrorotatory rotation of compound MHL-3 was proven by a polarimetric method with the $[\alpha]_{\mathrm{D}}^{25}$ +122.68. Therefore, comparing with the previous published data (Achenbach et al., 1987), absolute configurations at C-2 and C-3 were concluded as 2*R* and 3*R*.

From all of the above data, compound MHL-3 was identified as a neolignan conocarpan or (2*R*,3*R*)-2,3-dihydro-2-(4'-hydroxyphenyl)-3-methyl-5-[1-(*E*)-propenyl]benzofuran. Conocarpan has been found from *Krameria cystisoides* Cav. (Krameriaceae) (Seo et al., 2004) and *Piper solmsianum* C.DC (Kato and Furlan, 2007), *Piper regnellii* C.DC. (Piperaceae) (Luize et al., 2006), and *Miliusa mollis* Pierre (Annonaceae) (Sawasdee et al., 2010). This compound was reported for the first time in *Mitrephora*. Reported biological activities of conocarpan were such as antibacterial, antifungal, and antiprotozoal in Table 18 (Luize et al., 2006).

Table 16 ^{1}H and ^{13}C chemical shift (in ppm) of conocarpan (in $CDCl_3$) (Achenbach et al., 1987) and MHL-3 (in $CDCl_3$, 300 MHz)

Position	Conocarpan		MHL-3	
	^{1}H (multiplicity, coupling constant (Hz))	^{13}C	^{1}H (multiplicity, coupling constant (Hz))	^{13}C
1				
2	5.00 (*d*, 8.8)	93.1	5.07 (*d*, 8.1)	92.7
3	3.30 (*m*)	45.5	3.38 (*quintet*, 8.1)	45.1
3-CH_3	1.28 (*d*, 6.8)	17.9	1.37 (*d*, 6.9)	17.8
3a		133.1		132.4
4	7.02 (*m*)	121.4	7.10 (*br s*)	120.8
5		131.6		131.3
6	7.02 (*m*)	126.7	7.11 (*d*, 7.9)	126.3
7		109.4	6.78 (*d*, 7.9)	109.3
7a		159.0		158.1
8	6.30 (*d*, 16)	131.6	6.36 (*dd*, 15.6, 1.5)	130.7
9	6.08 (*m*)	122.7	6.08 (*dq*, 15.6, 6.6)	123.1
10	1.78 (*d*, 5.0)	18.3	1.85 (*dd*, 6.6, 1.5)	18.4
1'		132.3		132.6
2'	7.27 (*d*, 8.5)	128.2	7.25 (*d*, 7.6)	127.9
3'	6.78 (*d*, 9)	115.9	6.75 (*d*, 7.6)	115.5
4'		157.8		155.7
5'	6.78 (*d*, 9)	115.9	6.75 (*d*, 7.6)	115.5
6'	7.27 (*d*, 8.5)	128.2	7.25 (*d*, 7.6)	127.9

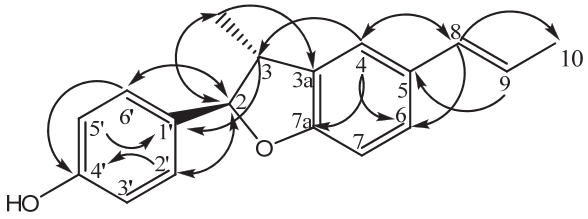

Figure 36 HMBC of MHL-3 or MDL-2

Table 17 HMBC spectral data of MHL-3 (in $CDCl_3$, 300 MHz)

Position	^1H	HMBC
2	5.07	3-$\underline{C}H_3$, C-2', C-6'
3	3.38	C-1'
3-CH_3	1.37	C-2, C-3a
4	7.10	C-3, C-6, C-7a, C-8
6	7.11	C-4
7	6.75	C-3a, C-5
8	6.36	C-4, C-6, C-9, C-10
9	6.08	C-5, C-10
10	1.85	C-8, C-9
2', 6'	7.25	C-2, C-4'
3', 5'	6.78	C-1'

Table 18 Biological activities of conocarpan.

Activity	Bacteria/Cell line name	Concentration used	Result	Reference
Antibacterial				
agar plate	*Bacillus subtilis*	200 µg/disc		Arnone et al., 1988
	Bacillus subtilis		IC_{50} 0.19 mg/ml	Arnone et al., 1988
	Escherichia coli	200 µg/disc		Arnone et al., 1988
	Escherichia coli		MIC 0.19 mg/ml	Ahmad et al., 1998
	Pseudomonas aeruginosa		IC_{50} 0.19 mg/ml	Ahmad et al., 1998
	Staphylococcus aureus		IC_{50} 0.38 mg/ml	Ahmad et al., 1998
Antifungal				
agar plate	*Aspergillus niger*	200 µg/disc		Arnone et al., 1988
	Microsporum gypseum		MIC 4.0 mg/ml	Freixa et al., 2001
	Trichophyton mentagrophytes		MIC 8.0 mg/ml	Freixa et al., 2001
Antiyeast				
agar plate	*Saccharomyces cerevisiae*	200 µg/disc		Arnone et al., 1988
	Saccharomyces cerevisiae		MIC 16.0 mg/ml	Freixa et al., 2001
	Candida albican		MIC 8.0 mg/ml	Freixa et al., 2001
	Cryptococcus neoformans		MIC 16.0 mg/ml	Freixa et al., 2001
Insecticide				
	Aedes atropalpus	10.0 µg/ml		Chauret et al., 1996

Table 18 Biological activities of conocarpan (Continued).

Activity	Bacteria/Cell line name/method	Concentration used	Result	Reference
Cytotoxic				
cell culture	CA-Human breast BC-1		ED_{50}> 20.0 µg/ml	Rimando et al., 1994
	fibrosarcoma HT-1080		ED_{50}> 20.0 µg/ml	Rimando et al., 1994
	CA-human lung LU-1		ED_{50} 17.6 µg/ml	Rimando et al., 1994
	melanoma SK MEL-2		ED_{50}> 20.0 µg/ml	Rimando et al., 1994
	CA-human colon COL-1		ED_{50}> 15.7 µg/ml	Rimando et al., 1994
	CA-9KB		ED_{50}> 20.0 µg/ml	Rimando et al., 1994
	LEUK-P388		ED_{50} 3.0 µg/ml	Rimando et al., 1994
	CA-A-431		ED_{50}> 20.0 µg/ml	Rimando et al., 1994
	CA-LNCAP		ED_{50}> 20.0 µg/ml	Rimando et al., 1994
	CA-Mammay ZR75		ED_{50} 8.7 µg/ml	Rimando et al., 1994
	Glioblastoma U-373		ED_{50}> 20.0 µg/ml	Rimando et al., 1994
Hemolysis inhibitory				
	Copper oxide induced hemolysis		IC_{50} 0.77 µg/ml	Carini et al., 2002
	UVB-induced hemolysis		IC_{50} 3.8 µg/ml	Carini et al., 2002

1.4.2 Compound MHL-1 ((2*R*,3*R*)-2,3-dihydro-2-(4'-methoxy phenyl)-3-methyl-5-[1-(*E*)-propenyl]benzofuran or methyl conocarpan)

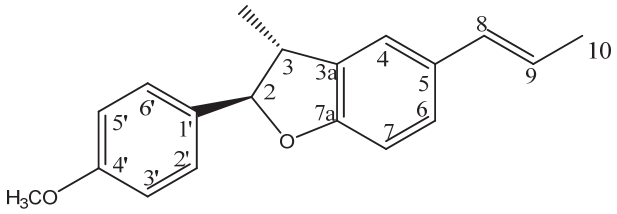

Figure 37 Structure of MHL-1

Compound MHL-1 was acquired as a colorless needle crystal. Its molecular formula was determined as $C_{19}H_{20}O_2$, according to the $[M+Na]^+$ ion peak in HRESI-MS at m/z 303.1295 (Figure 100). IR spectra showed bands of CH stretching at 2996-2839 cm^{-1}, overtone of out of plane C-H bending at 2025-1763 cm^{-1}, C=C stretching at 1610 cm^{-1}, and C-H bending at 1481 cm^{-1} (Figure 101).

Both ^1H and ^{13}C NMR data of MHL-1 (Figures 102 and 103, Table 19) and MHL-3 were very similar, except that the NMR data of MHL-1 showed a singlet signal at δ 3.80 (3H) and a quaternary carbon at δ 55.3 (4'-O<u>C</u>H_3). These signals implied a presence of a methoxy group in MHL-1, whereas the hydroxyl stretching bands observed in the IR spectra of MHL-3 was absent (Figure 101). The arrangement of aromatic protons of MHL-1 was in accordance with MHL-3, indicating the methoxy substitution on C-4'. Since both MHL-1 and MHL-3 showed equal number of aromatic protons on ^1H NMR spectrum, the methoxy substitution was suggested on C-4'. Dextrorotatory rotation of compound MHL-3 was proven by a polarimetric method with the $[\alpha]_D^{25}$ +129.43.

Comparison to the previous report, this compound was identified as (2*R*,3*R*)-2,3-dihydro-2-(4'-methoxyphenyl)-3-methyl-5-[1-(*E*)-propenyl]benzofuran or methyl conocarpan. The compound showed weak antibacterial activity (Pessini et al., 2003), and low activity against *Trypanosoma cruzi* with IC_{50} 24.5±2.1 μg/ml (Luize et al., 2006). It has been semi-synthesized from conocarpan and was identified to be 2*R*,3*R* configuration (Achenbach et al.,

1991), whereas its 2*S*,3*S* isomer was recently found (Sawasdee et al., 2010). NMR spectra of both configurations were similar, but their physical properties were different. For example, the 2*R*,3*R* was crystalline and insoluble in DMSO, while the 2*S*,3*S* was oil. The specific rotation of 2*R*, 3*R* was dextrorotatory, but that of 2*S*,3*S* was levorotatory. Thus, compound MHL-1 was (2*R*,3*R*)-2,3-dihydro-2-(4'-methoxyphenyl)-3-methyl-5-[1-(*E*)-propenyl]benzofuran. Moreover, this compound was isolated from nature for the first time.

Table 19 ^{1}H and ^{13}C chemical shift (in ppm) of methyl conocarpan (in $CDCl_3$) (Achenbach et al., 1991) and MHL-1(in $CDCl_3$, 300 MHz)

Position	methyl conocarpan		MHL-1	
	^{1}H (multiplicity, coupling constant(Hz))	^{13}C	^{1}H (multiplicity, coupling constant (Hz))	^{13}C
1				
2	5.10 (*d*, 9.0)	93.2	5.08 (*d*, 7.4)	92.7
3	3.36 (*m*)	46.0	3.39 (*quintet*, 7.4)	45.2
3-CH_3	1.39 (*d*, 7.0)	18.4[a]	1.38 (*d*, 7.0)	17.8
3a		132.1; 133.5; 133.9[b]		132.7
4	7.0-7.2 (*m*)	121.8	7.10 (*s*)	120.7
5		132.1; 133.5; 133.9[b]		131.2
6	7.0-7.2 (*m*)	127.1	7.12 (*d*, 8.2)	126.3
7	6.69 (*d*, 8.0)-	109.7	6.76 (*d*, 8.2)	109.3
7a		159.4, 160.7[c]		159.7
8	6.35 (*dm*, 16.0)	131.9	6.36 (*dd*, 15.7, 1.5)	130.8
9	5.9-6.2 (*m*)	123.1	6.09 (*dq*, 15.7, 6.4)	122.9
10	1.82 (*br d*, 5.0)	18.2[a]	1.85 (*dd*, 6.4, 1.5)	18.4
1'		132.1; 133.5; 133.9[b]		132.4
2'	7.38	128.4	7.34 (*d*, 8.7)	127.6
3'	6.95	114.8	6.90 (*d*, 8.7)	114.0
4'		159.4, 160.7[c]		158.3
5'	6.95	114.8	6.90 (*d*, 8.7)	114.0
6'	7.38	128.4	7.34 (*d*, 8.7)	127.6
4'-OCH_3	3.81 (*s*)	55.6	3.80 (*s*)	55.3

[a, b, c] interchangeable assignments

1.4.3 Compound MHL-2 or MDL-1 or MHT-1 ((2*R*,3*R*)-2,3-dihydro-2-(4'-hydroxy-3'-methoxyphenyl)-3-methyl-5-[1-(*E*)-propenyl]benzofuran or 3'-methoxy conocarpan)

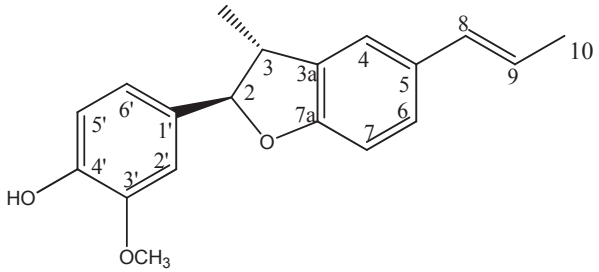

Figure 38 Structure of MHL-2 or MDL-1 or MHT-1

MHL-2 and MDL-1 and MHT-1 were obtained as a white amorphous powder. They were identified as the same compound. The HRESI-MS exhibited the $[M+Na]^+$ ion peak at *m/z* 319.1264 (Figure 104), corresponding to the molecular formula of $C_{19}H_{20}O_3$. IR spectra showed absorption bands for OH stretching at 3382 cm^{-1}, C-H stretching at 2963 cm^{-1}, overtone of out of plane C-H bending at 2058-1650 cm^{-1}, C=C stretching at 1610 cm^{-1}, and C-H bending at 1481 cm^{-1} (Figure 105).

The ^1H and ^{13}C NMR spectra of compound MHL-2 (Figure 106 and 107, Table 20) were quite similar to those of compounds MHL-1 and MHL-3. So, it was classified as a dihydrobenzofuran neolignan derivative.

From ^1H NMR spectrum, protons between H-5' and H-6' on the phenyl ring showed an *ortho* coupling constant of 6.0 Hz. Both ^1H and ^{13}C NMR data showed a singlet signal at δ 3.86 (3H) and a quaternary carbon at δ 55.9 (3'-O<u>C</u>H_3) which implied a methoxy group in this structure. From long range HMBC correlations (Table 21, Figures 39, 109), it was found that a quaternary carbon at δ 146.8 (C-3') was not only correlated to H-5', but also to methoxy protons. Thus, the substitution on C-3' implied a methoxy group. Correlation of aromatic protons at H-2' and H-6' was with a quaternary carbon on C-4'. The other substution on C-4' was suggested as a hydroxyl group. Then, signal at δ 6.90 (H-2') implied *meta*

position with H-6' with small coupling constant. The correlation between H-2 and two methine carbons as C-2' and C-6' confirmed the connection of the dihydrobenzofuran moiety on C-1' of the phenyl ring.

MHL-2 was identified as (2*R*,3*R*)-2,3-dihydro-2-(4'-hydroxy-3'-methoxyphenyl)-3-methyl-5-[1-(*E*)-propenyl]benzofuran or 3'-methoxy conocarpan by comparing with the previous report (Achenbach et al., 1987). This compound has been isolated from *Krameria cytisoides* Cav. (Achenbach et al., 1987), *Piper regnellii* (Miq.) C.CD. (Benevides et al., 1999), and *Miliusa mollis* Pierre var. sparsior Caib (Sawasdee et al., 2010).

Table 20 ^{1}H and ^{13}C chemical shift (in ppm) of 3'-methoxy conocarpan (in $CDCl_3$) (Achenbach et al., 1987) and MHL-2 (in $CDCl_3$, 300 MHz)

Position	3'-methoxy conocarpan		MHL-2	
	^{1}H (multiplicity, coupling constant (Hz))	^{13}C	^{1}H (multiplicity, coupling constant (Hz))	^{13}C
1				
2	5.08 (*d*, 9.3)	93.0	5.06 (*d*, 8.4)	93.1
3	3.35 (*m*)	45.2	3.40 (*quintet*, 8.4)	45.3
3-CH_3	1.37 (*d*, 7.1)	17.8	1.39 (*d*, 6.6)	17.6
3a		132.5		132.4
4	7.09 (*d*, 2.0)	120.7	7.14 (*s*)	120.7
5		131.4		131.3
6	6.84 (*d*, 8.5)	126.2	7.12 (*d*, 8.1)	126.3
7	6.91 (*dd*, 8.5, 2.0)	109.2	6.77 (*d*, 8.1)	109.3
7a		158.3		158.3
8	6.38 (*dd*, 15.7, 2.0)	130.9	6.37 (*dd*, 15.8, 1.4)	130.8
9	6.10 (*dq*, 15.7, 6.4)	122.9	6.09 (*dq*, 15.8, 6.5)	123.1
10	1.83 (*dd*, 6.4, 2.0)	18.2	1.86 (*dd*, 6.5, 1.4)	18.4
1'		132.3		132.4
2'	6.70 (*d*, 8.3)	108.7	6.90 (*br s*)	108.6
3'		146.8		146.8
4'		145.8		145.8
5'	7. 13 (*dd*, 8.3, 1.5)	114.3	6.92 (*d*, 6.0)	114.0
6'	7. 24 (*s*)	119.5	6.95 (*d*, 6.0)	119.7
3'-OCH_3	3.85(*s*)	55.9	3.86 (*s*)	55.9

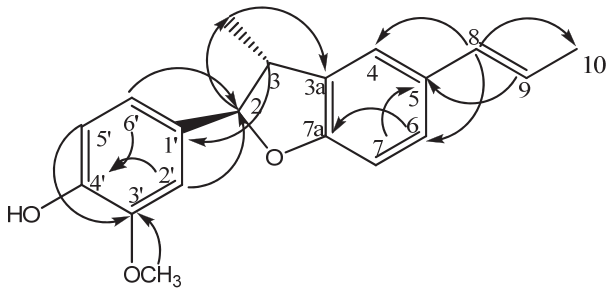

Figure 39 HMBC of MHL-2 or MDL-1

Table 21 HMBC spectral data of MHL-2 (in $CDCl_3$, 300 MHz)

Position	^1H	HMBC
2	5.06	3-$\underline{C}H_3$, C-2', C-6'
3	3.40	C-1'
3-CH_3	1.39	C-2, C-3a
4	7.14	C-7a, C-8
6	7.12	C-7a
7	6.77	C-5
8	6.37	C-4, C-6, C-10
9	6.09	C-5
10	1.86	C-8
2'	6.90	C-2, C-4'
5'	6.92	C-1', C-3'
6'	6.95	C-2, C-4'
3'-OCH_3	3.86	C-3'

1.5 Identification of Phenolic Amides

1.5.1 Compound MET-1 (*N-p*-coumaroyltyramine)

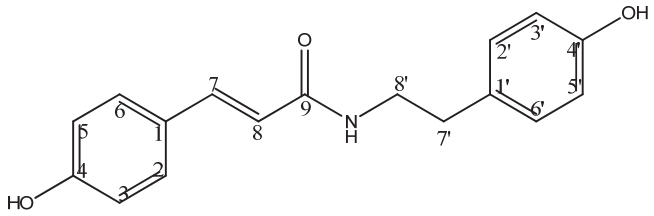

Figure 40 Structure of MET-1

Compound MET-1 was obtained as a white amorphous powder. The HRESI-MS spectra showed the $[M+Na]^+$ ion peak at *m/z* 306.1050 (Figure 124), corresponding to the molecular formula of $C_{17}H_{17}NO_3$. A calculated molecular weight of MET-1 compound was an odd number of 283.1050 amu which implied a presence of nitrogen atom in the structure. IR spectra presented a broad NH and OH stretching at 3433 cm^{-1}, overtone of out of plane C-H bending at 2080-1717 cm^{-1}, α, β-conjugated C=O stretching at 1660 cm^{-1}, C=C stretching at 1581 cm^{-1}, CH bending at 1448 cm^{-1}, and C-O stretching at 1242 cm^{-1} (Figure 125).

The ^{13}C-NMR and DEPT-135 spectra (Figures 127 and 128, Table 22) displayed two methylene carbons, ten methine carbons, four quaternary carbons, and one carbonyl carbon. The ^{1}H-NMR spectrum (Figures 126, Table 22) exhibited eight aromatic, two vinyl, and four methylene protons. Additionally, a broad singlet signal at δ 4.61 was identified as NH (Friebolin, 1993). Thus, MET-1 compound was suggested to contain an amide group by IR and NMR spectra. In ^{1}H NMR spectrum, signals at δ 7.41 (H-2 and H-6) and 6.80 (H-3 and H-5) were assigned to two pairs of symmetric aromatic protons with the *ortho* coupling constant of 8.5 Hz. Another pair of two proton doublets at δ 7.07 (H-2' and H-6') and 6.73 (H-3' and H-5') with the *ortho* coupling constant of 8.1 Hz were assigned to protons on the other phenyl ring. From COSY spectra (Figure 129), the coupling constant of 15.9 Hz between the methine protons at δ 7.48 (H-7) and δ 6.39 (H-8) suggested the *trans* configuration of these two vinylic protons. Moreover, two

coupled triplets (J = 7.2 Hz) at δ 3.47 (H-8') and 2.76 (H-7') corresponded to four methylene protons. The long range HMBC (Figures 41 and 131, Table 23) showed correlations between H-8 and two quaternary carbons at δ 126.3 (C-1) and at δ 167.8 (C-9) which implied a vinyl substitution on C-1 of the *p*-coumaroyl part. Whereas the correlations between a proton at δ 2.76 (H-7') and aromatic carbons (C-2' and C-6'), a proton at δ 7.07 (H-2') and a quaternary carbon (C-4') showed the presence of a tyramine moiety. The molecular formula implied that there were two more hydroxyl groups. The HMBC correlations between protons at δ 7.41 (H-2 and H-6) and a quaternary carbon C-4 and between protons at δ 7.07 (H-2' and H-6') and a quaternary carbon (C-4') indicated the hydroxyl substitution on these two quaternary carbons (C-4 and C-4'). Two units between a tyramine and a coumaroyl parts were connected by HMBC correlation between a proton at δ 3.47 (H-8') and a carbonyl carbon (C-9).

Comparison of ^{1}H and ^{13}C spectra with previous report (Treeratanapiboon et al., 2011), this compound was identified as *N-p*-coumaroyltyramine or paprazine. This compound was found in other families such as Solanaceae (*Datura metel* L.) (Yang et al., 2010), Rutaceae (*Aegle marmelos* (L.) Corr. Serr.) (Lambole, 2010), and Aristolochiaceae (*Aristolochia gigantea* Mart.) (Holzbach and Lopes, 2010). In Annonaceae, it had been isolated from *Annona glabra* Linn. (Chang et al., 2000), *A. montana* Macfad. (Wu et al., 1995) and *Mitrephora thorelii* Pierre (Ge et al., 2008). *N*-coumaroyltyramine was able to completely inhibit arachidonic acid induced platelet aggregation at the concentration of 60 μM. The IC_{50} for the cytotoxicity against P-388 cell line was 2.26 μg/ml (Wu et al., 1995).

Table 22 ^{1}H and ^{13}C chemical shift (in ppm) of *N*-*p*-coumaroyltyramine or paprazine (in CD_3OD) (Treeratanapiboon et al., 2011) and MET-1 (in CD_3OD, 300 MHz)

Position	*N*-*p*-coumaroyltyramine		MET-1	
	^{1}H (multiplicity, coupling constant(Hz))	^{13}C	^{1}H (multiplicity, coupling constant (Hz))	^{13}C
1		127.6		126.3
2	7.39 (*d*, 8.6)	130.4	7.41 (*d*, 8.5)	129.1
3	6.78 (*d*, 8.6)	116.6	6.80 (*d*, 8.5)	115.3
4		160.3		159.1
5	6.78 (*d*, 8.6)	116.6	6.80 (*d*, 8.5)	115.3
6	7.39 (*d*, 8.6)	130.4	7.41 (*d*, 8.5)	129.1
7	7.44 (*d*, 15.7)	141.7	7.48 (*d*, 15.9)	140.5
8	6.37 (*d*, 15.7)	118.3	6.39 (*d*, 15.9)	117.0
9		169.1		167.8
1'		131.2		129.9
2'	7.04 (*d*, 8.5)	130.6	7.07 (*d*, 8.1)	129.3
3'	6.72 (*d*, 8.5)	116.2	6.73 (*d*, 8.1)	114.8
4'		156.7		155.5
5'	6.72 (*d*, 8.5)	116.2	6.73 (*d*, 8.1)	114.8
6'	7.04 (*d*, 8.5)	130.6	7.07 (*d*, 8.1)	129.3
7'	2.75 (*t*, 7.4)	35.7	2.76 (*t*, 7.2)	34.4
8'	3.46 (*t*, 7.4)	42.4	3.47 (*t*, 7.2)	41.2

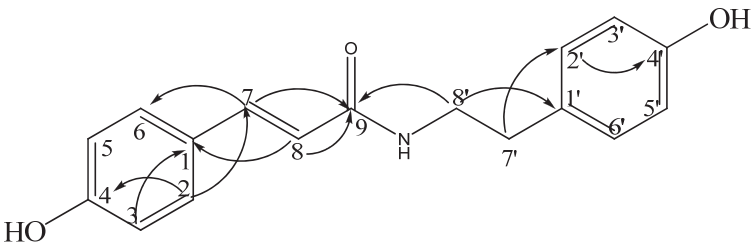

Figure 41 HMBC of MET-1

Table 23 HMBC spectral data of MET-1 (in CD_3OD, 300 MHz)

Position	^1H (multiplicity, coupling constant (Hz))	HMBC
2	7.41 (*d*, 8.5)	C-4, C-7
3	6.80 (*d*, 8.5)	C-1
5	6.80 (*d*, 8.5)	
6	7.41 (*d*, 8.5)	
7	7.45 (*d*, 15.9)	C-6, C-9
8	6.39 (*d*, 15.9)	C-1
2'	7.07 (*d*, 8.1)	C-4'
3'	6.73 (*d*, 8.1)	C-1', C-4'
5'	6.73 (*d*, 8.1)	
6'	7.07 (*d*, 8.1)	
7'	2.76 (*t*, 7.2)	C-2'
8'	3.47 (*t*, 7.2)	C-1', C-9

1.5.2 Compound MET-2 (*N*-caffeoyltyramine)

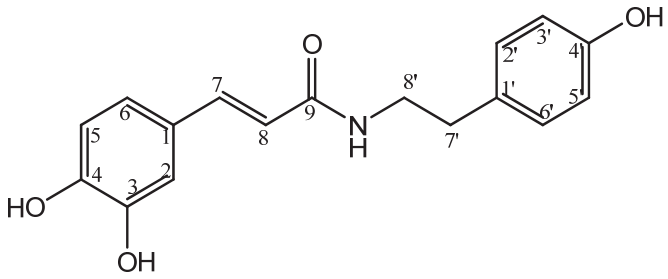

Figure 42 Structure of MET-2

Compound MET-2 was obtained as a yellow amorphous powder. The HRESI-MS spectra showed the $[M+Na]^+$ ion peak at *m/z* 322.1061 (Figure 132), which corresponded to the molecular formula of $C_{17}H_{17}NO_4$. IR spectra exhibited broad NH and OH stretching at 3333 cm^{-1}, overtone of out of plane C-H bending at 1887 cm^{-1}, α, β-conjugated C=O stretching at 1646 cm^{-1}, C=C stretching at 1581 cm^{-1}, CH bending at 1447 cm^{-1}, and C-O stretching at 1249 cm^{-1} (Figure 133).

The NMR spectra of MET-2 (Tables 24 and 25) indicated that it contained similar tyramine moiety as that of MET-1, but instead of connecting to a *p*-coumaroyl moiety, it was replaced by *p*-cafferoyl moiety which has two *ortho* hydroxyl groups.

In ^{13}C and DEPT-135 spectra (Figures 135 and 136, Tables 24), there were two methylene, nine methine, and six quaternary carbons. The ^1H NMR spectrum (Figure 134) displayed proton signals which were seven aromatic protons, two vinylic protons, and four methylene protons. The structure of tyramine moiety was identified in the same manner as MET-1. For the *p*-cafferoyl moiety, the *ortho* coupling between H-5 and H-6 presented a doublet signal with a coupling constant of 8.2 Hz, whereas the *meta* coupling between H-6 and H-2 showed a doublet signal with a coupling constant of 1.9 Hz. The HMBC correlation (Figures 43 and 139) confirmed the connction between the carbonyl, the vinyl, and the phenyl group of the *p*-cafferoyl moiety. The correlations were between a proton at δ 6.63 (H-5) and

a quaternary carbon (C-3) and between a proton at δ 6.86 (H-2) and a quaternary carbon (C-4) were also found. Moreover, the molecular formular suggested two other hydroxyl groups in the molecule and from the HMBC correlation, they indicated that these two hydroxyl groups were substituted on C-3 and C-4.

Compound MET-2 was identified as *N*-caffeoyltyramine or typheramide by comparison with published reports (Han et al., 2002; Yang et al., 2010; Park, 2011). This compound has been found in *Allium sativum* L., *Allium fistulosum* L. (Alliaceae) (Park, 2011), and *Lycium chinenses* Miller (Solanaceae) (Han et al., 2002). *N*-caffeoyltyramine completely inhibited arachidonic acid induced platelete aggregation and showed cytotoxicity against P-388 cell line (Wu et al., 1995). Moreover, this compound inhibited both COX (cyclooxygenase)-1 and COX-2 enzymes (Park, 2011). For Annonaceous family, this compound was isolated from *Annona montana* (Wu et al., 1995), and *Mitrephora thorelii* (Ge et al., 2008).

Table 24 ^{1}H and ^{13}C NMR chemical shift (in ppm) of *N*-caffeoyltyramine (in CD_3OD) (Yang et al., 2010) and MET-2 (in CD_3OD, 300 MHz)

Position	*N*-caffeoyltyramine		MET-2	
	^{1}H (multiplicity, coupling constant (Hz))	^{13}C	^{1}H (multiplicity, coupling constant (Hz))	^{13}C
1		128.3		128.3
2	6.99 (*d*, 2.0)	115.1	6.86 (*d*, 1.9)	115.1
3		146.7		146.7
4		148.7		148.7
5	6.76 (*d*, 8.3)	116.5	6.63(*d*, 8.2)	116.5
6	6.89 (*dd*, 8.3, 2.0)	122.1	6.77 (*dd*, 8.2, 1.9)	122.1
7	7.38 (*d*, 15.7)	142.1	7.24 (*d*, 15.7)	142.2
8	6.33 (*d*, 15.7)	118.4	6.20 (*d*, 15.7)	118.4
9		169.3		169.3
1'		131.3		131.3
2'	7.05 (*d*, 8.6)	130.7	6.92 (*d*, 8.7)	130.7
3'	6.72 (*d*, 8.6)	116.3	6.58 (*d*, 8.7)	116.3
4'		156.9		156.9
5'	6.72(*d*, 8.6)	116.3	6.58 (*d*, 8.7)	116.3
6'	7.05(*d*, 8.6)	130.7	6.92 (*d*, 8.7)	130.7
7'	2.74 (*t*, 7.3)	35.8	2.62 (*t*, 7.1)	35.8
8'	3.45 (*t*, 7.3)	42.5	3.32 (*t*, 7.1)	42.5

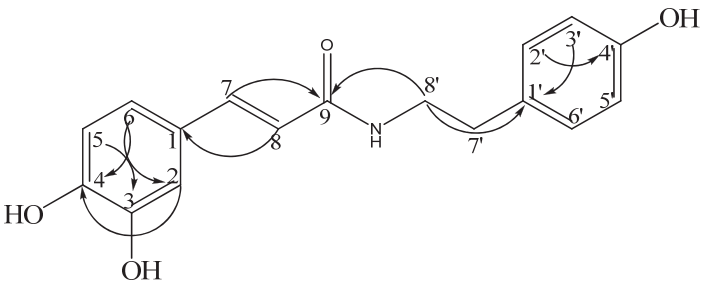

Figure 43 HMBC of MET-2

Table 25 HMBC spectral data of MET-2 (in CD_3OD, 300 MHz)

Position	^1H	HMBC
1		
2	6.86	C-4, C-7
3		
4		
5	6.63	C-3
6	6.77	C-2, C-4, C-7
7	7.24	C-2, C-6, C-9
8	6.20	C-1
9		
1'		
2'	6.92	C-4'
3'	6.58	C-1'
4'		
5'	6.58	C-1'
6'	6.92	C-4'
7'	2.62	C-6'
8'	3.32	C-1', C-9

1.6 Identification of Aporphine Alkaloids

1.6.1 Compound MBT-2 (magnoflorine)

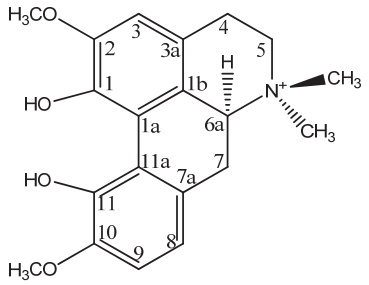

Figure 44 Structure of MBT-2

Compound MBT-2 was obtained as a slightly brownish yellow amorphous powder. HRESI-MS exhibited the $[M-H+Na]^+$ ion peak at *m/z* 364.1335 (Figure 162), corresponding the molecular formula of $C_{20}H_{24}NO_4$. IR spectra showed absorption at 3424, 2934, 1602, 1458-1384, and 1248 cm^{-1} (Figure 163), corresponding to OH stretching, C-H stretching, overtone of out of plane C-H bending, CH bending, and C-O stretching bands, respectively. Based on extensive NMR study, the aporphine alkaloid skeleton was indicated.

^{13}C-NMR and DEPT-135 spectra (Figures 165 and 166, Table 26) revealed twenty carbon atoms which were three methylene, four methyl, four methine, and nine quaternary carbons. ^{1}H-NMR spectra (Figure 164, Table 26) displayed two singlet signals of *N*-methyl protons at δ 2.83 and 3.21 (Cave et al., 1987), six methylene protons at δ 2.56, 2.71, 2.99, and 3.44 (H-4β, H-5α, H-5β), one methine proton at δ 4.04, two methoxy groups at δ 3.70 and 3.71 and three aromatic protons at δ 6.48, 6.49, and 6.63. Coupling of *ortho* aromatic protons (*J*=6.7 Hz) between δ 6.63 (H-9) and 6.48 (H-8) was observed, whereas the other aromatic proton (H-3) was a singlet.

HMBC long-range correlations (Figures 45 and 169, Table 27) from H-3 to C-1b, H-8 to C-11a, and H-9 to C-7a, confirmed the assignment of aporphine alkaloid skeleton. HMBC spectrum (Figure 169) also indicated the correlations from two singlet signals of *N*-methyl protons to *N*-methyl carbons of

one another, and C-6a and C-5. The other two singlet methyl signals were those of methoxy groups at δ 3.70 (2-OC<u>H</u>$_3$) and 3.71 (10-OC<u>H</u>$_3$). From long range HMBC, methoxy protons at δ 3.70 (2-OC<u>H</u>$_3$) and 3.71 (10-OC<u>H</u>$_3$) correlated to two quaternary carbons at C-2 (δ 153.4) and C-10 (δ 151.9), respectively, indicating the methoxy substitutions on positions 2 and 10. Moreover, NOESY correlation which assigned two adjacent protons (Figure 170) between δ 3.70 (2-OC<u>H</u>$_3$) and H-3 and δ 3.71 (10-OC<u>H</u>$_3$) and H-9 confirmed the methoxy positions. From these spectroscopic information, compound MBT-2 was identified as magnoflorine. Its absolute stereochemistry was assigned *S*-configuration on C-6a by comparing its specific rotation with that of previous report (Chen et al., 2009).

Magnoflorine has been isolated from several plant species, such as *Magnolia grandiflora* L. (Magnoliaceae) (Nakano, 1954), *M. denudata* Desr. (Magnoliaceae) (Nakano, 1956a), *Cocculus trilobus* DC. (Menispermaceae) (Nakano, 1956b), and *Coptis chinensis* Franch (Ranunculaceae) (Hung et al., 2007) Magnoflorine has been found to significantly inhibit Cu^{2+}-induced HDL oxidation. At low concentration of 3.0 μM, this compound was more effective than vitamin C, but less effective than vitamin E (Hung et al., 2007).

Table 26 ^{1}H and ^{13}C NMR chemical shift (in ppm) of magnoflorine (in CD_3OD) (Barbosa-Filho et al., 1997; Han et al., 2001; Chen et al., 2009) and MBT-2 (in CD_3OD, 300 MHz)

Position	Magnoflorine		MBT-2	
	^{1}H (multiplicity, coupling constant (Hz))	^{13}C	^{1}H (multiplicity, coupling constant (Hz))	^{13}C
1		150.4		150.9
1a		123.3		123.7
1b		121.1		121.0
2		152.9		153.4
3	6.48 (*s*)	109.5	6.49 (*s*)	109.5
3a		116.1		115.8
4	α 2.63 (*m*) β3.17 (*m*)	24.7	α 2.71 (*br d*, 15.6) β 3.44 (*m*)	24.8
5	α 3.45 (*m*) β 3.11 (*m*)	62.4	A 3.44 (*m*) B 3.44 (*m*)	62.6
6a	3.48 (*m*)	71.0	4.04 (*br d*, 13.8)	71.5
7	α 2.96 (*m*) β 2.45 (*t*, 11.6)	31.6	α 2.99 (*br d*, 13.8) β 2.56 (*br t*, 13.8)	31.9
7a		126.1		126.1
8	6.49 (*d*, 8.0)	117.5	6.48 (*d*, 6.7)	116.9
9	6.67 (*d*, 8.0)	110.5	6.63 (*d*, 6.7)	110.6
10		151.6		151.9
11		149.6		149.9
11a		123.4		123.8
N-CH_3	α 3.21 (*s*) β 2.75 (*s*)	54.0 43.6	α 3.21 (*s*) β 2.83 (*s*)	53.9 43.5
2-OCH_3	3.76 (*s*)	56.4	3.70 (*s*)	56.3
10-OCH_3	3.81 (*s*)	56.1	3.71 (*s*)	56.0

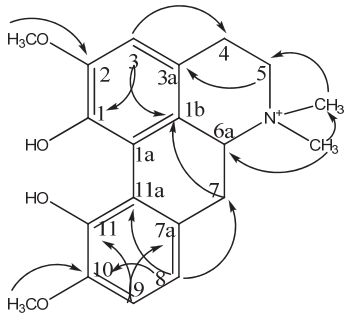

Figure 45 HMBC of MBT-2

Table 27 HMBC spectral data of MBT-2 (in CD_3OD, 300 MHz).

Position	^1H	HMBC
1		
1a		
1b		
2		
3	6.47	C-1, C-1b, C-2, C-4
3a		
4	2.71, 3.44	
5	3.44	C-3a
6a	4.04	
7	2.56, 2.99	C-1b
7a		
8	6.48	C-7, C-11a
9	6.63	C-7a, C-10, C-11
10		
11		
11a		
N-CH_3	α 3.21	N-$CH_{3\beta}$, C-5, C-6a
	β 2.83	N-$CH_{3\alpha}$, C-5, C-6a
2-OCH_3	3.71	C-2
10-OCH_3	3.70	C-10

1.6.2 Compound MBT-1 (corytuberine)

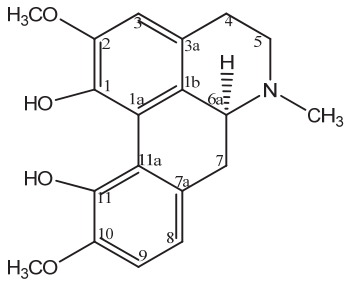

Figure 46 Structure of MBT-1

Compound MBT-1 was obtained as dark orange oil. HRESI-MS exhibited the $[M+H]^+$ ion peak at *m/z* 328.1792 (Figure 153), corresponding to the molecular formula of $C_{19}H_{21}NO_4$. IR spectra showed absorption at 3422, 2924, and 1252 cm^{-1} (Figure 154) which corresponded to OH stretching, C-H stretching, and C-O stretching bands, respectively. Based on extensive NMR study, the aporphine alkaloid skeleton was indicated.

^{13}C-NMR and DEPT-135 spectra (Figures 156 and 157, Table 28) revealed nineteen carbon atoms which were three methylene, three methyl, four methine, and nine quaternary carbons. The structure of MBT-1 was identified in the same manner as the MBT-2. ^{1}H-NMR spectrum (Figure 155, Table 28) displayed one methyl proton at δ 2.69, six methylene protons at δ 2.47, 2.75, and 3.12, one methine proton at δ 4.29, two methoxy groups at δ 3.82 and three aromatic protons at δ 6.65 (2H) and 6.79. Coupling of four methylene protons was exhibited as two triplets between δ 2.47 (H-4) and 3.12 (H-5) which was an *ortho* position (*J*=6.3, 6.3 Hz). Coupling between H-6a and H-7A and H-7B showed doublet of doublet signals with coupling constant of 2.5 Hz.

From HMBC correlations (Figures 47 and 160, Table 29), aromatic protons at H-9 and H-8 correlated to C-11 and C-10, respectively. The other aromatic proton at H-3 correlated to C-1. Two methoxy protons (6H, δ 3.82) correlated to two quaternary carbons that were C-2 and C-10 on HMBC spectra and to aromatic protons at C-3 and C-9 on NOSEY spectra (Figure 161) that confirmed these methoxu groups on C-2 and C-10. There are 34 amu missing, implying the

substitutions of hydroxyl groups on C-1 and C-11. Other proton positions showed correlation in Table 29.

From these spectroscopic information, compound MBT-1 was identified as corytuberine (Lu et al., 1989). Its absolute stereochemistry was assigned *S*-configuration by its specific rotation which showed dextrorotatory. Corytuberine was an intermediate of MBT-2 (magnoflorine). The first report of corytuberine was its isolation from *Corydalis cava* (L.) Schweigg. & Körte (Papaveraceae) in 1893 (Lakshmi et al., 2009).

Table 28 ^{1}H NMR and ^{13}C NMR chemical shift (in ppm) of corytuberine (in DMSO-d_6) (Lu et al., 1989) and MBT-1 (in CD_3OD, 300 MHz)

Position	Corytuberine	MBT-1	
	^{1}H (multiplicity, coupling constant (Hz))	^{1}H (multiplicity, coupling constant (Hz))	^{13}C
1			150.0
1a			ND
1b			120.5
2			153.0
3	6.53 (*s*)	6.65 (*s*)	109.2
3a			ND
4		A 2.47 (*t*, 6.3)	32.6
		B 2.47 (*t*, 6.3)	
5		A 3.12 (*t*, 6.3)	47.3
		B 3.12(*t*, 6.3)	
6a		4.29 (*dd*, 13.5, 2.5)	71.1
7		A 3.19 (*dd*, 13.5, 2.5)	31.5
		B 2.75 (*dd*,13.5, 2.5)	
7a			125.7
8	6.80 (*d*, 8.0)	6.65 (*d*, 8.1)	116.9
9	6.58 (*d*, 8.0)	6.79 (*d*, 8.1)	110.3
10			151.9
11			149.0
11a			123.2
N-CH_3	2.55	2.69 (*s*)	32.8
2-OCH_3	3.75	3.82 (*s*)	55.6
10-OCH_3	3.75	3.82 (*s*)	55.9

Remark: ND = not determined

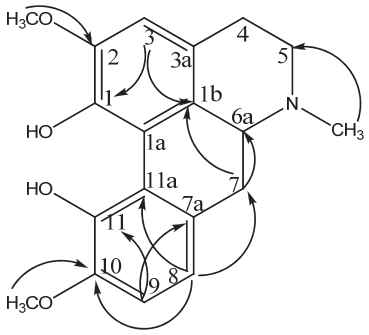

Figure 47 HMBC of MBT-1

Table 29 HMBC spectral data of MBT-1 (in $CDCl_3$, 300 MHz)

Position.	^1H	HMBC
1		
1a		
1b		
2		
3	6.65	C-1b, C-1, C-2
3a		
4	2.47	
5	3.12	
6a	4.29	
7	2.75	C-1b, C-6a
7a		
8	6.65	C-11a, C-7, C-10
9	6.79	C-7a, C-11
10		
11		
11a		
NCH_3	2.69	C-5
2-OCH_3	3.82	C-2
10-OCH_3	3.82	C-10

1.7 Identification of Cyclitol

1.7.1 Compound MET-3 (quebrachitol)

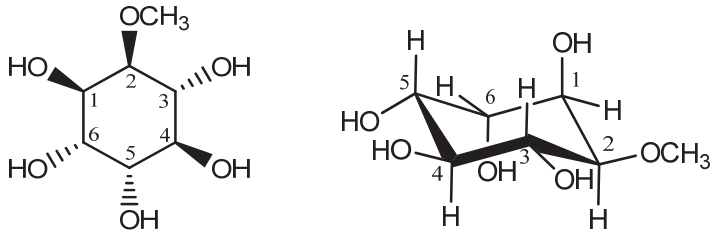

Figure 48 Structure of MET-3

Compound MET-3 was a crystalline white powder. The $[2M+Na]^+$ ion peak at *m/z* 411.1517 (Figure 140), corresponding to the molecular formula $C_7H_{14}O_6$, was obtained from HRESI-MS. IR spectra showed absorption bands of broad hydroxyl group at 3500-3200 cm^{-1} and broad C-O stretching at 1200-1100 cm^{-1} (Figure 141). Seven carbon signals were shown in ^{13}C-NMR and DEPT-135 spectra (Figures143 and 144, Table 30) as a methoxy carbon at δ 57.5, and six methine carbons at δ 68.5, 70.9, 72.5, 72.6, 73.7, and 81.5. ^{1}H-NMR spectrum (Figure 142, Table 30) revealed seven proton signals, including a methoxy group at δ 3.31, and six methine protons. The hydroxyl signals and their coupling constants on this compound were observed.

The cyclohexane skeleton was suggested by ^{1}H NMR (Figure 142, Table 30) and COSY spectra (Figure 145). Arrangement of each proton was determined based on their coupling constants. The correlations of protons between δ 3.09 (H-2) and 3.39 (H-3) and between δ 3.09 (H-2) and 3.86 (H-1) showed a coupling constants with 7.5 and 3.0 Hz, respectively which implied the axial-axial and the axial-equatorial arrangements, respectively. The signals between δ 3.86 (H-1) and 3.67 (H-6) exhibited the coupling constant with 3.0 Hz which suggested as the equatorial-equatorial arrangement. Additionally, the coupling constants with 7.5 and 3.0 Hz were the axial-axial and the axial-equatorial arrangement,

respectively which showed the correlations between H-5 (δ 3.44) and H-4 (δ 3.27) and between H-5 and H-6, respectively. The proton at H-4 coupled with H-3 with *J* = 7.5 Hz which implied to be the axial-axial arrangement. The long range HMBC spectra (Figures 49 and 146, Table 31) supported the cyclohexane arrangements. The singlet signal of methoxy protons at δ 3.31 correlated to a methine carbon at δ 81.5 (C-2), whereas H-2 correlated to a quaternary carbon (2-OCH_3). Then data confirmed the substitution of methoxy group on C-2. NMR data of this compound was compared with *L*-quebrachitol (Huang and Luo, 1994, Diaz et al., 2008a). Moreover, the hydroxyl signals at δ 4.00-5.00 and coupled to their vicinal protons which was generally found in DMSO solvent. These hydroxyl groups were assigned by long range HMBC. The hydroxyl proton at δ 4.67 (1-OH) correlated to methine carbon at δ 81.5 (C-2) and 72.5 (C-6). The correlation between hydroxyl at δ 4.66 (6-OH) and methine carbons C-1 and C-5 showed on HMBC. In the same manner, other hydroxyl positions were identified from HMBC data in Table 31 and Figure 49. This compound exhibited levorotatory specific rotation ($[\alpha]_D^{25}$ 88.89^o). All results are the comparable with previous reports (Huang and Luo, 1994, Diaz et al., 2008a, Sureshan et al., 2009). Therefore, compound MET-3 was identified as *L*-quebrachitol or *L*-2-*O*-methyl-chiro-inositol.

L-quebrachitol was found in many plants such as *Allophyllus edulis* Radlk (Sapindaceae) (Diaz et al., 2008b), *Klainedoxa gabonensis* Pierre (Irvingiaceae) (Dongo et al., 2009), and *Paullinia pinnata* L. (Sapindaceae) (Dongo et al., 2009). In Annonaceae, *L*-quebrachitol was isolated from *Uvaria kurzii* (King) P.T.Li. (Lu et al., 2009) and *Mitrephora vulpina* C.E.C. Fisch (Moharam et al., 2010). This compound showed a strong antagonistic effect on rabbit platelet activating factor (PAF) with 65.5% inhibition at the concentration of 18.2 μg/ml (Moharam et al., 2010).

Table 30 ^{1}H and ^{13}C NMR chemical shift (in ppm) of *L*-quebrachitol (in D_2O) (Diaz et al., 2008a) and MET-3 (in DMSO-d_6, 300 MHz)

Position	*L*-quebrachitol		MET-3	
	^{1}H (multiplicity, coupling constant(Hz))	^{13}C	^{1}H (multiplicity, coupling constant (Hz))	^{13}C
1	4.25 (*dd*, 3.6, 3.5)	67.6	3.86 (*dd*, 3.0)	68.5
2	3.39 (*dd*, 9.5, 3.2)	80.6	3.09 (*dd*, 7.5, 3.0)	81.5
2-OCH_3	3.44 (*s*)	57.3	3.31 (*s*)	57.5
3	3.60 (*m*)	73.2	3.39 (*dd*, 7.5)	73.7
4	3.60 (*m*)	72.3	3.27 (*dd*, 7.5)	72.6
5	3.73 (*dd*, 9.6, 3.2)	70.8	3.44 (*dd*, 7.5, 3.0)	70.9
6	4.05 (*dd*, 3.7, 3.6)	71.8	3.67 (*dd*, 3.0, 3.0)	72.5
1-OH			4.67 (*d*, 3.6)	
3-OH			4.47 (*d*, 5.1)	
4-OH			4.48 (*d*, 5.1)	
5-OH			4.32 (*d*, 5.7)	
6-OH			4.66 (*d*, 3.6)	

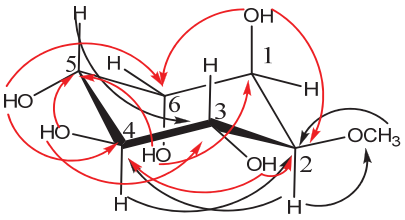

Figure 49 HMBC of MET-3

Table 31 HMBC spectral data of compound MET-3 (in DMSO-d_6, 300 MHz)

Position.	^{1}H (multiplicity, coupling constant (Hz))	HMBC
1	3.86 (*dd*, 3.0)	
2	3.09 (*dd*, 7.5, 3.0)	C-4, 2-O<u>C</u>H$_3$
2-OCH$_3$	3.31 (s)	C-2
3	3.39 (*dd*, 7.5)	
4	3.27 (*dd*, 7.5)	
5	3.44 (*dd*, 7.5, 3.0)	C-3
6	3.67 (*dd*, 3.0, 3.0)	
1-OH	4.67 (*d*, 3.6)	C-2, C-6
3-OH	4.47 (*d*, 5.1)	C-2, C-4
4-OH	4.48 (*d*, 5.1)	C-3, C-5
5-OH	4.32 (*d*, 5.7)	C-6
6-OH	4.66 (*d*, 3.6)	C-1, C-5

1.8 Identification of Fatty Acid

1.8.1 Compound MHL-4 (linoleic acid)

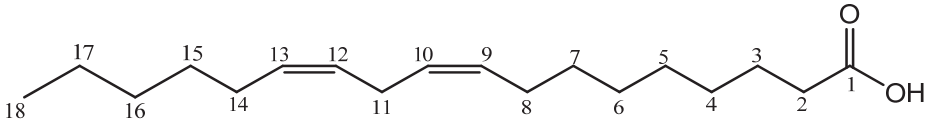

Figure 50 Structure of MHL-4

Compound MHL-4 was obtained as pale yellow oil, soluble in dichloromethane and chloroform. HRESI-MS showed the $[M-H]^+$ ion peak at m/z 279.2278 (Figure 117), corresponding to the molecular formula of $C_{18}H_{32}O_2$. IR spectra exhibited broad OH stretching at 3422-2849 and C=O at 1704 cm^{-1} of carboxylic acid (Figure 118).

In ^{13}C-NMR spectrum (Figure 120, Table 32), there were a methyl, twelve methylene, four methine, and a carbonyl carbons. The spectrum showed a carbonyl carbon at δ 180.27. The ^{1}H-NMR spectrum (Figure 119, Table 32) presented four olefinic protons, twelve methylene groups, and a methyl group. There was a triplet signal at δ 0.88 (J = 6.6 Hz, H-18) which coupled with H-17 (δ 1.28). The coupling constant among δ 2.34 (H-2), δ 1.62 (H-3) and δ 1.28 (H-4) was 7.3 Hz. The triplet signals of two methylene protons at 2.79 (H-11) which coupled with two methine protons at δ 5.36 (H-10 and H-12) showed a coupling constant of 6.0 Hz. From the molecular formula, the double bond equivalent was 3 which were a carbonyl and two double bonds. A coupling constant (J = 5.1 Hz.) of four vinyl protons at δ 5.36 (H-9 and H-10, H-12 and H-13) implied a *cis* configuration of each double bond. Comparing those spectra of MHL-4 with available spectra of previous literatures (Shimada et al., 1999; Mannina et al., 2004), this compound was identified as linoleic acid or octadeca-9,12-dienoic acid (Shimada et al., 1999; Mannina et al., 2004). Linoleic acid is a ubiquitous component of plant lipids, found in several plant families such as Rubiaceae (Kohler et al., 2002), Malvaceae (Kihc et al., 2011), and Asteraceae (Kohler et al.,

2002). For Annonaceae, linoleic acid was isolated from *Annona amazonica* R. E. Fries (Pinheiro et al., 2009), and *Xylopia aethiopica* A. (Elhassan et al., 2009). Linoleic acid inhibited two *Plasmodium falciparum* strains (a chloroquine-sensitive strain and a chloroquine-resistant strain) with IC_{50} values of 6.1 and 8.7 μg/ml, respectively (Kohler et al., 2002).

Table 32 ^{1}H and ^{13}C NMR NMR chemical shift (in ppm) of linoleic acid (in $CDCl_3$) (Shimada et al., 1999; Mannina et al., 2004) and MHL-4 (in $CDCl_3$, 300 MHz)

Position	linoleic acid		MHL-4	
	^{1}H (multiplicity, coupling constant (Hz))	^{13}C	^{1}H (multiplicity, coupling constant (Hz))	^{13}C
1		176.5		180.2
2	2.22 (m)	34.1	2.34 (*t*, 7.3)	34.0
3	1.54 (*m*)	25.1	1.62 (*quintet*, 7.3)	24.4
4-7	1.28 (*br s*)	29.3-29.7	1.28 (*br s*)	29.0-29.6
8	1.99 (*q*, 7.0)	27.3	2.05 (*m*)	27.2
9	5.30 (*m*)	130.0	5.36 (*m*, 5.1)	130.0
10	5.30 (*m*)	128.0	5.36 (*m*, 5.1)	128.0
11	2.71 (*t*, 7.0)	25.7	2.79 (*t*, 6.0)	24.6
12	5.30 (*m*)	128.0	5.36 (*br d*, 5.1)	127.9
13	5.30 (*m*)	130.2	5.36 (*br d*, 5.1)	129.7
14	1.99 (*q*, 7.0)	27.3	2.05 (*m*)	27.2
15	1.28 (*br s*)	29.3	1.28 (*br s*)	29.0-29.6
16	1.28 (*br s*)	31.6	1.28 (*br s*)	31.9
17	1.28 (*br s*)	22.7	1.28 (*br s*)	22.7
18	0.83 (*t*, 7.0)	14.1	0.88 (*t*, 6.6)	14.1

1.9 Identification of Purine Derivative

1.9.1 Compound MET-4 (allantoin)

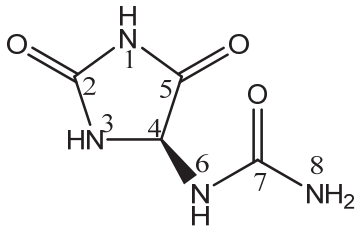

Figure 51 Structure of MET-4

Compound MET-4 was obtained as a white crystal. HRESI-MS displayed the $[2M+Na]^+$ ion peak at *m/z* 399.0740 (Figure 147), corresponding to the molecular formula of $C_4H_6N_4O_3$. IR spectra exhibited broad NH_2 and NH group at 3439-3062, C=O group at 1781-1661, NH bending at 1603, and 1531 cm^{-1} (Figure 148). This compound was identified as allantoin which contained two principal parts as purine base and ureido substitution.

The ^{13}C-NMR and DEPT-135 spectra (Figures 150 and 151 Table 33) revealed one methine carbon and three carbonyl carbons. The ^{1}H NMR spectrum (Figure 149, Table 33) showed six protons. Two protons at δ 8.06 (3-NH) and 10.54 (1-NH), adjacent to electron withdrawing groups, appeared as downfield broad singlet signals. Singlet signal of two protons at δ 5.79 belonged to 8-NH_2. Two vicinal protons at δ 5.24 (H-4) and 6.86 (6-NH) displayed as doublet signals with a coupling constant of 8.1 Hz. From long-range HMBC (Figures 52 and 152 Table 34), H-4 correlated to two carbonyl carbons as C-5 and C-7. The proton at δ 6.86 (6-NH) also displayed correlations to C-5 and C-7 and a methine carbon (C-4) which confirmed the position of ureido substitution on C-4.

The ^{13}C and ^{1}H NMR chemical shifts were compared to the previous reports (Park et al., 2009; Xu et al., 2011) and MET-4 was identified as allantoin, the purine derivative. This compound was isolated from several plants such as *Pisonia grandis* R. Br. (Nyctaginaceae) (Sripathi et al., 2011), and *Aristolochia gigantea* Mart. & Zucc. (Aritolochiaceae) (Holzbach and Lopes,

2010). In *Mitrephora* genus, it was found in *M. maingayi* Hook (Yu et al., 2005). This compound was used in cosmetics and showed anti-inflammatory and antifungal activities (Silva et al., 2007; Sripathi et al., 2011).

Table 33 ^{1}H and ^{13}C NMR chemical shift (in ppm) of allantoin (in DMSO-d_6) (Park et al., 2009) and MET-4 (in DMSO-d_6, 300 MHz)

Position	allantoin		MET-4	
	^{1}H (multiplicity, coupling constant (Hz))	^{13}C	^{1}H (multiplicity, coupling constant (Hz))	^{13}C
1	10.56 (*br s*)		10.54 (*br s*)	
2		156.9		157.2
3	8.07 (*s*)		8.06 (*s*)	
4	5.23 (*d*, 8.1)	62.5	5.24 (*d*, 8.1)	62.8
5		173.7		174.0
6	6.90 (*d*, 8.1)		6.86 (*d*, 8.1)	
7		157.4		157.8
8	5.80 (*s*)		5.79 (*s*)	

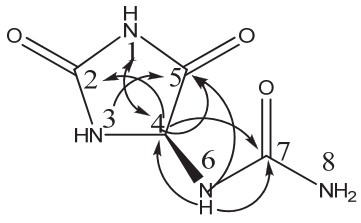

Figure 52 HMBC of MET-4

Table 34 HMBC spectral data of MET-4 (in DMSO-d_6, 300 MHz)

Position.	^{1}H (multiplicity, coupling constant (Hz))	HMBC
1	10.54 (*br s*)	C-2, C-4
2		
3	8.06 (*s*)	C-5
4	5.24 (*d*, 8.1)	C-1, C-2, C-5, C-7
5		
6	6.86 (*d*, 8.1)	C-4, C-5, C-7
7		
8	5.79 (*s*)	C-4

2. Biological Activities of the Extracts from *Pterospermum grande* and *Mitrephora wangii*

2.1 Brine Shrimp Lethality Assay

The brine shrimp lethality assay is considered a preliminary toxicity test since *Artemia salina* eggs are inexpensive, rapid, and sensitive to small amount of chemical compound. Two plant extracts were tested on this assay according to bioassay-guided fractionation. The criteria for toxicity were highly (LC_{50} of less than 20.0 μg/ml), moderately (LC_{50} from 20.1 to 100.0 μg/ml), weakly toxic (LC_{50} from 100.1 to 1,000 μg/ml), and inactive (LC_{50} of higher than 1,000 μg/ml) (Meyer et al., 1982; Mclaughlin, 1991; Colegate and Molyneux, 1993).

All extracts of *P. grande* leaves were examined and only the aqueous extract showed moderate toxicity with LC_{50} value of 80.76 μg/ml, while others were inactive (Table 35).

The ethyl acetate extract of *M. wangii* leaves exhibited moderate toxicity with the LC_{50} value of 63.18 μg/ml. For *M. wangii* twigs, the hexane, ethyl acetate and aqueous phase displayed weak activity with the LC_{50} values of 156.83, 150.93, and 147.94 μg/ml, respectively (Table 35).

Table 35 Brine shrimp lethality assay of extracts from *P. grande* and *M. wangii*.

Extracts	Brine shrimp lethality assay; LC_{50} (μg/ml)		
	P. grande leaves	*M. wangii* leaves	*M. wangii* twigs
Hexane	187.96	>1,000	156.83
Dichloromethane	181.18	747.23	0
Ethyl acetate	115.62	63.18	150.93
Aqueous phase	80.76	303.37	147.94
n-Butanol	ND	ND	473.37

Remark: ND = not determined

2.2 DPPH Assay

In DPPH assay, a stable free radical with a characteristic absorption at 517 nm was used to test the radical scavenging effects of extracts. Antioxidative compounds donate hydrogen atoms to DPPH radical and lead to decrease in absorption which measured by UV spectroscopy. The decrease in absorption implied the radical scavenging activity (Molyneux, 2004). The criteria of antioxidant activity for plant extracts were highly (IC_{50} < 10.0 μg/ml), moderately (IC_{50} = 10.1-50.0 μg/ml), weakly (IC_{50} = 50.1-100.0 μg/ml), and inactive (IC_{50} > 100.0 μg/ml).

All extracts of *P. grande* leaves showed different antioxidative activity (Table 36). The extract with strong antioxidative activity was the ethyl acetate extract with an IC_{50} value of 7.35 μg/ml. The ones with moderate activity were the dichloromethane and aqueous extract with IC_{50} values of 16.75 and 11.78 μg/ml, respectively. The hexane extract was weakly active with the IC_{50} value of 42.71 μg/ml. Ascorbic acid, which was a positive control, gave an IC_{50} value of 3.53 μg/ml.

For *M. wangii*, all extracts were not tested on antioxidative assay, since the methanol extract showed weak activity.

Table 36 DPPH and HFI assays of extracts from *P. grande* and *M. wangii*.

Extract	*P grande* leaves		*M.wangii* leaves
	DPPH IC_{50} (μg/ml))	HFI CZI/BZI (mm)	HFI CZI/BZI (mm)
Hexane	42.72	0	12 (BZI)
Dihloromethane	16.75	0	21 (CZI)
Ethyl acetate	7.35	15 (CZI)	22 (BZI)
Aqueous	11.78	0	0

2.3 Hyphae Formation Inhibition (HFI) Assay

Protein kinases, the enzymes that transfer phosphate group of ATP to serine, tyrosine, and threonine residues in proteins, play important roles in signal transduction which involves in the initiation, propagation, and regulation of immunological responses. Additionally, the roles of protein kinases have emerged as cellular regulatory proteins in many diseases such as cancer, inflammatory, and heart diseases. The hyphae formation inhibition (HFI) assay is a cell-based assay that is a simple and inexpensive alternative to *in vitro* enzyme assays for the evaluation of microbial and plant extracts. Inhibition of the formation of *Streptomyces* 85E hyphae involves the activity of protein kinase. The results of this test are presented as clear zone inhibition (CZI) and bald zone inhibition (BZI). Clear zone indicates that the extract inhibits both growth and sporulation of *Streptomyces* 85E cells which implied the cytotoxicity. The bald zone indicates that the extract inhibits aerial hyphae formation, but no inhibition of cellular growth. Thus, the bald zone of the extract exhibits protein kinase inhibition. This test is used as alternative to cytotoxicity and protein kinase inhibition screening. Plant extract producing an inhibition zone of greater than 9 mm with 80 μg/disc is considered active (Carmichael et al., 1987; Waters et al., 2002).

The hexane, dichloromethane, ethyl acetate, and aqueous extracts from *P. grande* leaves were examined for HFI assay (Table 36). The ethyl acetate extract showed significant inhibition of *Streptomyces* 85E with 15 mm clear zone.

The hexane, dichloromethane and ethyl acetate extract from *M. wangii* leaves showed various activity against *Streptomyces* 85E. The dichloromethane extract presented the widest clear zone of inhibition at 21 mm. The ethyl acetate extract exhibited more activity than the hexane extract with a bald zone of inhibition at 22 and 12 mm, respectively, suggesting the inhibitory activity on protein kinase enzymes of both extracts. The aqueous phase extract was inactive. The extracts of *M. wangii* twigs were not tested in HFI assay.

3. Biological Activities of Pure Compounds

Due to limited quantities, only four compounds from *M. wamgii*, including three neolignans and quebrachitol (MET-3), were investigated for their biological activities.

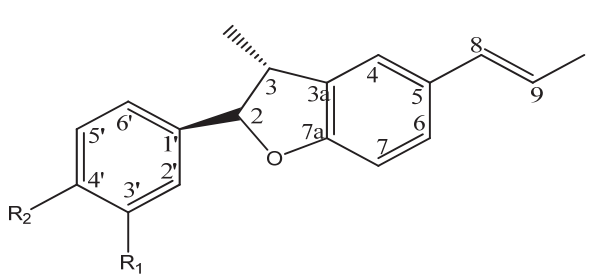

MHL-1= (2*R*,3*R*)-2,3-dihydro-2-(4'-methoxyphenyl)-3-methyl-5-[1-(*E*)-propenyl]benzofuran or methyl conocarpan

MHL-2 = (2*R*,3*R*)-2,3-dihydro-2-(4'-hydroxy-3'-methoxyphenyl)-3-methyl-5-[1-(*E*)-propenyl] benzofuran or 3'-methoxy conocarpan

MHL-3 = (2*R*,3*R*)-2,3-dihydro-2-(4'-hydroxyphenyl)-3-methyl-5-[1-(*E*)-propenyl]benzofuran or conocarpan

Figure 53 Structures of dihydrobenzofuran neolignans

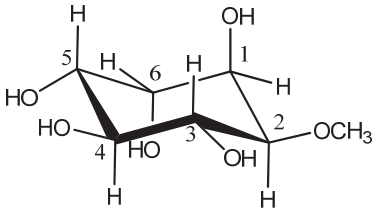

Figure 54 Structures of quebrachitol (MET-3)

Table 37 Biological activities of pure compounds from *M. wangii*.

Compounds	Brine shrimp lethality (IC_{50} µg/ml)	HFI assay Zone of inhibition (mm)	MTT assay (IC_{50} µg/ml)		
			HeLa	HepG2	U937
MHL-1	157.90	0	ND	ND	ND
MHL-2	148.79	11 (BZI)	11.0	18.8	5.9
MHL-3	6.21	21(CZI)	13.7	18.6	6.3
MET-3	ND	0	>500	>500	ND

Remark: ND = not determined

3.1 Brine Shrimp Lethality Assay

Three neolignans from *M. wangii* were examined on brine shrimp lethality. MHL-3 gave the strongest activity than the others with the IC_{50} value of 6.21 μg/ml. The MHL-1 and MHL-2 showed weak activity (Table 37).

3.2 Hyphae Formation Inhibition Assay

The compounds were tested at the concentration of 20 μg/disk for HFI assay (Table 37). MHL-1 was inactive, while MHL-2 and MHL-3 exhibited significant activity against *Streptomyces* 85E with bald zone of inhibition and clear zone of inhibition at 11 and 21 mm, respectively. The criterion for active compound was inhibition zone of higher than 9 mm. The result implied that MHL-2 inhibited protein kinase activity, while MHL-3 indicated its cytotoxicity against *Streptomyces* 85E cell. The quebrachitol (MET-3) was inactive in HFI assay.

3.3 MTT Assay

The compounds were tested in HeLa, HepG2, and U937 (Table 37). In HeLa, the IC_{50} values were 11.0 μg/ml for MHL-2 and 13.7 μg/ml for MHL-3. In HepG2, IC_{50} values were 18.8 for MHL-2 and 18.6 μg/ml for MHL-3. In U937, IC_{50} values were 5.9 μg/ml for MHL-2 and 6.3 μg/ml for MHL-3. MET-3 was inactive against all three cell lines

The biological activities of three neolignans were discussed according to their structures. The methoxy substitution on C-4' of MHL-1 and on C-3' of MHL-2 greatly reduced the BSL, implying that the methoxy group on a phenyl ring affected the solubility of the compounds. The absence of a methoxy group on a phenyl ring as in compound MHL-3 increased its activity in BSL and HFI assays, indicating that hydroxyl substitution on C-4' might be required for the activity.

CHAPTER 5
CONCLUSION

Eighteen plants from fifteen families were investigated in brine shrimp lethality and DPPH assay. Two plants, *P. grande* (Sterculiaceae) and *M. wangii* (Annonacea), were carried on for the isolation and biological activities testing of chemical constituents.

Isolation of the leaves of *Pterospermum grande* yielded seven compounds, including three triterpenoids, a steroid, and three phenolic compounds. Four compounds from the hexane leaf extract were taraxerol, taraxerol acetate, simiarenol, and *β*-sitosterol. The ethyl acetate leaf extract gave three phenolic compounds, consisting of two flavonol glycosides, kaempferol-3-*O*-*β*-galactopyranoside and kaempferol-3-*O*-*β*-D-6"(4-hydroxy-*E*-cinnamoyl)-(*β*)-glucopyranoside, and a flavan-3-ol, (-)-epicatechin.

Separated chemical compounds from the hexane, dichloromethane, ethyl acetate, and *n*-butanol leaf and twig extracts of *M. wangii* were a steroid, a steroidal glycoside, three neolignans, two phenolic amides, sugar, two alkaloids, a fatty acid, and allantoin. For the genus *Mitrephora*, the isolation of three neolignans, a tertiary aporphine alkaloid and a quaternarium aporphine alkaloid, including methyl conocarpan, 3'-methoxy conocarpan, conocarpan, corytuberine, and magnoflorine were reported for the first time.

In addition, three neolignans were examined for biological activities. From brine shrimp lethality, HFI assay, and cytotoxicity, it was found that conocarpan showed the strongest activities than the other compounds.

BIBLIOGRAPHY

Thai

เต็ม สมิตินันทน์ 2544. *ชื่อพรรณไม้แห่งประเทศไทย*, กรุงเทพ, บริษัทประชาชน จำกัด.

ปิยะ เฉลิมกลิ่น 2544. พรรณไม้วงศ์กระดังงา, กรุงเทพฯ, สำนักพิมพ์บ้านและสวน.

สุธรรม อารีกุล 2552. องค์ความรู้เรื่องพืชป่าที่ใช้ประโยชน์ทางภาคเหนือของไทย, เชียงใหม่, มูลนิธิโครงการหลวง.

English

Achenbach, H., Grob, J., Dominguez, X., A, Cano, G., Star, J., Verde, Brussolo, L., Del, Carmen, Munoz, G., Salgada, F. & Lopez, L. 1987. Lignans, Neolignans and Norneolignans from *Krameria cystisoides*. *Phytochemistry,* 26**,** 1159-1166.

Achenbach, H., Utz, W., Usubillaga, A. & Rodriguez, H. A. 1991. Lignans from *Krameria ixina*. *Phytochemistry,* 30**,** 3753-3757.

Adeloye, O. A., Akinpelu, A. D., Ogundaini, O. A. & Obafemi, A. C. 2007. Studies on Antimicrobial, Antioxidant and Phytochemical Analysis of *Urena lobata* Leave. *Journal of Physical and Natural Sciences,* 1**,** 1-9.

Agrawal, P. K. 1992. NMR Spectroscopy in the Structural Elucidation of Oligosaccharides and Glycosides. *Phytochemistry*, 31**,** 3307-3330.

Agrawal, P. K. & Thakur, R. S. 1985. ^{13}C NMR Spectroscopy of Lignan and Neolignan Derivatives. *Magnetic Resonance in Chemistry,* 23**,** 389-418.

Ahmad, F., Bakar, S. & Read, R. 1998. Benzofurans From the Leaves of *Piper magnibacum* C.DC. *ACGC Chemical Research Communications,* 7**,** 33-37.

Ali, M. S., Ali, M. I., Ahmed, Z. & Waffo, A. F. K. 2011. Vogelate: A New Long-chained Ester from *Erythrina vogelii* Hook. (Fabaceae) of Cameroon. *Journal of the Chemical Society of Pakistan,* 33**,** 412-416.

Anjaneyulu, A. S. R. & Raju, S. N. 1987a. Cyclotriterpenes from the Heartwood of *Pterospermum heyneanum*. *Phytochemistry*, 26**,** 2805-2810.

Anjaneyulu, A. S. R. & Raju, S. N. 1987b. The Heartwood of *Pterospermum heyneanum*. *Phytochemistry*, 26**,** 2805-2810.

Anjaneyulu, A. S. R. & Raju, S. N. 1988. Chemical Constituents of the Bark and Leaves of *Pterospermum heyneanum* Wall. *Journal of Indian Chemical Society,* 65**,** 147-148.

Arnone, A., Modugno, D. V., Nasini, G. & Venturini, I. 1988. Isolation and Structure Determination of New Active Neolignans and Norneolignans From Ratanhia. *Gazzetta Chimica Italiana* 118**,** 675-682.

Arthur, H. R. & Hui, W. H. 1965. The Structure of Simiarenol from the Hong Kong Species of *Rhododendron simiarum*. *Tetrahedron Letters,* 14**,** 937-943.

Asbagh, L. A., Deniz, A., Uzunoglu, S. & Uslu, R. 2008. Translation Perspective of Mathematical Models Used in the Assessment of Cellular Synergy in Cytotoxicity Assays. *Cape Breton University Journal of Science,* 41**,** 127-134.

Atal, C. K., Srivastava, J. B., Wali, B. K., Chakravarty, R. B., Dhawan, B. N. & Rastogi, R. P. 1978. Screening of Indian Plants for Biological Activity: Part VIII. *Indian Journal of Experimental Biology.,* 16**,** 330-349.

Balunas, M. J. & Kinghorn, D. A. 2005. Drug Discovery from Medicinal Plants. *Life Sciences,* 78**,** 431-441.

Barbosa-Filho, J., Maria, Da-Cunha, E., V. L. , Cornelio, M., Lopes, Dias, C., Da Silva & Gray, A., I 1997. Cissaglaberrimine, an Aporphine Alkaloid From *Cissampelos glaberrima*. *Phytochemistry,* 44**,** 959-961.

Benevides, P., J. C., Sartorelli, P. & Kato, M., J. 1999. Phenylpropanoids and Neolignans from *Piper regnellii*. *Phytochemistry,* 52**,** 339-343.

Bingtao, L., Weerasooriya, A. D. & Saunders, R. M. K. 2011. Mitrephora *Flora of China,* 19**,** 687-688.

Bishnoi, P. & Gupta, P. C. 1979. Structure of a new Acid-Polysaccharide from the Bark of *Pterospermum acerifolium*. *Journal of the Chemical Society Perkin Transactions 1,* 1979**,** 1680-1683.

Bohannon, M. B. & Kleiman, R. 1978. Cyclopropene Fatty Acids of Selected Seed Oils from *Bombaceae Malvaceae*, and *Sterculiaceae*. *Lipids,* 13**,** 270.

Brophy, J., Goldsack, R. & Forster, P. 2004. *Essential Oils from the Leaves of Some Queensland Annonaceae* [Online]. Available: http://findarticles.com/ p/ articles/mi_qa4091/is_200403/ai_n9368485/ [Accessed March 22, 2011].

Calderon-Montana, J. M., Burgos-Moron, E., Perez-Guerrero, C. & Lopez-Lazaro, M. 2011. A Review on Dietary Flavonoid Kaempferol. *Medicinal Chemistry,* 11**,** 298-344.

Carini, M., Aldini, G., Orioli, M. & Facino, R. 2002. Antioxidant and Photoprotective Activity of a Lipophilic Extract Containing Neolignans from *Krameria triandra* Roots. *Planta Medica,* 68**,** 193-197.

Carmichael, J., Degraff, W. G., Gazdar, A. F., Minna, J. D. & Mitchell, J. B. 1987. Evaluation of a Tetrazolium-based Semiautomated Colorimetric Assay: Assessment of Chemosensitivity Testing*Cancer Research,* 47**,** 936-942.

Carr, G. G. 2006. ***Sterculiaceae*** [Online]. Available: http://www.botany.hawaii.edu /faculty/carr/sterculi.htm [Accessed March 05, 2011].

Cave, A., Leboeuf, M. & Waterman, P. G. 1987. The Aporphine Alkaloids of the Annonaceae. *In:* PELLETIER, S. W. (ed.) *Alkaloids: Chemical and Biological Perspectives.* New York: John Wiley & Sons, Inc.

Chakravarty, A. K. 1994. Unambiguous Assignment of ^{13}C Chemical Shifts of Some Hopane and Migrated Hopane Derivatives by 2D NMR. *Tetrahedron,* 50**,** 2865-2876.

Chang, F.-R., Chen, C.-Y., Hsieh, T.-J., Cho, C.-P. & Wu, Y.-C. 2000. Chemical Constituents from *Annona glabra* III. *Journal of the Chinese Chemical Society,* 47**,** 913-920.

Chauret, D., Bernard, C., Arnason, J., Krishnamurty, H., Sanchez-Vandas, P., Nmorenon, N., Roman, L. & Poveda, L. 1996. Insaecticidal Neolignans from *Piper decurrens*. *Journal of Natural Product,* 59**,** 152-155.

Chen, J.-H., Du, Z.-Z., Shen, Y.-M. & Yang, Y.-P. 2009. Aporphine Alkaloids From *Clematis parviloba* and Their Antifungal Activity. *Archives of Pharmacal Research* 32**,** 3-5.

Chen, Z.-S., Lai, J.-S. & Kuo, Y.-H. 1991. The Constituents of *Cynanchum taiwanianum*. *Journal of the Chinese Chemical Society,* 38**,** 393-396.

Chou, T. C. 2006. Theoretical Basis, Experimental Design, and Computerized Simulation of Synergism and Antagonism in Drug Combination Studies. *Pharmacological Reviews,* 58**,** 621-681.

Chuakul, W. & Sornthornchareonon, N. 2003. Ethnomedicinal Used of Thai Annonaceous Plant (1). *Thai Journal of Phytopharmacy,* 10**,** 25-32.

Colegate, S. M. & Molyneux, R. J. 1993. Separation, Structure Elucidation, and Bioassay of Cytotoxic Natural Products. *In:* CORDELL, G. A., KINGHORN, D. A. & PEZZUTO, J. M. (eds.) *Bioactive Natural Products: Detection, Isolation, and Structure Determination.* Florida: CRC Press, Inc.

Cordell, G. A., Beecher, C. W. W. & Pezzuto, J. M. 1991. Can Ethnopharmacology Contribute to the Development of New Anticancer Drugs? *Journal of Ethnopharmacology,* 32**,** 117-133.

Cordell, G. A., Kinghorn, A. D. & Pezzuto, J. M. 1993. Separation, Structure Elucidation, and Bioassay of Cytotoxic Natural Products. *In:* COLEGATE, S. M. & MOLYNEUX, R. J. (eds.) *Bioactive Natural Products: Detection, Isolation, and Structural Determination.* London: CRC Press.

Cui, C.-B., Tezuka, Y., Kikuchi, T., Nakano, H., Tamaoki, T. & Park, J.-H. 1992. Constituents of a Fern, *Davallia mariesii* Moore. II. Identification and ^{1}H- and ^{13}C-Nuclear Magnetic Resonance Spectra of Procyanidin B-5, Epicatechin-(4*b*->6)-epicatechin, and Epicatechin-(4*b*->6)-epicatechin-(4*b*->8)-epicatechin-(4*b*->6)-epicatechin. *Chemical & Pharmaceutical Bulletin,* 40**,** 889-898.

Daengrot, C., Ponglimanont, C. & Karalai, C. 2005. Chemical Constituents from the Braks of *Heritiera littoralis*. 31st Congress on Science and Technology of Thailand at Suranaree Univeristy of Technology.

Dahl, R., Kapp, A., Colombo, G., Monchy, J. G. R., Rak, S., Emminger, W., Rivas, M. F., Ribel, M. & Durham, S. R. 2006. Efficacy and Safety of Syblingual Immunotherapy with Grass Allergen Tablets for Seasonal Allergic Rhinoconjunctivitis. *Journal of Allergy and Clinical Immunology,* 118**,** 434-440.

Dan, S. & Dan, S. S. 1988. Chemical Investigation in the Family *Sterculiaceae*. *Fitoterapia,* 59**,** 348-349.

Deepralard, K., Pengsuparp, T., Moriyasu, M., Kawanishi, K. & Suttisri, R. 2007. Chemical Constituents of *Mitrephora maingayi*. *Biochemical Systematic and Ecology,* 35**,** 696-699.

Dias, G. C. D., Gressler, V., Hoenzel, S. C. S. M., Silva, U. F., I, D. I. & F, M. A. 2007. Constituents of Roots of *Melochia chamaedrys*. *Phytochemistry,* 68**,** 668-672.

Diaz, M., Gonzalez, A., Castro-Gamboa, I., Gonzalez, D. & Rossini, C. 2008a. First Record of *L*-Quebrachitol in *Allophyllus edullis* (Sapindaceae). *Carbohydrate Research,* 343**,** 2699-2700.

Diaz, M., Gonzalez, A., Castro-Gamboa, I., Gonzalez, D. & Rossini, C. 2008b. First Record of *L*-Quebrachitol in *Allophylus edulis* (Sapindaceae). *Carbohydrate Research,* 343**,** 2699-2700.

Dobson, A. 1995. Biodiversity and Human Health. *TREE,* 10**,** 390-391.

Dongo, E., Hussain, H., Miemanang, R. S., Tazoo, D., Schulz, B. & Krohn, K. 2009. Chemical Constituents of *Klainedoxa gabonenses* and *Paullinia pinnata*. *Records of Natural Products,* 3**,** 165-169.

Duarte, N., Ramalhete, C., Varga, A., Molnar, J. & Ferreira, M.-J. U. 2009. Multidrug Resistance Modulation and Apoptosis Induction of Cancer Cells by Terpenic Compounds Isolated from *Euphorbia* Species. *Anticancer Research,* 29**,** 4467-4472.

Elhassan, I. A., Elamin, E. E. & Ayoub, S. M. H. 2009. Characterization of Lipid Compounds of the Dried Fruits of *Xylopia aethiopica* (Dunal) A. Rich Growing in Sudan. *Pakistan Journal of Nutrition,* 8**,** 1592-1595.

Fabricant, D. S. & Farnsworth, N. R. 2001. The Value of Plants Used in Traditional Medicine for Drug Discovery. *Environmental Health Perspectives,* 109**,** 69-75.

Finney, D. J. 1971. *Probit Analysis,* Cambridge, Cambridge University Press

Freixa, B., Vila, R., Ferro, E., Adzet, T. & Cangueral, S. 2001. Antifungal Principles from *Piper fulvescens*. *Planta Medica,* 67**,** 873-875.

Friebolin, H. 1993. *Basic One- and Two-Dimensional NMR Spectroscopy,* New York, WILEY-VCH.

Ge, F., Tang, C.-P. & Ye, Y. 2008. Lignanamides and Sesquiterpenoids from Stems of *Mitrephora theorelii*. *Helvetica Chemica Acta,* 91**,** 1023-1030.

Gohar, A. A., El-Olemy, M. M., Abdel-Sattar, E., El-Said, M. & Niwa, M. 2000. Cardenolides and *b*-Sitosterol Glucoside from *Pergularia tomentosa* L. *Natural Product Sciences,* 6**,** 142-146.

Gossell-Williams, M., Simon, O. R. & West, M. E. 2006. The Past and Present Use of Plants for Medicines. *West Indian Medical Journal,* 55**,** 217-218.

Gunasegaran, R. & Subramanian, S. S. 1979. Flavonoids of Three *Pterospermum* Species. *Indian Journal of Pharmaceutical Science,* 41**,** 72-73.

Han, Q. B., Jiang, B., Mei, S. X., Ding, G., Sun, H. D., Xie, J. X. & Liu, Y. Z. 2001. Constituents From the Roots of *Semiaquilegia adoxoides*. *Fitoterapia,* 72**,** 86-88.

Han, S. H., Lee, H. H., Lee, I. S., Moon, Y. H. & Woo, E. R. 2002. A New Phenolic Amide from *Lycium chinense* Miller. *Archives of Pharmacal Research,* 433-437.

Heywood, V. H. 1985. *Flowering Plants of the World,* London, Croom Helm.

Holzbach, J. C. & Lopes, L. M. X. 2010. Aristolactams and Alkamides of *Aristolochia gigantea*. *Molecules,* 15**,** 9462-9472.

Hou, W. C., Lin, R. D., Cheng, K. T., Hung, Y. T., Cho, C. H., Chen, C. H., Hwang, S. Y. & Lee, M. H. 2003. Free Radical-scavenging Activity of Taiwanese Native Plants. *Phytomedicine,* 10**,** 170-175.

Hras, A. R., Hadolin, M., Knez, Z. & Bauman, D. 2000. Comparison of Antioxidative and Synergistic Effects of Rosemary Extract with Tocopherol, Ascorbyl Palmitate and Citric acid in Sunflower oil. *Food Chemistry,* 71**,** 229-233.

Huang, K.-F. & Luo, W.-L. 1994. Crystal Structure of *L*-Quebrachitol. *Journal of the Chinese Chemical Society,* 41**,** 115-117.

Hung, T., Manh, Lee, J., Pill, Min, B., Sun, Choi, J., Sue, Na, M., Kyun, Zhang, X., Feng, Ngoc, T., Minh, Lee, I., Soo & Bae, K., Hwan 2007. Magnoflorine from Coptine Rhizoma Protects High Density Lipoprotein During Oxidant Stress. *Biological & Pharmaceutical Bulletin,* 30**,** 1157-1160.

Hutchinson, J. 1959. *The Families of Flowering Plants,* New York, OXford: Clarendon Press.

Jachak, S. M. & Saklani, A. 2007. Challenges and Opppotunities in Drug Discovery From Plants. *Current science,* 92**,** 1251-1257.

Jayaprakasha, G. K., Yaligar, J., Gowda, G. a. N. & Patil, B. S. 2009. NMR Structure CHaracterization and Inhibition of Colon Cancer Cells by Components of *Citrus aurantium* L. *International Society for Magnetic Resonance in Medicine,* 17**,** 4163.

Jin, W. Y., Cai, X. F., Na, M. K., Lee, J. J. & Bae, K. H. 2007. Triterpenoids and Diaryheptanoids from *Alnus hirsuta* inhibit HIF-1 in AGS Cells. *Archives of Pharmacal Research,* 30**,** 412-418.

Kato, M., J. & Furlan, M. 2007. Chemistry and Evolution of the Piperaceae. *Pure and Applied Chemistry,* 79**,** 529-538.

Khallouki, F., Haubner, R., Hull, W. E., Erben, G., Spiegelhalder, B., Bartsch, H. & Owen, R. W. 2007. Isolation, Purification and Identification of Ellagic Acid Derivatives, Catechins, and Procyanidins from the Root Bark of *Anisophyllea dichostyla* R. Br. *Food and Chemical Toxicology,* 45**,** 472-485.

Khan, M. S. H., Nahar, N., Mosihuzzaman, M. & Rashid, M. A. 2005. Neoliganan and Megastigmane Glycosides from the Leaves of *Pterospermum semisagittatum*. *Pharmazie,* 60**,** 72-74.

Kihc, C. S., Aslan, S., Kartal, M. & Coskun, M. 2011. Fatty acid Composition of *Hibicus trinum* L. (Malvaceae). *Records of Natural Products,* 5**,** 65-69.

Kim, G.-S., Zeng, L., Alali, F., Rogers, L. L., Wu, F.-E., Mclaughlin, J. L. & Sastrodihardjo, S. 1998. Two New Mono-tetrahydrofuran Ring Acetogenin, Annomuricin E and Muricapetocin, from the Leaves of *Annona muricata*. *American Chemical Society and American Society of Pharmacognosy*.

Kim, Y. H., Yang, H. E., Park, B. K., Heo, M. Y., Jo, B. K. & Kim, H. P. 2002. The Extract of the Flowers of *Prunus persica*, a New Cosmetic Ingredient, Protects against Solar Ultraviolet-induced Skin Damage *in vivo*. *Journal of Cosmetic Science,* 53**,** 27-34.

Kofink, M., Papagiannopoulos, M. & Galensa, R. 2007. (-)-Catechin in Cocoa and Chocolate: Occurence and Analysis of an Atypical Flavan-3-ol Enantiomer. *Molecules,* 12**,** 1274-1288.

Kohler, I., Jenett-Siems, K., Siems, K., Hernandez, M. A., Ibarra, R. A., Berendsohn, W. G., Bienzle, U. & Eich, E. 2002. *In vitro* Antiplasmodial Investigation of Medicinal Plants from El Salvador. *Verlag der Zeitschrift fur Naturforschung,* 57c**,** 277-281.

Kong, J.-M., Goh, N.-K., Chia, L.-S. & Chia, T.-F. 2003. Recent Advances in Traditional Plant Drugs and Orchids. *Acta Pharmacologica Sinica,* 24**,** 7-21.

Kornwongwan, P. & Luangkamin, S. 2011. Pentacyclic Triterpenoids and Steroids from the Rhizomes of *Agapetes hosseana* Diels. *In:* PATTANAPRATEEB, P. (ed.) *Pure and Applied Chemistry International Conference 2011* Miracle Grand Convention Hotel.

Kuljanabhagavad, T., Suttisri, R., Pengsuparp, T. & Ruangrungsi, N. 2009. Chemical Structure and Antiviral Activity of Aerial Part From *Laggera Pterodonta*. *Journal of Health Research,* 23**,** 175-177.

Lagnika, L., Weniger, B., Vonthron-Senecheau, C. & Ambaliou, S. 2009. Antiprotozoal Activities of Compounds Isolated From *Croton lobatus L.* *African Journal of Infectious Diseases,* 3**,** 1-5.

Lakshmi, V., Pandey, K., Mishra, S. K., Srivastava, S., Mishra, M. & Agarwal, S. K. 2009. An Overview of Family Hermandiaceae. *Records of Natural Products,* 3**,** 1-22.

Lambole, V. B. 2010. Phytopharmacological Properties of *Aegle marmelos* as A Potential Medicinal Tree: An Overview. *Internaltional journal of Pharmaceutical Sciences Review and Research,* 5**,** 67-72.

Lee, N. H. S., Xu, Y.-J. & Goh, S. H. 1999. 5-Oxonoraporphines from *Mitrephora* cf. maingayi. *Journal of Natural Product,* 62**,** 1158-1159.

Lekphrom, R., Kanokmedhakul, S. & Kanokmedhakul, K. 2009. Bioactive Stryllactones and Alkaloids from Flowers of *Goniothalamus laotica*. *Journal of Ethnopharmacology,* 125**,** 47-50.

Li, C., Lee, D., Graf, T. N., Phifer, S. S., Nakanishi, Y., Burgess, J. P., Riswan, S., Setyowati, F. M., Saribi, A. M., Soejarto, D. D., Farnsworth, N. R., Falkinham, J. O., Kroll, D. J., Kinghorn, D., Wani, M. C. & Oberlies, N. H. 2005. A Hexacyclic *ent*-Trachylobane Diterpenoids Possessing an Oxetane Ring from *Mitrephora glabra*. *Organic Letters,* 7**,** 5709-5712.

Li, C., Lee, D., Graf, T. N., Phifer, S. S., Nakanishi, Y., Riswan, S., Setyowati, F. M., Saribi, A. M., Soejarto, D. D., Farnsworth, N. R., Falkinham, J. O., Kroll, D. J., Kinghorn, D., Wani, M. C. & Oberlies, N. H. 2009. Bioactive Constituents of the Stem Bark of *Mitrephora glabra*. *Journal of Natural Product,* 72**,** 1949-1953.

Litaudon, M., Bousserouel, H., Awang, K., Nosjean, O., Martin, M.-T., Dau, M. E. T. H., Hadi, H. A., Boutin, J. A., Sevenet, T. & Gueritte, F. 2009. A Dimer Sesquiterpenoid from a Malaysian *Meiogyne* as a New Inhibitory of Bcl-xL/BakBH3 Domain Peptide Interaction. *Journal of Natural Product,* 72**,** 480-483.

Lopes, G., O, Rocha, J., C. B., Almeida, G., C. De & Mello, J., C. P. 2009. Condensed Tannins from the Bark of *Guazuma ulmifolia* Lam. (Sterculiaceae). *Journal of the Brazilian Chemical Society,* 2009**,** 1103-1109.

Lu, S.-T., Tsai, I.-L. & Leou, S.-P. 1989. Alkaloids of *Dehaasia Triandra*. *Phytochemistry,* 28**,** 615-620.

Lu, Z., Huang, L., Chen, R. & Yu, D. 2009. Chemical Constituents of *Uvaria kurzii*. *Zhongguo Zhong Yao Za Zi,* 34**,** 2203-2205.

Luize, P., Shima, Ueda-Nakamura, T., Filho, B., Prado, Dias & Cortez, D., Aparicio, Garcia 2006. Activity of Neolignans Isolated from *Piper regnellii* (Miq.)

C.DC. var. pallescens (C.DC.) Yunck Against Trypanosoma cruzi. *Biol Pharm Bull* 29**,** 2126-2130.

Madan, S., Singh, G., Kumar, Y., Singh, R. M., Mir, S. & Ahmad, S. 2008. A New Flavanone from *Flemingia strobilifera* (Linn) R. Br. and its Antimicrobial Activity. *Tropical Journal of Pharmaceutical Research* 7**,** 921-927.

Mahato, S. B. & Kundu, A. P. 1994. ^{13}C NMR Spectra of Pentacyclictriterpenoids-A Compilation and Some Salient Features. *Phytochemistry,* 37**,** 1517-1575.

Manna, A., Kumar, Jena, J., Behera, A., Kumar, Roy, D., Manna, S., Karmakar, S. & Kar, S. 2009. Effect of *Pterospermum acerifolium* Bark Extract on Oxidative Damages in The Gastric Tissue During Alcohol Induced Ulceration. *Internaltional journal of Pharmacy and Pharmaceutical Sciences* 1**,** 51-59.

Mannina, L., Cristinzio, M., Sobolev, A., P, Ragni, P. & Segre, A. 2004. High-Field Nuclear Magnetic Resonance (NMR) Study of Truffles (*Tuber aestivum vittadini*). *Journal of Agricutural and Food Chemistry,* 52**,** 7988-7996.

Martinez-Vazquez, M., Apan, T. O. R., Lazcano, M. E. & Bye, R. 1999. Anti-inflammatory Active Compounds from the *n*-Hexane Extract of *Euphorbia hirta*. *Journal of the Maxican Chemical Society,* 43**,** 103-105.

Maxwell, J. F. 2007. Vegetation of Doi Tung, Chiang Rai province, northern Thailand. *Maejo International Journal of Science and Technology,* 1**,** 10-63.

Mclaughlin, J. L. 1991. Crown Gall Tumours on Potato Disc and Brine Shrimp Lethality: Two Simple Bioassays for Higher Plant Screening and Fractionation. *In:* HOSTETTMANN, K. (ed.) *Methods in Plant Biochemistry.* San Diego: Academic Press Limited.

Meng, D.-H., Xu, Y.-P., Chen, W.-L., Zou, J., Lou, L.-G. & Zhao, W.-M. 2007. Anti-tumour Clerodane-Type Diterpenes from *Mitrephora thorelii*. *Journal of Asian Natural Products Research,* 9**,** 679-684.

Meselhy, M. R. 2003. Constituents from Moghat, the Roots of *Glossostemon bruguieri* (Desf.). *Molecules,* 8**,** 614-621.

Meyer, B. N., Ferrigni, N. R., Putnam, J. E., Jacobsen, L. B., Nicholas, D. E. & Mclaughlin, J. L. 1982. Brine shrimp: Convenient General Bioassay for Activeplant Constituents. *Planta Medica,* 45**,** 31-34.

Moghaddam, F. M., Farimani, M. M., Salahvarzi, S. & Amin, G. 2006. Chemical Constituents of Dichloromethane Extract of Cultivated *Satureja khuzistanica*. *Evidence-Based Complementary and Alternative Medicine (eCAM),* 4**,** 195-198.

Moharam, B. A., Jantan, I., Jalil, J. & Shaari, K. 2010. Inhibitory Effects of Phylligenin and Quebrachitol Isolated from *Mitrephora vulpina* on Platelet Activating Factor Receptor Binding and Platelet Aggregation *Molecules,* 15**,** 7840-7848.

Molyneux, P. 2004. The Use of the Stable Free Radical Diphenylpicryl-Hydrazyl (DPPH) for Estimating Antioxidant Activity. *Songklanakarin Journal of Science and Technology,* 26**,** 211-219.

Mosmann, T. 1983. Rapid Cplorimetric Assay for Cellular Growth and Survival: Application to Proliferation and Cytotoxicity Assays. *Journal of Immunological Methods,* 65**,** 55-63.

Mueller, D., Davis, R. A., Duffy, S., Avery, V. M., Camp, D. & Quinn, R. J. 2009. Antimalarial Activity of Azafluorenone Alkaloids from the Australian Tree *Mitrephora diversifolia*. *Journal of Natural Product,* 72**,** 1538-1540.

Muhit, A., Khanam, S., Shultana, Islam, S., Rahman, M., S. & Begum, B. 2010. Phytochemical and Biological Investigations of *Pterospermum acerifolium* Wild Bark. *Journal of Pharmacy Research,* 3**,** 2643-2646.

Nakano, T. 1954. Studies on the Alkaloids of *Magnoliaceous* Plants. XIII. Alkaloids of *Magnolia grandiflora* L. *Chemical & Pharmaceutical Bulletin,* 2**,** 326-328.

Nakano, T. 1956a. Studies on the Alkaloids of *Magnoliaceous* Plant. XVI. Alkaloids of *Magnolia denudata*. *Chemical & Pharmaceutical Bulletin,* 4**,** 67-68.

Nakano, T. 1956b. Studies on the Alkaloids of *Menispermaceous* Plants. CXXXI. Isolation of Magnoflorine From *Cocculus trilobus* DC. *Chemical & Pharmaceutical Bulletin,* 4**,** 69-70.

Ogle, N. 2009. Green Tea *Camellia sinensis*. *Australian Journal of Medical Herbalism,* 21**,** 44-48.

Panchal, H. S., Master, S. M., Shah, U. D., Saluja, A. K. & Dholwani, K. K. 2010. Anti-convulsion Activity of Leaf of *Trema orientalis*. *International Journal of Pharmaceutical Research,* 2**,** 53-55.

Park, J. B. 2011. Effects of Typheramide and Alfrutamide Found in *Allium* Species on Cyclooxygenase and Lipoxygenase. *Journal of Medicinal Food* 14**,** 226-231.

Park, J. Y., Lee, S., Han, S., Kim, H. M., Lee, J. M., Ahn, Y.-H., Lee, S. Y. & Lee, S. 2009. Phytochemical Constituents from the Seed of *Lithospermum erythrorhizon*. *Natural Product Sciences,* 15**,** 181-184.

Patra, A., Jha, S., Murthy, P. N. & Sharone, A. 2010. Isolation and Characterization of Stigmasterol-5-en-3B-ol (B-sitosterol) from the Leaves of *Hygrophila spinosa* T. Anders. *International Journal of Pharma Sciences and Research,* 1**,** 95-100.

Pattanaik, P. & Parida, S. 2010. Antimicrobial and Anthelmintic Activity of Barks of *Pterospermum acerifolium (Sterculiaceae)*. *Internaltional journal of Pharma World Research,* 1**,** 1-38.

Pessini, G., Lorena, Filho, B., Prado, Dias, Nakamura, C., Vataru & Cortez, D., Aparicio, Garcia 2003. Antibacterial Activity of Extracts and Neolignans from *Piper regnellil* (Miq.) C. DC. var. pallescens (C. DC.) Yunck. *Mem Inst Oswalda Cruze,* 98**,** 1115-1120.

Pinheiro, M. L. B., Xavier, C. M., Souza, A. D. L., Rabelo, D. D. M., Batista, C. L., Batista, R. L., Costa, E. V., Campos, F. R., Barison, A., Valdez, R., Tania, U.-N. & Nakamura, C., Vataru 2009. Acanthoic Acid and other Constituents from the Stem of *Annona amazonica* (Annonaceae). *Journal of Brazilian Chemical Society,* 20**,** 1095-1102.

Qiao, W., Zhao, C., Qin, N., Zhai, H. Y. & Duan, H. Q. 2011. Identification of trans-tiliroside as Active Principle with Anti-hyperglycemic, Anti-hyperlipidemic and Antioxidant Effects from *Potentilla chinesis*. *Journal of Ethnopharmacology,* 135**,** 515-521.

Rachchh, M. A. & Jain, S. M. 2008. Gastoprotective Effect of *Benincasa hispida* Fruit Extract. *Indian Journal of Pharmacology,* 40**,** 271-275.

Rahman, M. S., Begum, B., Chowdhury, R., Rahman, K. M. & Rashid, M. A. 2008. Preliminary Cytotoxicity Screening of Some Medicinal Plants of Bangladesh. *University of Dhaka Journal of Pharmaceutical Sciences,* 7**,** 47-52.

Rahman, S. M. M., Mulkta, Z. A. & Hossain, M. A. 2009. Isolation and Characterization of *b*-Sitosterol-D-glycoside from Petroleum Extract of the Leaves of *Ocimum sanctum* L. *Asian Journal of Food and Agro-Industry,* 2**,** 39-43.

Rai, N. P., Adhikari, B. B., Paudel, A., Masuda, K., Mckelvey, R. D. & Manandhar, M. D. 2006. Phytochemical Constituents of the Flowers of *Sarcococca coriacea* of Nepalese origin. *Journal of Nepal Chemical Society,* 21**,** 1-7.

Rimando, A., Pezzuto, J., Farnsworth, N., Santisuk, T. & Reutrakul, V. 1994. Revision of the NMR Assigments of Pterostilbene and of Dihydrodehydroconiferyl Alcohol: Cytotoxic Constituents From *Anogeissus acuminata*. *Natural Product Letter,* 4**,** 267-272.

Rizvi, S. a. I. & Sultana, T. 1972. Phytochemical Studies of the Flowers of *Pterospermum acerifolium. Phytochemistry,* 11**,** 856-858.

Saboo, S., Tapadiya, R., Khadabadi, S. S. & Deokate, U. A. 2010. *In vitro* Antioxidant Activity and Total Phenolic, Flavonoid Contents of the Crude Extracts of *Pterospermum acerifolium* Willd Leaves (*Sterculiaceae*). *Journal of Chemical and Pharmaceutical Research,* 2**,** 417-423.

Saklani, A. & Kutty, S. K. 2008. Plant-derived Compounds in Clinical Trials. *Drug Discovery Today,* 13**,** 161-171.

Sam, T. W. 1993. Toxicity Testing Using the Brine Shrimp *Artemia salina*. *In:* MOLYNEUX, R. J. (ed.) *Bioactive Natural Products Detection, Isolation, and Structural Determination.* Boca Raton: CRC Press.

Sannigrahi, S., Parida, S., Patro, J., Mishra, U., Shankar & Pathak, A. 2010. Antioxidant and Anti-inflammatory Potential of *Pterospermum acerifolium*. *International Journal of Pharmaceutical Sciences Review and Research,* 2**,** 1-5.

Saripah, S. S. a. A., Mat Ropi, M., Hadi, A. H., A., Abdullah, N. R. & Awang, K. 2009. Isoquinoline Alkaloids and Antimalarial Properties of *Popowia perakensis* Extract. *Jurnal Sains dam Matematik,* 1**,** 80-86.

Sawasdee, K., Chaowasku, T. & Likhitwitayawuid, K. 2010. New Neolignans and a Phenylpropanoid Glycoside from Twigs of *Miliusa mollis*. *Molecules,* 15**,** 639-648.

Seo, P.-J., Choi, H. D. & Son, B.-W. 2004. Total Synthesis of Norneolignans from *Krameria* Species. *Archives of Pharmacal Research,* 27**,** 1189-1193.

Sharma, A., Vijayakumar, M., Verma, A. R., Talib, M., Unnikrishnan, M. K. & Rao, C. V. 2009. *In vitro* a-Amylase Inhibition and Antihyperglycemic Activity of *Helicteres isora* in Streptozotocin-Induced Rats. *International Journal ofPharmaceutical and Clinical Research,* 1**,** 15-18.

Sherine, G., Bhalerao, S., V., Lidstone, E., A., Ahmad, I., S., Abbasi, A., Cunningham, B., T. & Watkin, K., L. 2010. Cytotoxicity Screening of Bangladeshi Medicinal Plant Extracts on Pancreatic Cancer Cells. *BioMedCentral Complementary and Alternative Medicine,* 10**,** 1-11.

Shimada, A., Takeuchi, S., Nakajima, A., Tanaka, S., Kawano, T. & Kimura, Y. 1999. Phytotoxicity of Indole-3-acetic acid Produced by the Fungus, *Pythium aphanidermatum*. *Bioscience, Biotechnology, and Biochemistry,* 63**,** 187-189.

Shu, S.-H., Han, J.-L., Du, G.-H. & Qin, H.-L. 2008. A New Flavonoid from Heartwood of *Caesalpinia sappan*. *China Journal of Chinese Materia Medica,* 33**,** 905-908.

Sichaem, J., Ruksilp, T., Worawalia, W., Siripong, P., Khumkratok, S. & Tip-Pyang, S. 2011. A New Dimeric Aporphine from the Roots of *Artabotrys spinosus*. *Fitoterapia,* 82**,** 422-425.

Silva, D. B. D., Tulli, E. C. O., Garcez, W., Nascimento, E. V. & Siqueira, J. M. 2007. Chemical Constituents of the Underground Stem Bark of *Duguetia furfuracea* (Annonaceae). *Journal of the Brazilian Chemical Society,* 18**,** 1560-1565.

Sivonova, M., Zitnanova, I., Horakova, L., Strosova, M., Muchova, J., Balgavy, P., Dobrota, D. & Durackova, Z. 2006. The Combined Effect of Pycnogenol with Ascorbic Acid and Trolox on the Oxidation of Lipids and Proteins. *General Physiology and Biophysics,* 25**,** 379-396.

Sripathi, S. K., Gopal, P. & Lalitha, P. 2011. Allantoin from the Leaves of *Pisonia grandis* R. Br. *International Journal of Pharmacy & Life Science,* 2**,** 815-818.

Subhadhirasakul, S. & Pechpongs, P. 2004. A Terpenoid and Two Steroids from the Flowers of *Mammea siamensis*. *Songklanakarin Journal of Science and Technology,* 27**,** 555-561.

Sudjaroen, Y. 2008. Antihypertensive and Antioxidant Activities of Methanol Extract from Malva Nut (*Scaphium scaphigerum*). *The Public Health Journal of Burapha University,* 3**,** 24-27.

Supudompol, B., Chaowasku, T., Kingfang, K., Burud, K., Wongseripipatana, S. & Likhitwitayawuid, K. 2004. A New Pimarane from *Mitrephora tomentosa*. *Natural Product Research,* 18**,** 387-390.

Sureshan, K. M., Murakami, T. & Watanabe, Y. 2009. Total Syntheses of Cyclitol Based Natural Products from *myo*-inositol: Brahol and Pinpollitol. *Tetrahedron,* 65**,** 3998-4006.

Tanamatayarat, P., Sotanaphun, U. & Poobrasert, O. 2011. Thai Plant from Doi Tung: Brine Shrimp Lethality, Antioxidative Activity, and Combination Effect with L-Ascorbic Acid. *Natural Product Research***,** 1-7.

The Mae Fahluang Foundation under Royal Patronage. 2008. *Doi Tung* [Online]. Available: http://www.doitung.org/home.php [Accessed October 16, 2008].

Tiwari, K. P., Choudhary, R. N. & Singh Rathore, Y. K. 1977. Chemical Examination of Stem Cuttings of *Pterospermum heyneanum*. *Journal of Indian Chemical Society,* 54**,** 916B.

Traditional Chineses Medicine Daynetwork. 2010. *big red hair leaf* [Online]. Available:http://babelfish.yahoo.com/translate_url?trurl=http%3A%2F%2Fwww.ywkaitai.com%2Fzhongcaoyao%2FDaHongMaoYe%2F&lp=zh_en&.intl=us&fr=altavista [Accessed March 09 2011].

Treeratanapiboon, L., Worachartcheewan, A., Suksrichavalit, T., Kiatfuengfoo, R., Prachayasittikul, S., Ruchirawat, S. & Prachayasittikul, V. 2011. Bioactive

4-Hydroxycinnamide and Bioactivities of *Polyalthia cerasoides*. *Experimental and Clinical Science International Online Journal for Advances in Science*, 10**,** 16-22.

Tsao, C.-C., Shen, Y.-C., Su, C.-R., Li, C.-Y., Liou, M.-J., Dung, N.-X. & Wu, T.-S. 2008. New Diterpenoids and the Bioactivity of *Erythrophleum fordii*. *Bioorganic & Medicinal Chemistry,* 16**,** 9867-9870.

Vrchotova, N., Sera, B. & Triska, J. 2007. The Stilbene and Catechin Content of the Spring Sprouts of *Reynoutria* Species. *Acta Chromatographica,* 19**,** 21-28.

Waters, B., Saxena, G., Wanggui, Y., Kau, D., Wrigley, S., Stokes, R. & Davies, J. 2002. Identifying Protein Kinase Inhibitors Using an Assay Based on Inhibition of Aerial Hyphae Formation in *Streptomyces*. *The Journal of Antibiotics,* 55**,** 407-416.

Weerasooriya, A., D, Chalermglin, P. & Saunders, R., M. K. 2006. *Mitrephora sirikitiae* (Annonaceae): A Remarkable New Species Endemic to Northern Thailand. *Nordic Journal of Botany,* 24**,** 201-206.

Wu, Y.-C., Chang, G.-Y., Ko, F.-N. & Teng, C.-M. 1995. Bioactive Constituents from the Stems of *Annona montana*. *Planta Medica,* 61**,** 146-149.

Xu, B., Sung, C. & Han, B. 2011. Crystal Structure Characterization of Natural Allantoin from Edible Lichen *Umbilibaria esculenta*. *Crystals,* 1**,** 128-135.

Xu, J., Ze, Yeung, S., Ying, Venus, Chang, Q., Huang, Y. & Chen, Z.-Y. 2004. Comparison of Antioxidant Activity and Bioavailability of Tea Epicatechins with Their Epimers. *British Journal of Nutrition,* 91**,** 873-881.

Ya, T., Gilbert, M. G. & Dorr, L. J. 2010. *Sterculiaceae* [Online]. Available: http://hua.huh.harvard.edu/china/mss/volume12/Sterculiaceae.pdf [Accessed March 05 2010].

Yang, B.-Y., Xia, Y.-G., Chen, D. & Kuang, H.-X. 2010. Chemical Constituents from the Flower of *Datura metel*. *Chinese Journal of Natural Medicines,* 8**,** 429-432.

Yao, G., Sebisubi, F. M., Voo, L. Y. C., Ho, C. C., Tan, G. T. & Chang, L. C. 2011. Citrinin Derivatives from the Soil Filamentous Fungus *Penicillium* sp. H9318. *Journal of the Brazilian Chemical Society*22**,** 1125-1129.

Yoo, N. H., Jang, D. S. & Kim, J. S. 2008. Phytochemical Constituents of the Roots of *Erigeron annuus*. *Journal of Korean Society for Applied Biological Chemistry,* 51**,** 305-308.

Yu, R., Li, B.-G., Ye, Q. & Zhang, G.-L. 2005. A Novel Alkaloids from *Mitrephora maingayi*. *Natural Product Research,* 1**,** 359-362.

Zgoda-Pols, J. R., Freyer, A. J., Killmer, L. B. & Porter, J. R. 2002. Antimicrobial Diterpenoids from the Stem Bark of *Mitrephora celebica*. *Fitoterapia,* 73**,** 434-438.

Zgoda, J. R., Freyer, A. J., Killmer, L. B. & Porter, J. R. 2001. Polyacetylene Carboxylic Acids from *Mitrephora celebica*. *Journal of Natural Product,* 64**,** 1348-1349.

Zhong, Y. L., Zeng, L. M., Tu, G. Z., Ma, L. B. & Hong, S. L. 1993. Triterpenes from the Leaves of *Pterospermum lanconfolium* Roxb. *Gaodeng Xuexiao Huaxue Xuebao,* 14**,** 214-216.

APPENDICES

APPENDIX A

LIST OF ABBREVEATIONS AND SYMBOLS

α	=	Alpha
$[\alpha]^t_D$	=	Specific rotation at t ^oC and sodium D line
β	=	Beta
BSL	=	Brine Shrimp Lethality
BZI	=	Bald Zone Inhibition
^oC	=	Degree Celsius
calcd.	=	Calculated
CC	=	Columm Chromatography
$CDCl_3$	=	Deuterated chloroform
CD_3OD	=	Deuterated methanol
CI	=	Combination index
CZI	=	Clear Zone Inhibiton
CH_2Cl_2	=	Dichloromethane
cm^{-1}	=	Reciprocal centimeter
^{13}C-NMR	=	Carbon-13 Nuclear Magnetic Resonance
2D-NMR	=	Two Dimensional Nuclear Magnetic Resonance
d	=	Doublet
dd	=	Doublet of doublet
DEPT	=	Distortionless Enhancement by Polarization Transfer
DMSO	=	Dimethyl sulfoxide
DMSO-d_6	=	Deuterated dimethyl sulfoxide
D_2O	=	Deuterium oxide
DPPH	=	1,1-Diphenyl-2-picrylhydrazyl
δ	=	Chemical Shift
EtOAc	=	Ethyl acetate
g	=	gram
Hex	=	Hexane
hr	=	Hour
HFI	=	Hyphae Forrnation Inhibition
^{1}H-NMR	=	Proton Nuclear Magnetic Resonance

HMBC	=	Heteronuclear Multiple Bond Coherence
HMQC	=	Heteronuclear Multiple Quantum Coherence
HRESIMS	=	High Resolution Electrospray Ionization Mass Spectrometry
H_2O	=	water
Hz	=	Hertz
IC_{50}	=	Inhibition Concentration at 50%
IR	=	Infrared Spectrum
J	=	Coupling constant
Kg	=	Kilogram
K_i	=	inhibition constant of a compound determined at equilibrium with reference
L	=	Liter
µg	=	Microgram
µL	=	Microliter
λ_{max}	=	Wavelength at maximal absorption
ε	=	Molar absorptivity
M^+	=	Molecular ion
m	=	Multiplet
MeOH	=	Methanol
mg	=	Milligram
$[M+H]^+$	=	Protonated molecular ion
MHz	=	Megahertz
mm	=	Millimeter
ml	=	Milliliter
mp	=	Melting point
MS	=	Mass spectrometry
MTT	=	3-(4,5-dimethylthiazol-2-yl)-2,5-diphenyltetrazolium bromide
MW	=	Molecular weight
m/z	=	Mass to charge ratio
nm	=	nanometer

NOESY	=	Nuclear Overhauser Enhancement Spectroscopy
ppm	=	Part per million
q	=	Quartet
s	=	Singlet
t	=	Triplet
TLC	=	Thin Layer Chromatography
UV-VIS	=	Ultraviolet and Visible Spectrophotometry
µg	=	Microgram
µl	=	Microliter
ν_{max}	=	Wave number at maximal absorption
5-FU	=	5-fluorouracil
ϕ	=	diameter

APPENDIX B

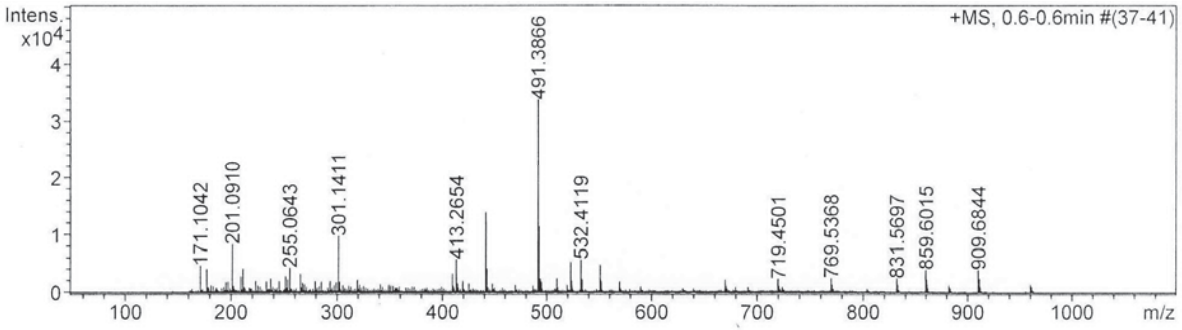

Figure 55 IR (KBr) spectrum of compound PGH-1

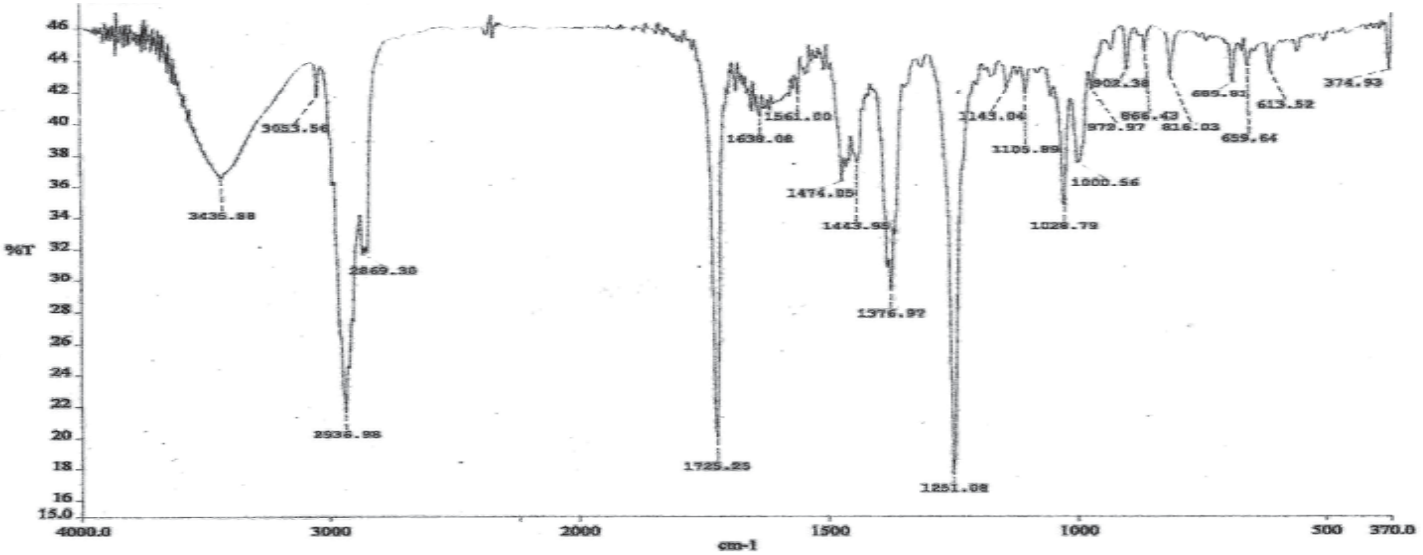

Figure 56 IR (KBr) spectrum of compound PGH-1

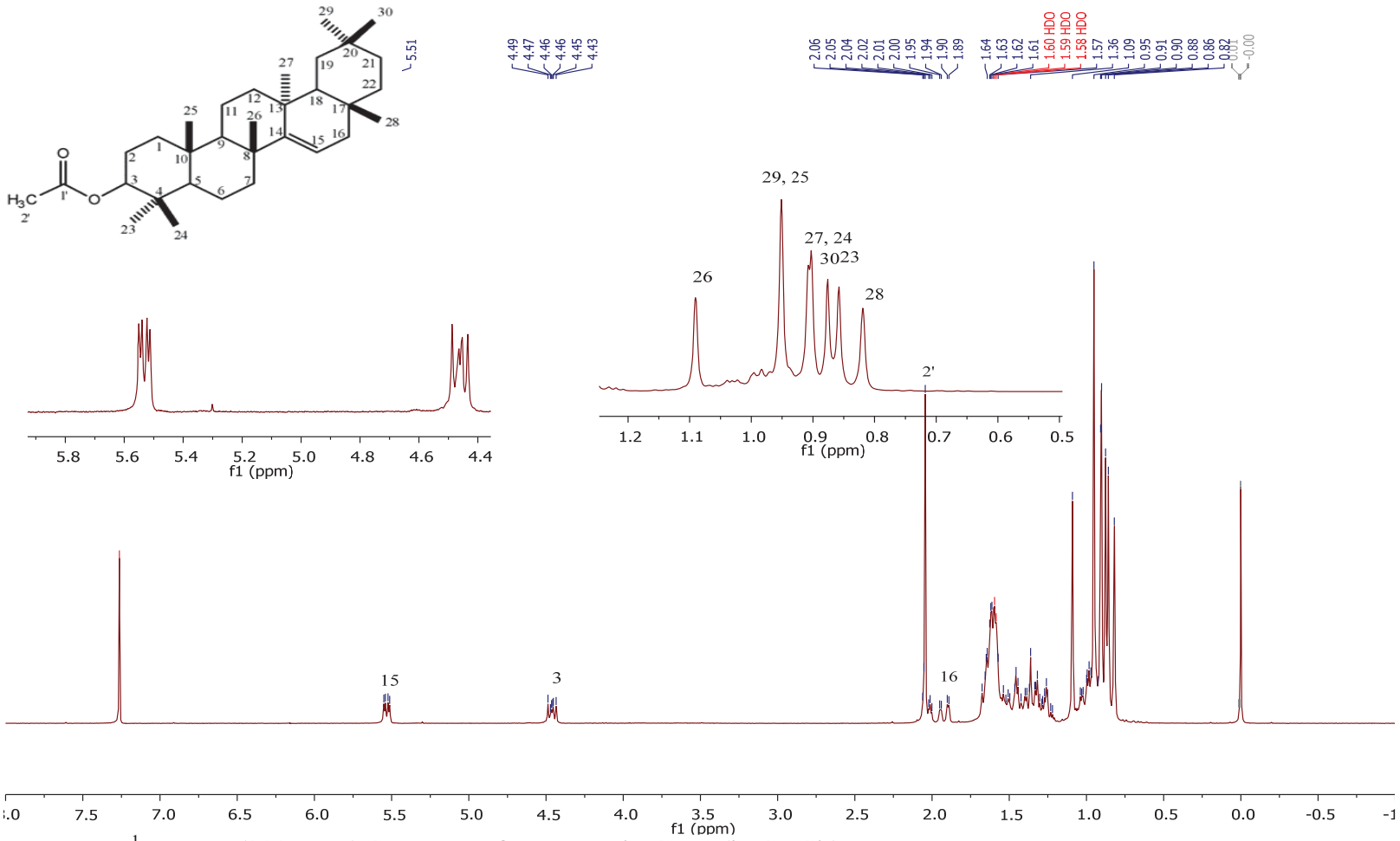

Figure 57 ^{1}H NMR (300 MHz) Spectrum of compound PGH-1 (in $CDCl_3$)

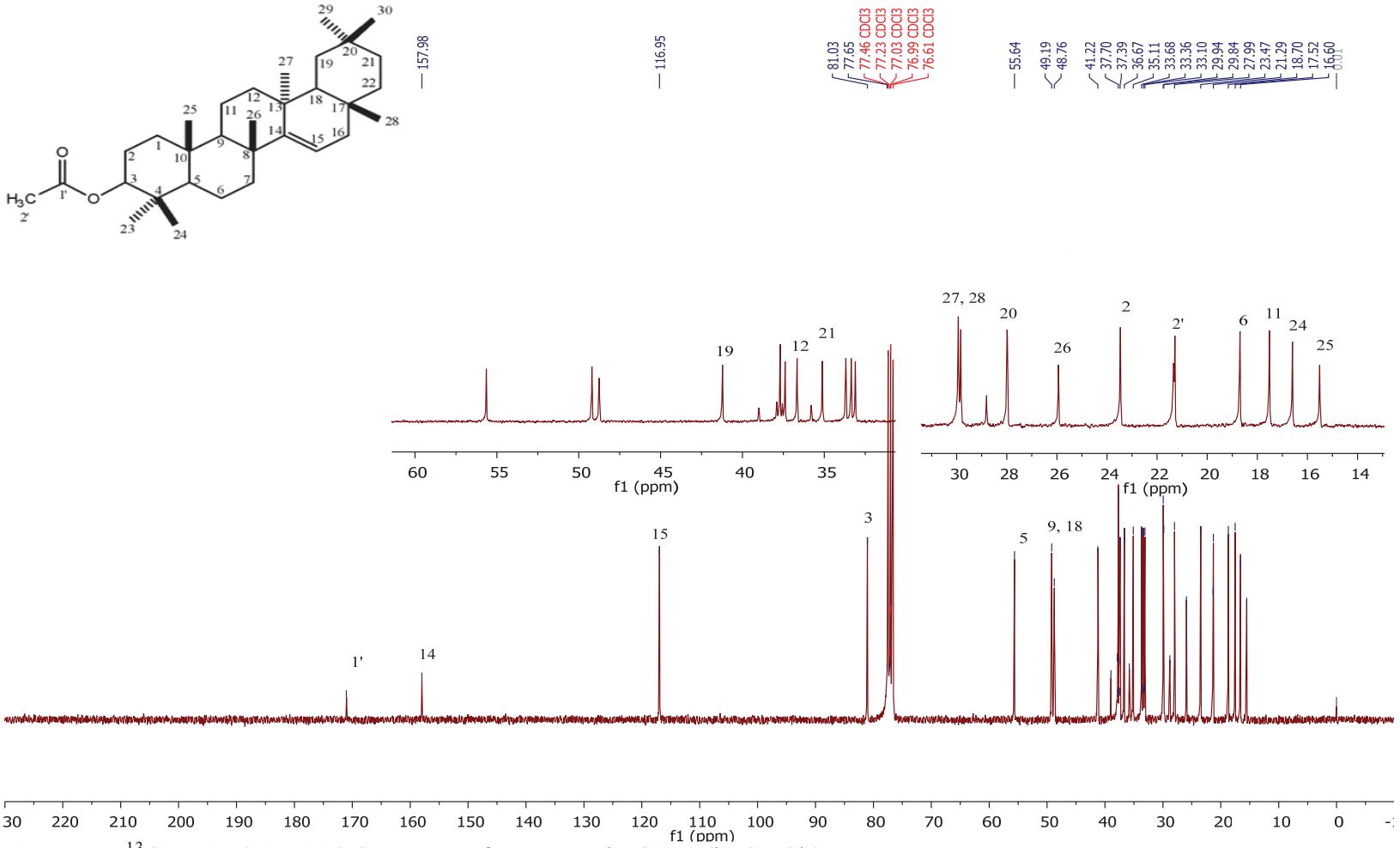

Figure 58 ^{13}C NMR (75 MHz) Spectrum of compound PGH-1 (in $CDCl_3$)

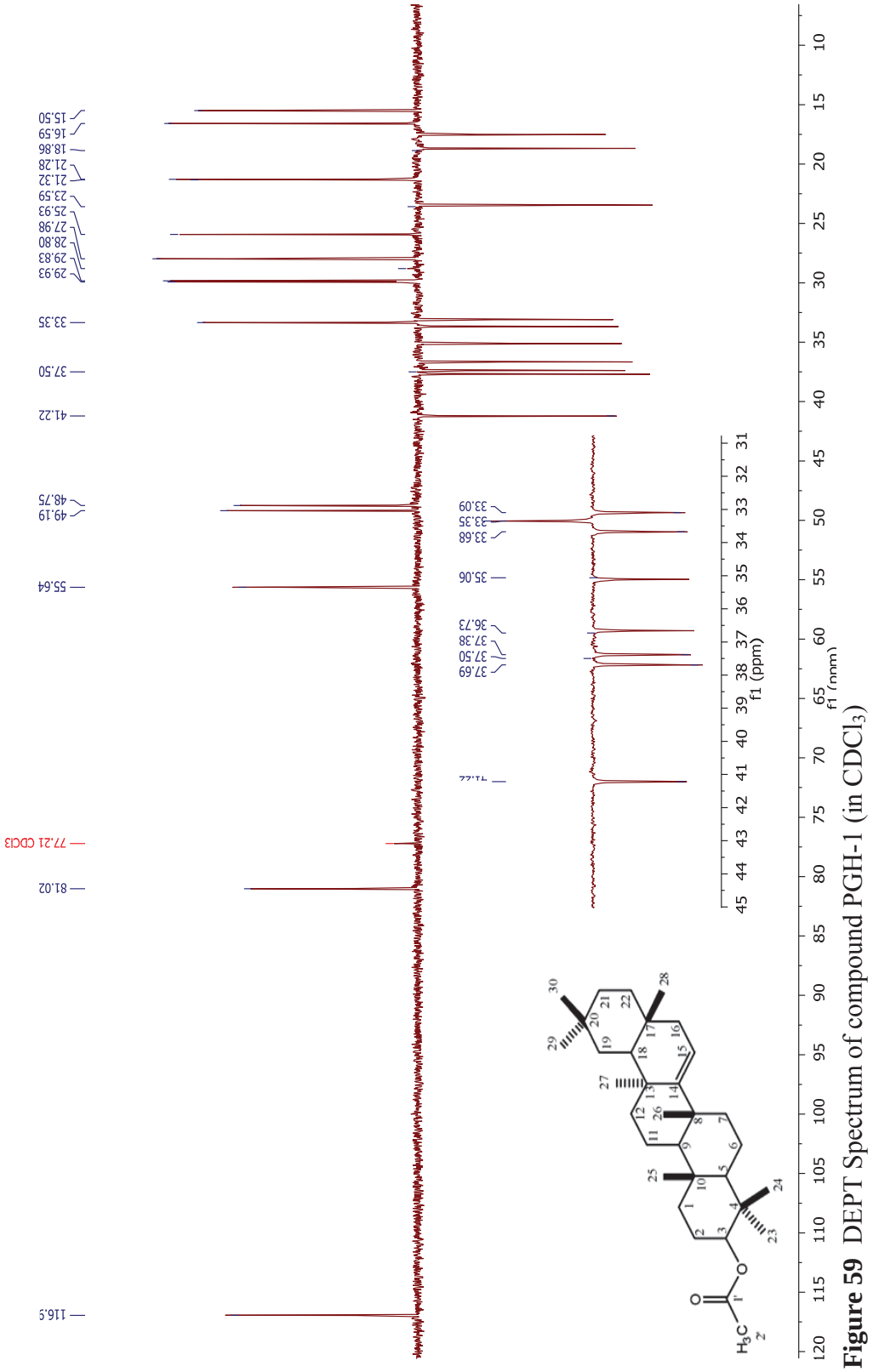

Figure 59 DEPT Spectrum of compound PGH-1 (in $CDCl_3$)

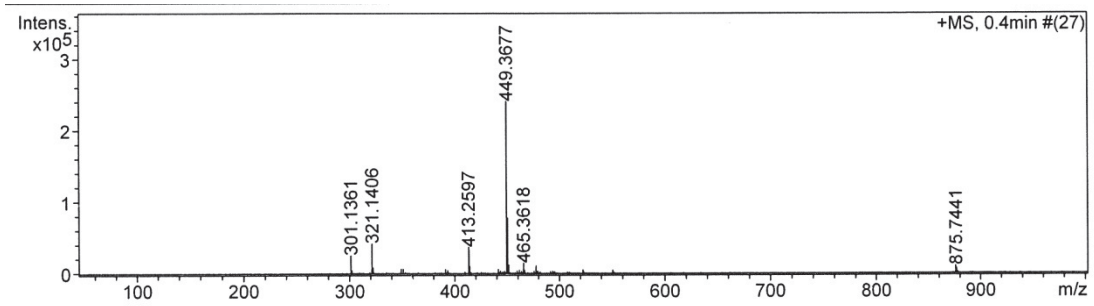

Figure 60 IR (KBr) spectrum of compound PGH-2

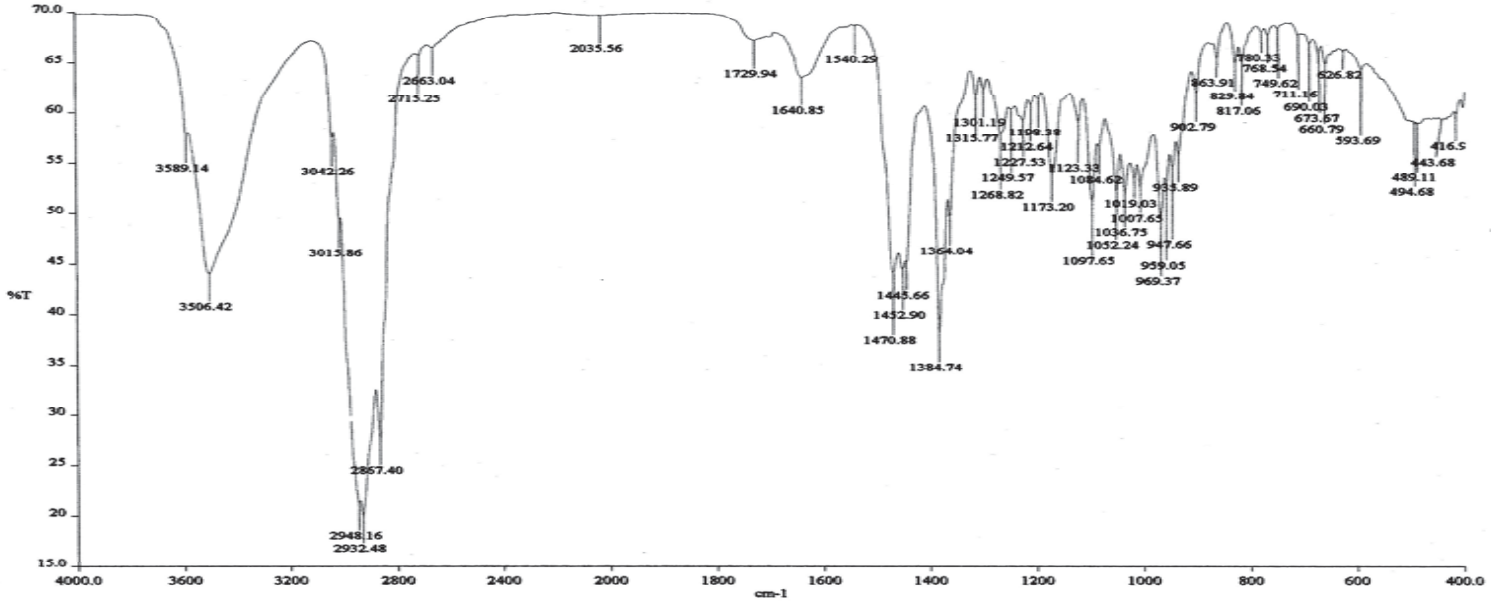

Figure 61 IR (KBr) spectrum of compound PGH-2

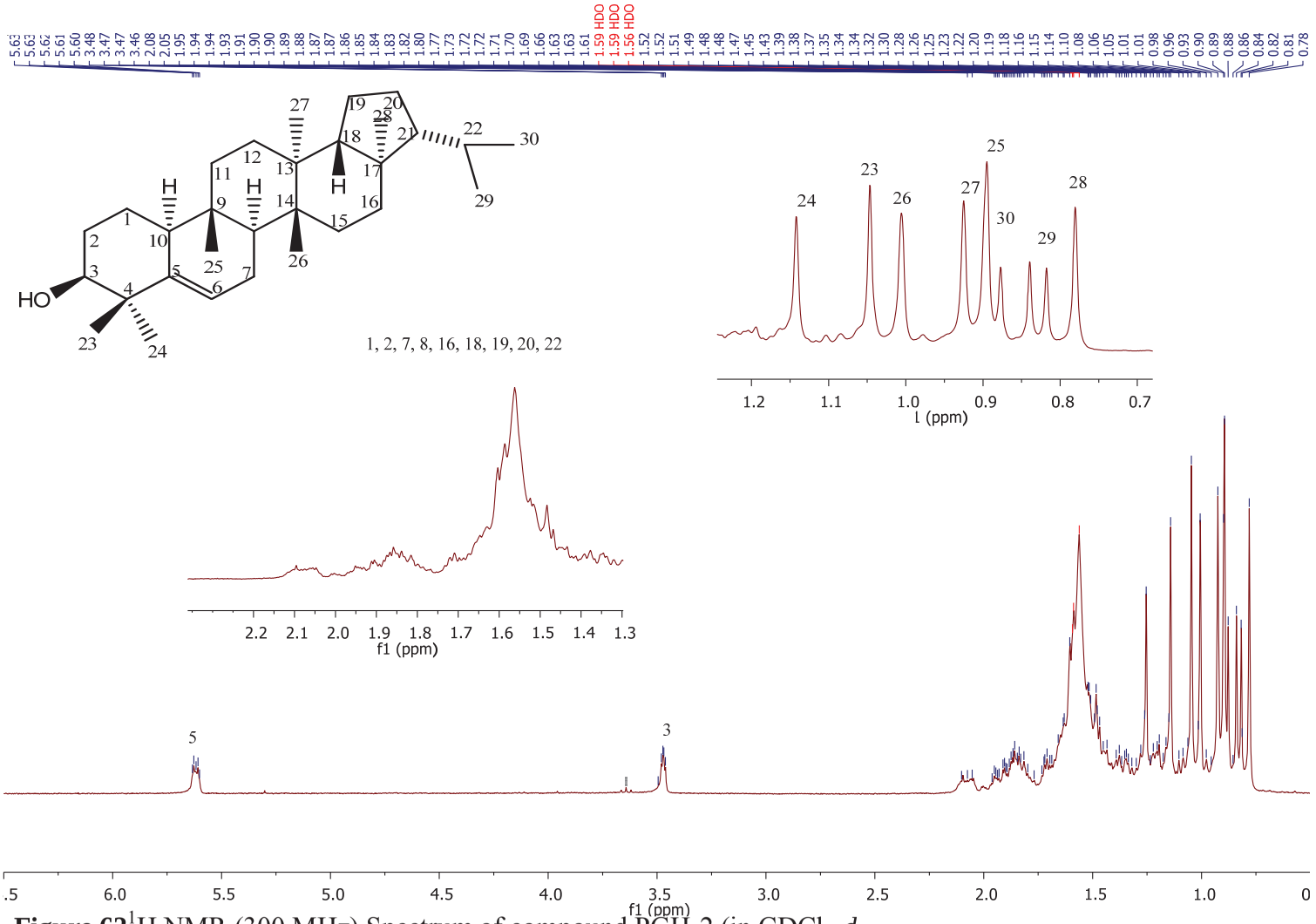

Figure 62^{1}H NMR (300 MHz) Spectrum of compound PGH-2 (in $CDCl_3$-*d*

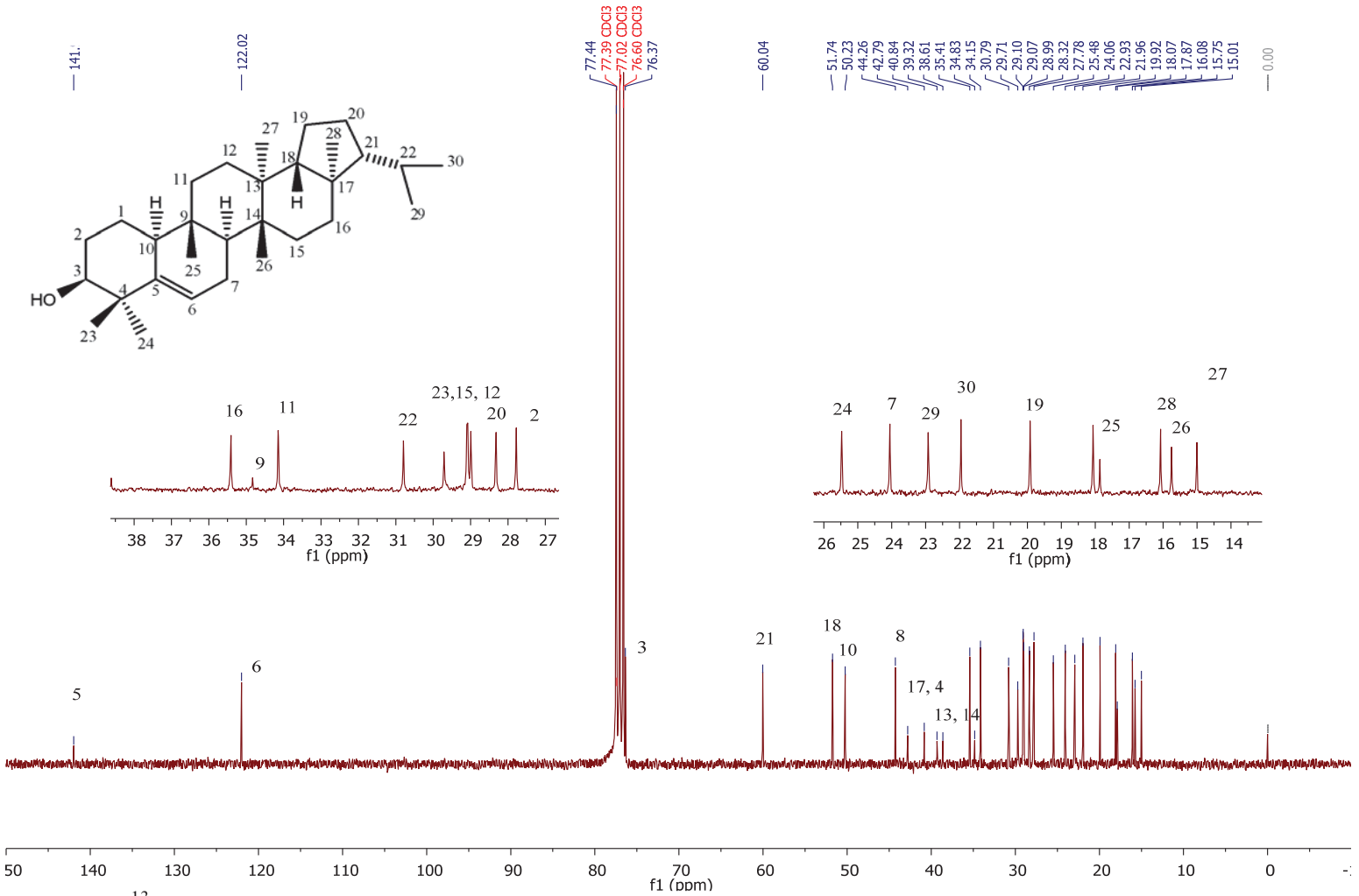

Figure 63 ^{13}C NMR (75 MHz) Spectrum of compound PGH-2(in $CDCl_3$)

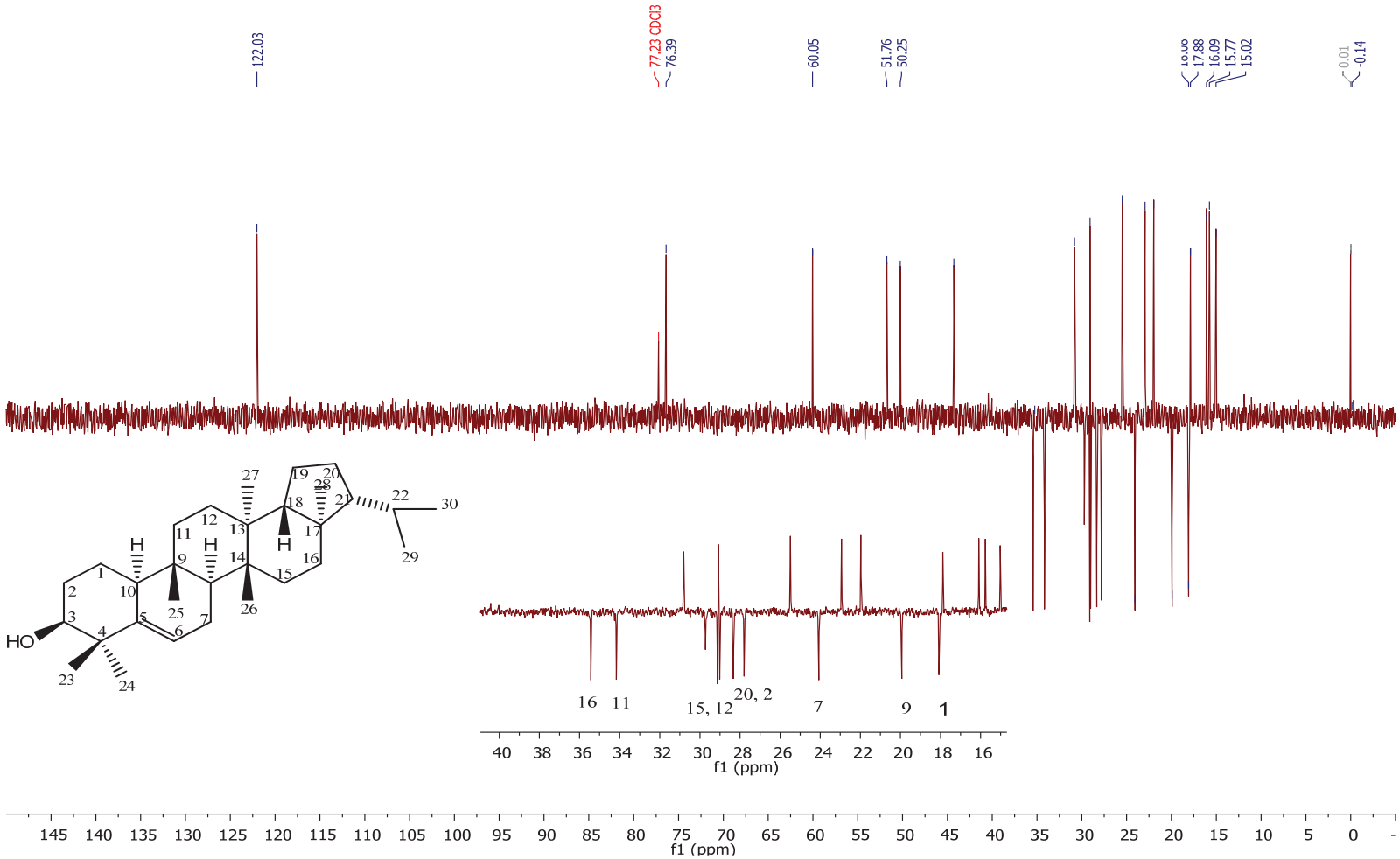

Figure 64 DEPT Spectrum of compound PGH-2 (in $CDCl_3$)

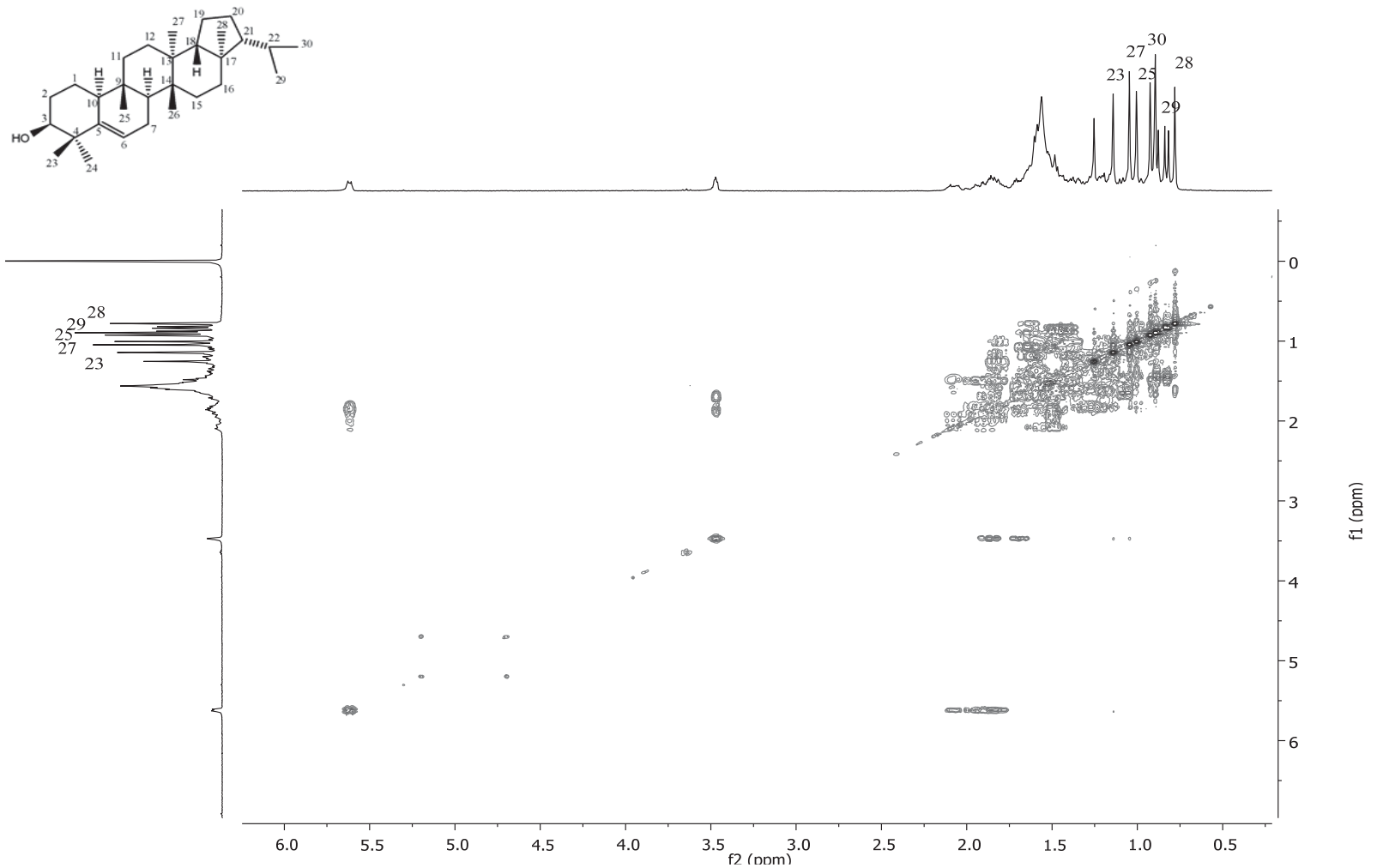

Figure 65 COSY Spectrum of compound PGH-2 (in $CDCl_3$)

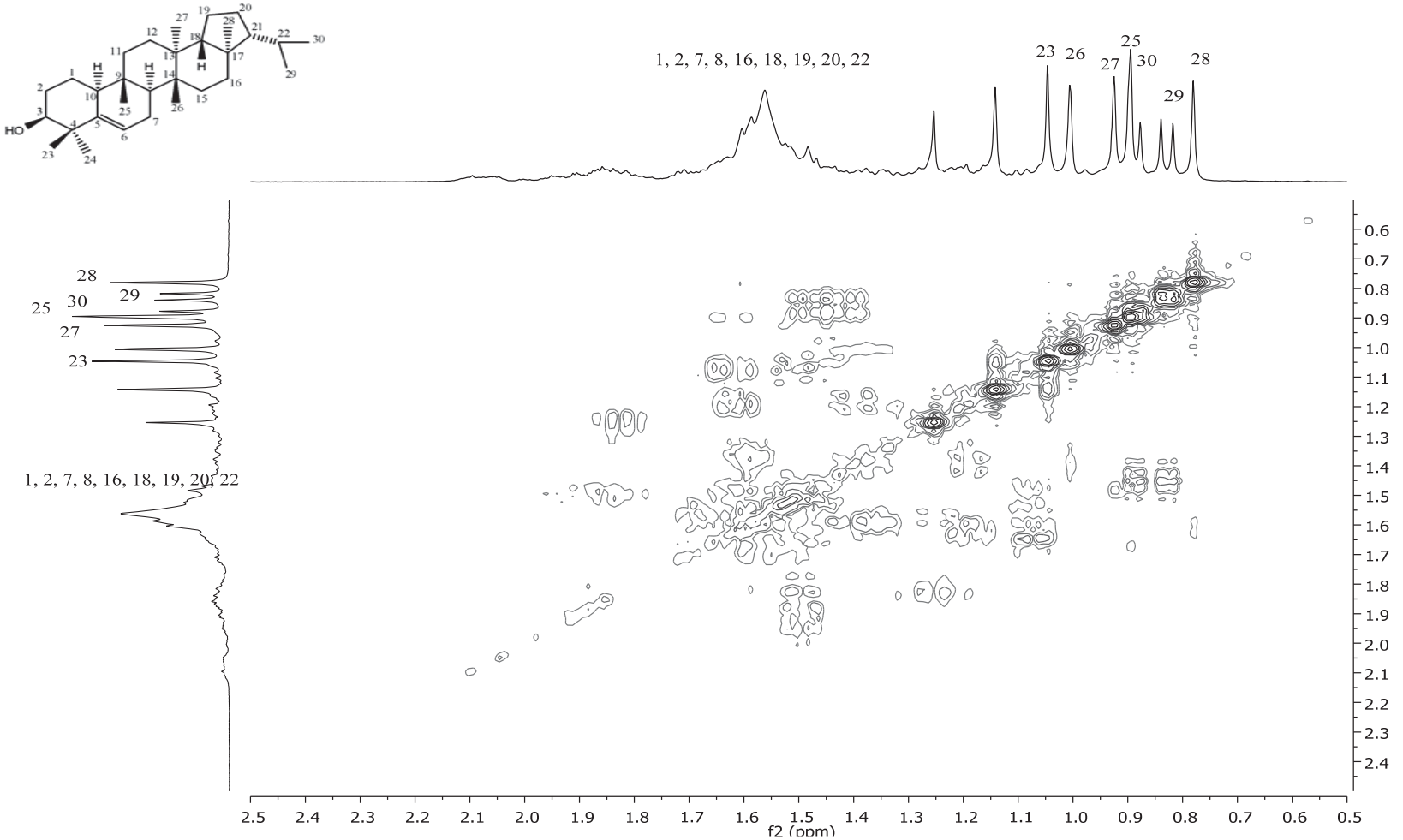

Figure 65 (Continued) COSY Spectrum of compound PGH-2 (in $CDCl_3$)

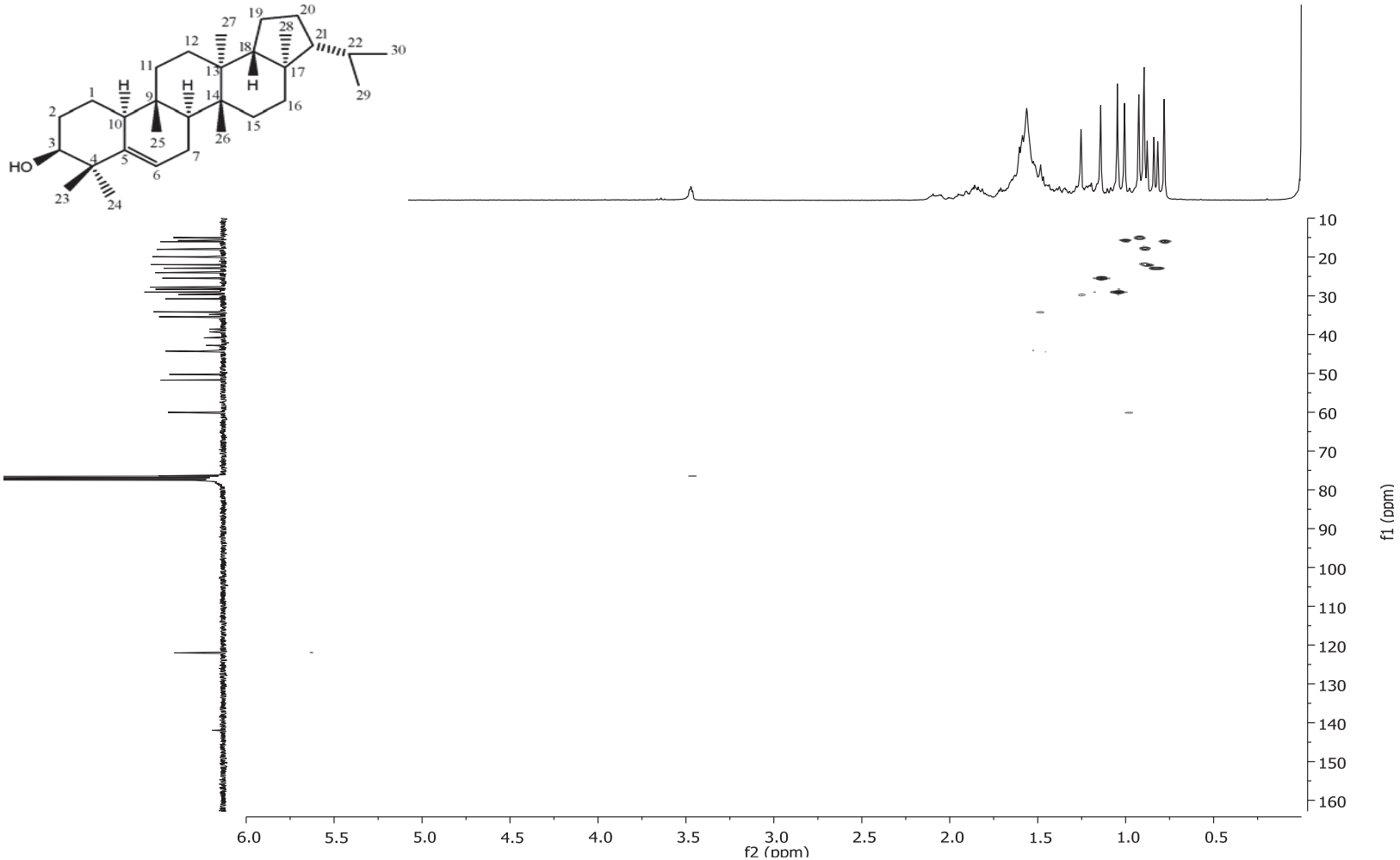

Figure 66 HMQC Spectrum of compound PGH-2 (in $CDCl_3$)

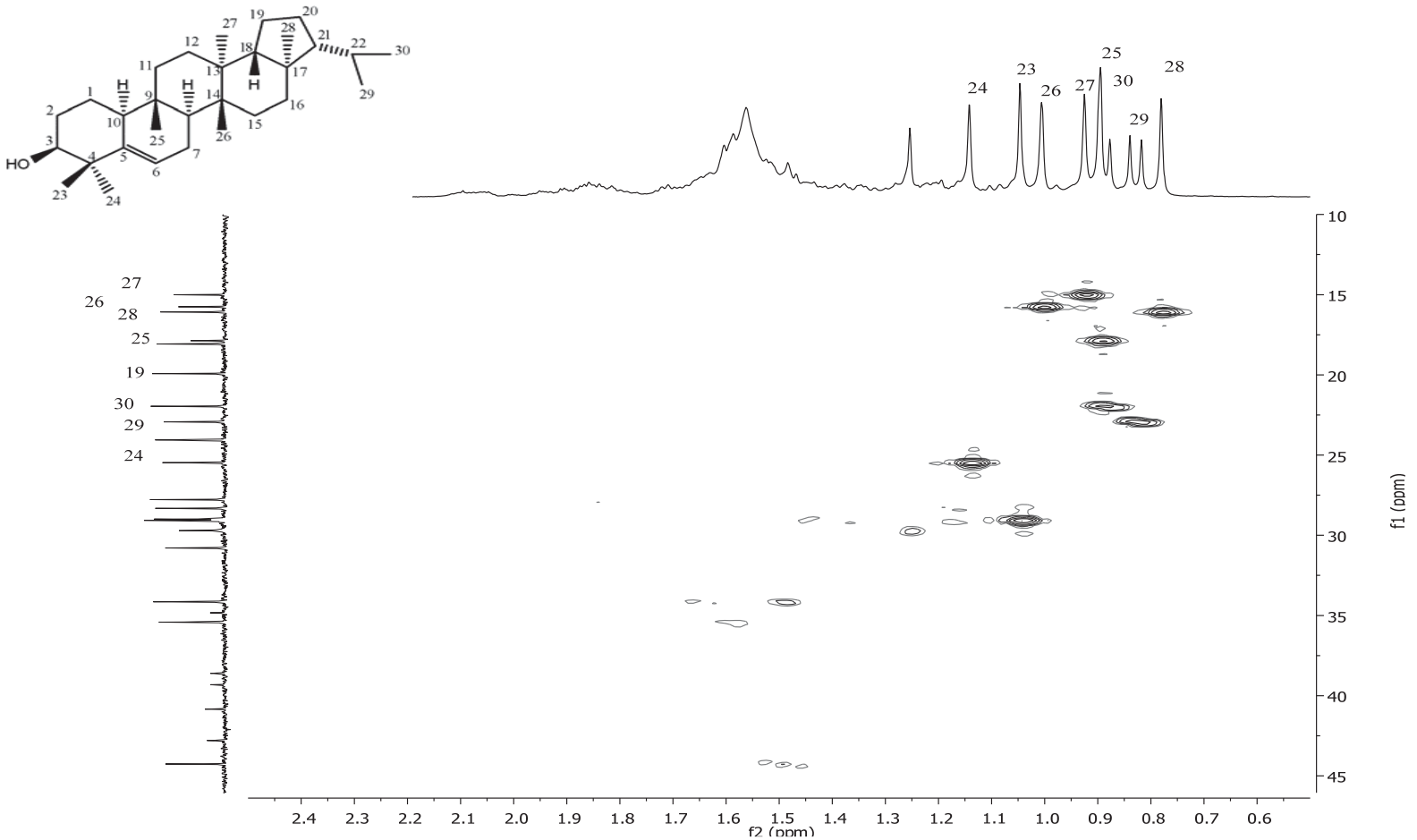

Figure 66 (Continued) HMQC Spectrum of compound PGH-2 (in $CDCl_3$) (Continued)

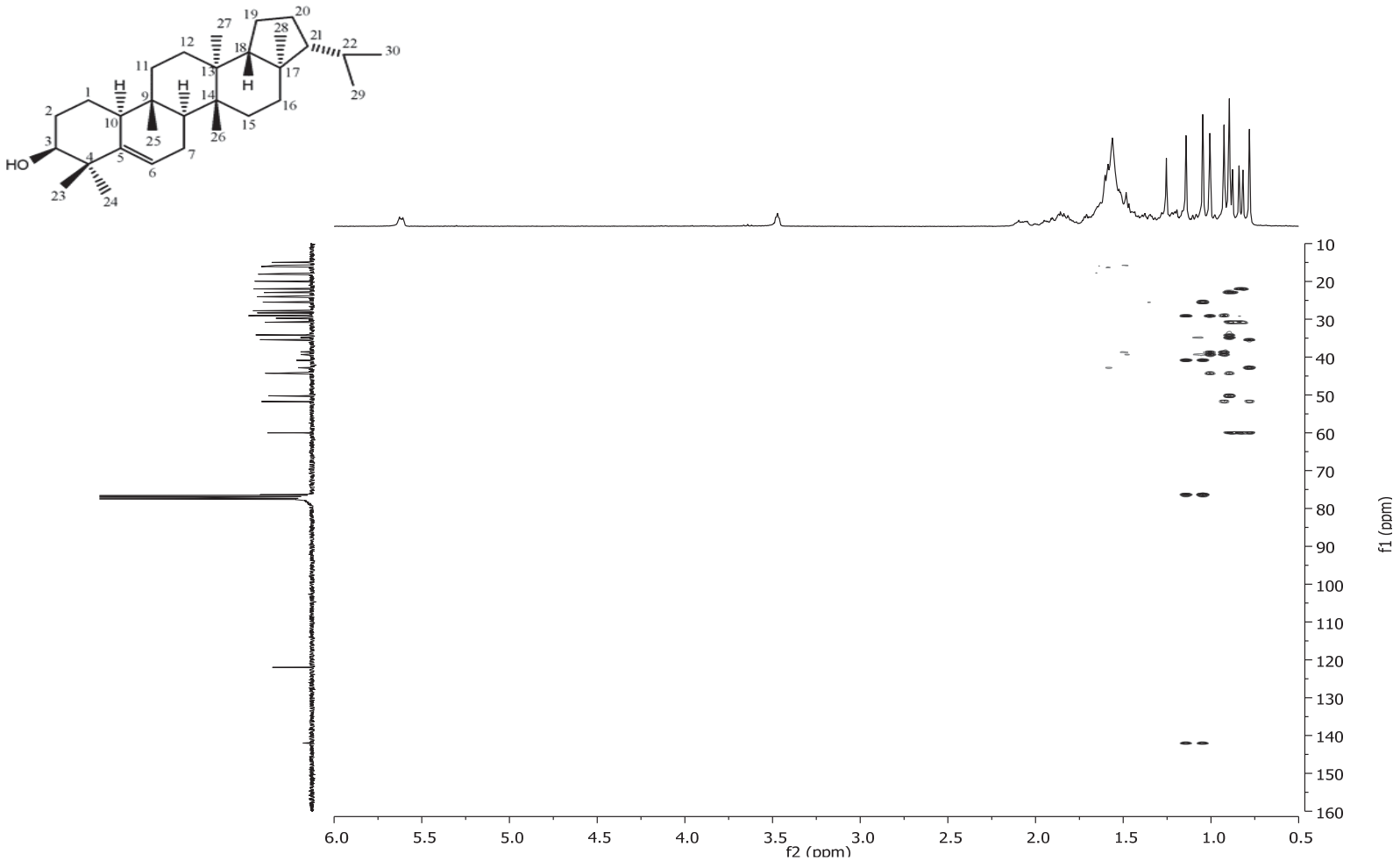

Figure 67 HMBC Spectrum of compound PGH-2 (in $CDCl_3$)

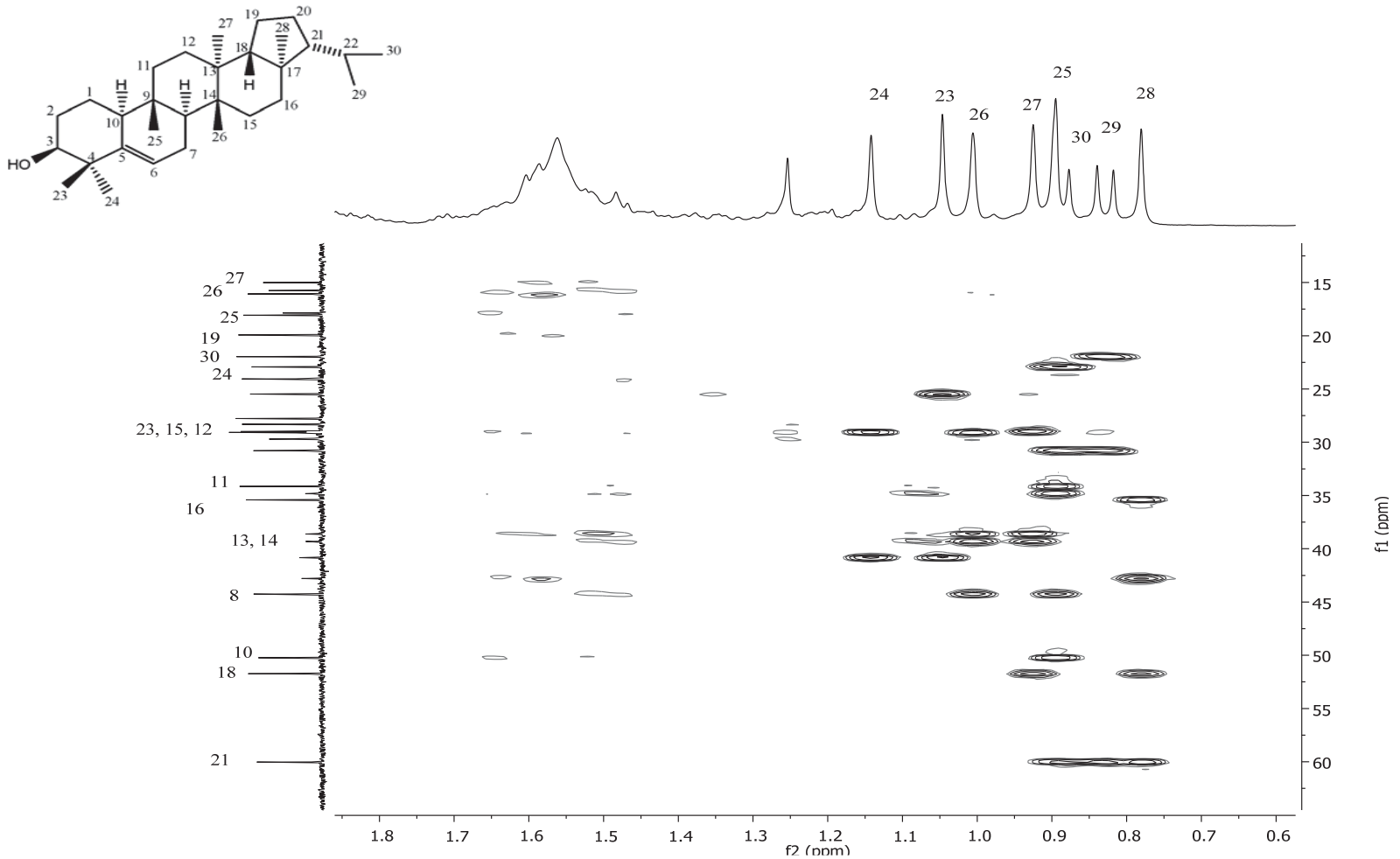

Figure 67 (Continued) HMBC Spectrum of compound PGH-2 (in $CDCl_3$)

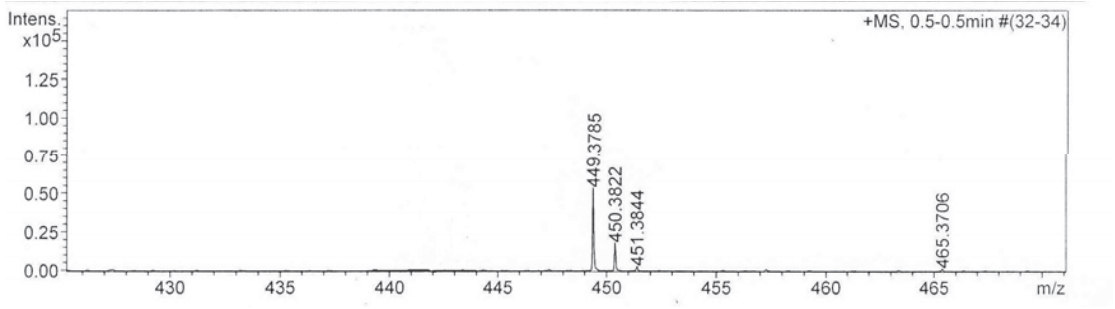

Figure 68 IR (KBr) spectrum of compound PGH-3

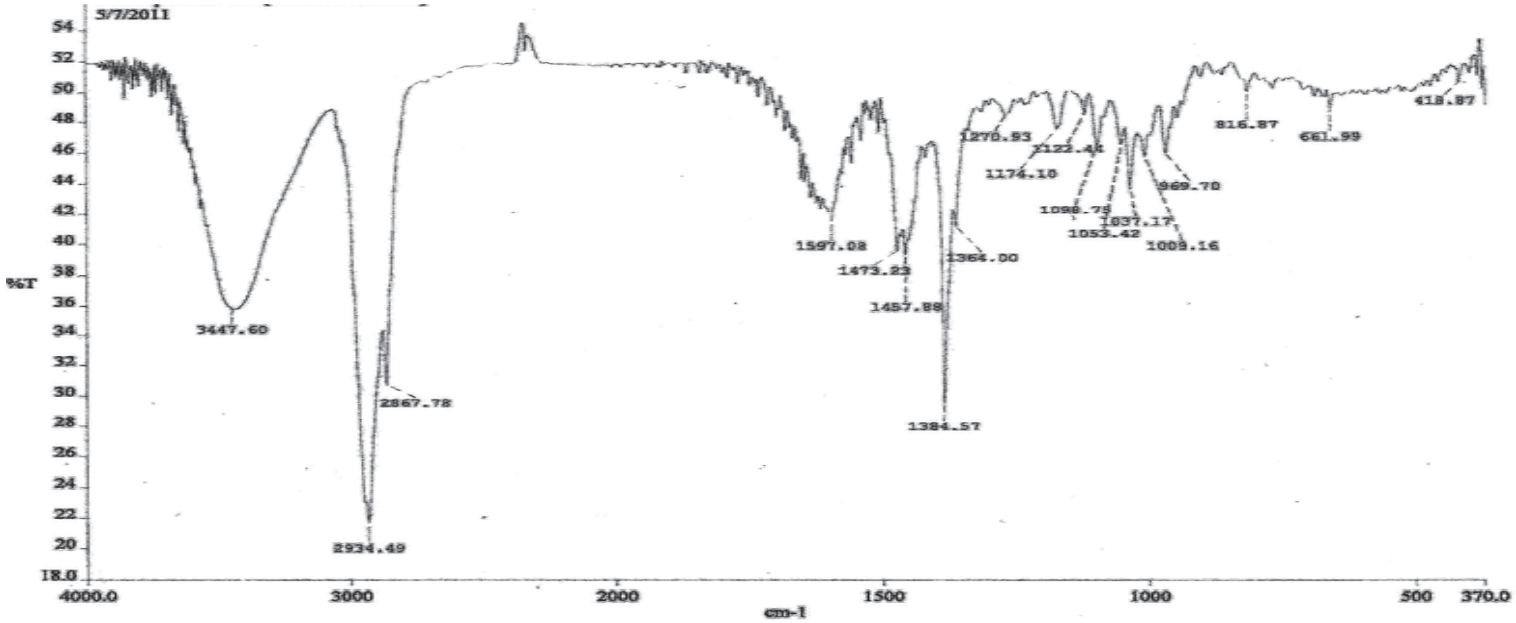

Figure 69 IR (KBr) spectrum of compound PGH-3

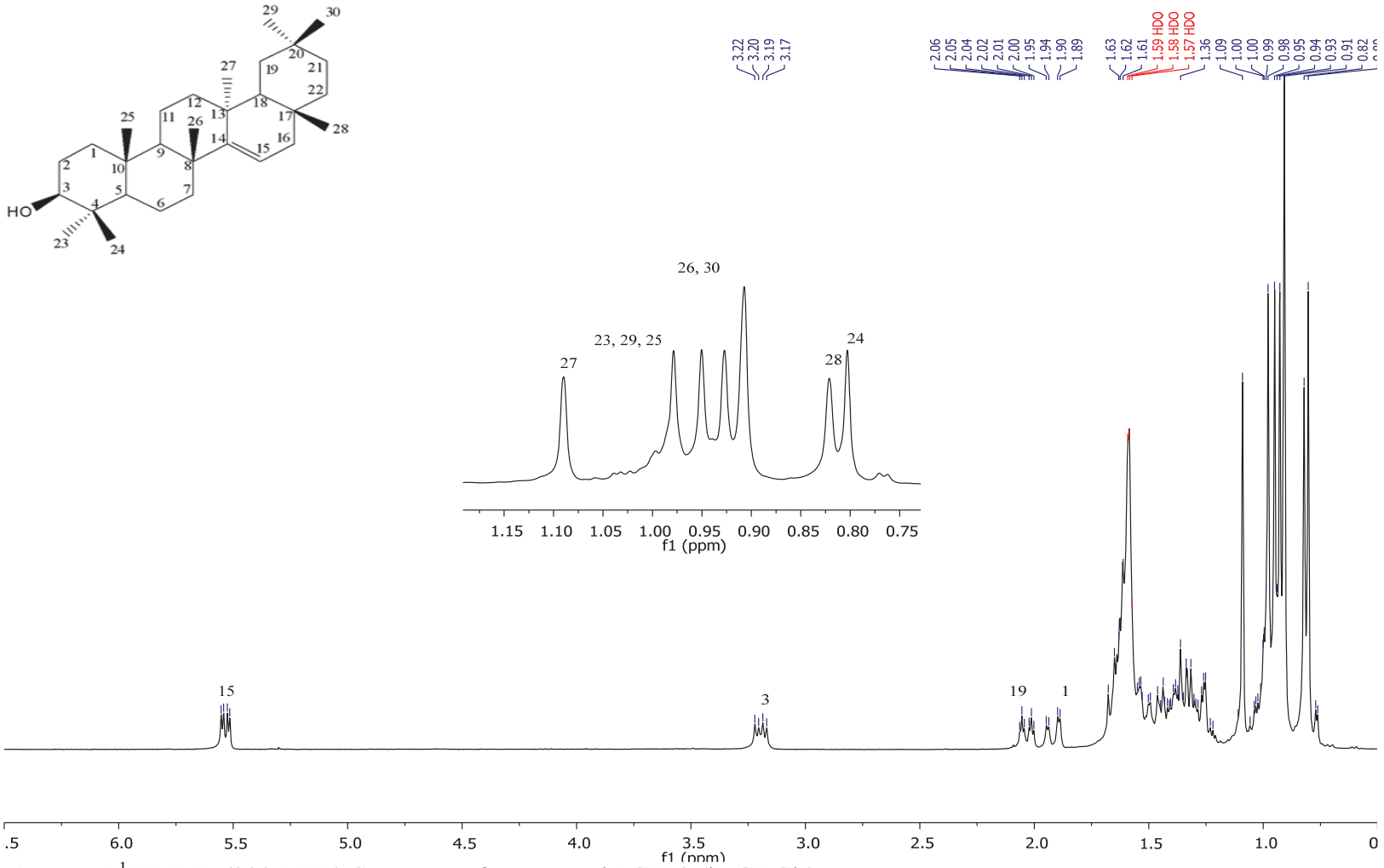

Figure 70 ^{1}H NMR (300 MHz) Spectrum of compound PGH-3 (in $CDCl_3$)

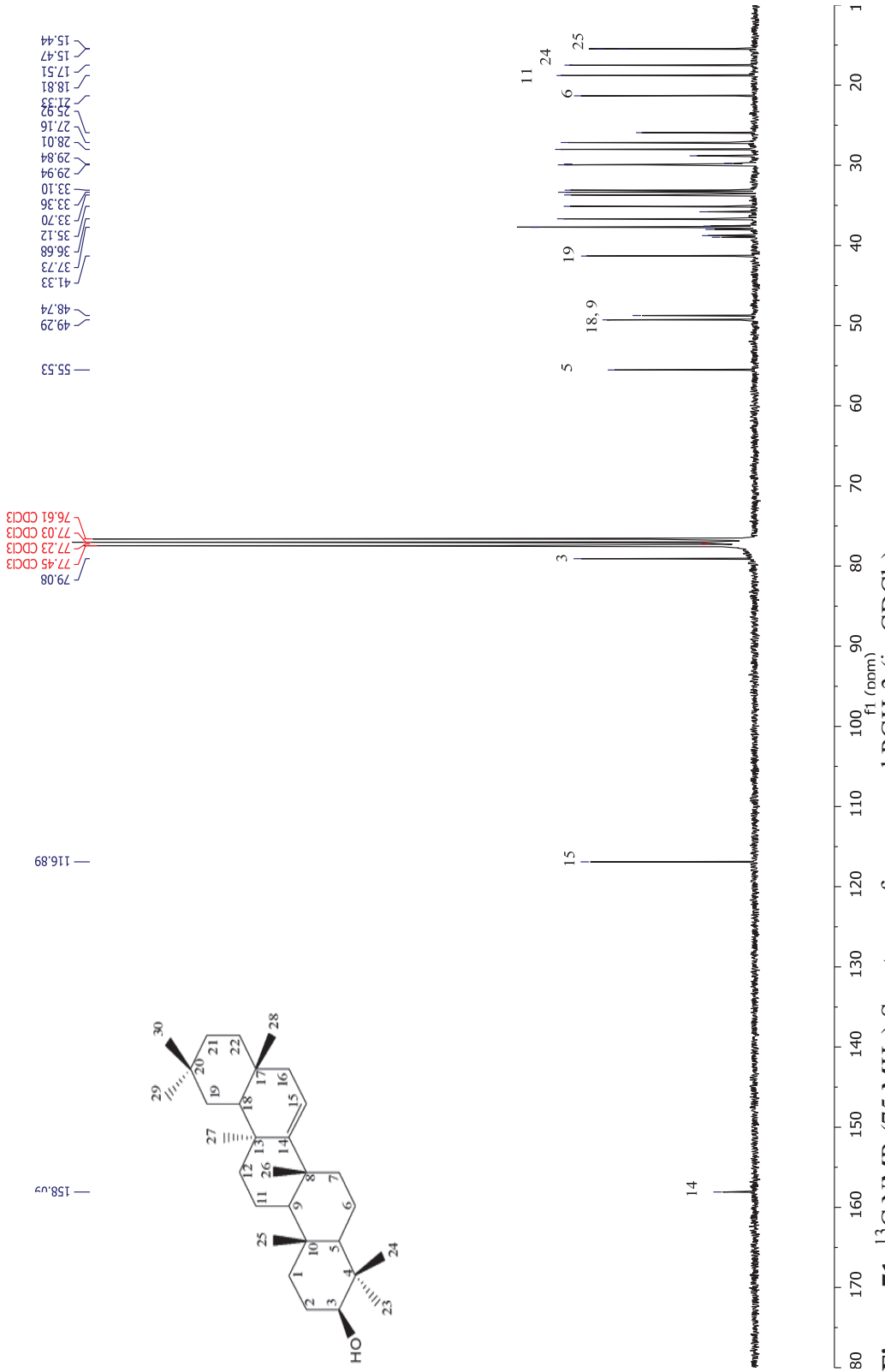

Figure 71 ^{13}C NMR (75 MHz) Spectrum of compound PGH-3 (in $CDCl_3$)

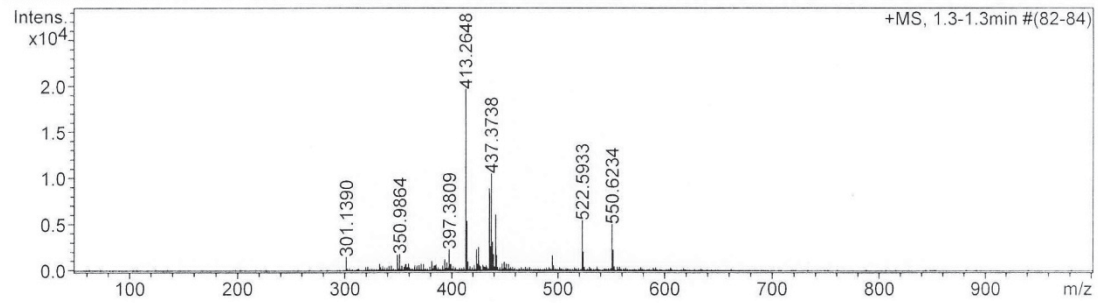

Figure 72 MS spectrum of compound PGH-4

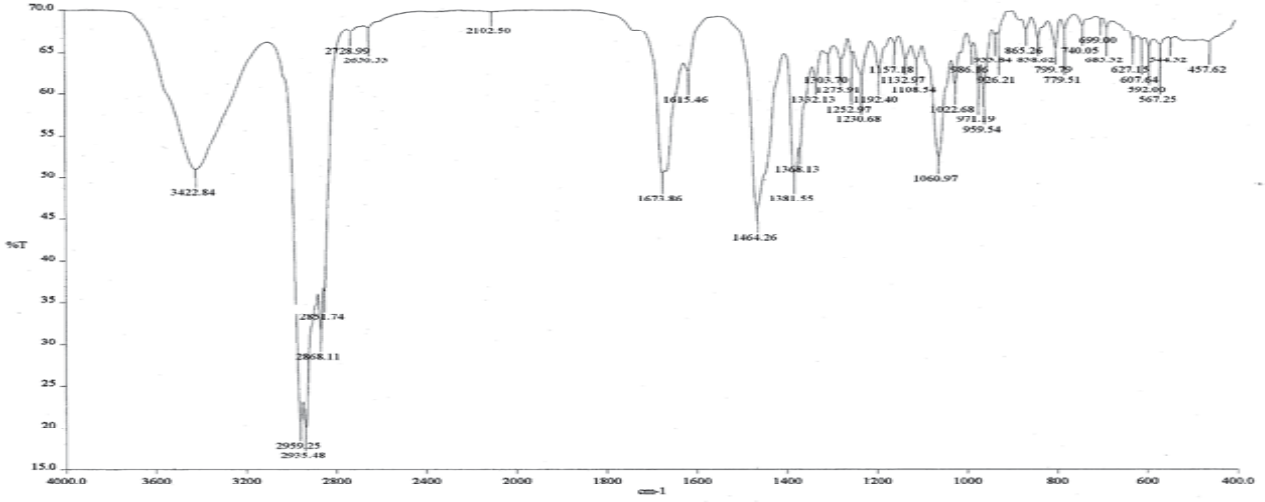

Figure 73 IR (KBr) spectrum of compound PGH-4

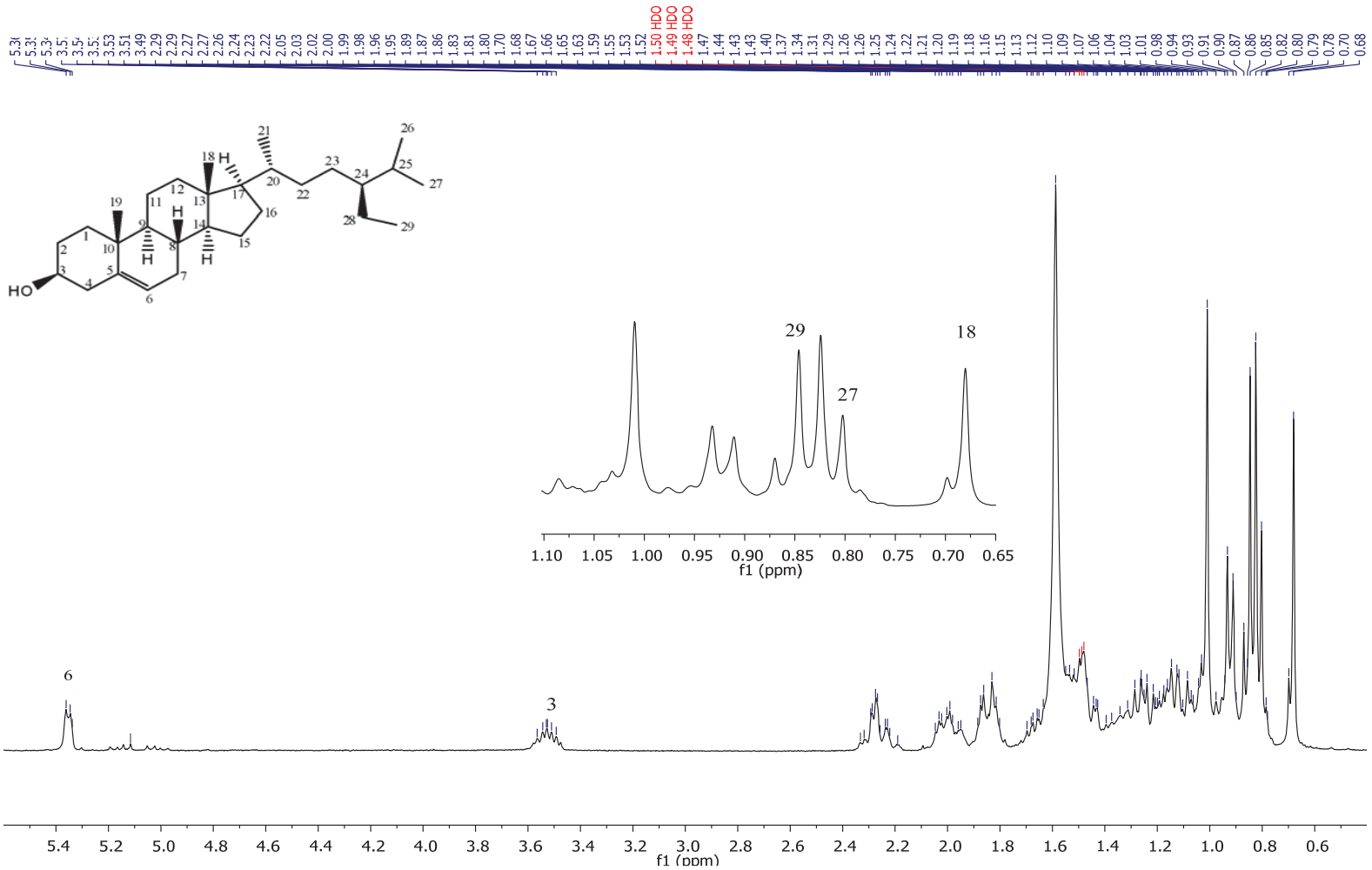

Figure 74 ^{1}H NMR (300 MHz) Spectrum of compound PGH-4 (in $CDCl_3$)

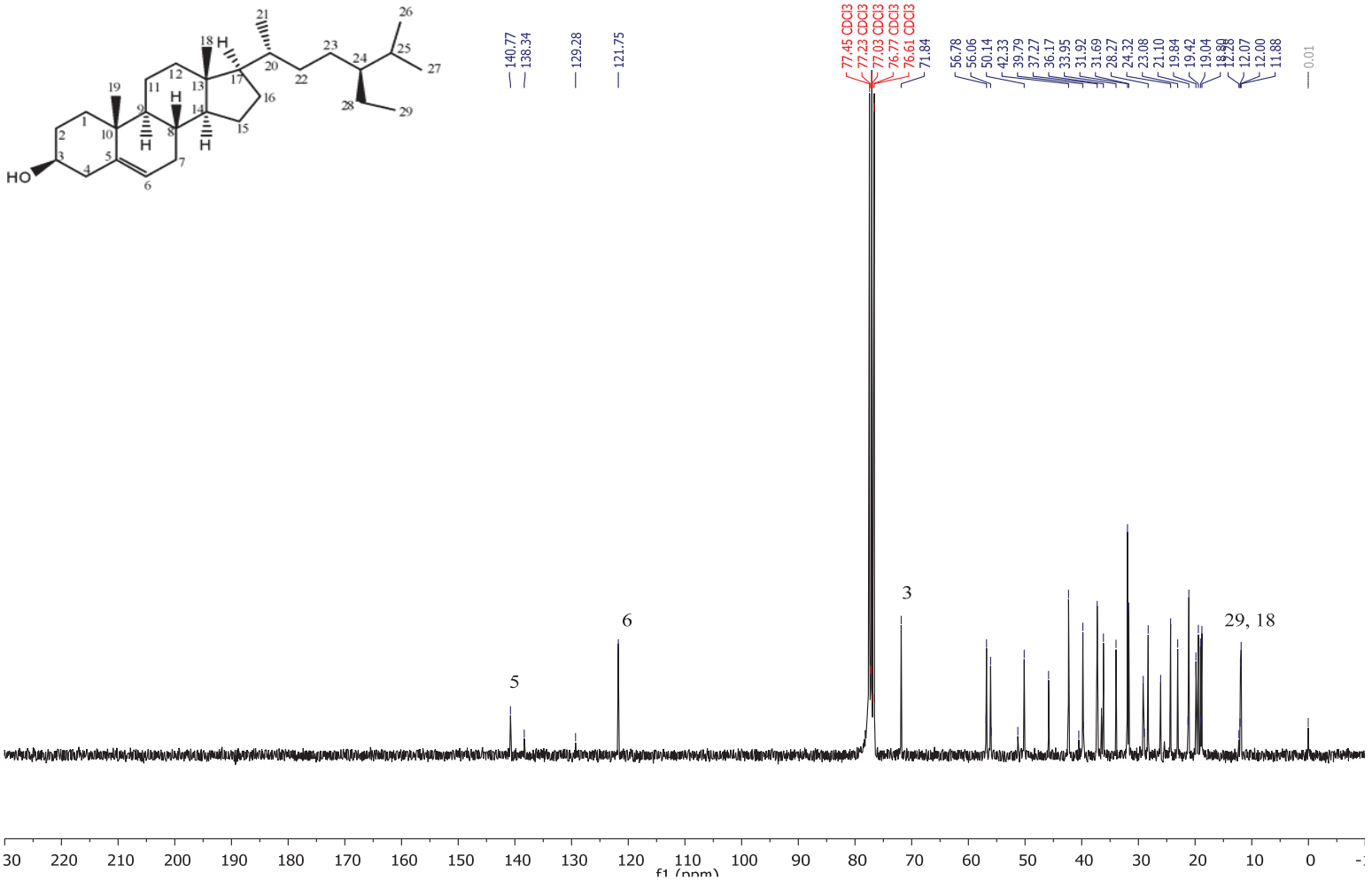

Figure 75 ^{13}C NMR (75 MHz) Spectrum of compound PGH-4 (in $CDCl_3$)

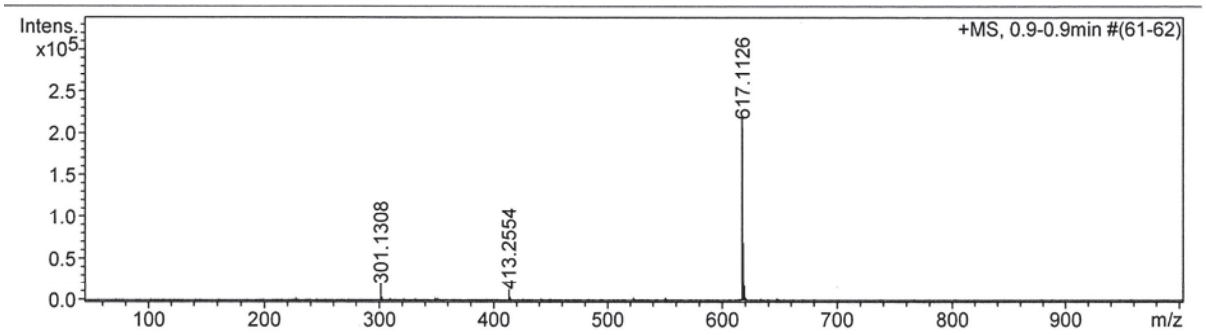

Figure 76 MS spectrum of compound PGE-1

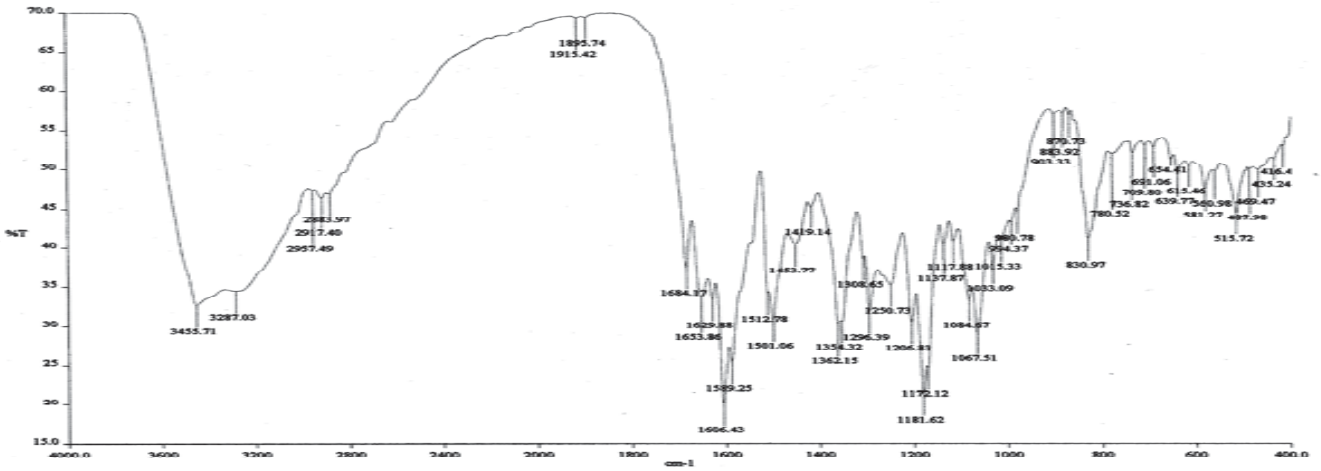

Figure 77 IR (KBr) spectrum of compound PGE-1

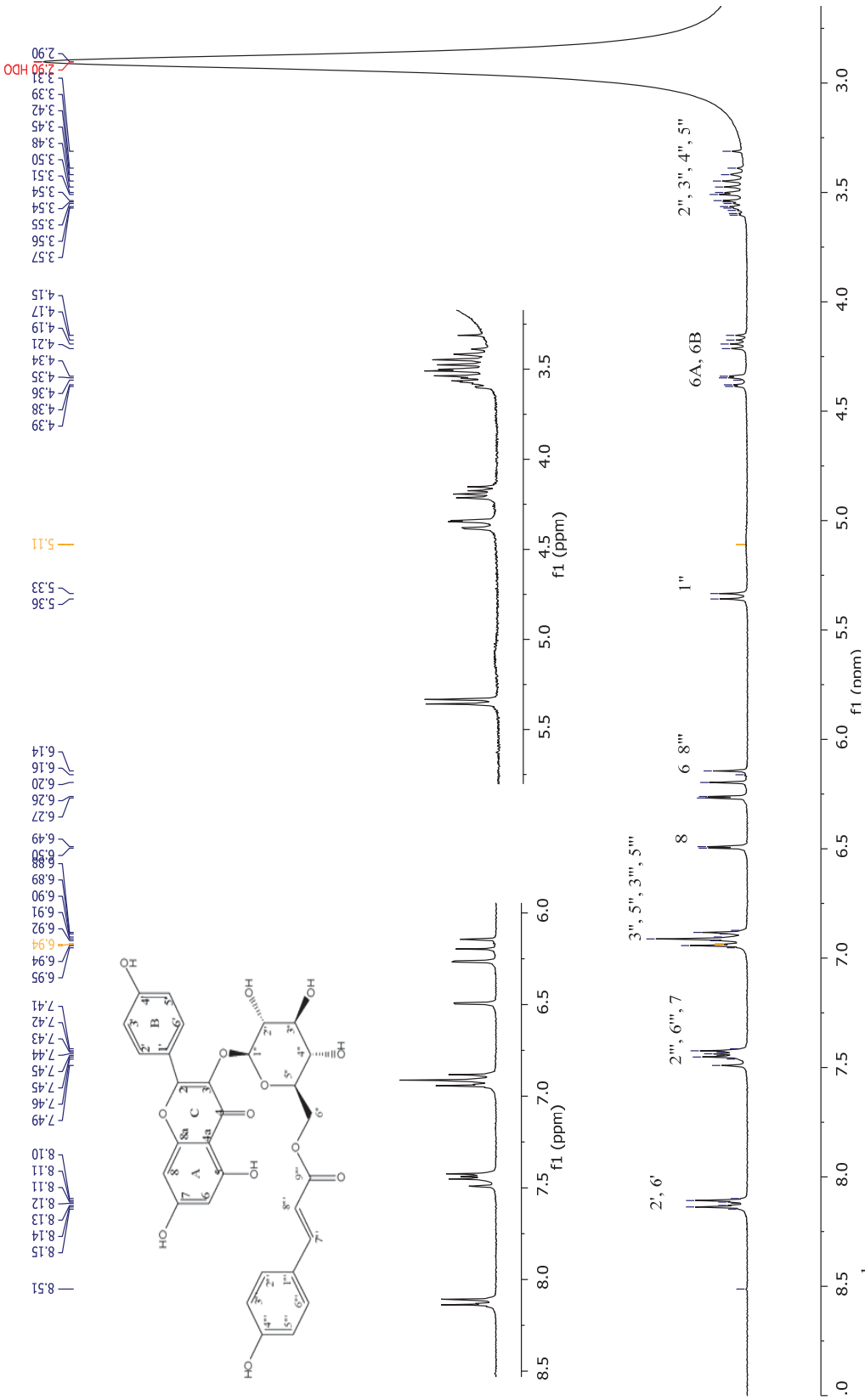

Figure 78 ^{1}H NMR (300 MHz) Spectrum of PGE-1 (in acetone-d_6)

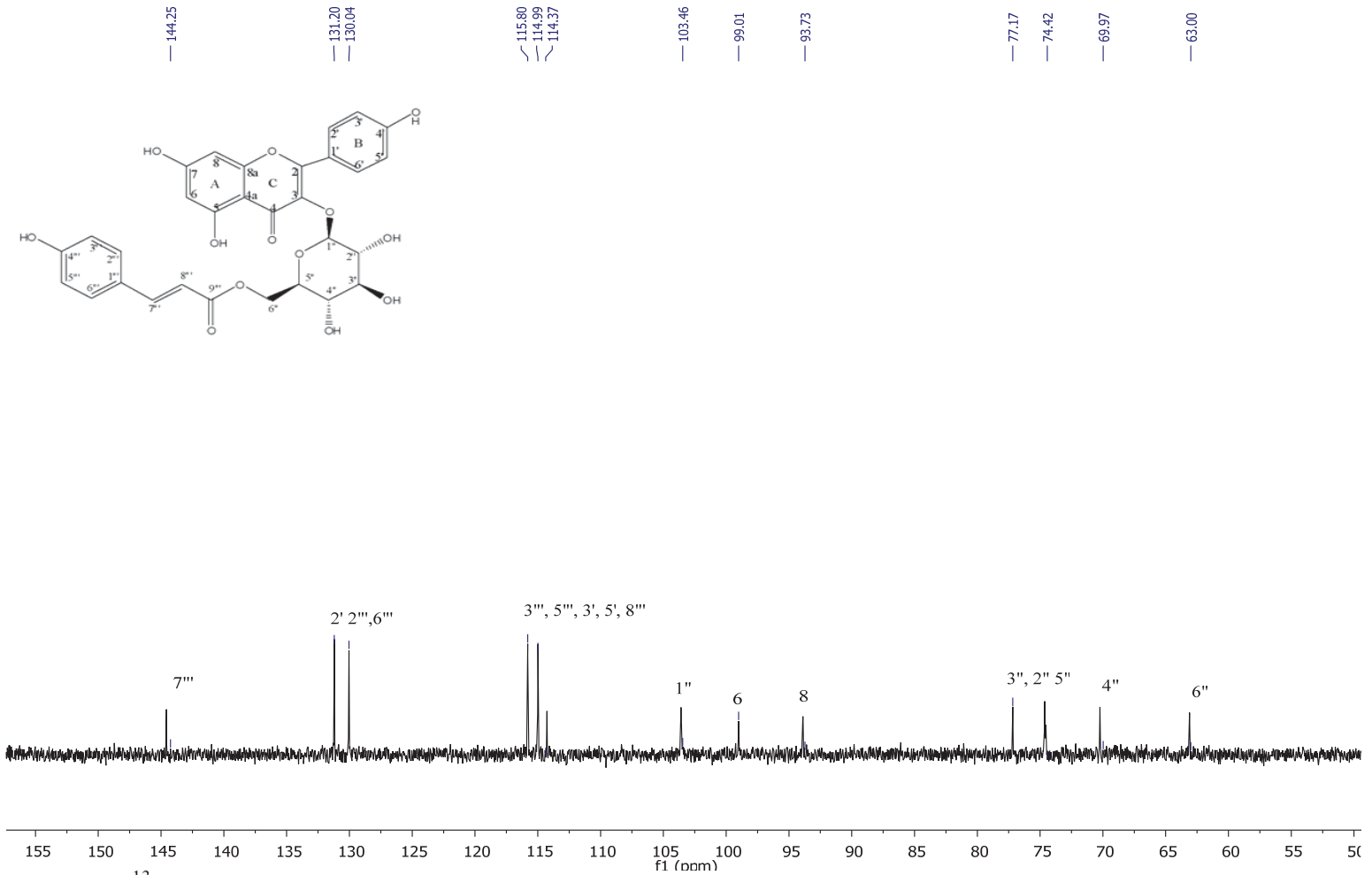

Figure 79 ^{13}C NMR (75 MHz) Spectrum of compound PGE-1(in acetone-d_6)

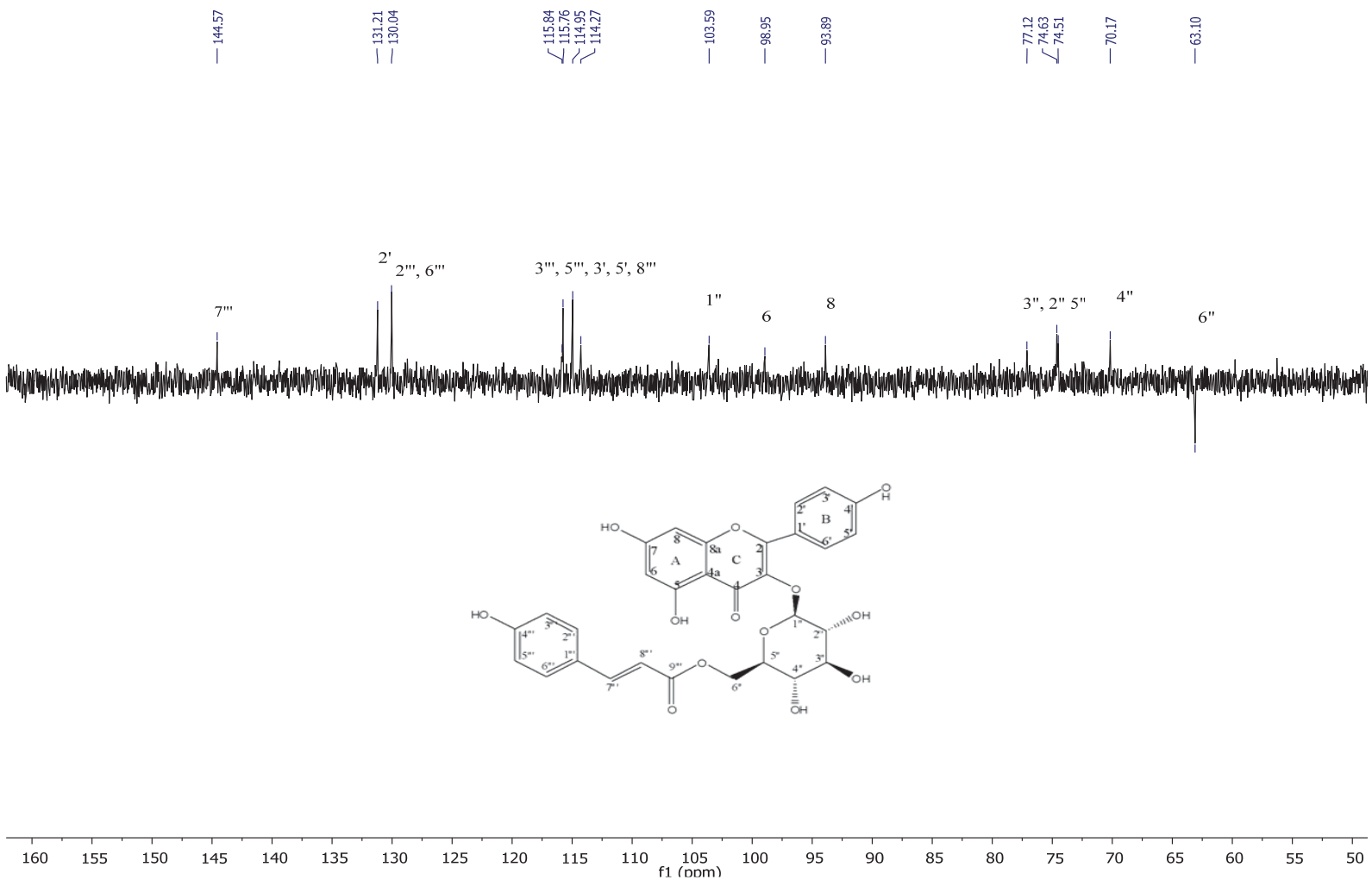

Figure 80 DEPT Spectrum of compound PGE-1(in acetone-d_6)

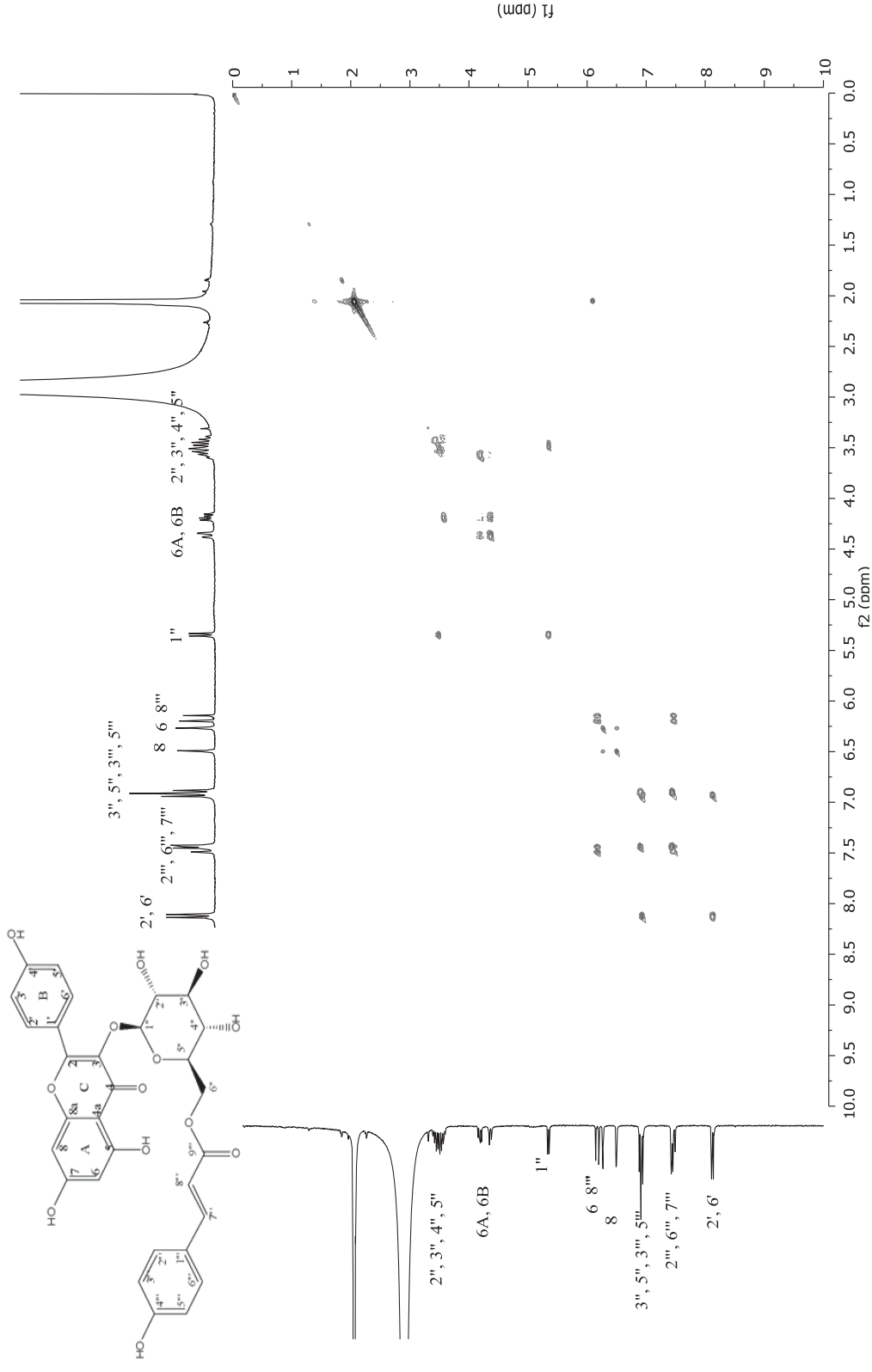

Figure 81 COSY Spectrum of compound PGE-1(in acetone-d_6)

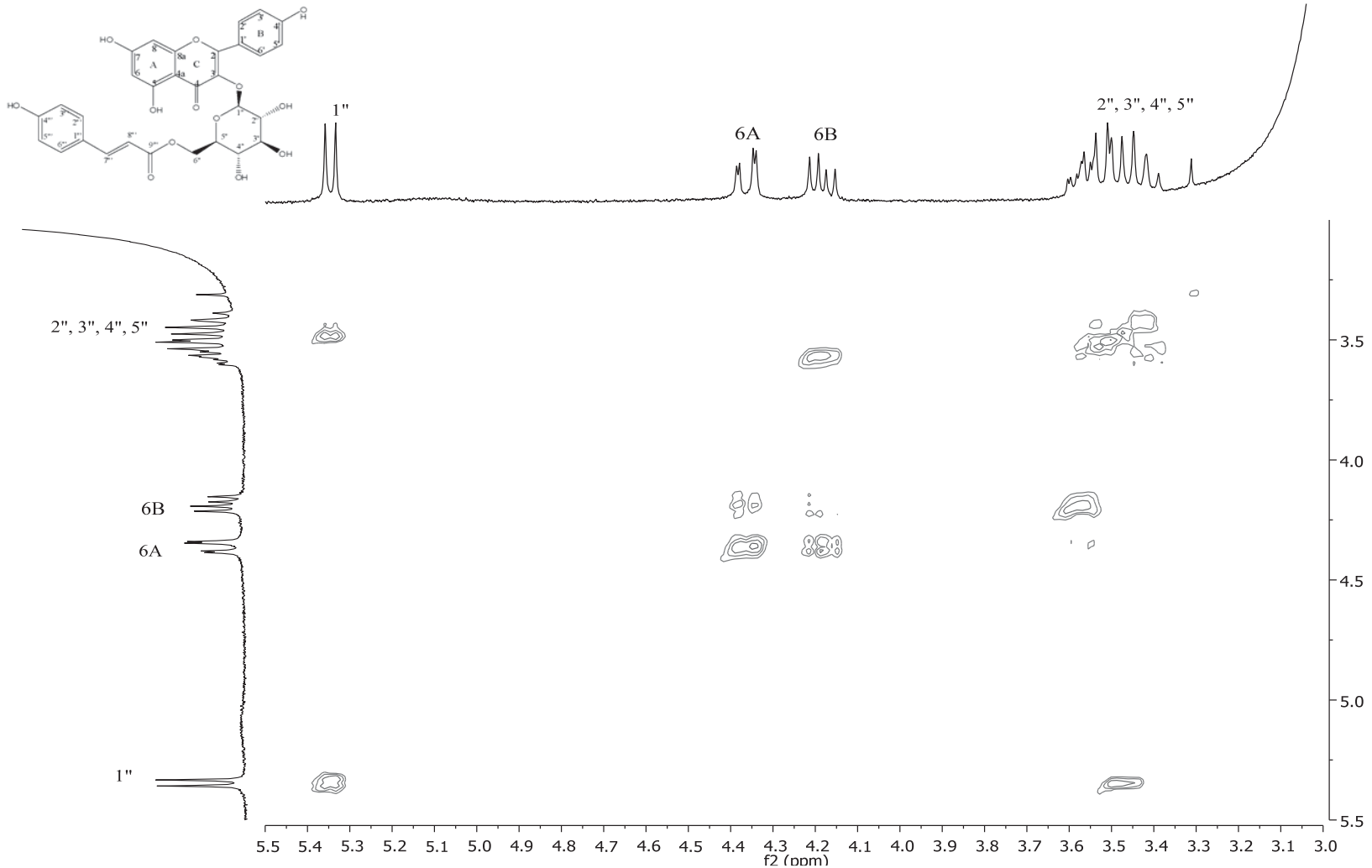

Figure 81 (Continued) COSY Spectrum of compound PGE-1(in acetone-d_6)

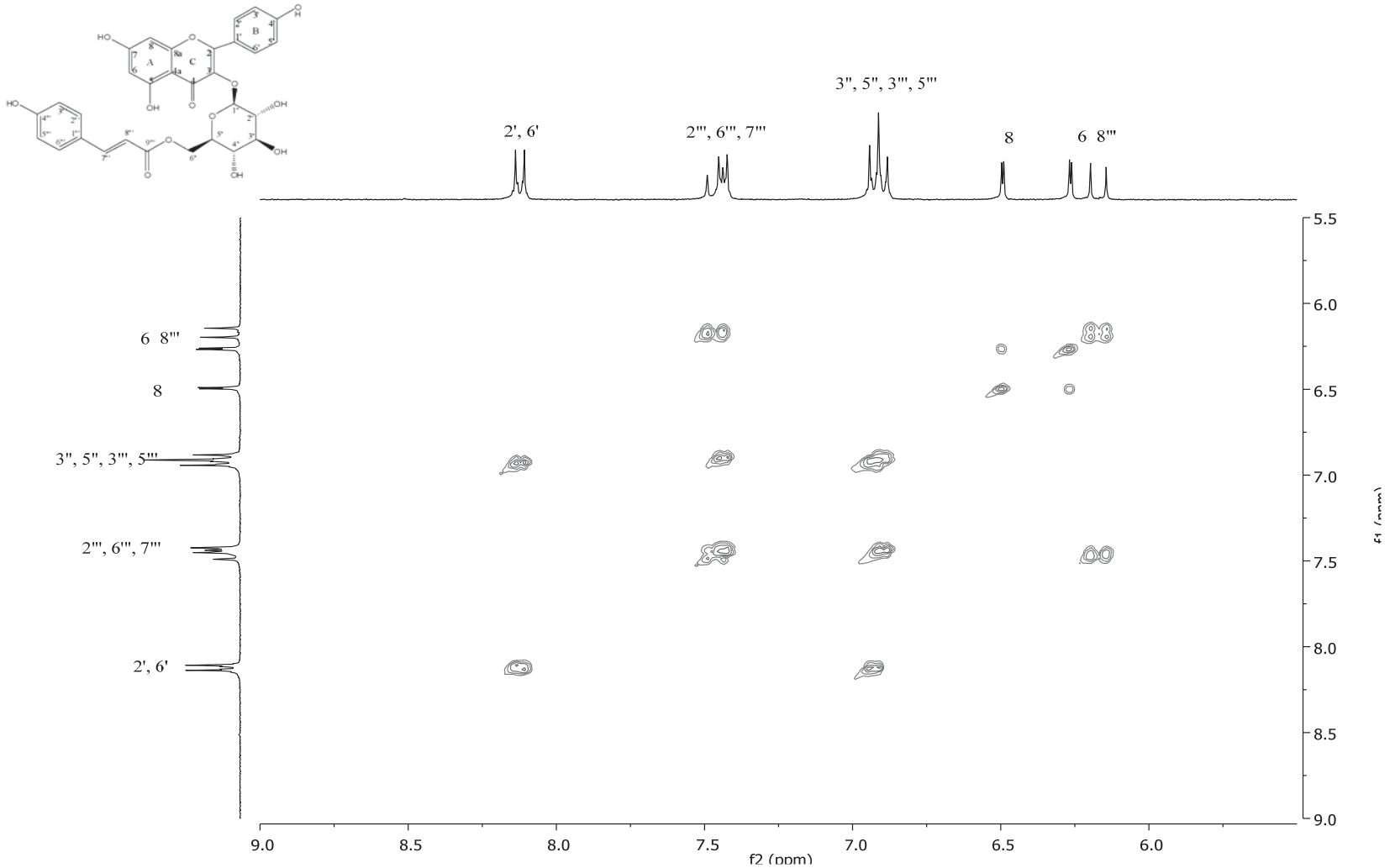

Figure 81 (Continued) COSY Spectrum of compound PGE-1(in acetone-d_6)

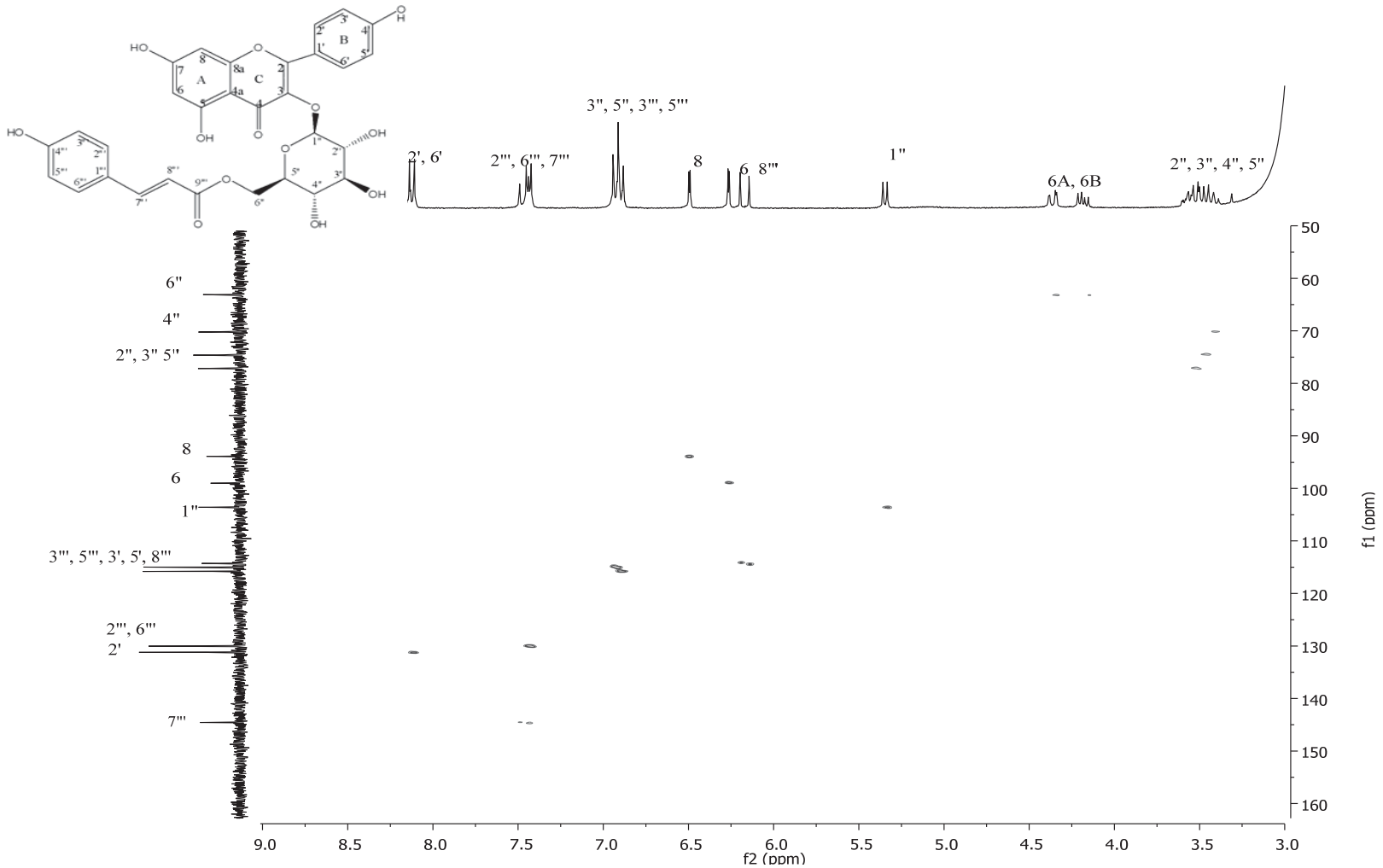

Figure 82 HMQC Spectrum of compound PGE-1(in acetone-d_6)

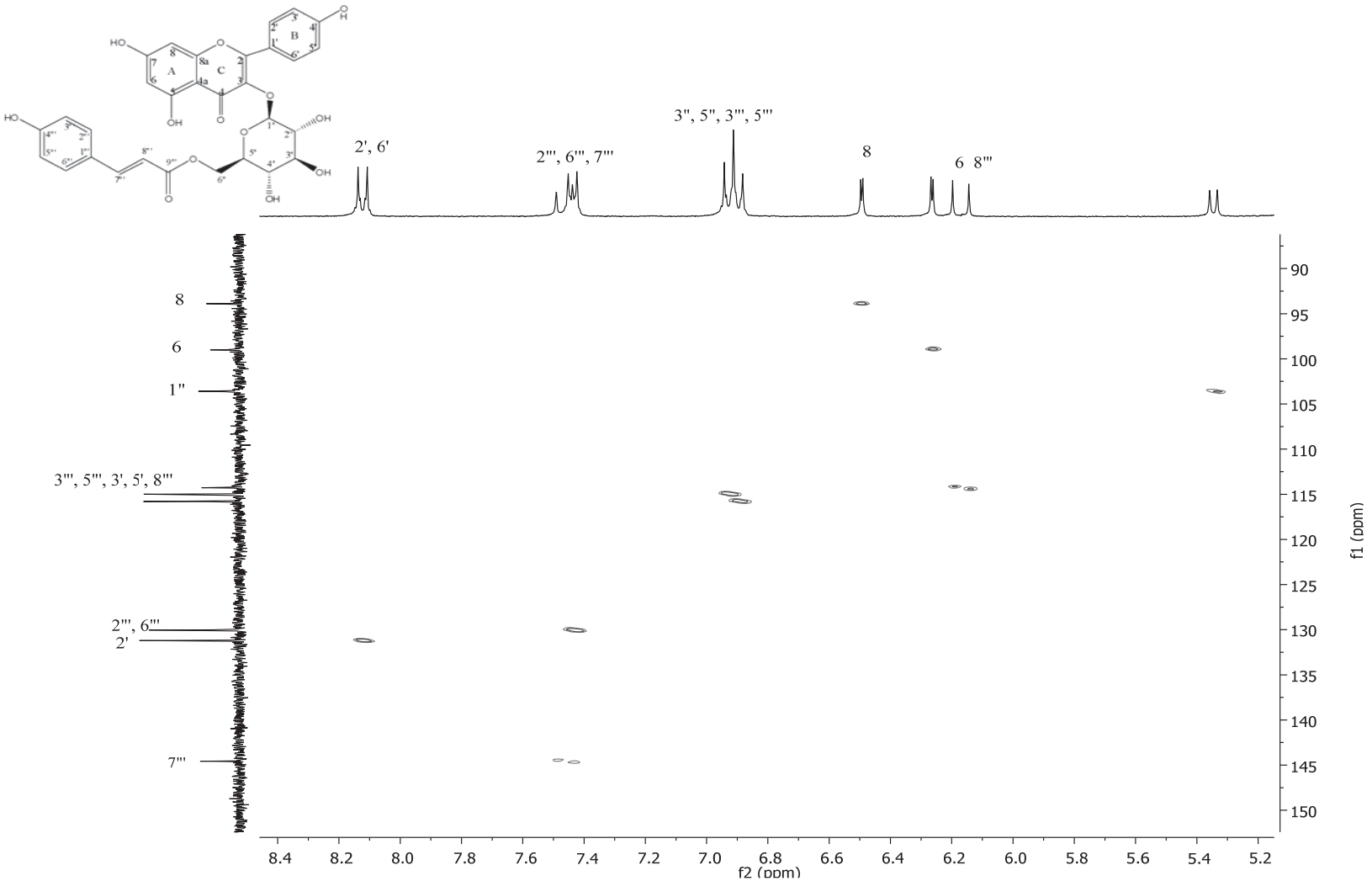

Figure 82 (Continued) HMQC Spectrum of compound PGE-1(in acetone-d_6)

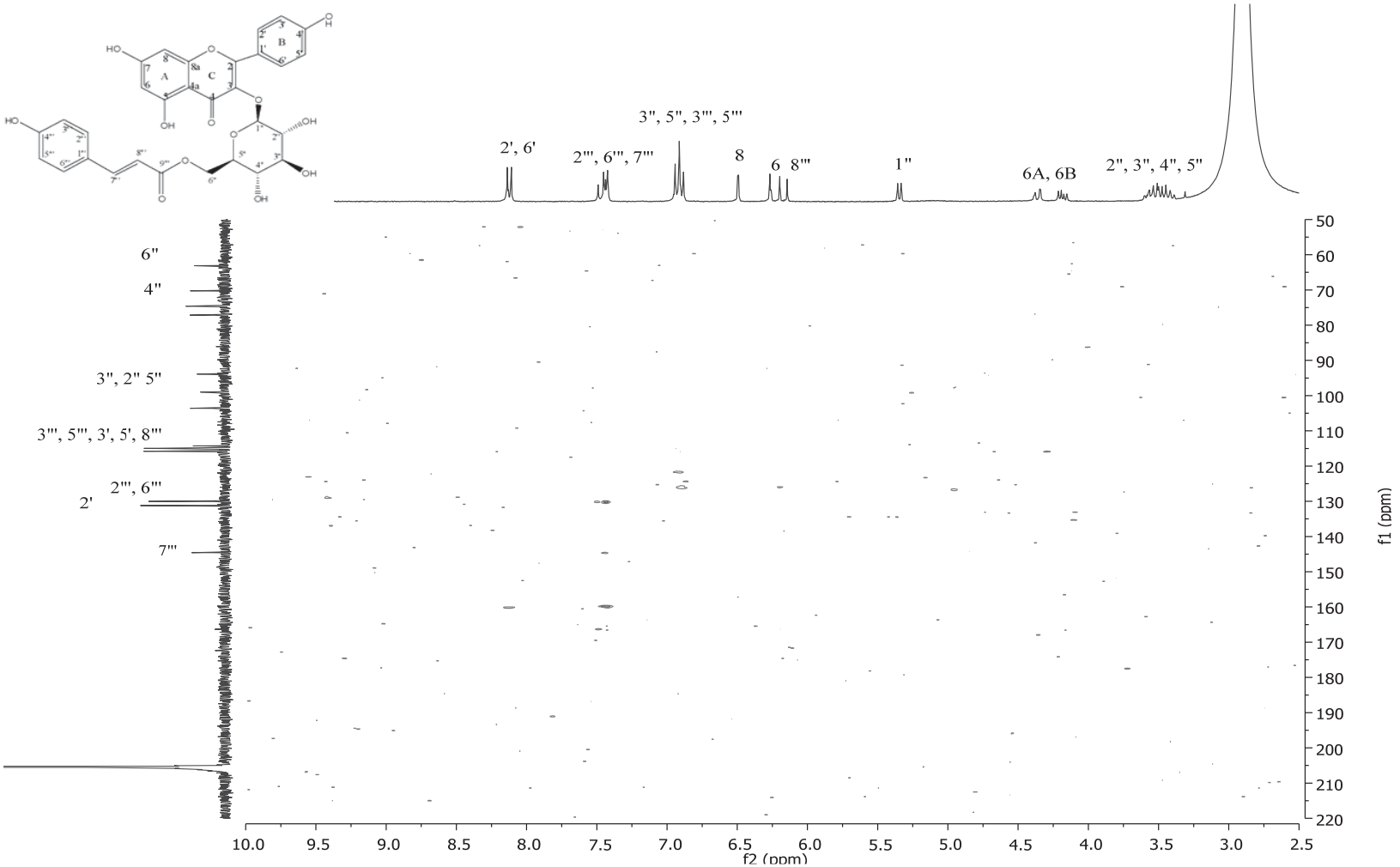

Figure 83 HMBC Spectrum of compound PGE-1(in acetone-d_6)

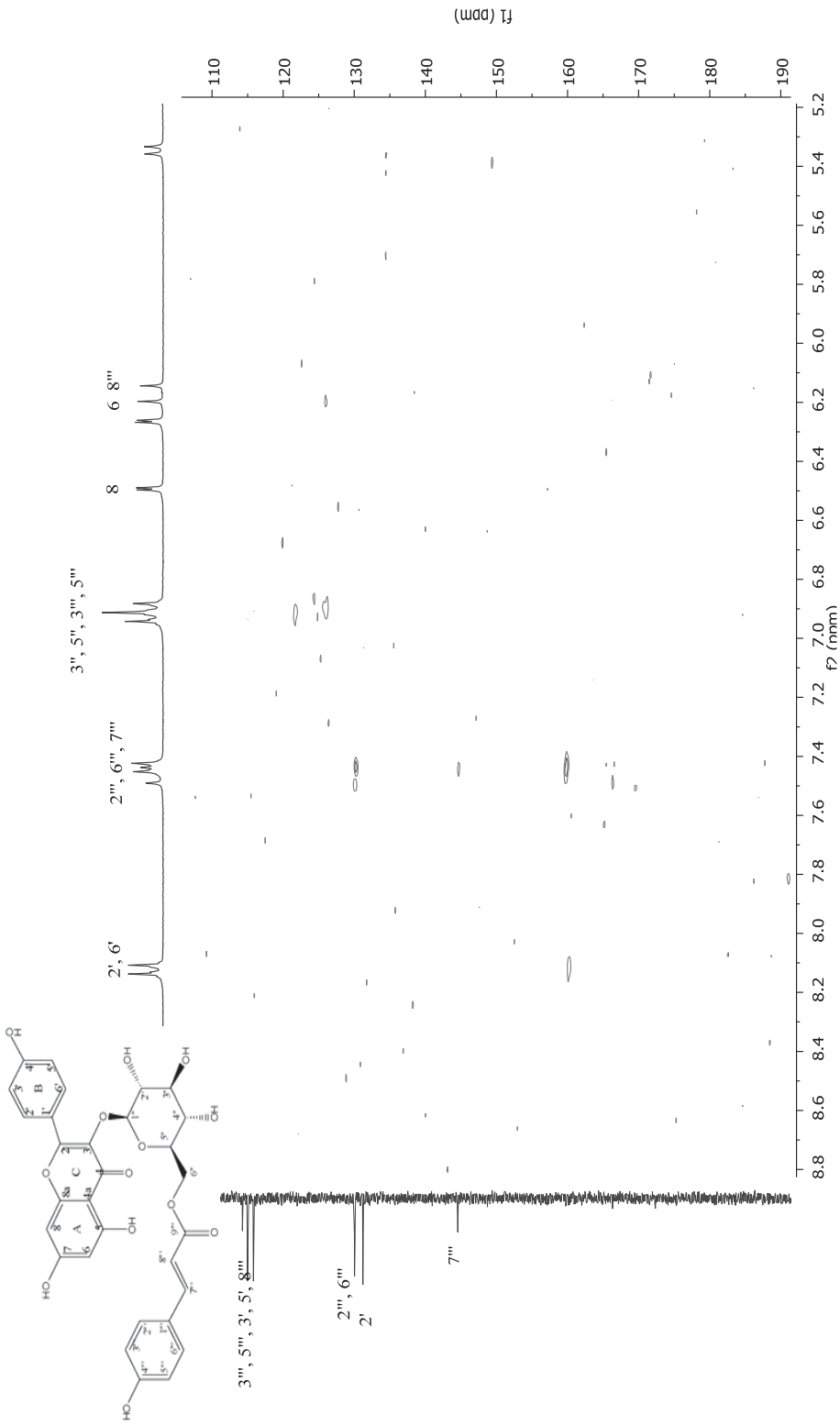

Figure 83 (Continued) HMBC Spectrum of compound PGE-1(in acetone-d_6)

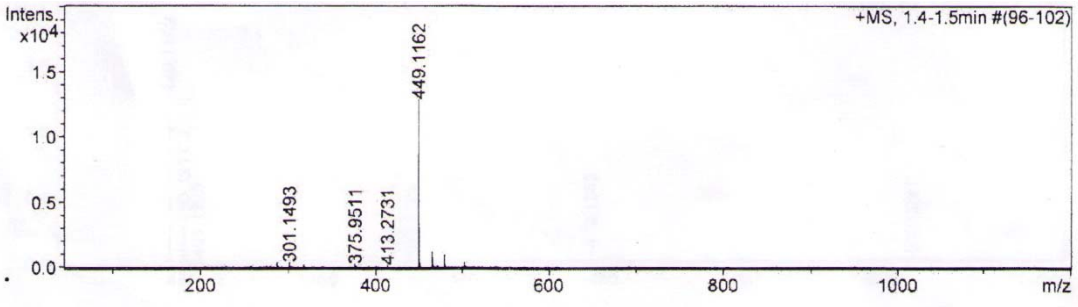

Figure 84 IR (KBr) spectrum of compound PGE-2

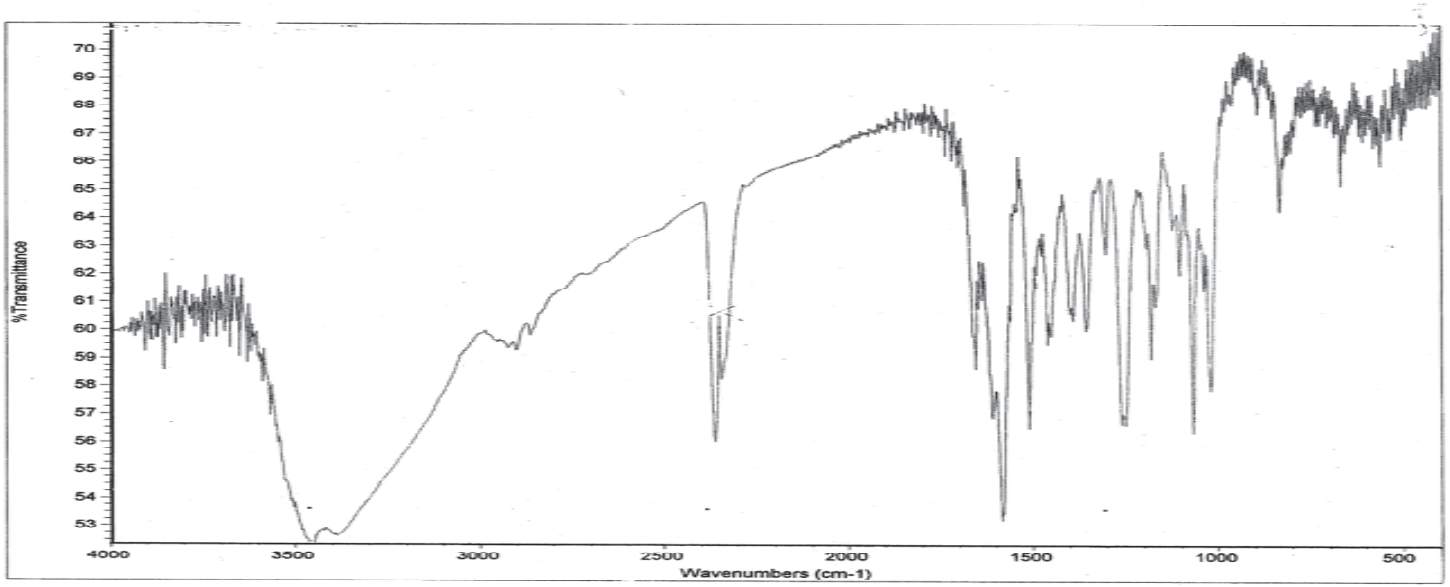

Figure 85 IR (KBr) spectrum of compound PGE-2

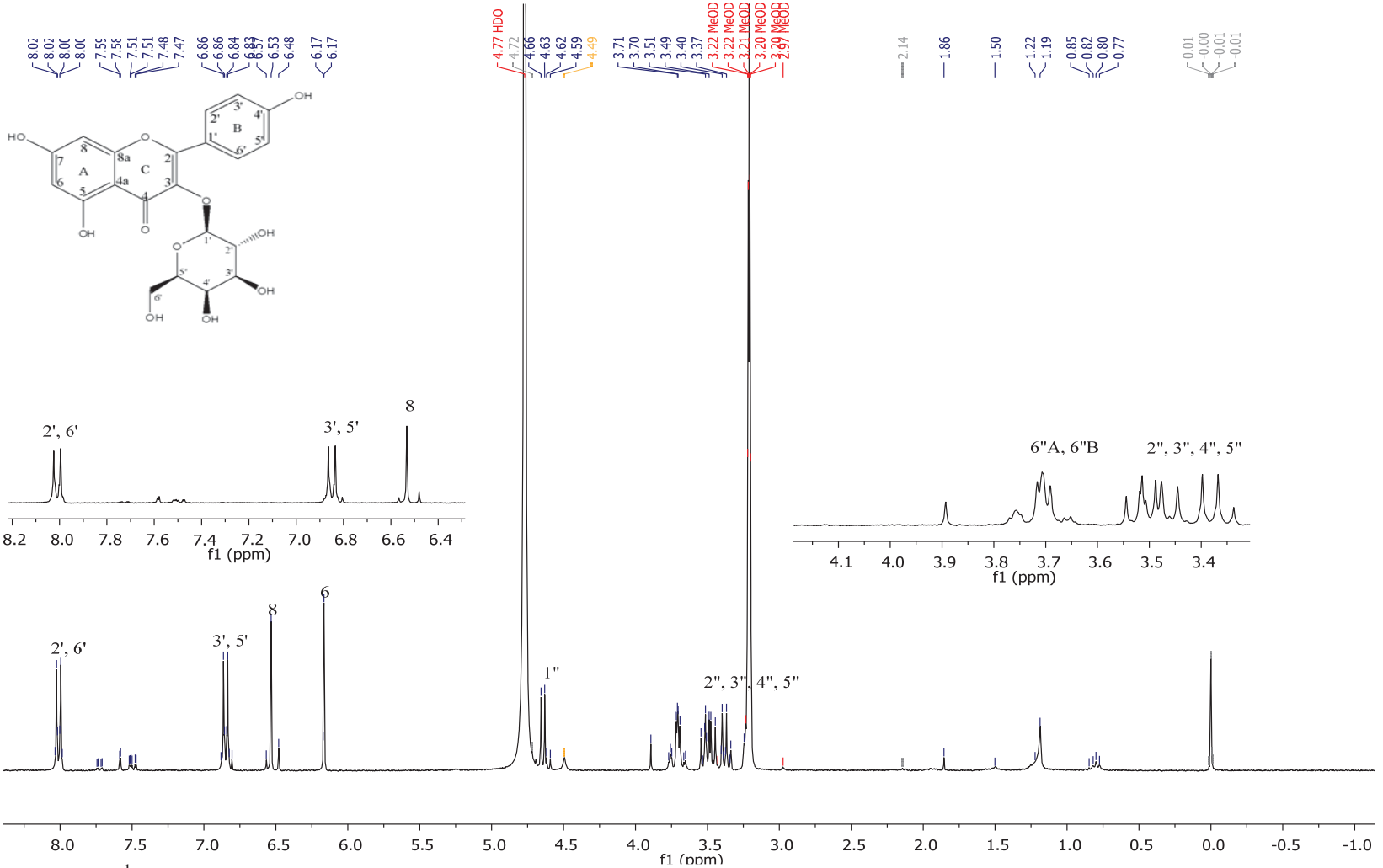

Figure 86 ^{1}H NMR (300 MHz) Spectrum of compound PGE-2 (in CD_3OD)

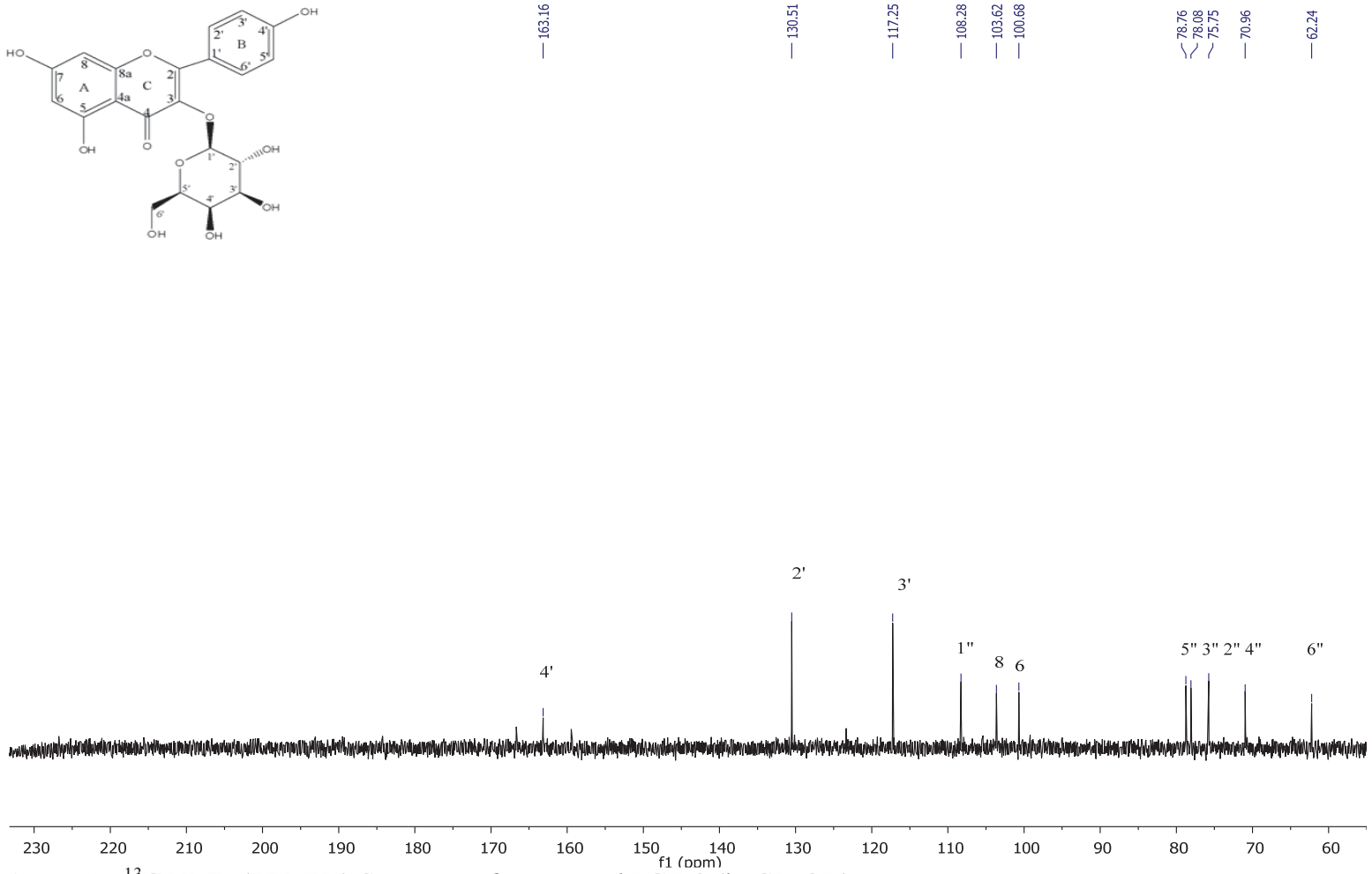

Figure 87 ^{13}C NMR (75 MHz) Spectrum of compound PGE-2 (in CD_3OD)

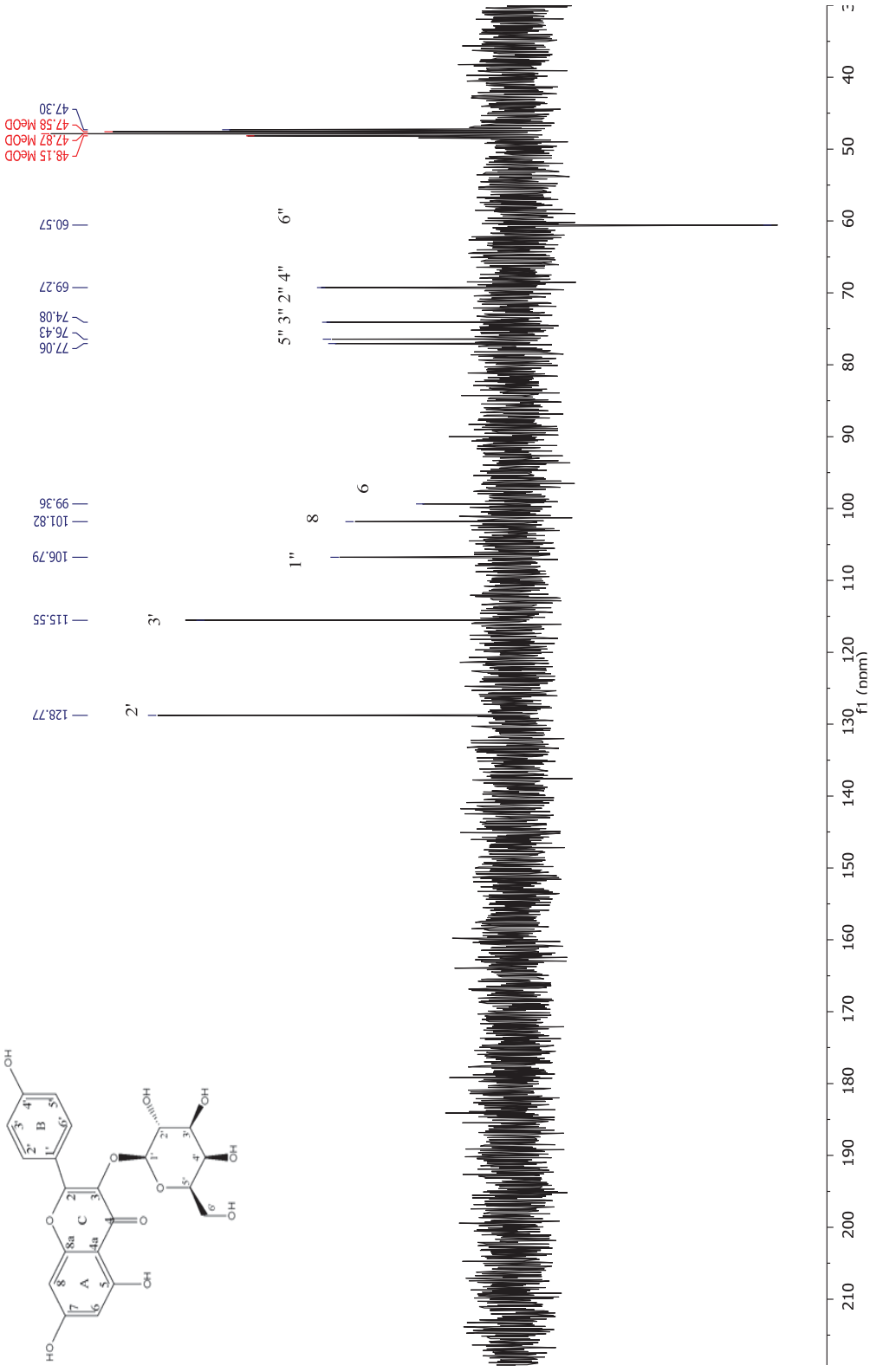

Figure 88 DEPT Spectrum of compound PGE-2 (in CD_3OD)

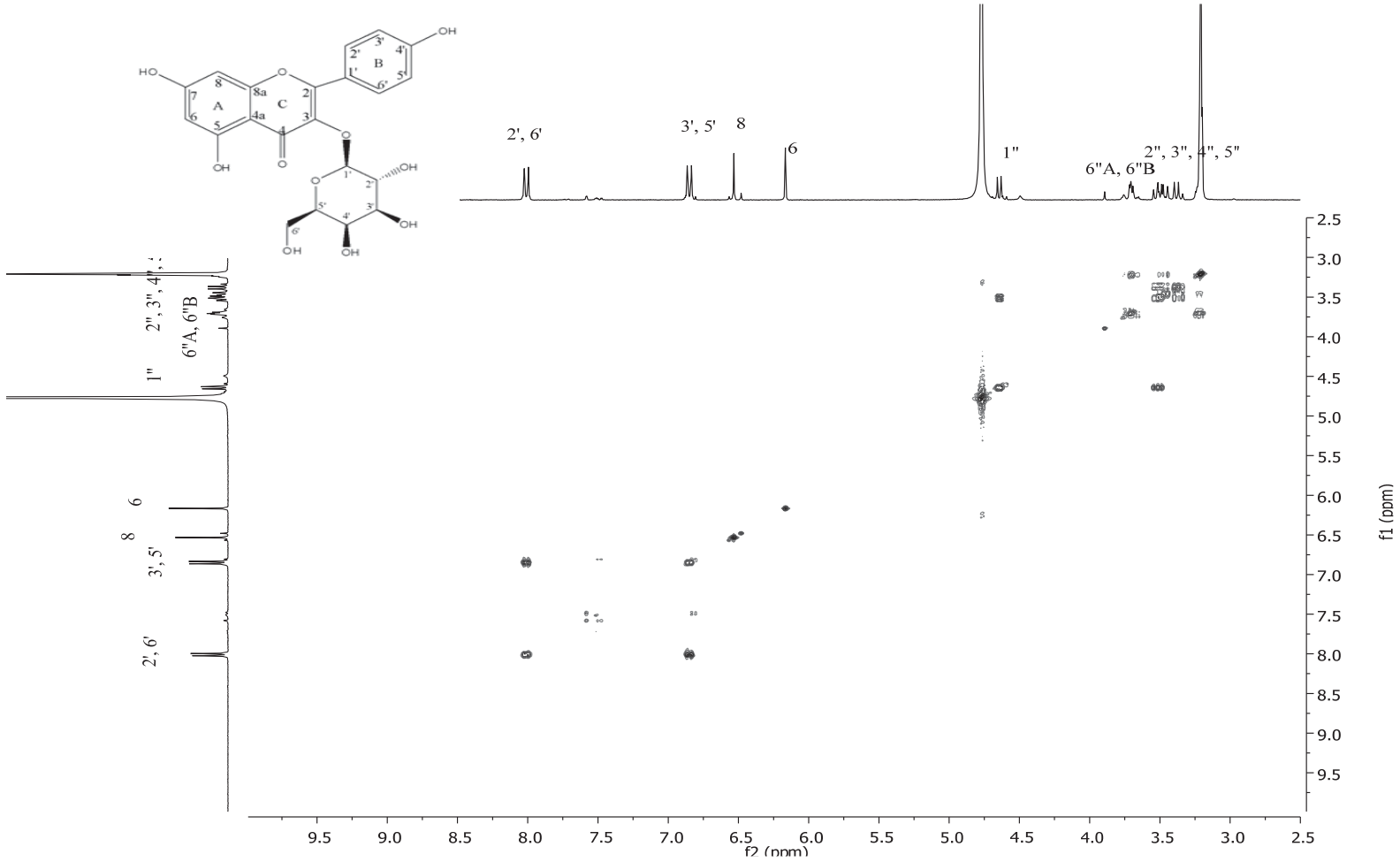

Figure 89 COSY Spectrum of compound PGE-2 (in CD_3OD)

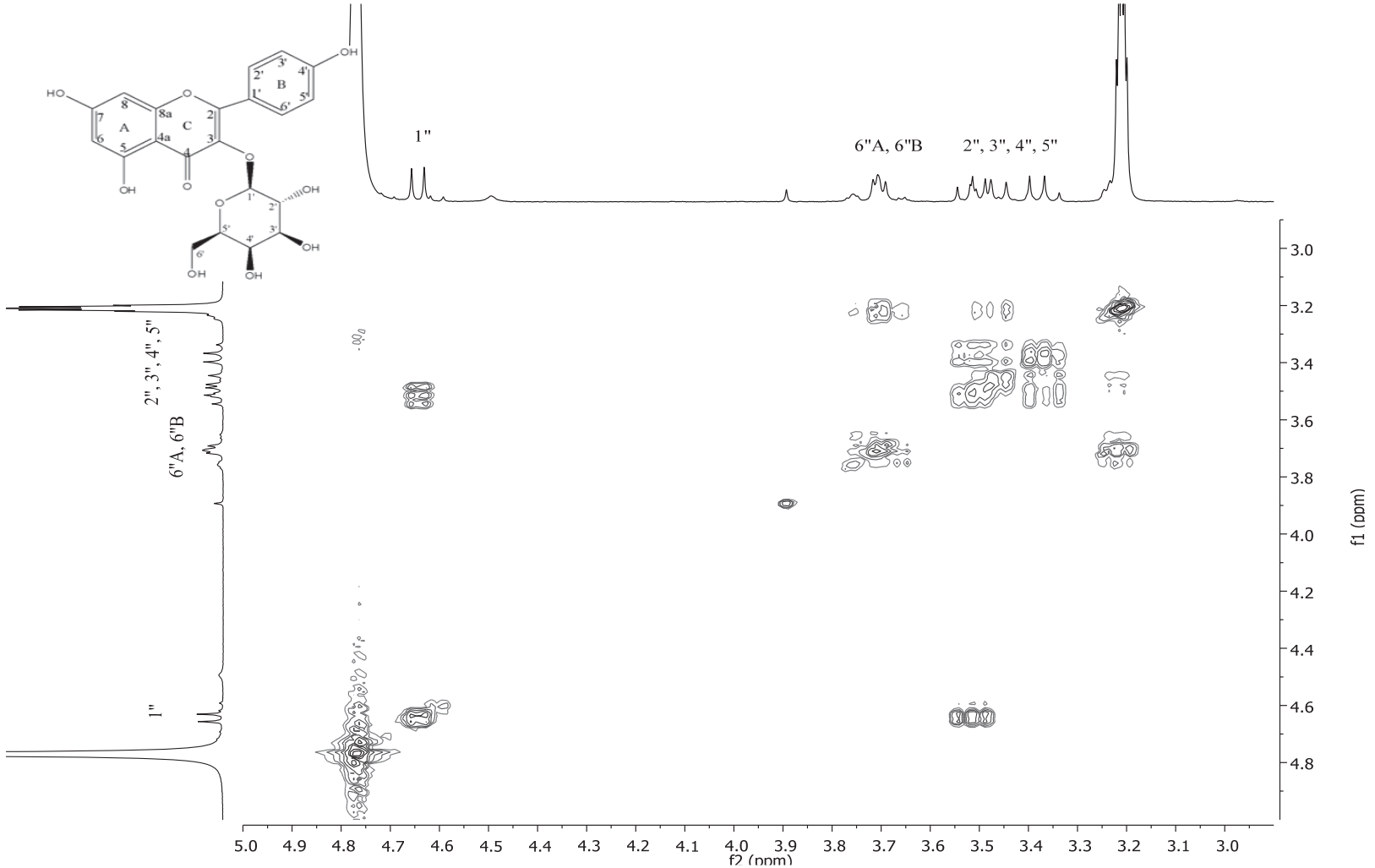

Figure 89 (Continued) COSY Spectrum of compound PGE-2 (in CD_3OD)

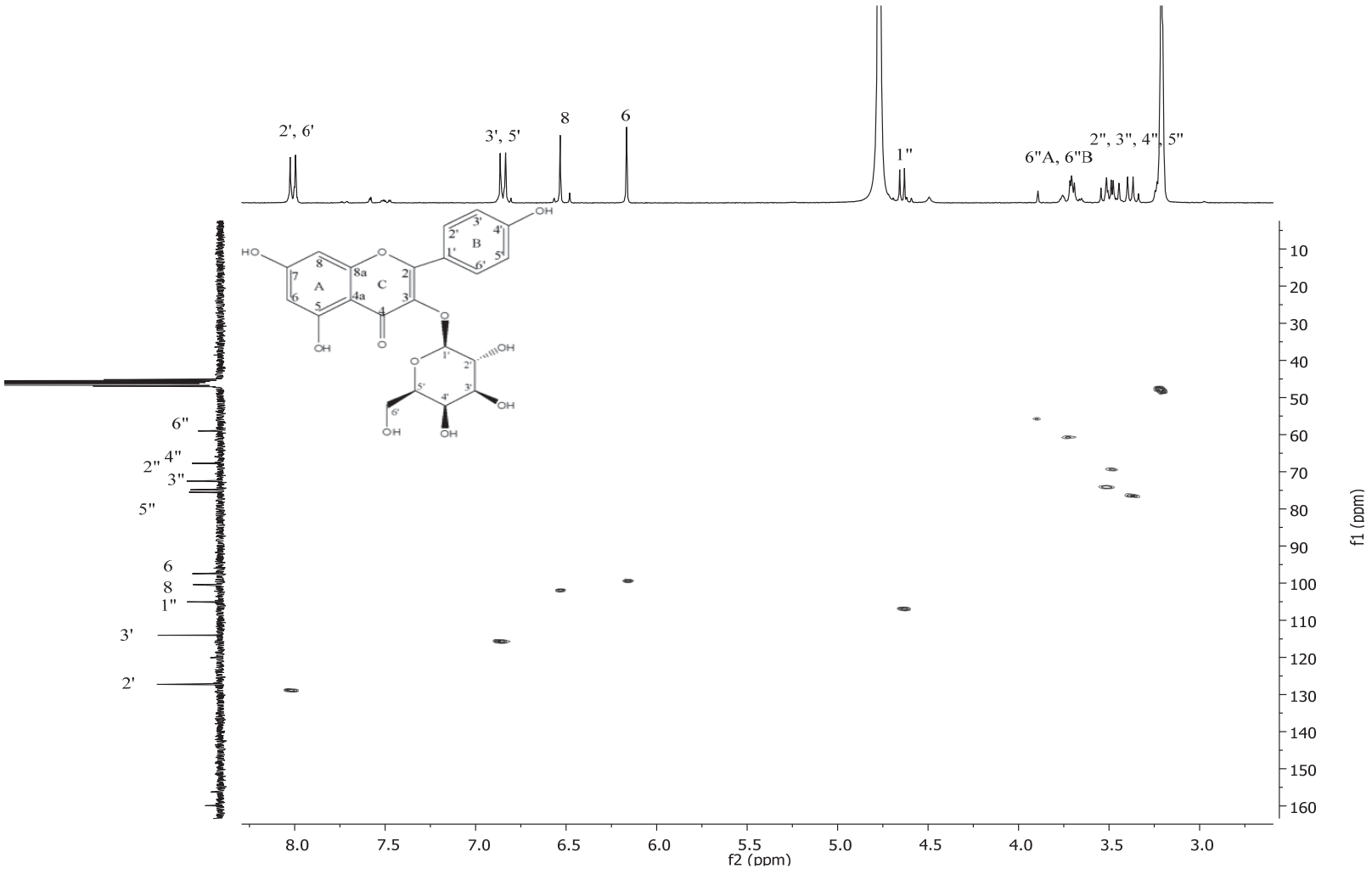

Figure 90 HMQC Spectrum of compound PGE-2 (in CD_3OD)

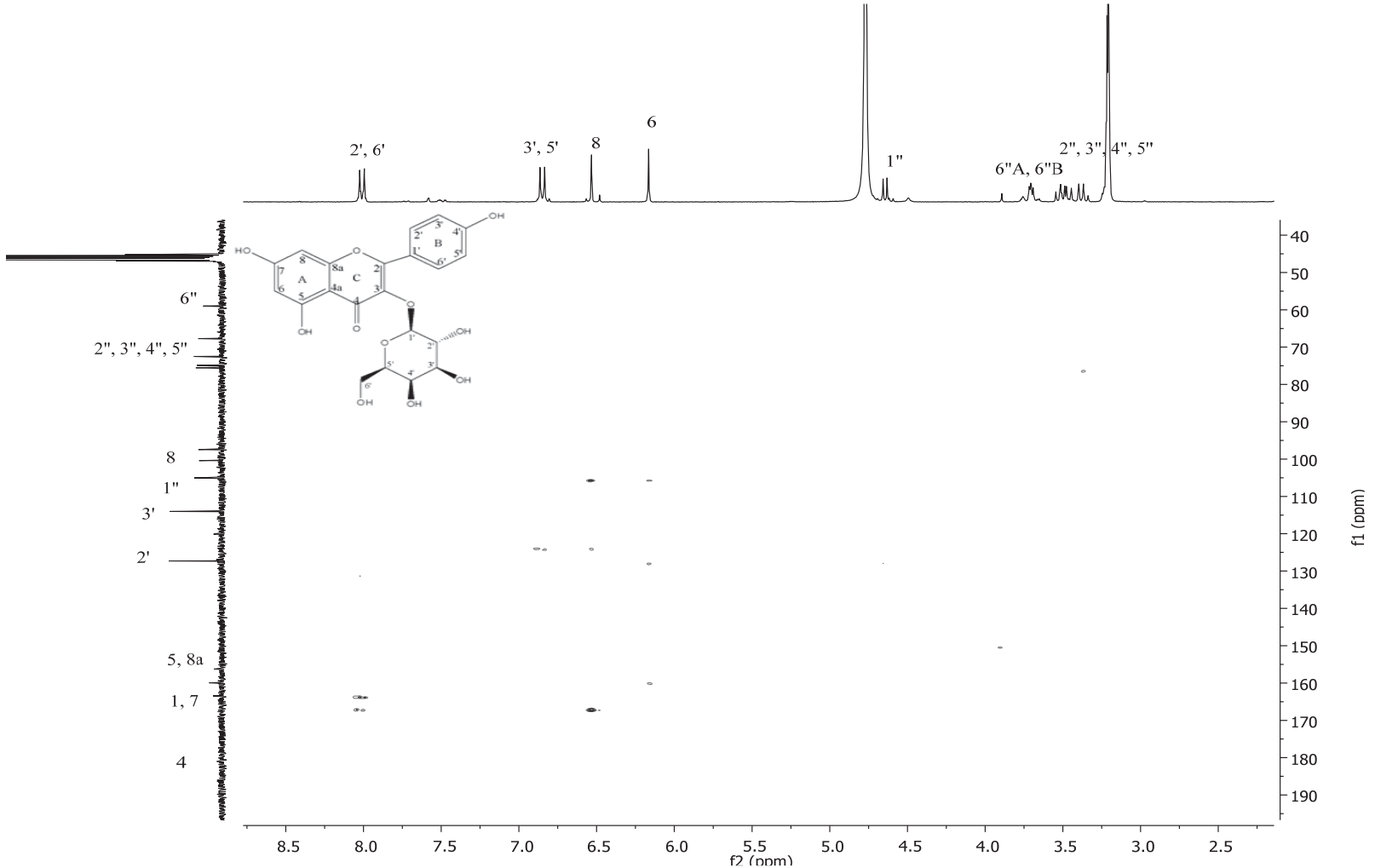

Figure 91 HMBC Spectrum of compound PGE-2 (in CD_3OD)

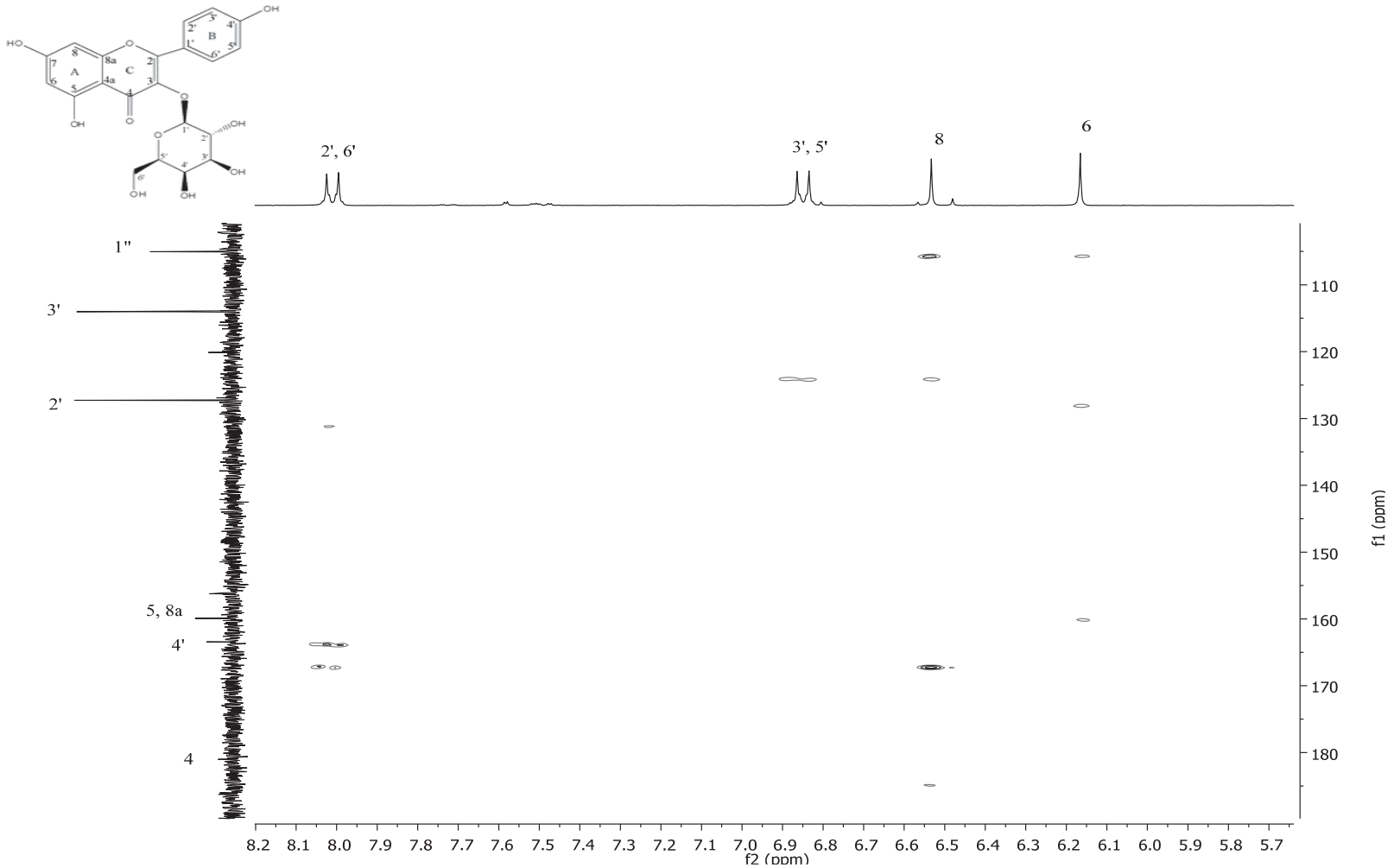

Figure 91 (Continued) HMBC Spectrum of compound PGE-2 (in CD_3OD)

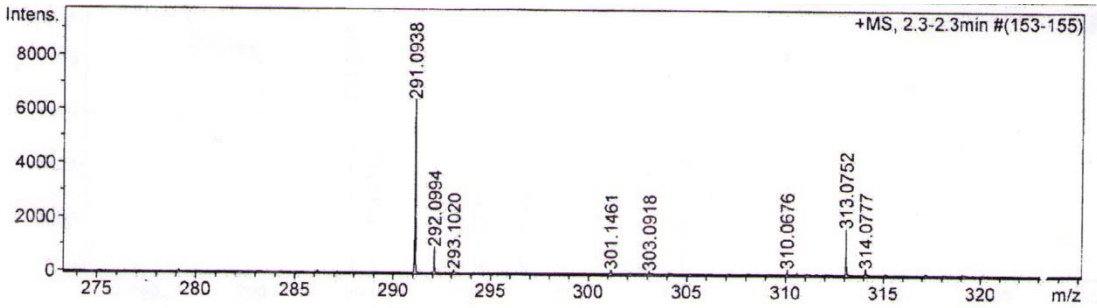

Figure 92 MS spectrum of compound PGE-3

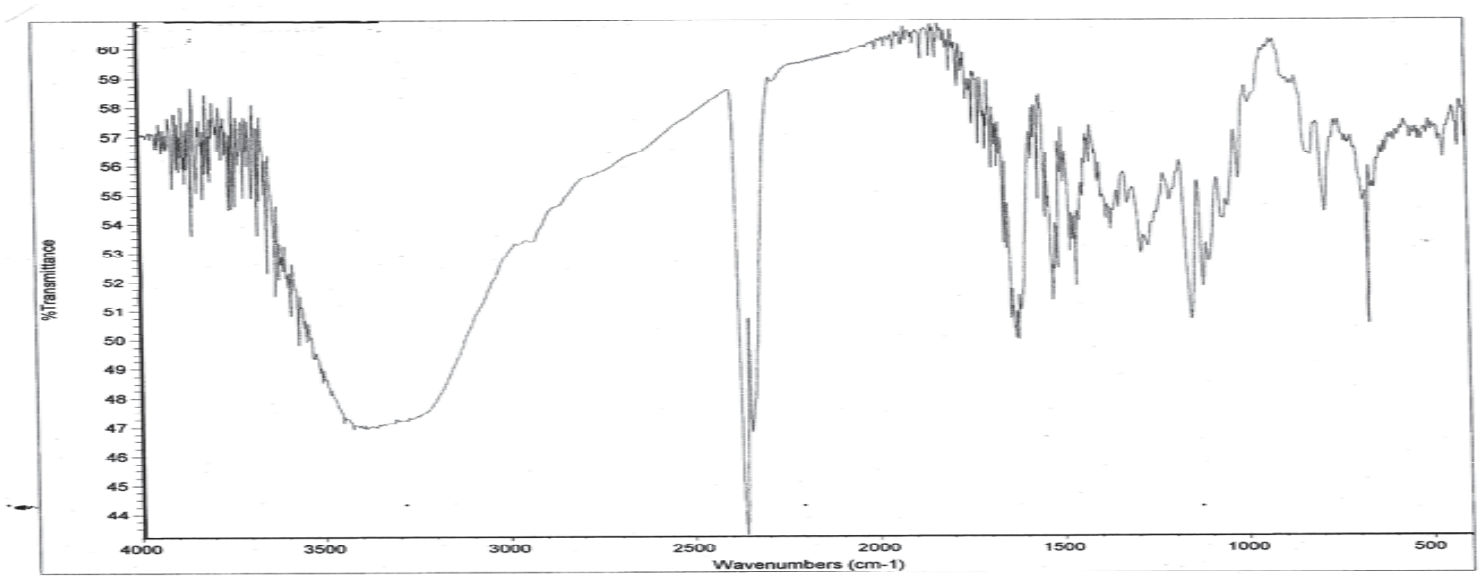

Figure 93 IR (KBr) spectrum of compound PGE-3

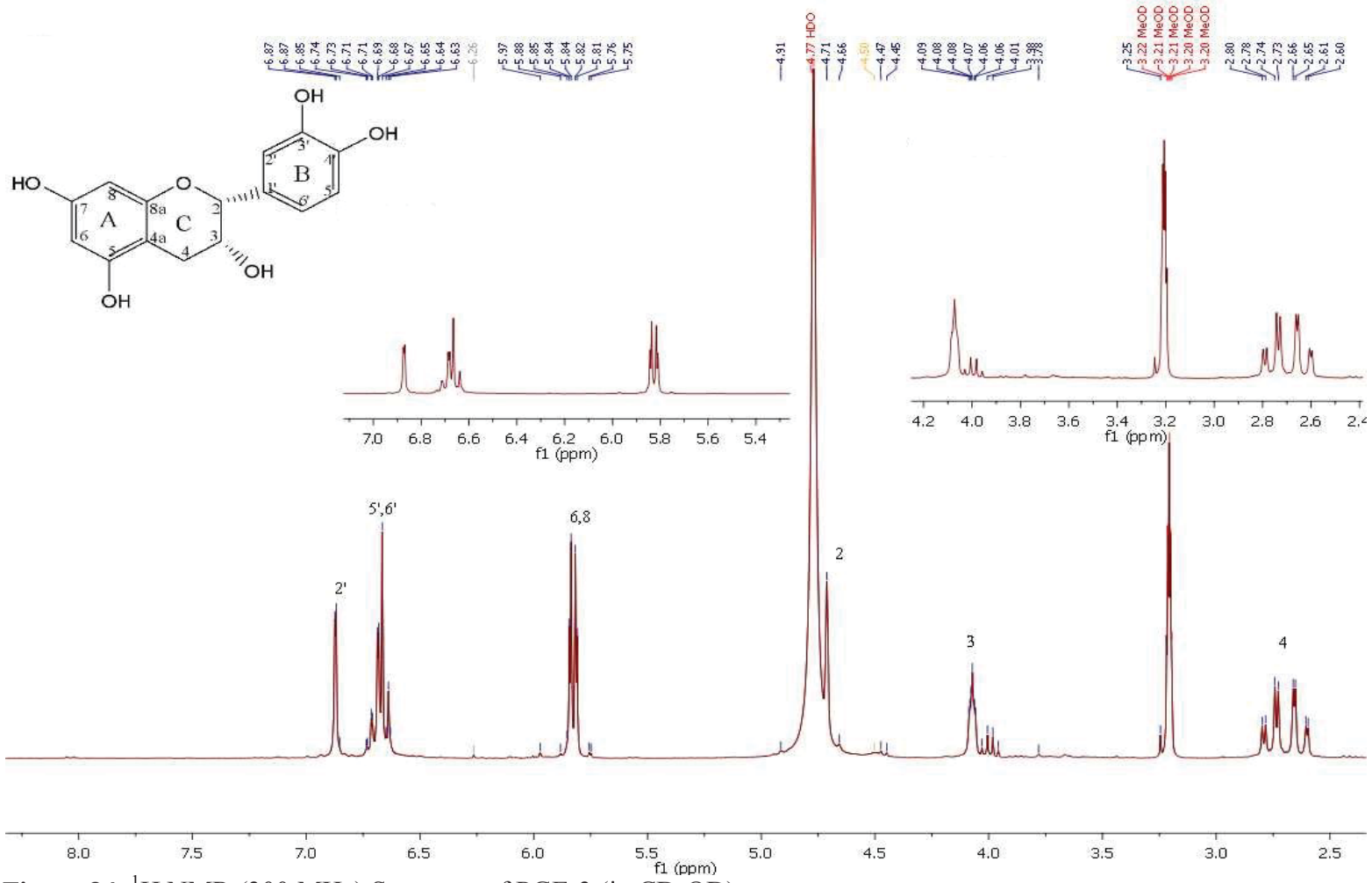

Figure 94 ^{1}H NMR (300 MHz) Spectrum of PGE-3 (in CD_3OD)

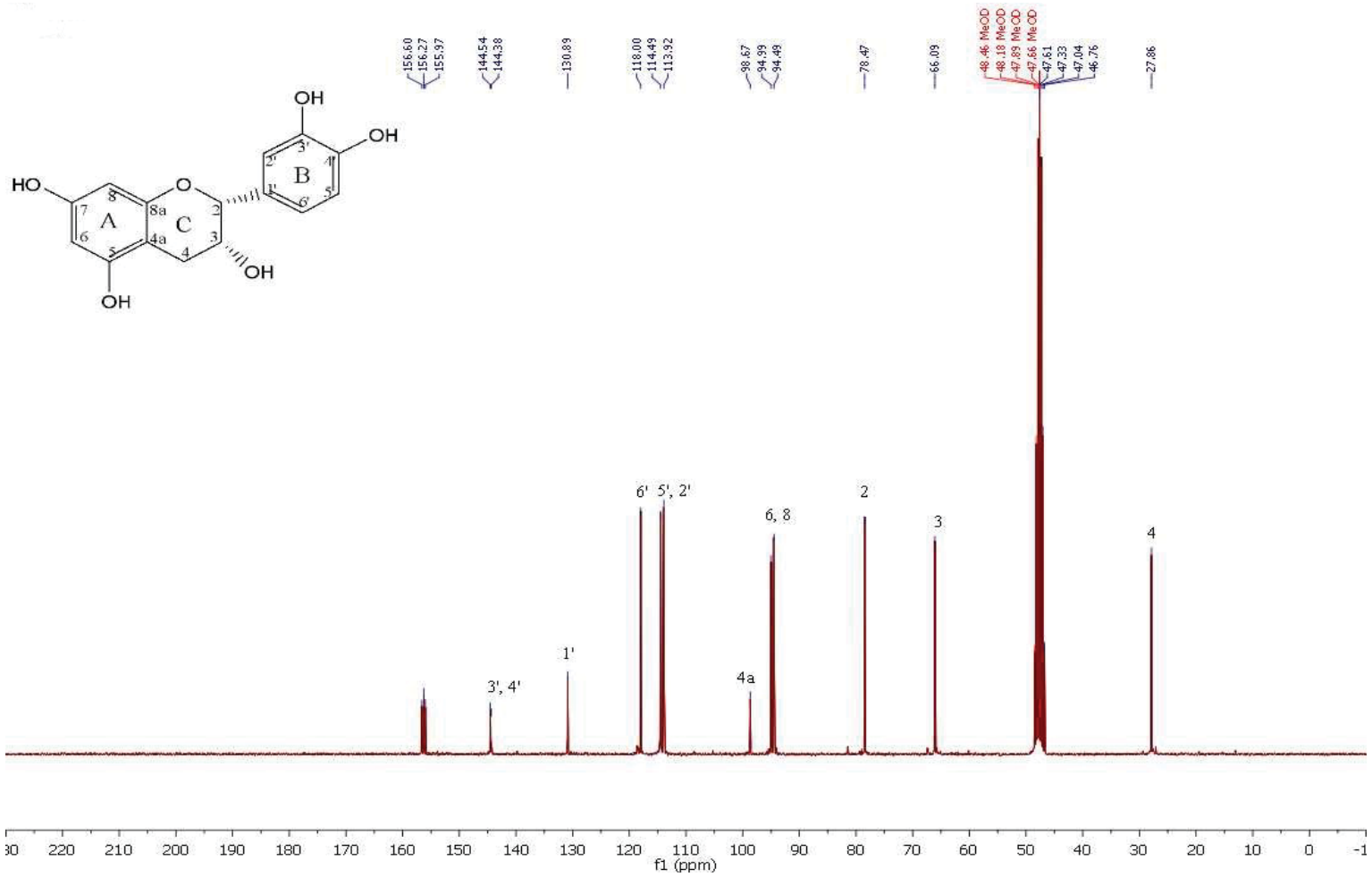

Figure 95 ^{13}C NMR (75 MHz) Spectrum of compound PGE-3 (in CD_3OD)

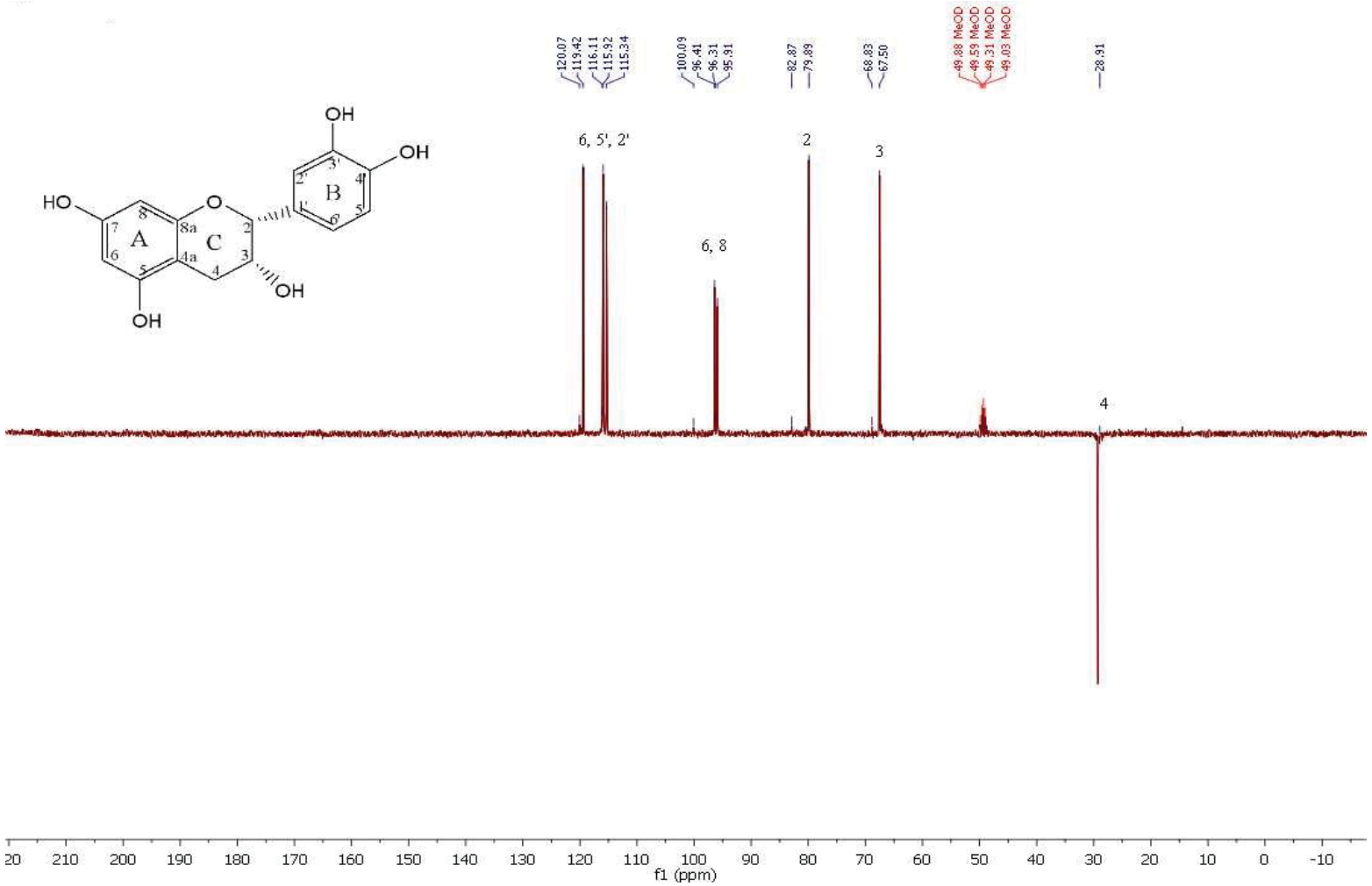

Figure 96 DEPT Spectrum of compound PGE-3 (in CD_3OD)

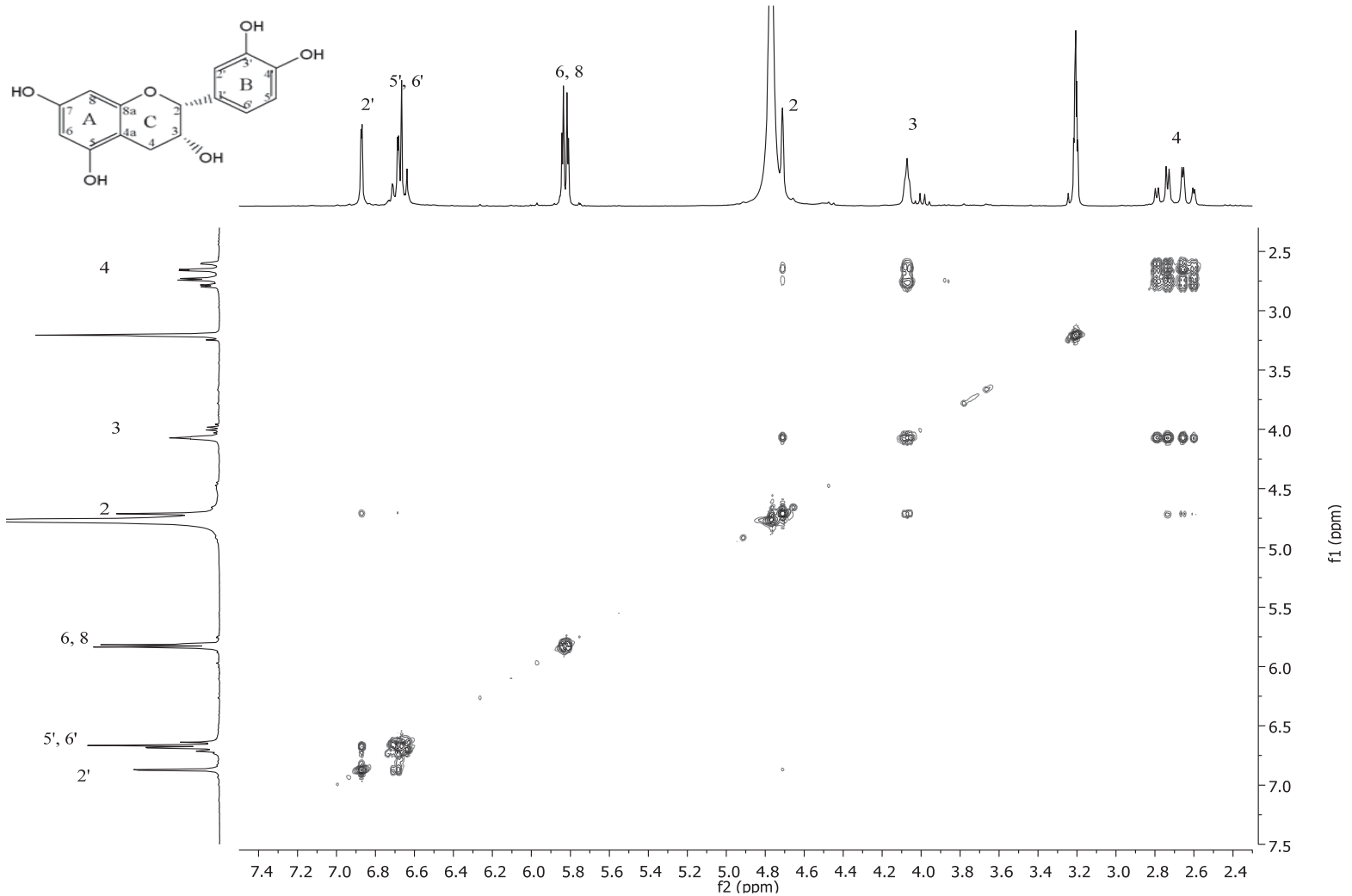

Figure 97 COSY Spectrum of compound PGE-3 (in CD_3OD)

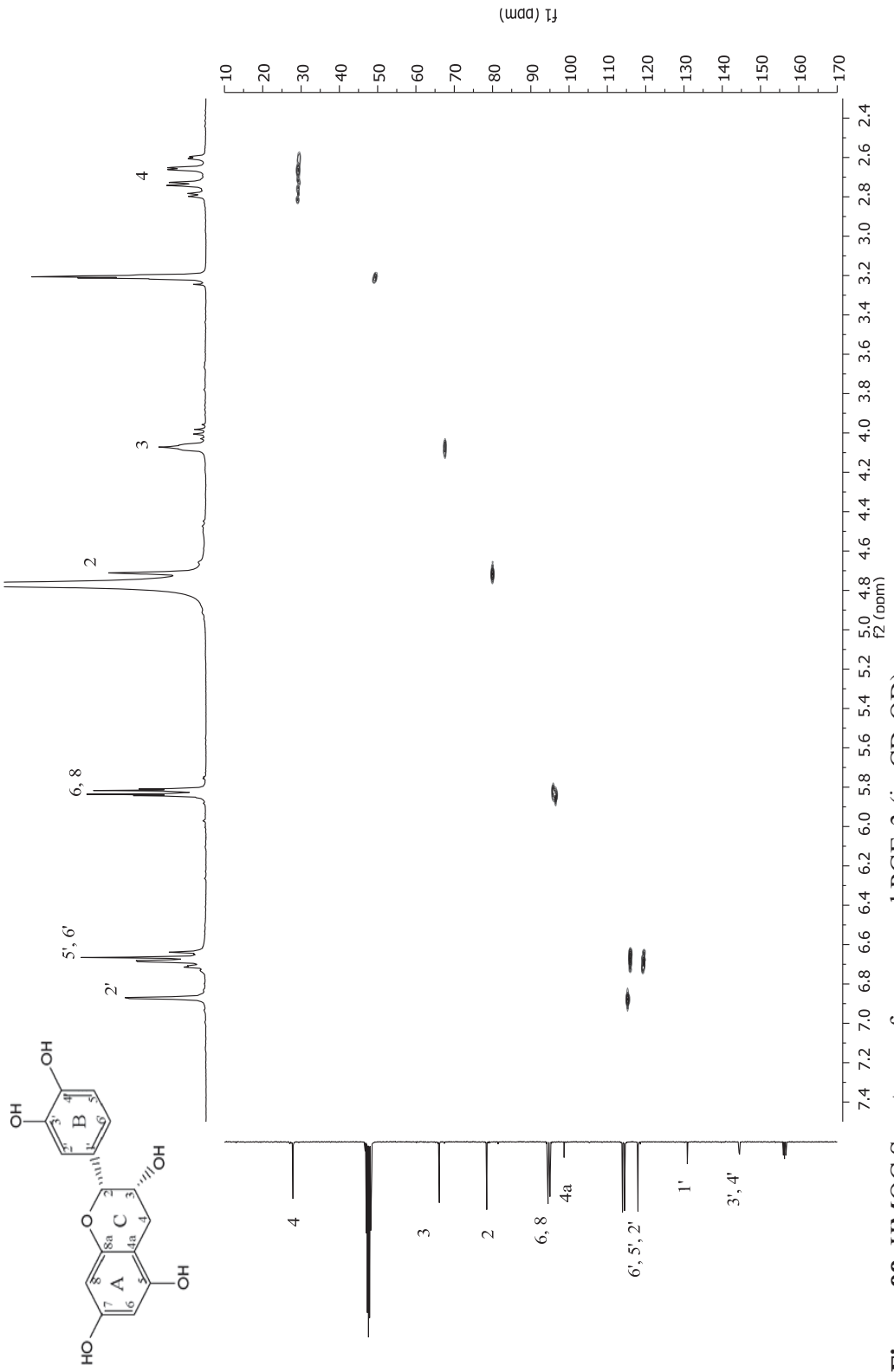

Figure 98 HMQC Spectrum of compound PGE-3 (in CD_3OD)

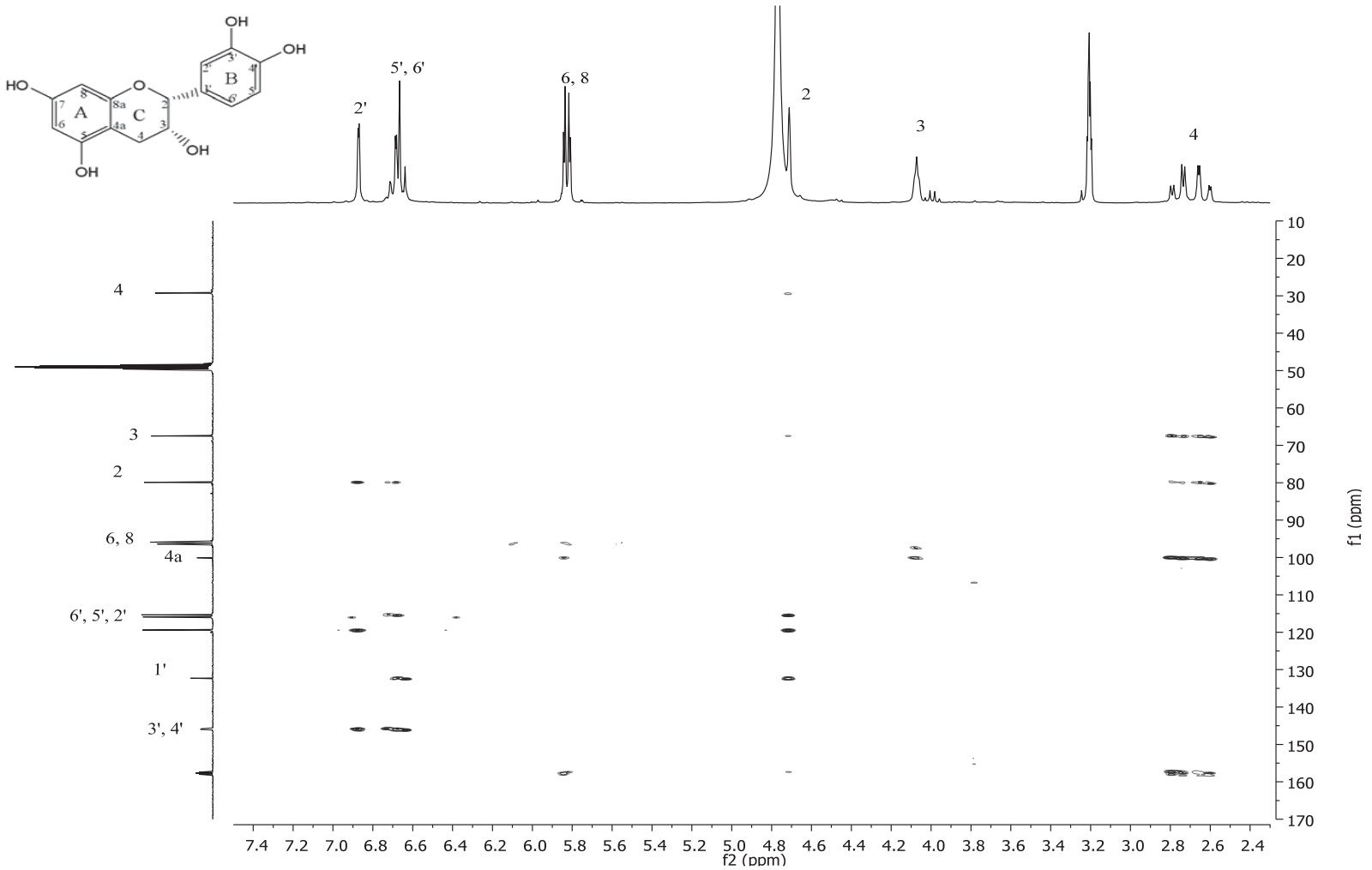

Figure 99 HMBC Spectrum of compound PGE-3 (in CD_3OD)

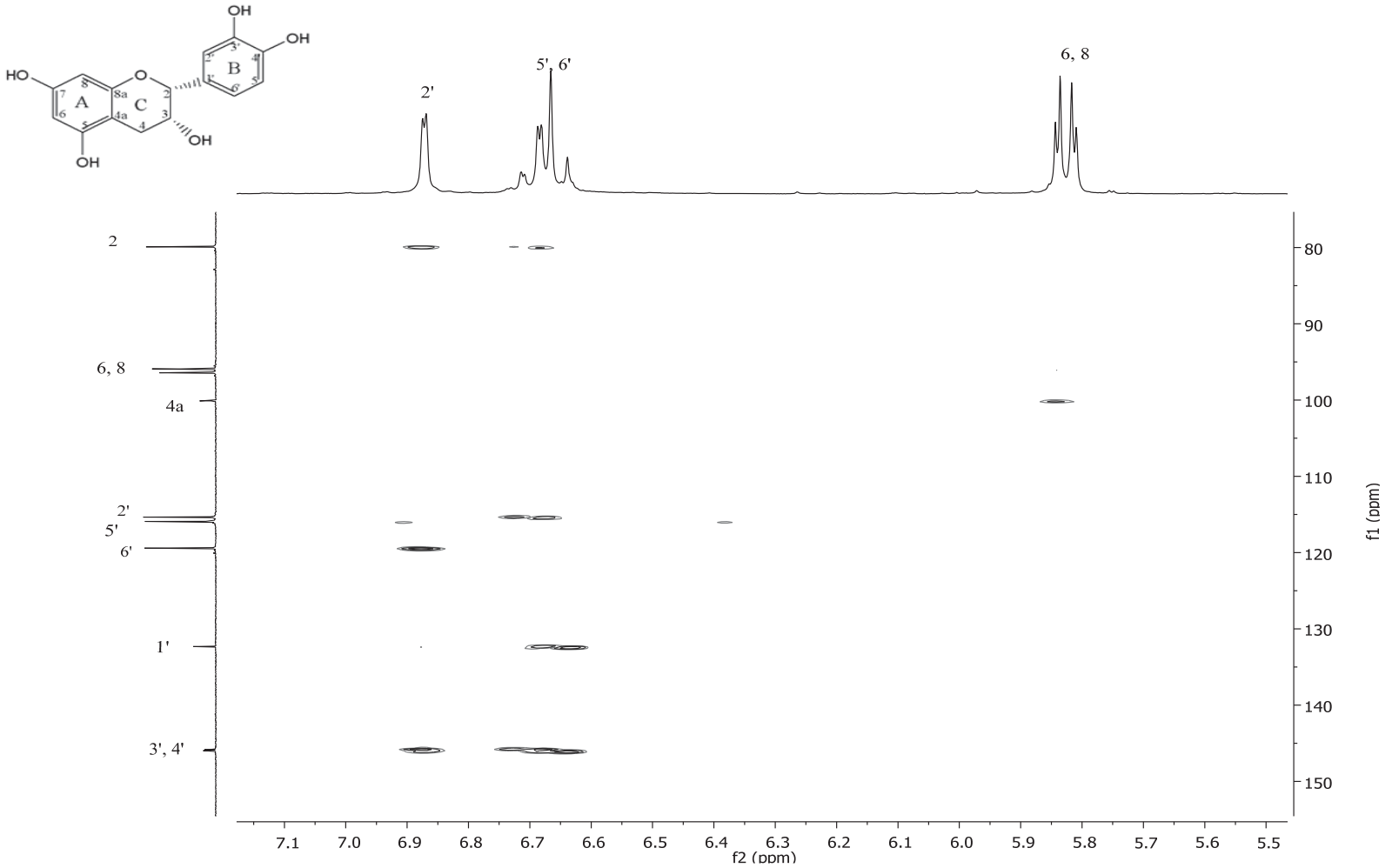

Figure 99 (Continued) HMBC Spectrum of compound PGE-3 (in CD_3OD)

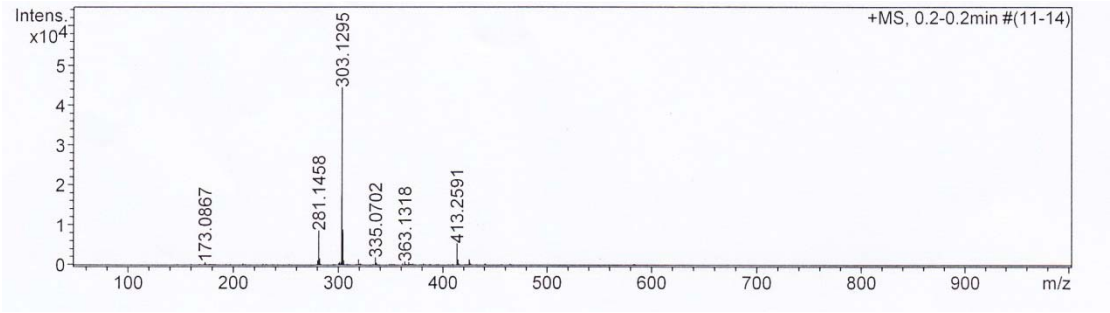

Figure 100 MS spectrum of compound MHL-1

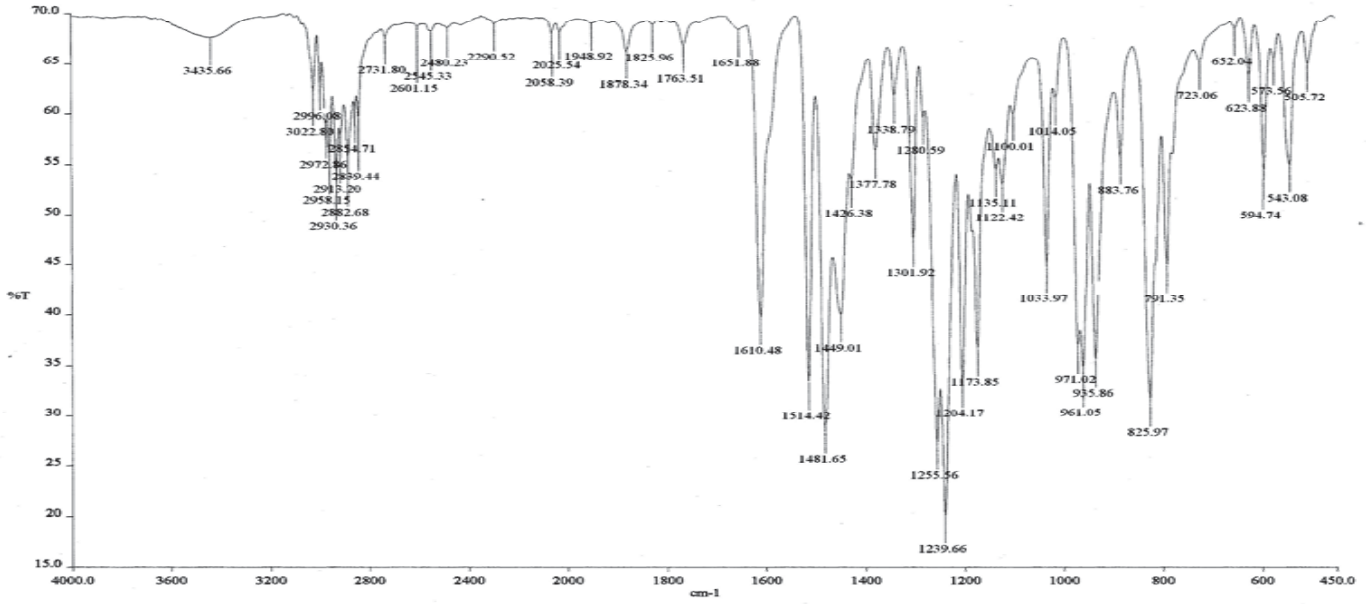

Figure 101 IR (KBr) spectrum of compound MHL-1

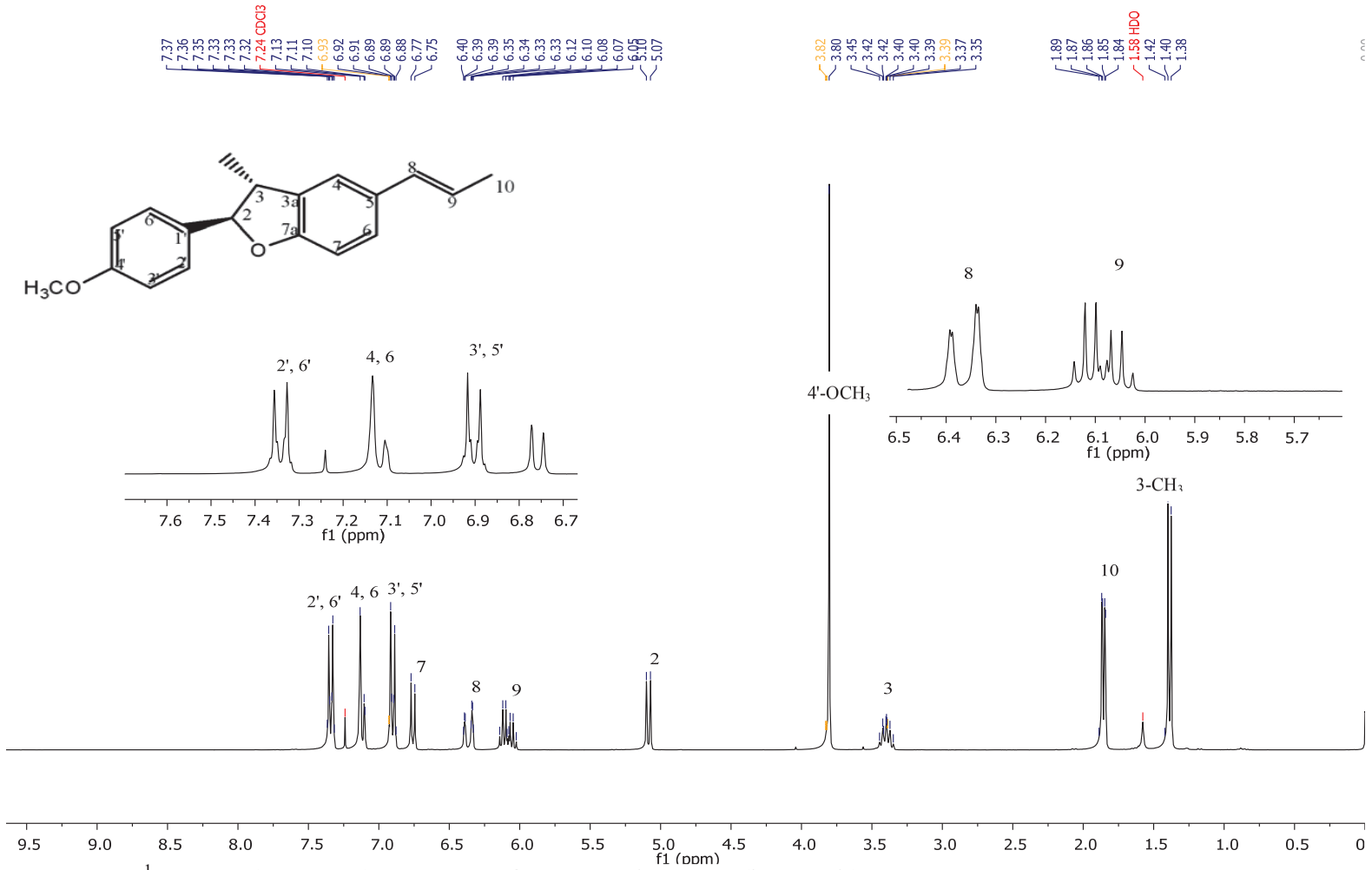

Figure 102 ^{1}H NMR (300 MHz) Spectrum of compound MHL-1 (in $CDCl_3$)

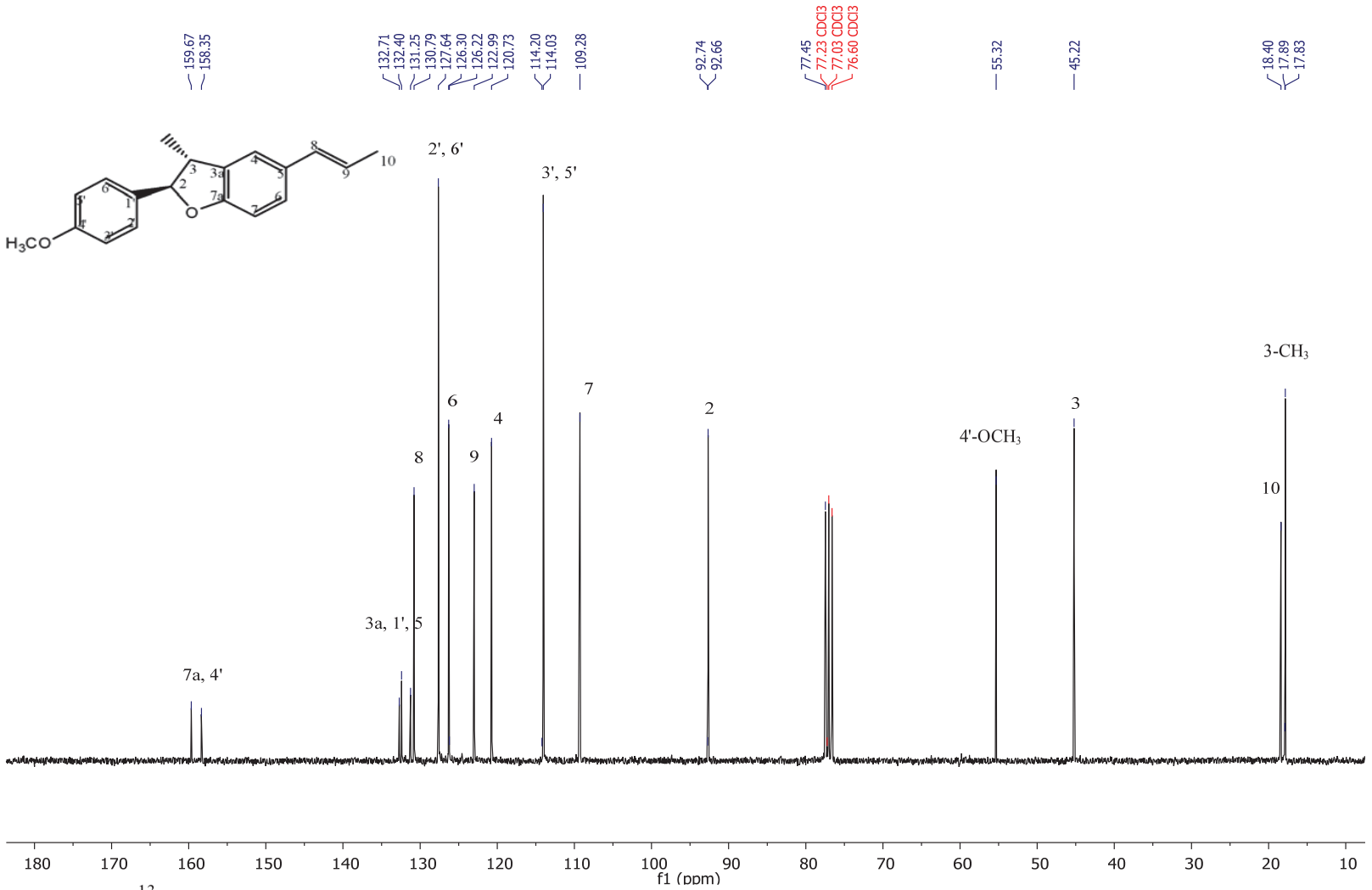

Figure 103 ^{13}C NMR (75 MHz) Spectrum of compound MHL-1 (in $CDCl_3$)

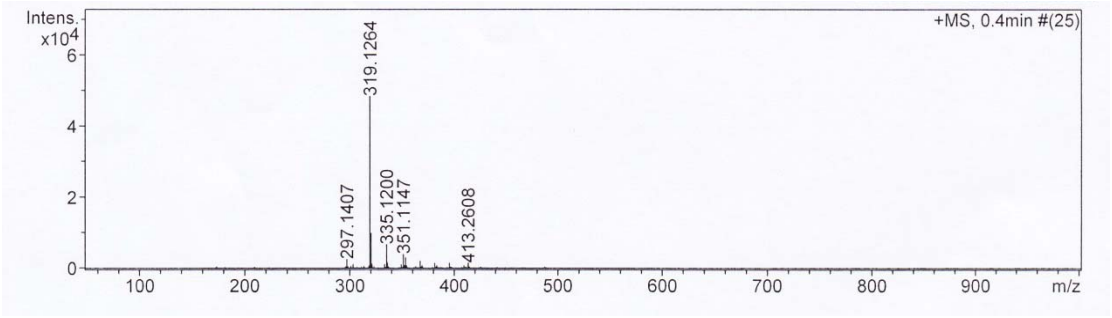

Figure 104 MS spectrum of compound MHL-2

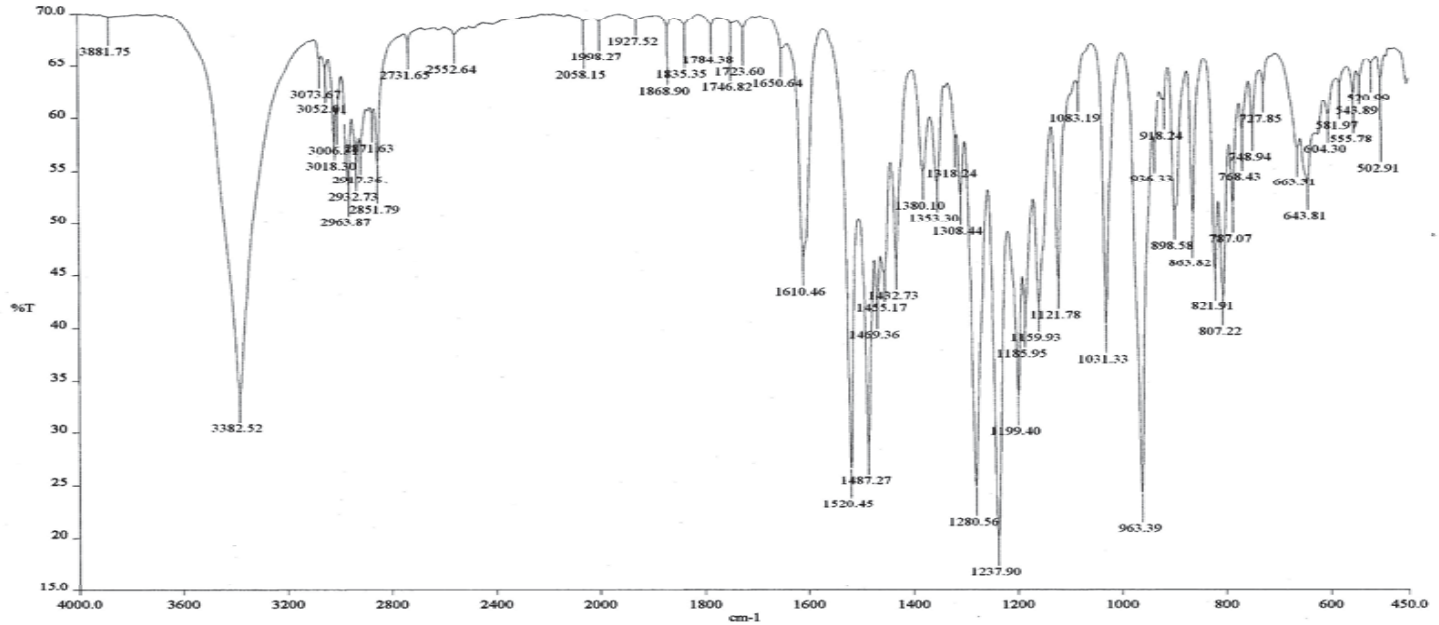

Figure 105 IR (KBr) spectrum of compound MHL-2

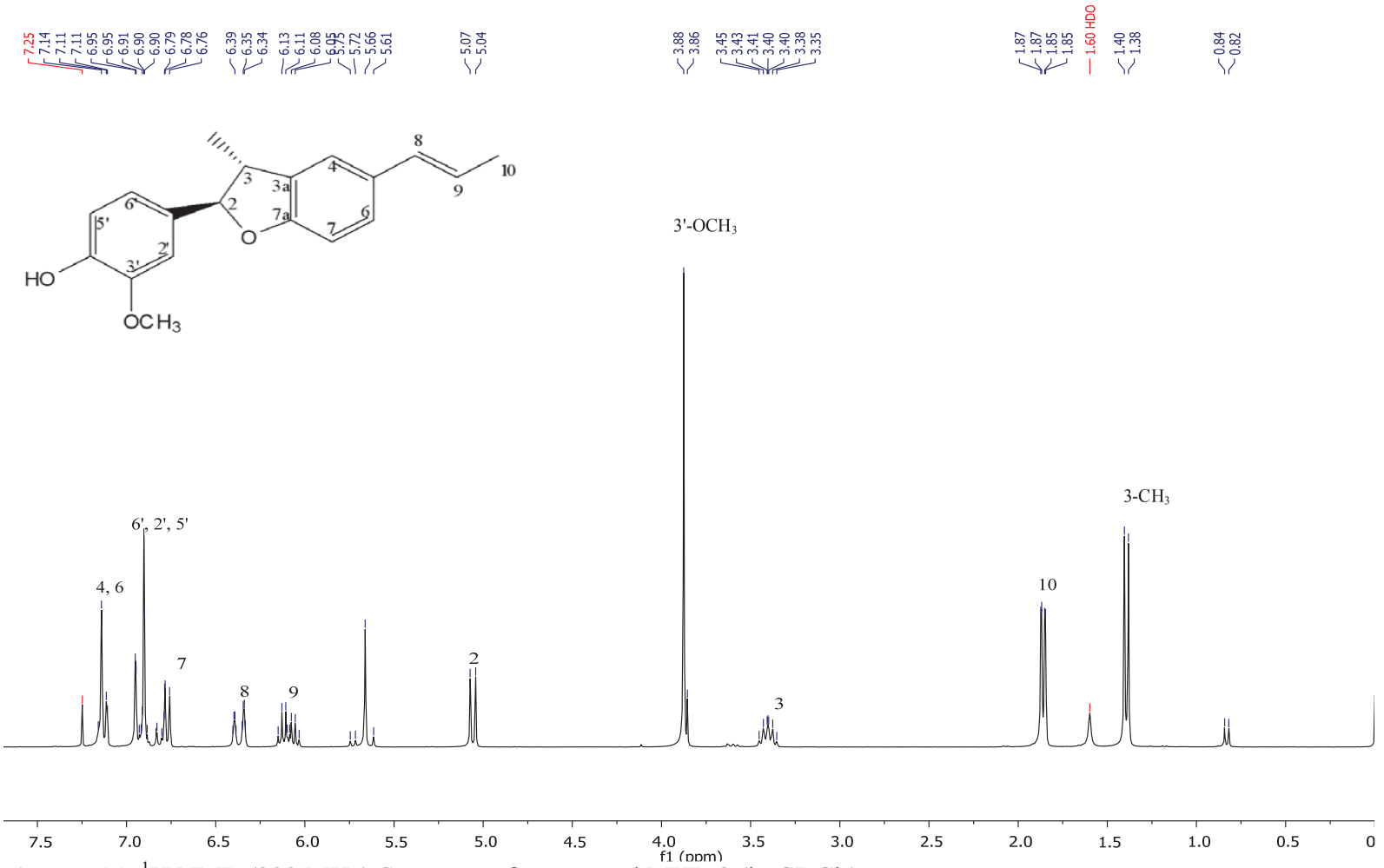

Figure 106 ^{1}H NMR (300 MHz) Spectrum of compound MHL-2 (in $CDCl_3$)

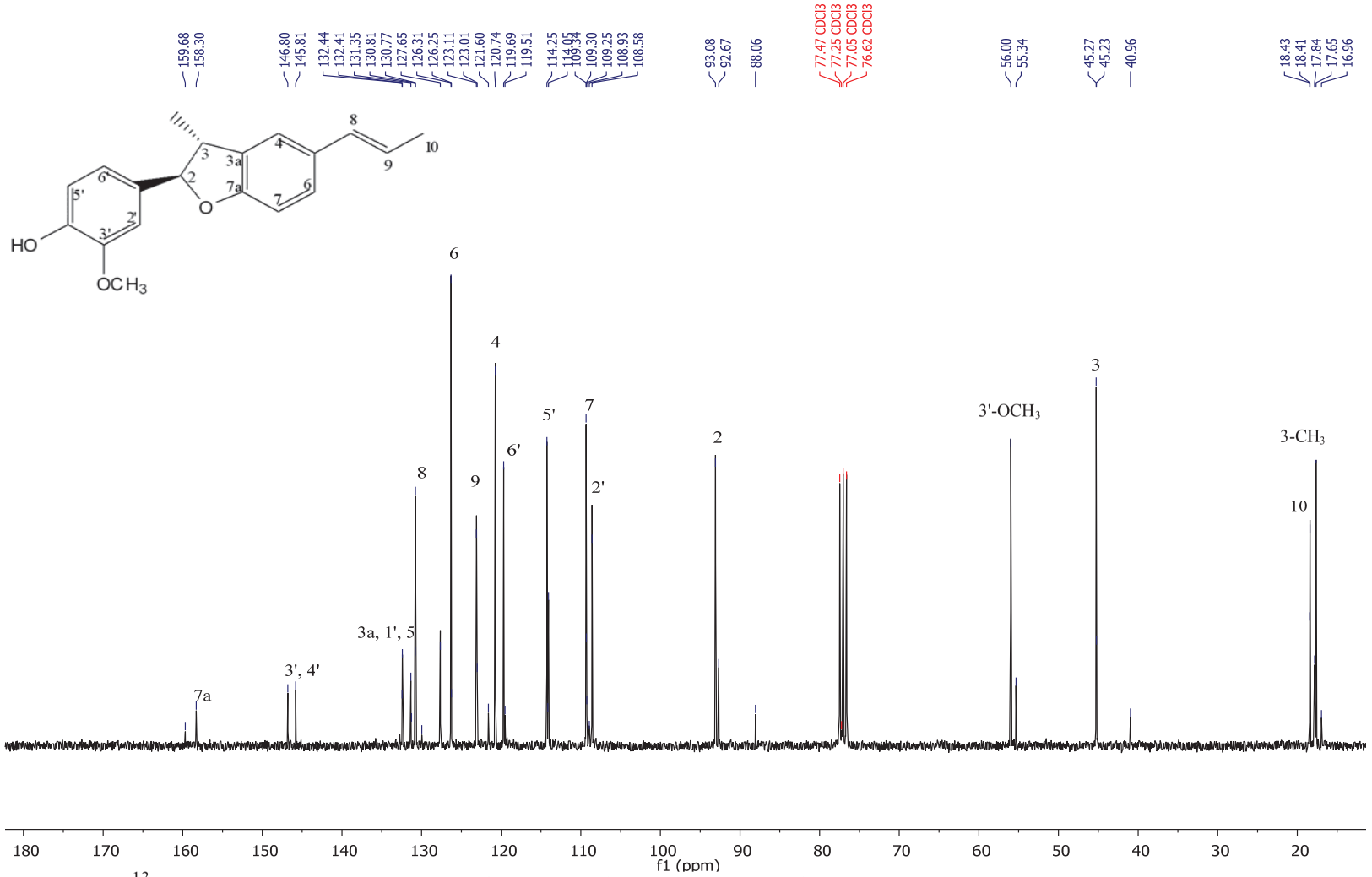

Figure 107 ^{13}C NMR (75 MHz) Spectrum of compound MHL-2 (in $CDCl_3$)

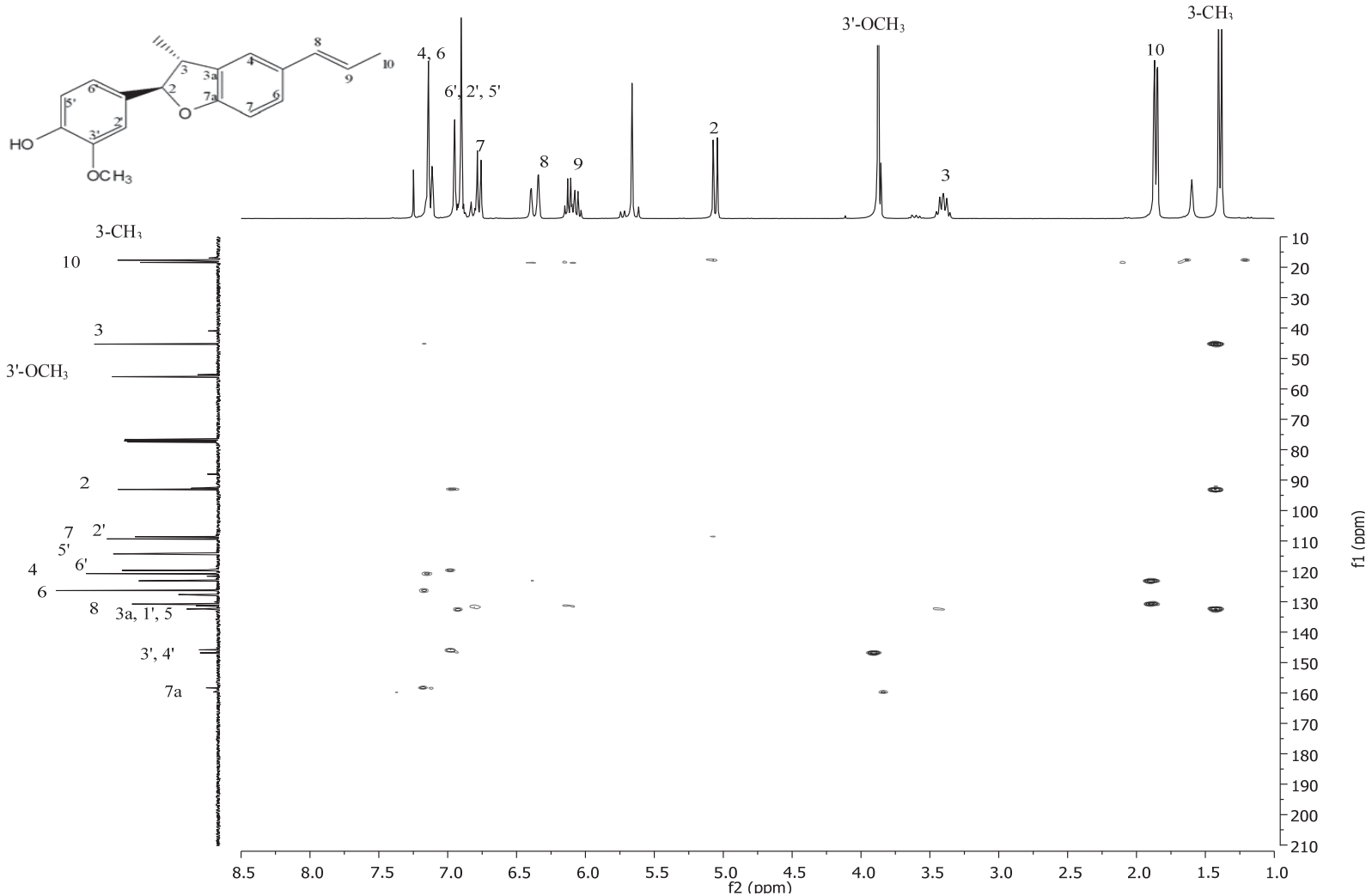

Figure 108 HMBC Spectrum of compound MHL-2 (in $CDCl_3$)

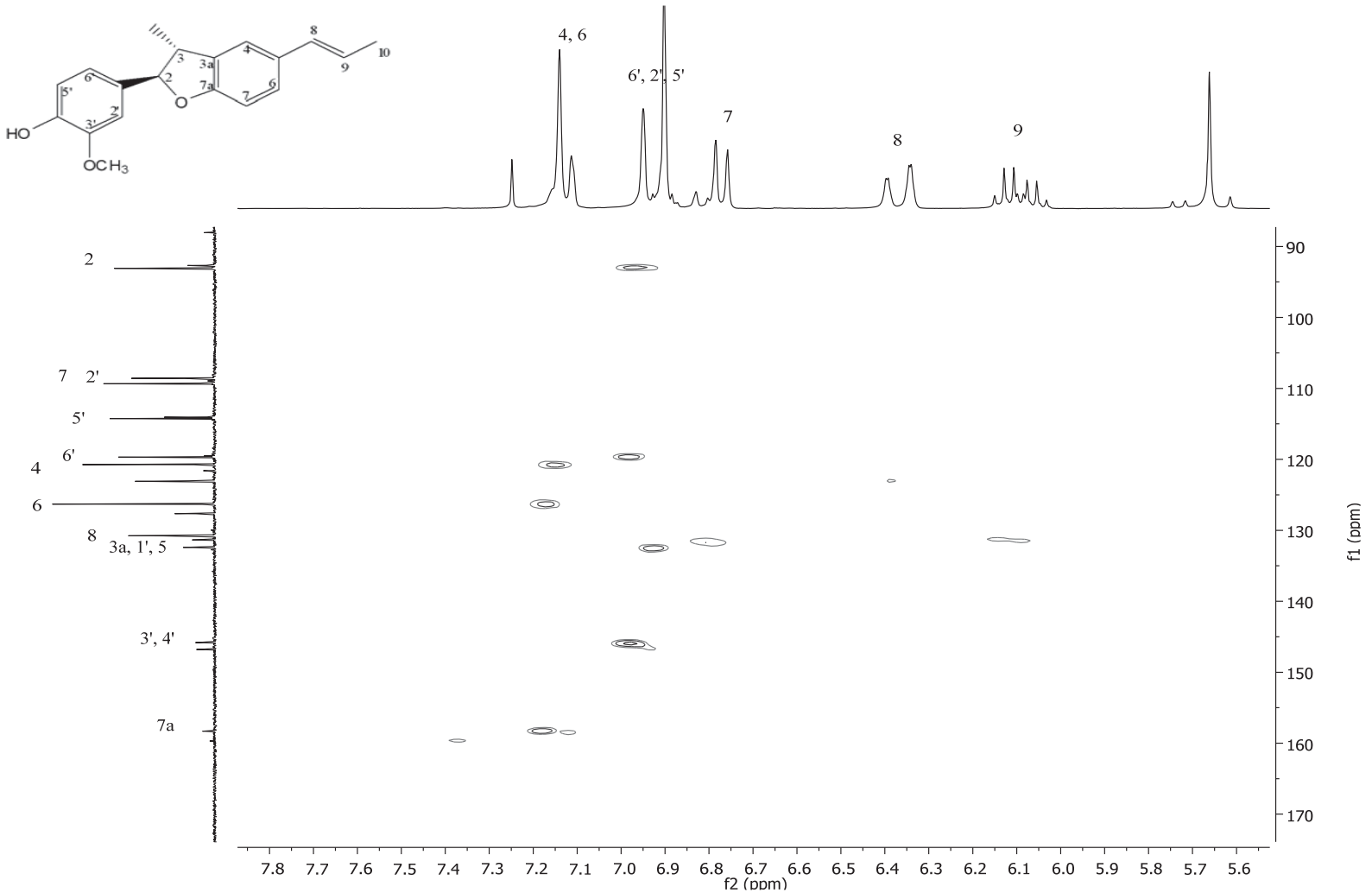

Figure 108 (Continued) HMBC Spectrum of compound MHL-2 (in $CDCl_3$)

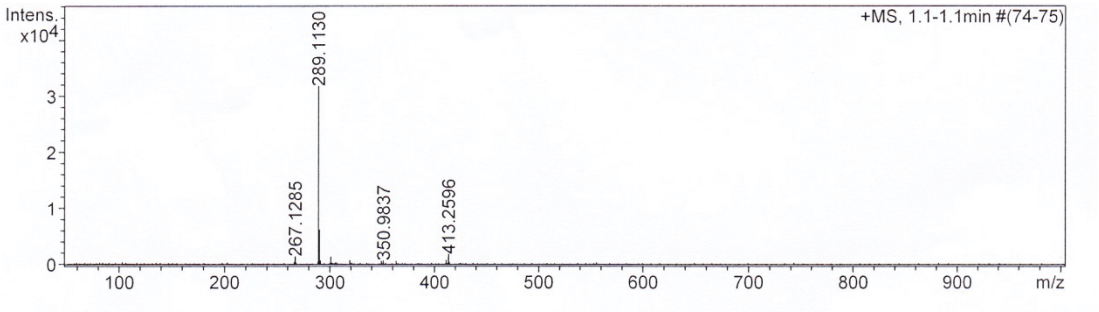

Figure 109 MS spectrum of compound MHL-3

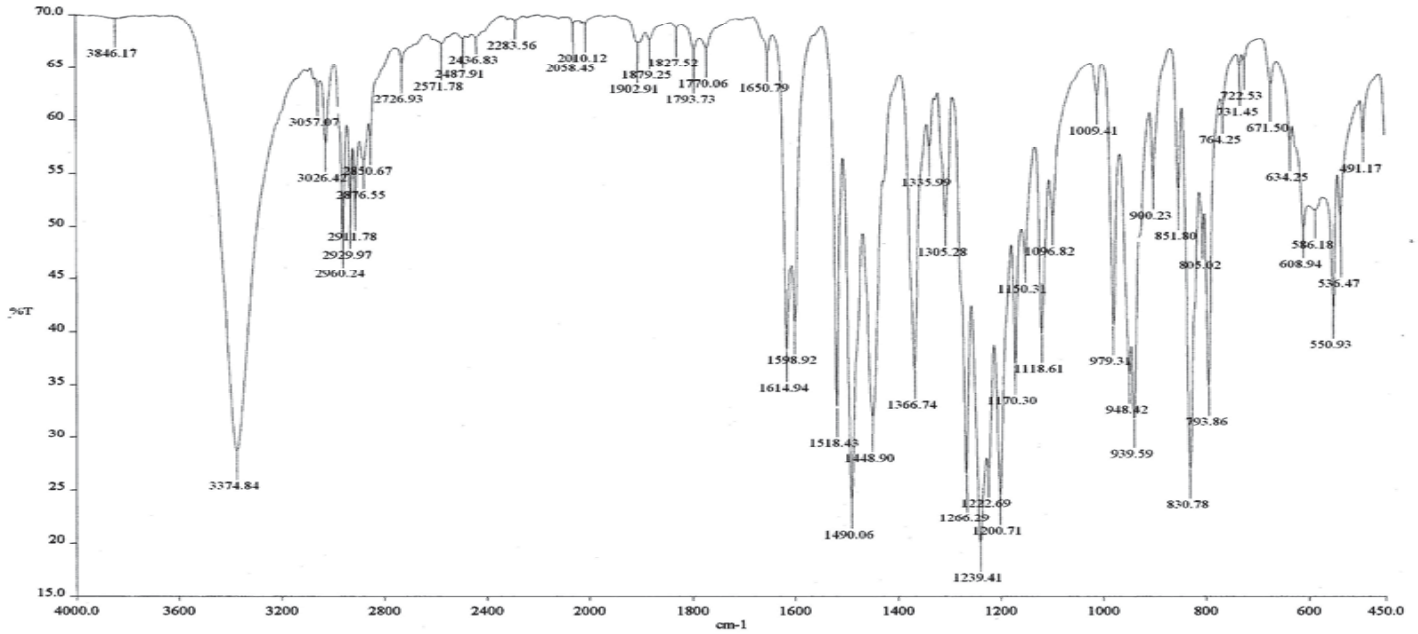

Figure 110 IR (KBr) spectrum of compound MHL-3

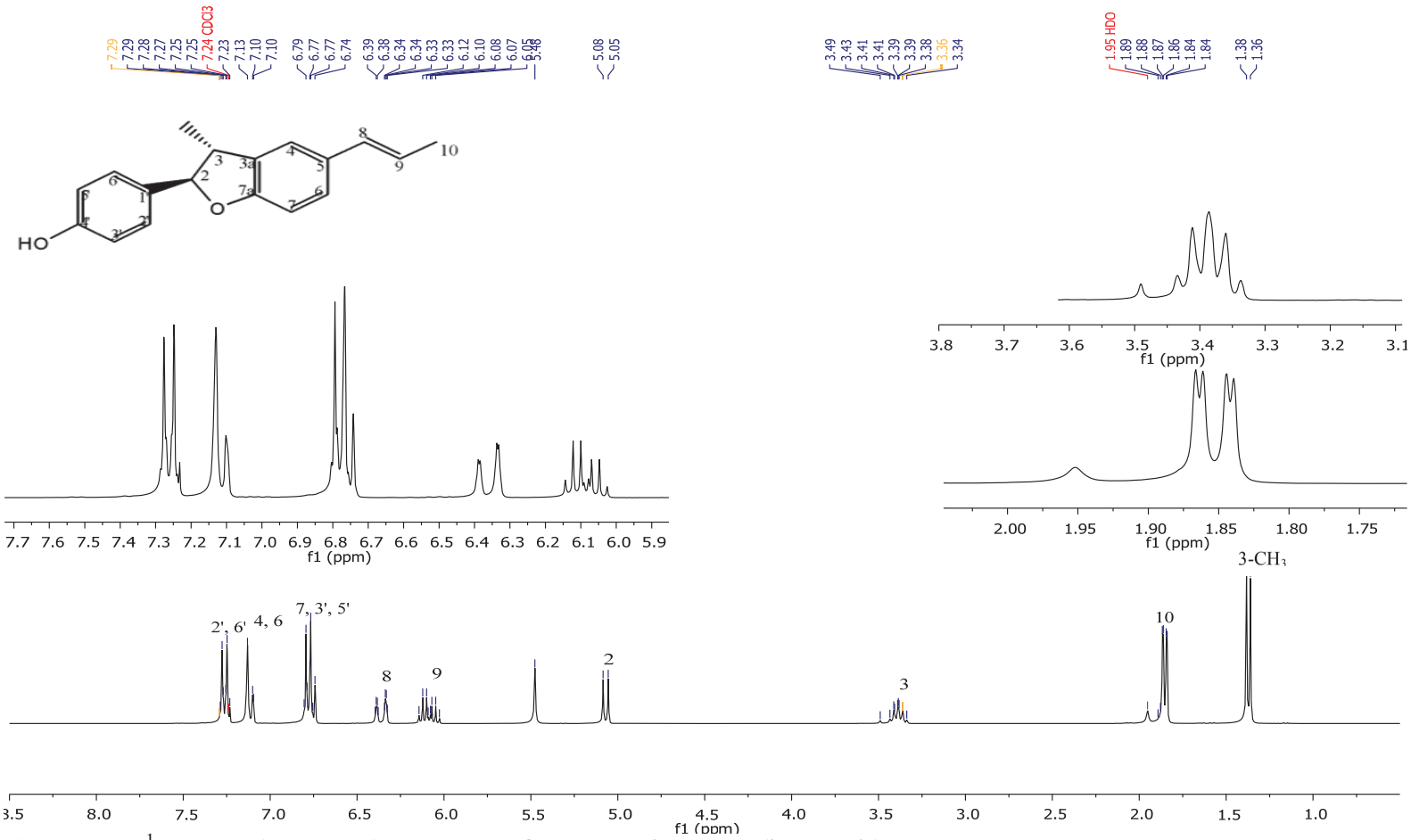

Figure 111 ^{1}H NMR (300 MHz) Spectrum of compound MHL-3 (in $CDCl_3$)

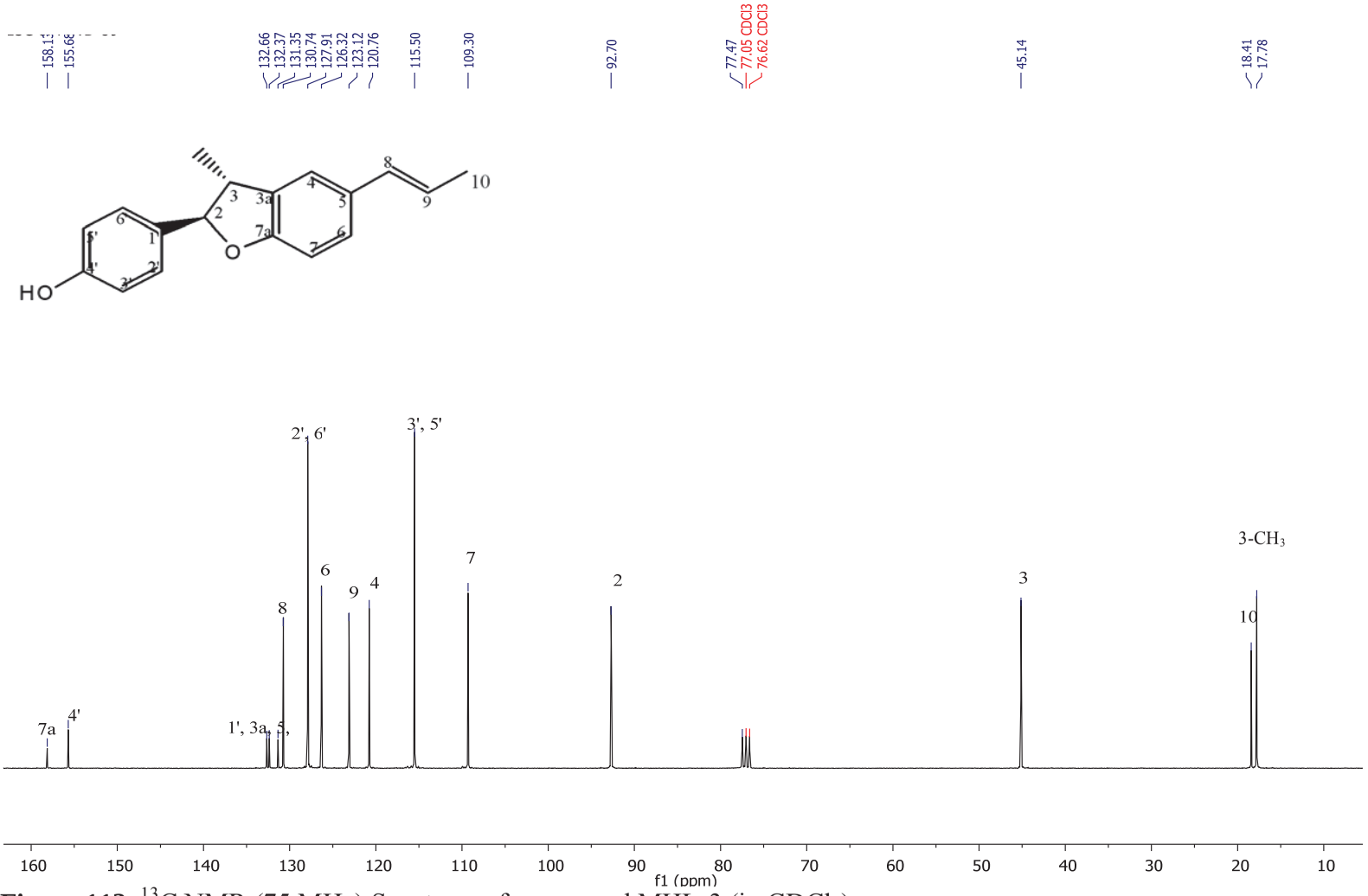

Figure 112 ^{13}C NMR (75 MHz) Spectrum of compound MHL-3 (in $CDCl_3$)

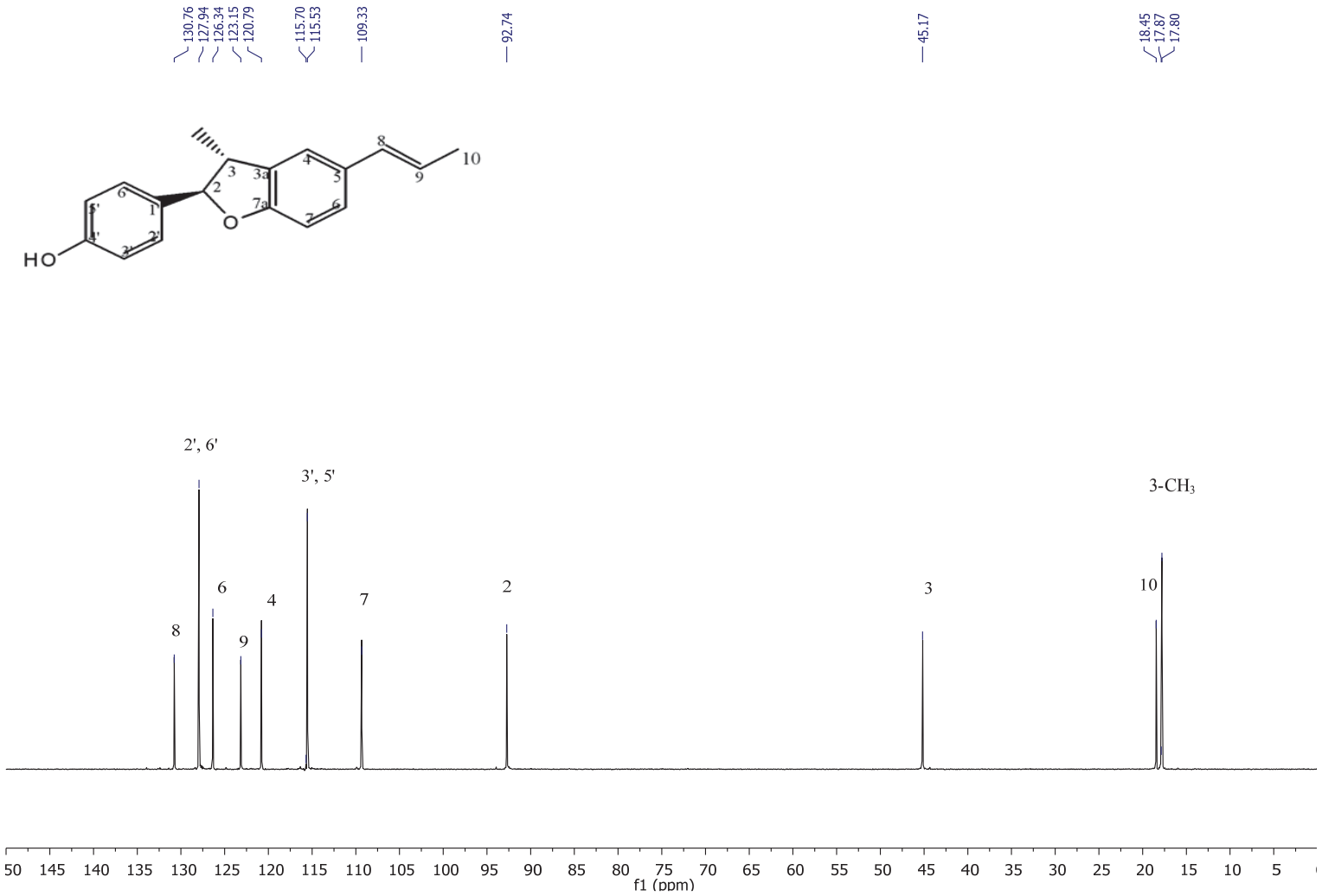

Figure 113 DEPT Spectrum of compound MHL-3 (in $CDCl_3$)

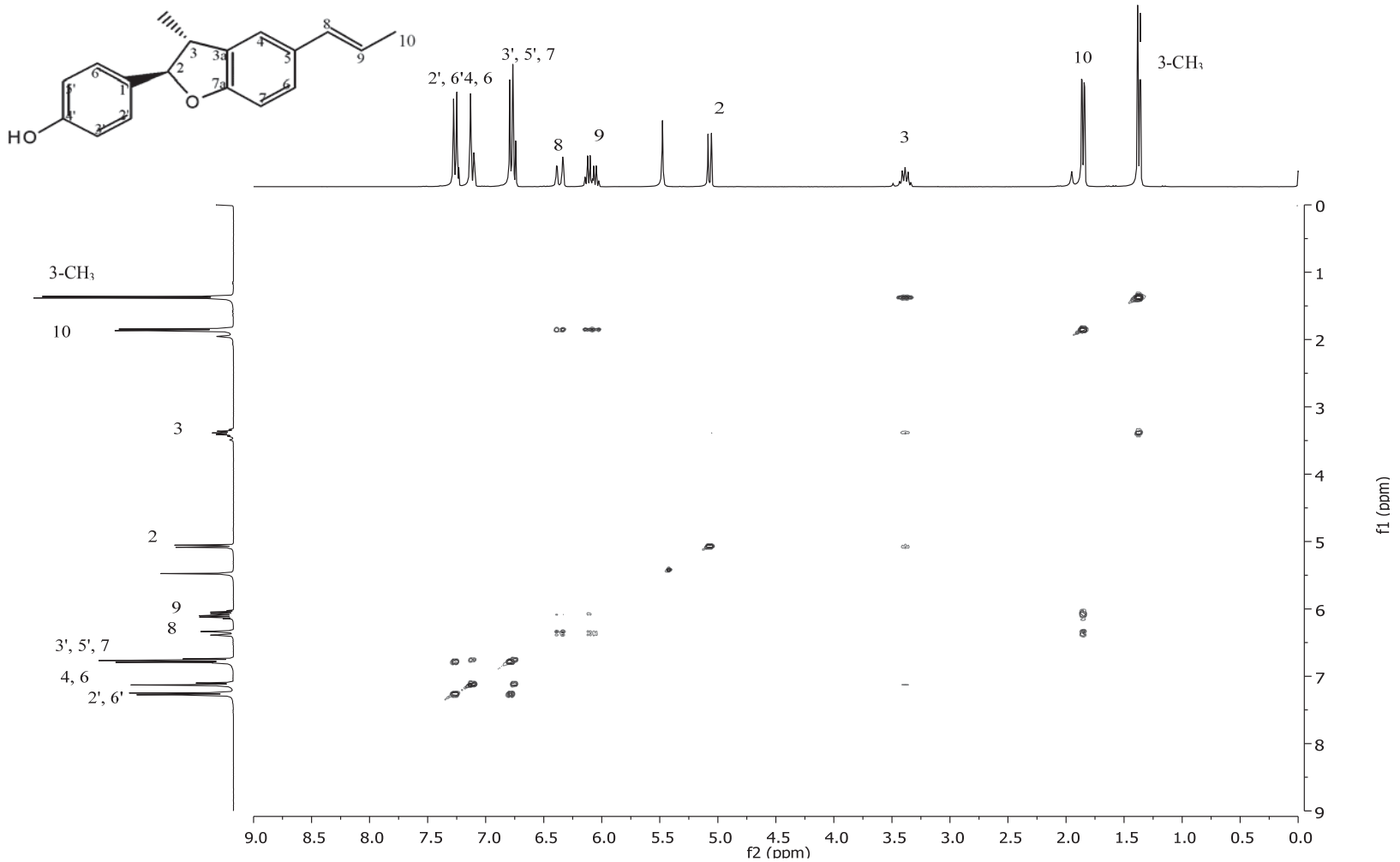

Figure 114 COSY Spectrum of compound MHL-3 (in $CDCl_3$)

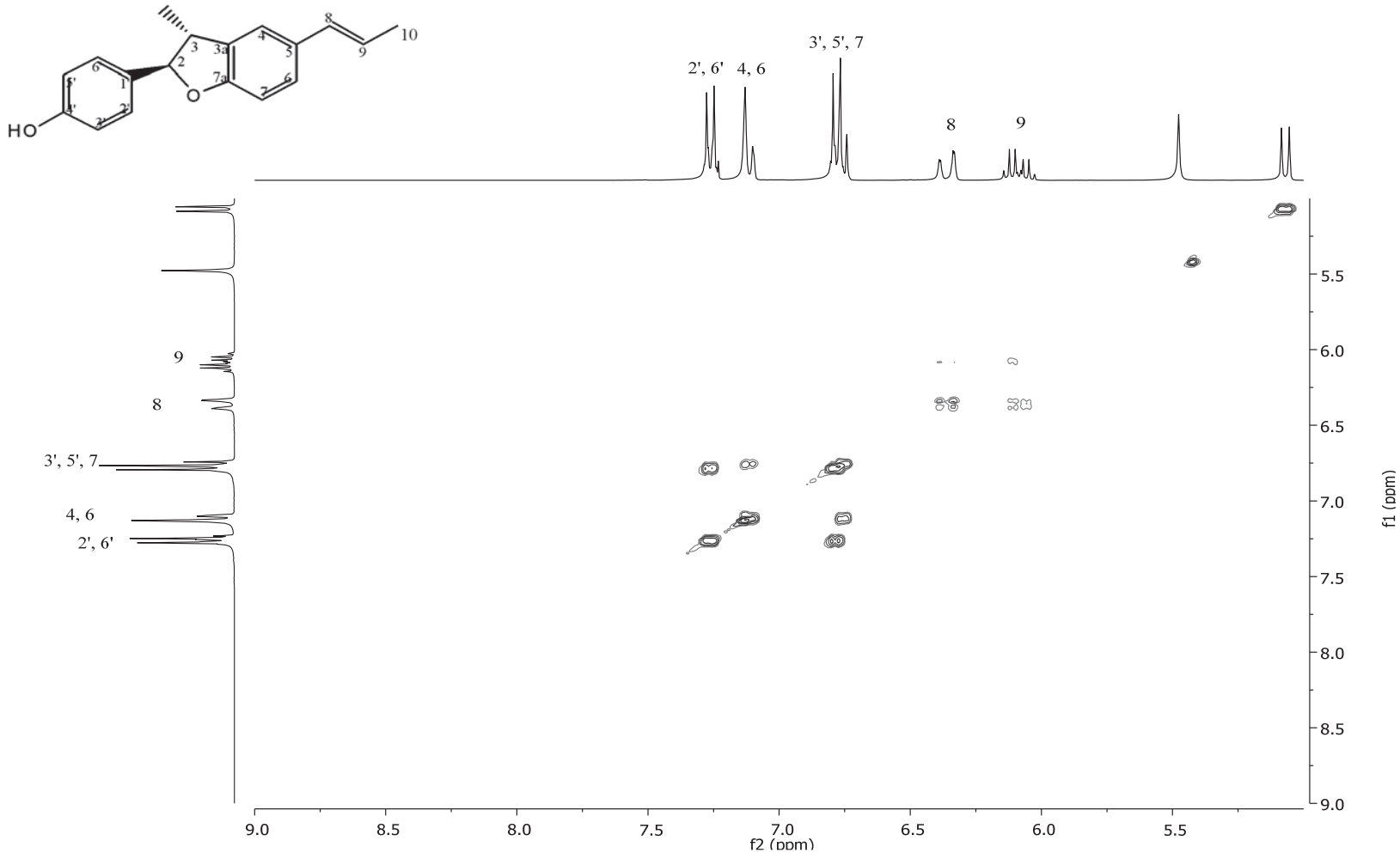

Figure 114 (Continued) COSY Spectrum of compound MHL-3 (in $CDCl_3$)

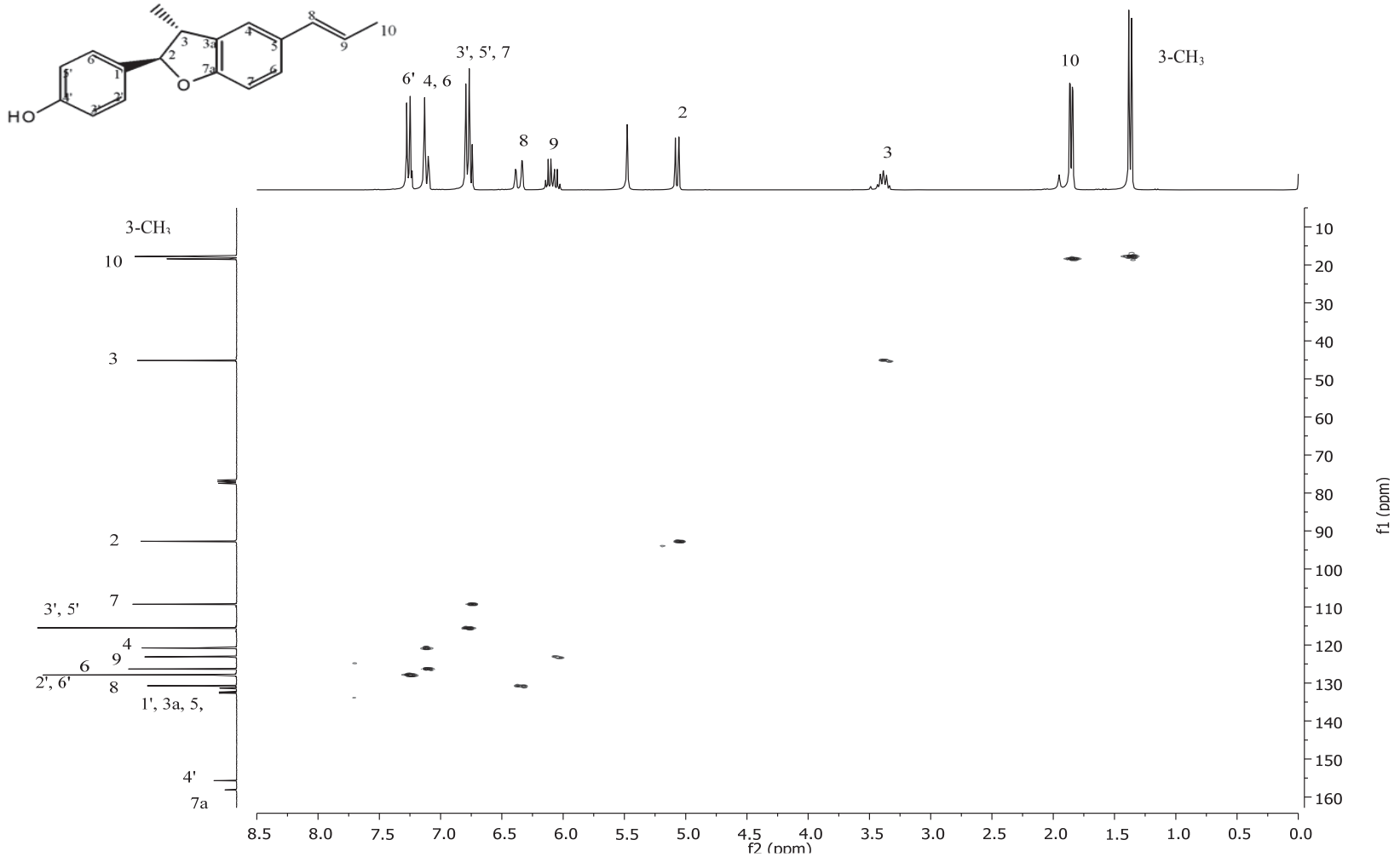

Figure 115 HMQC Spectrum of compound MHL-3 (in $CDCl_3$)

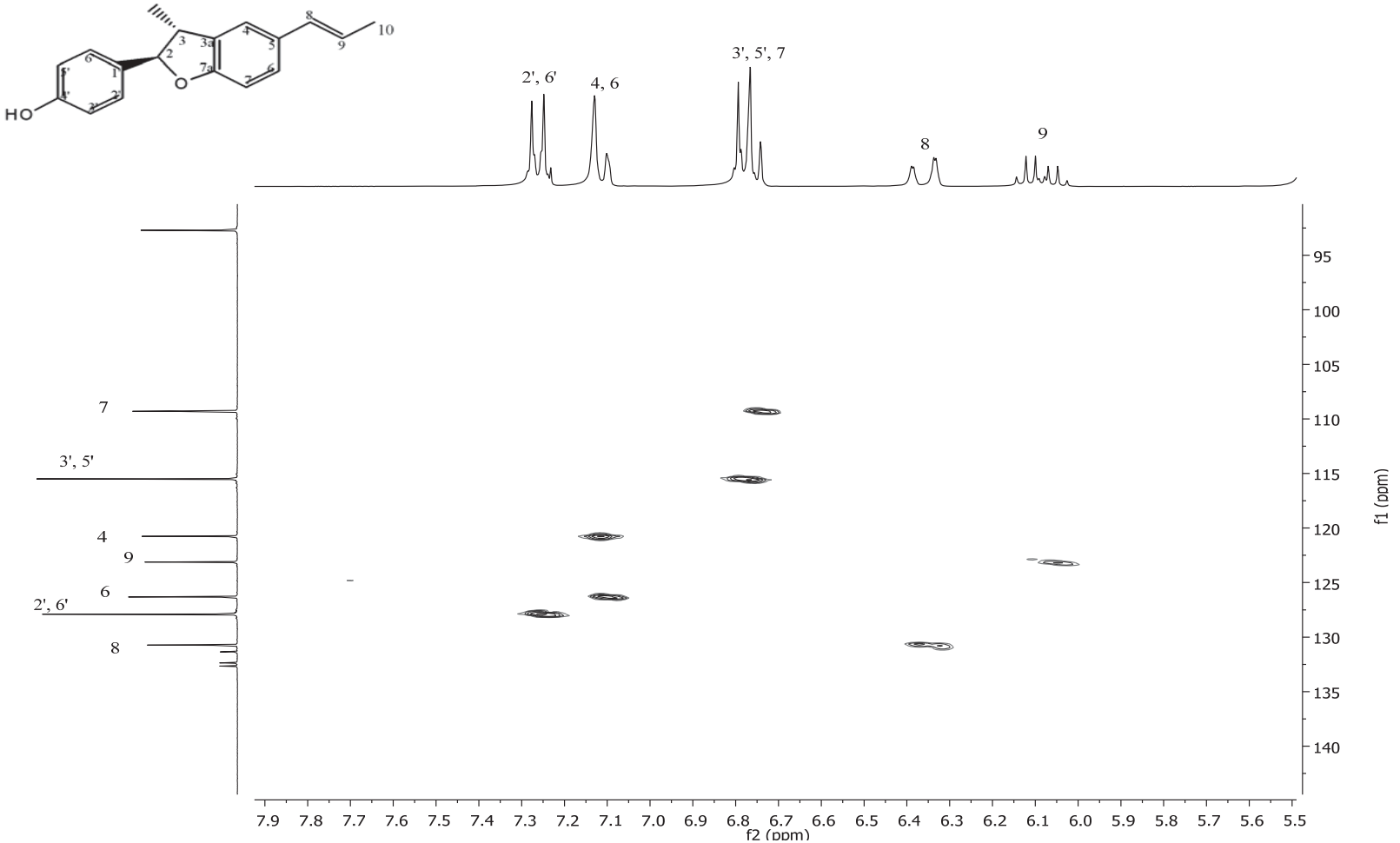

Figure 115 (Continued) HMQC Spectrum of compound MHL-3 (in $CDCl_3$)

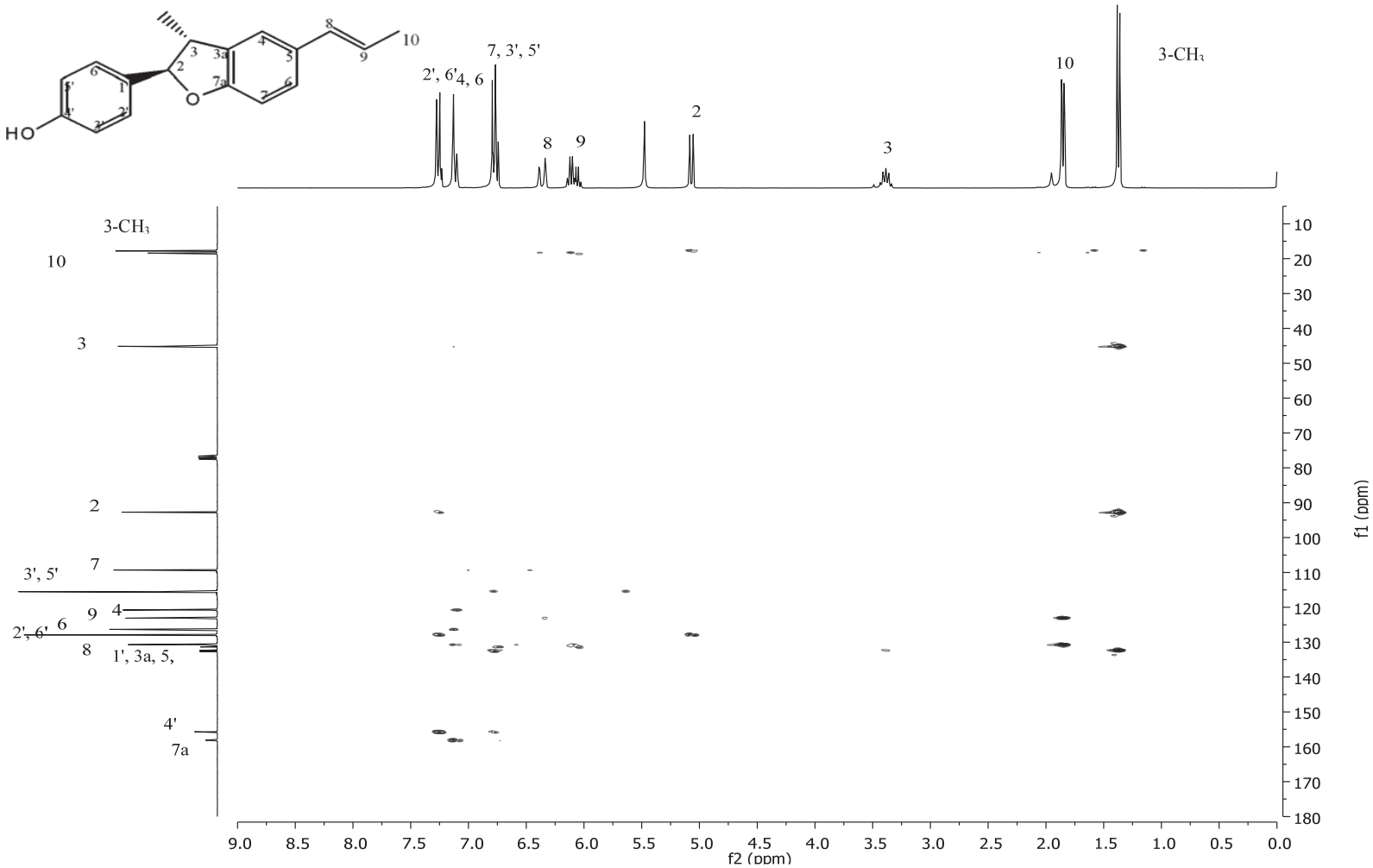

Figure 116 HMBC Spectrum of compound MHL-3 (in $CDCl_3$)

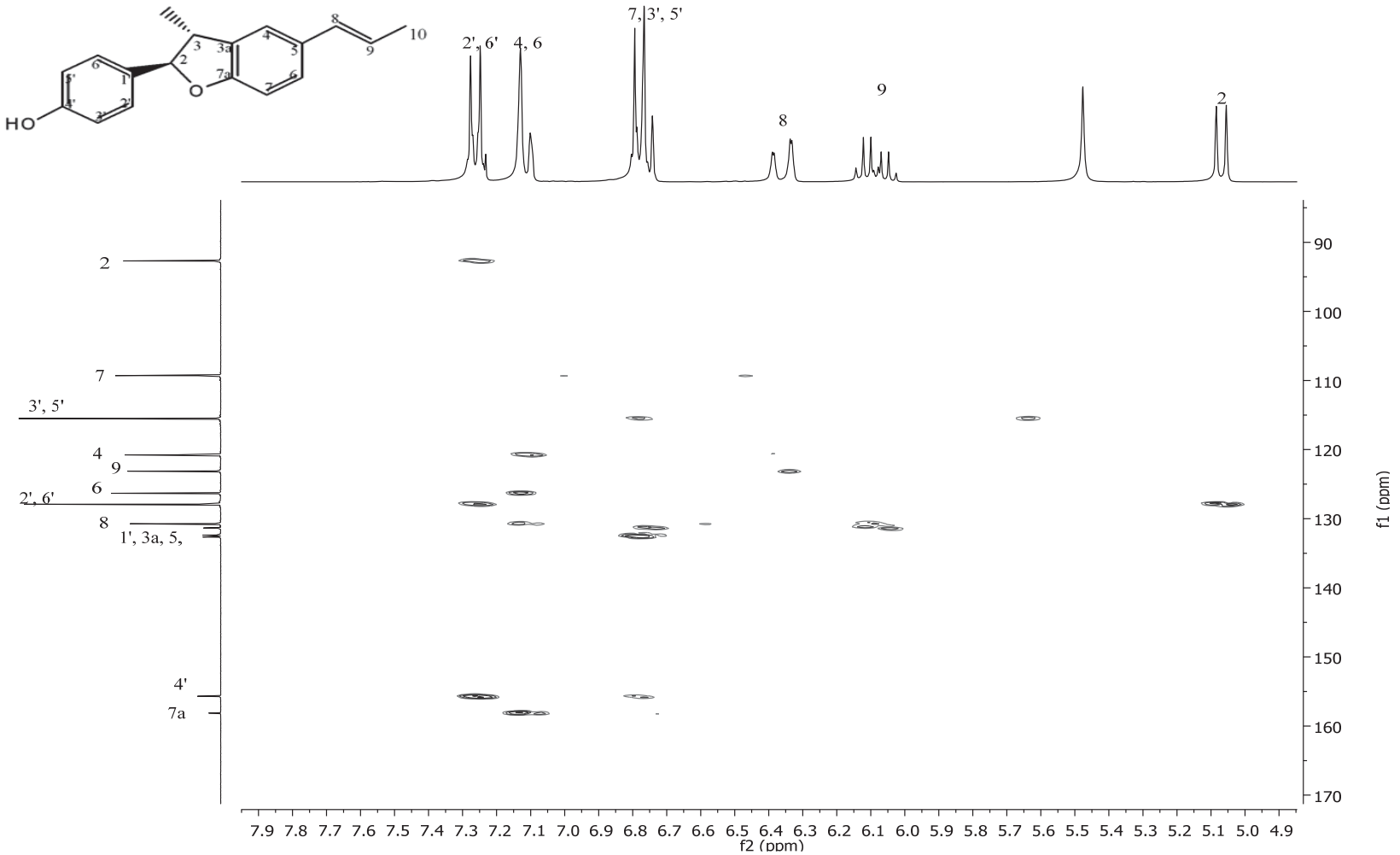

Figure 116 (Continued) HMBC Spectrum of compound MHL-3 (in $CDCl_3$)

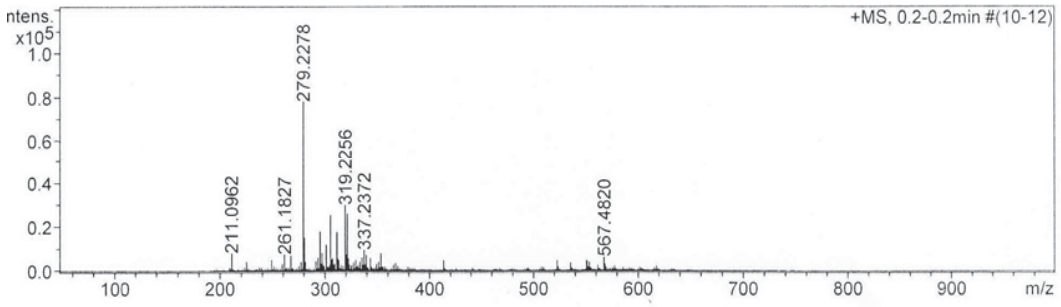

Figure 117 MS spectrum of compound MHL-4

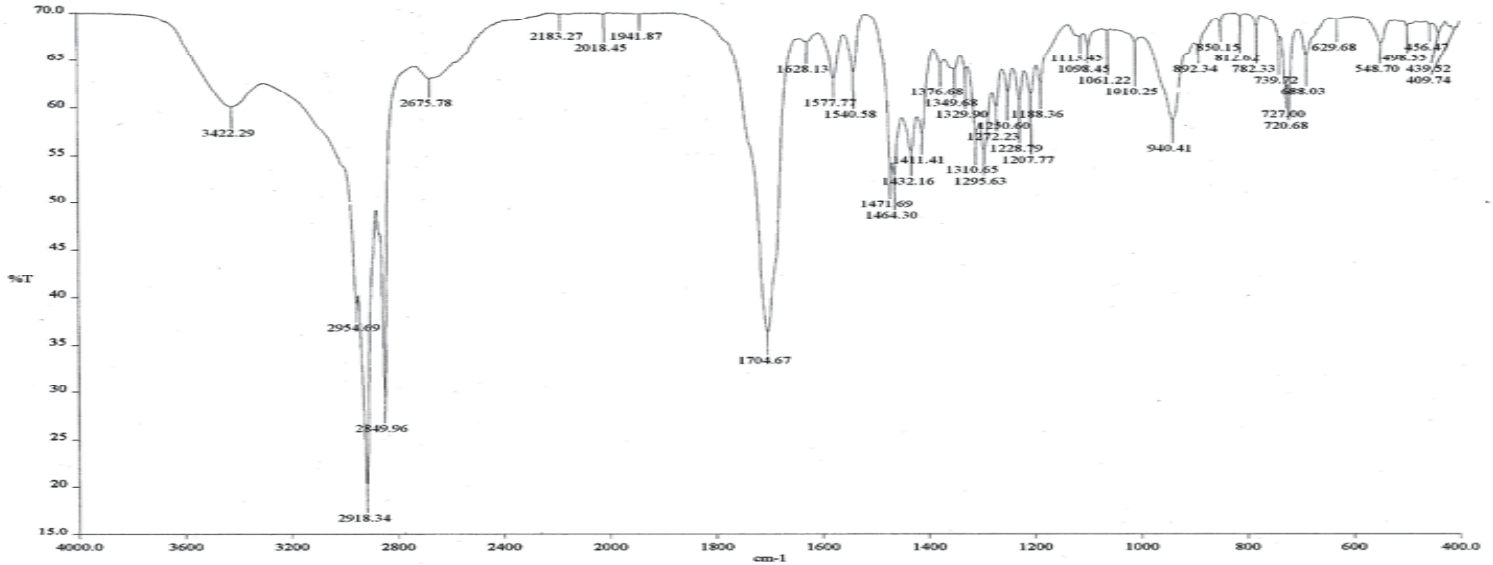

Figure 118 IR (KBr) spectrum of compound MHL-4

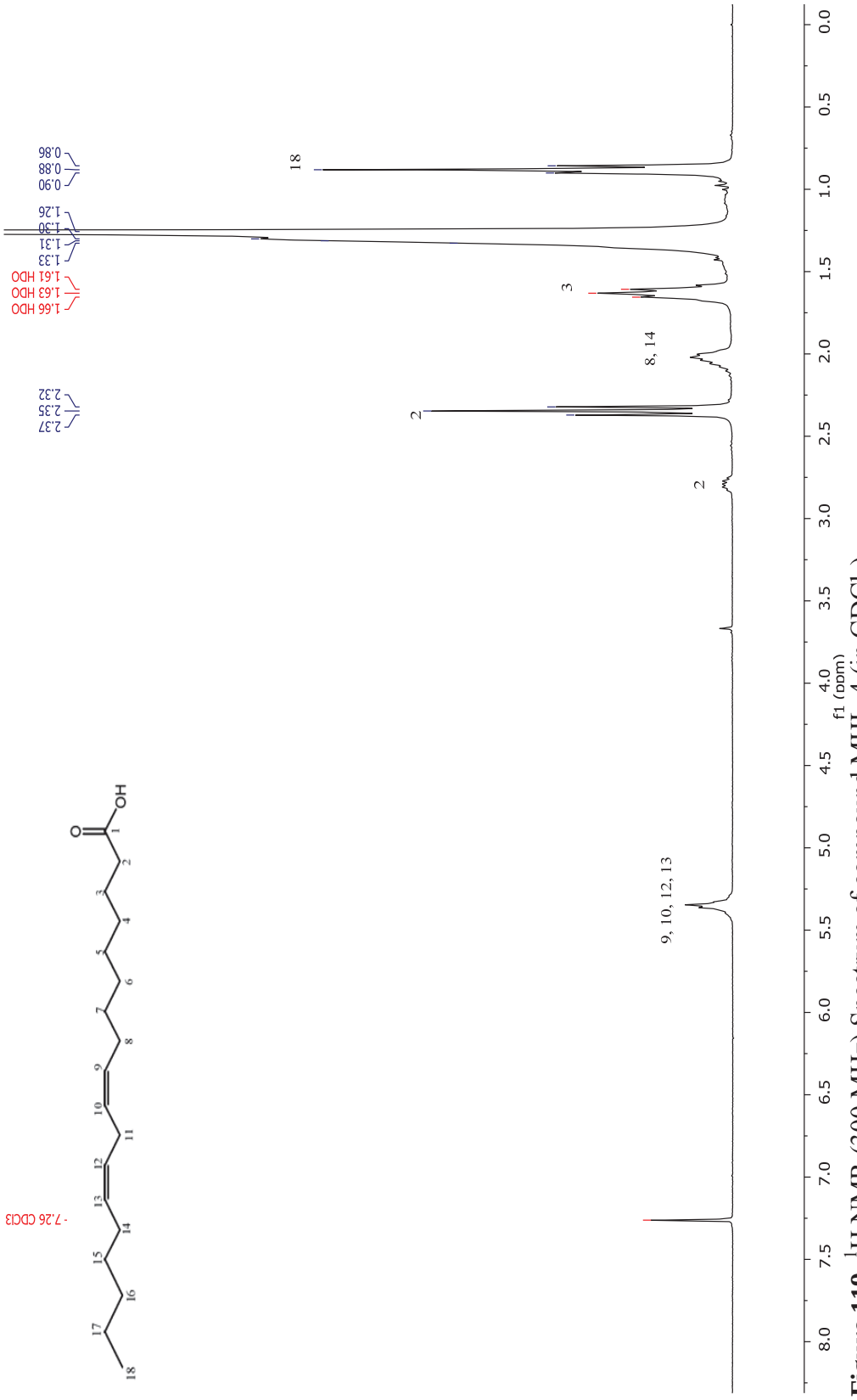

Figure 119 ^{1}H NMR (300 MHz) Spectrum of compound MHL-4 (in $CDCl_3$)

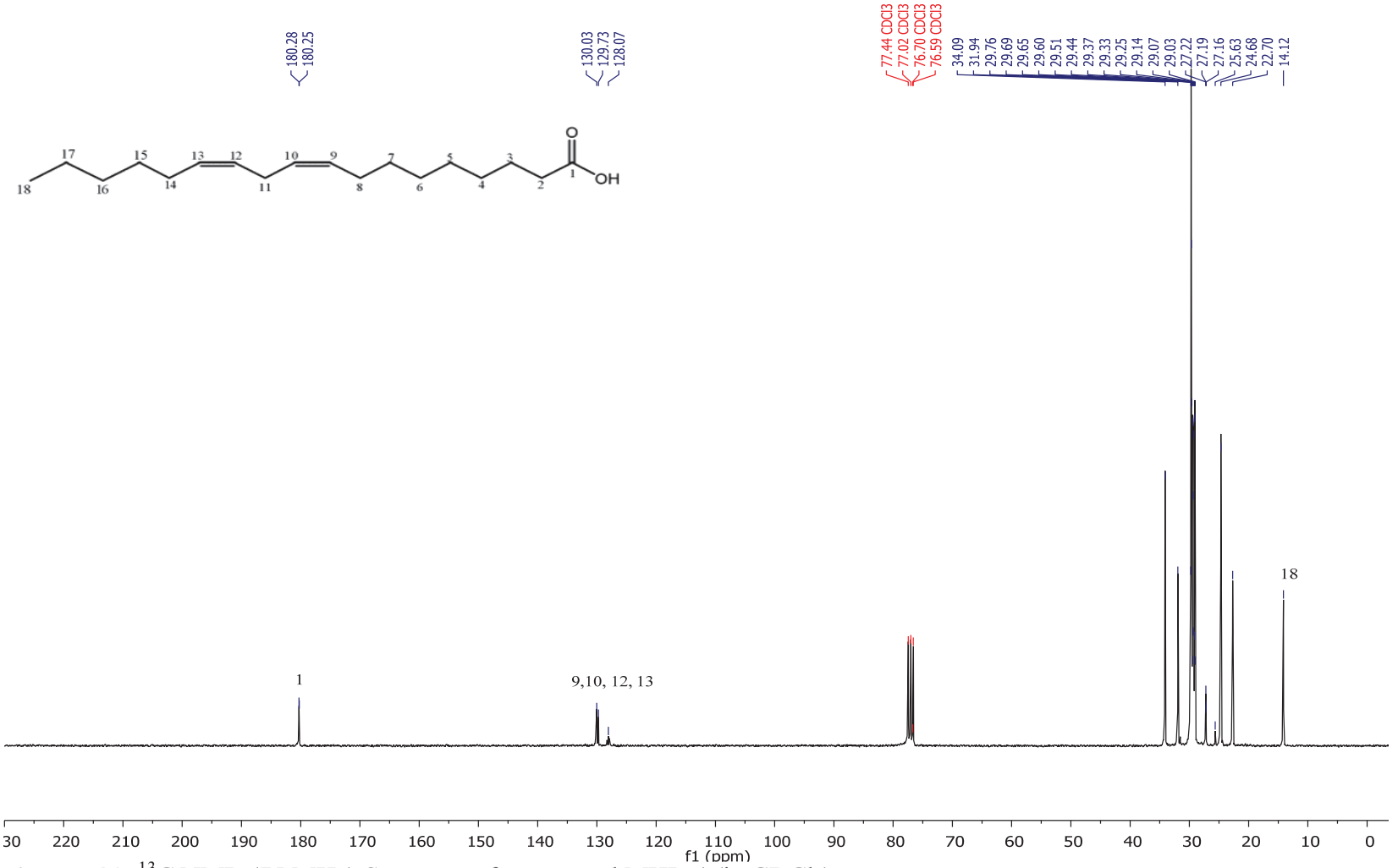

Figure 120 ^{13}C NMR (75 MHz) Spectrum of compound MHL-4 (in $CDCl_3$)

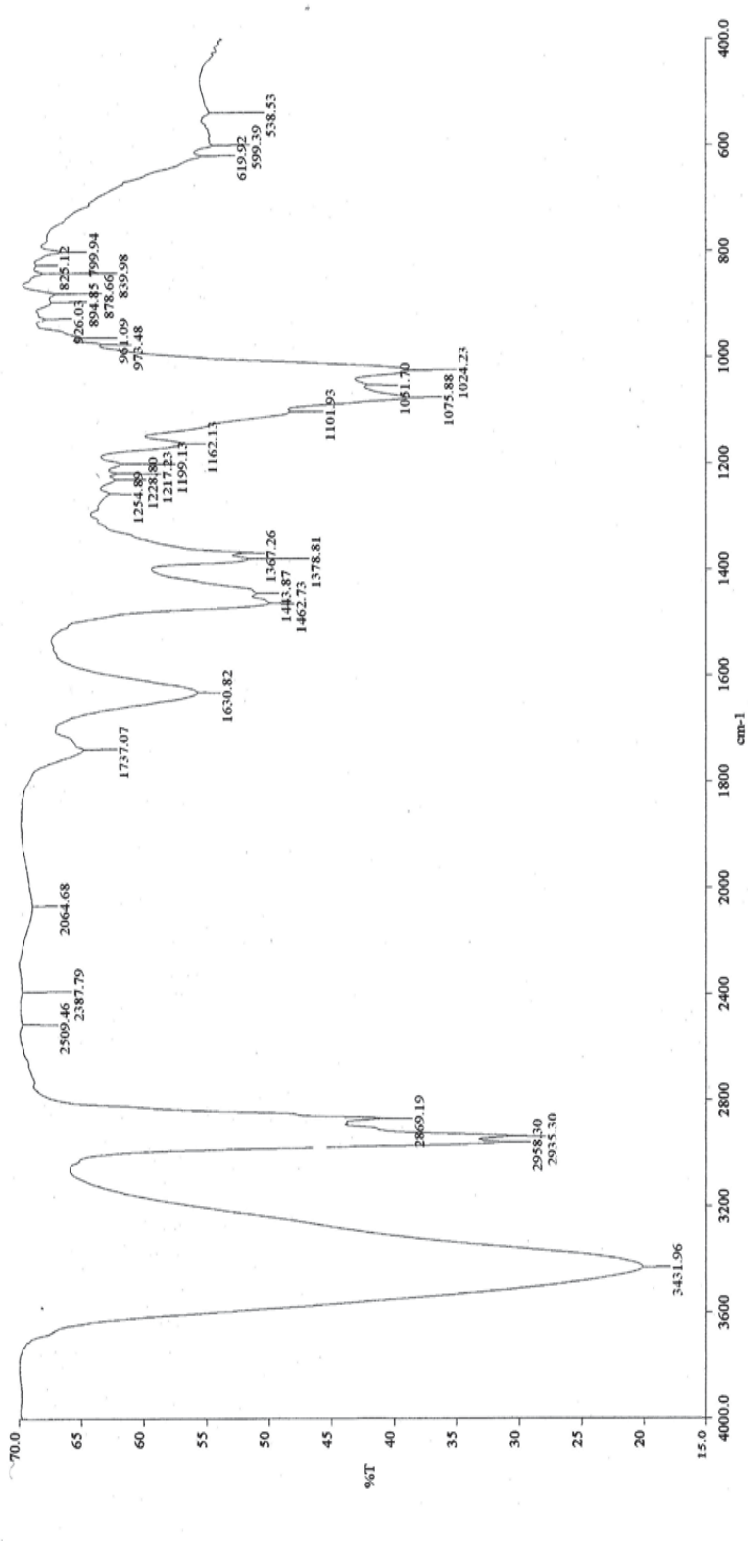

Figure 121 IR (KBr) spectrum of compound MEL-1

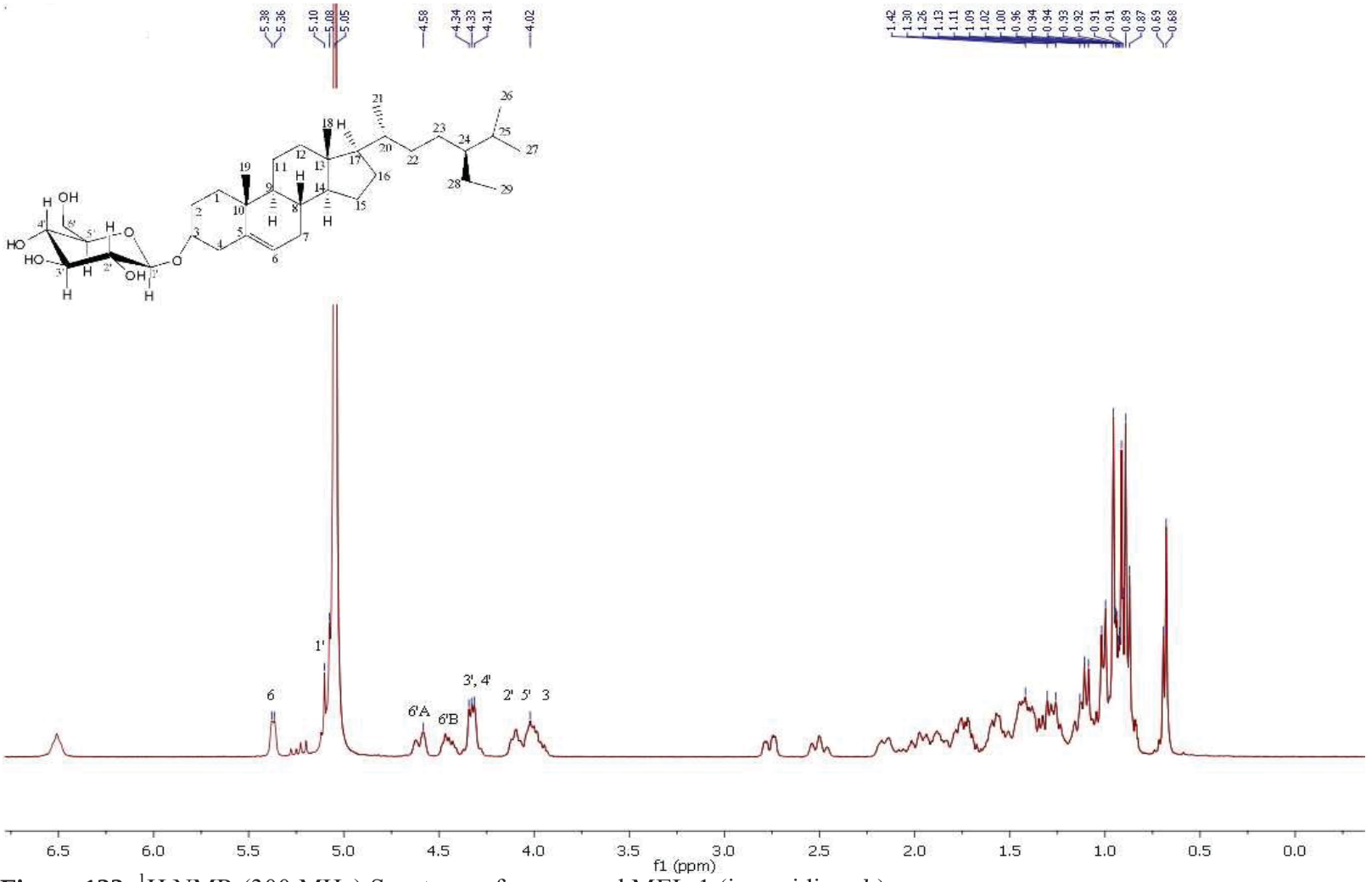

Figure 122 ^{1}H NMR (300 MHz) Spectrum of compound MEL-1 (in pyridine-d_5)

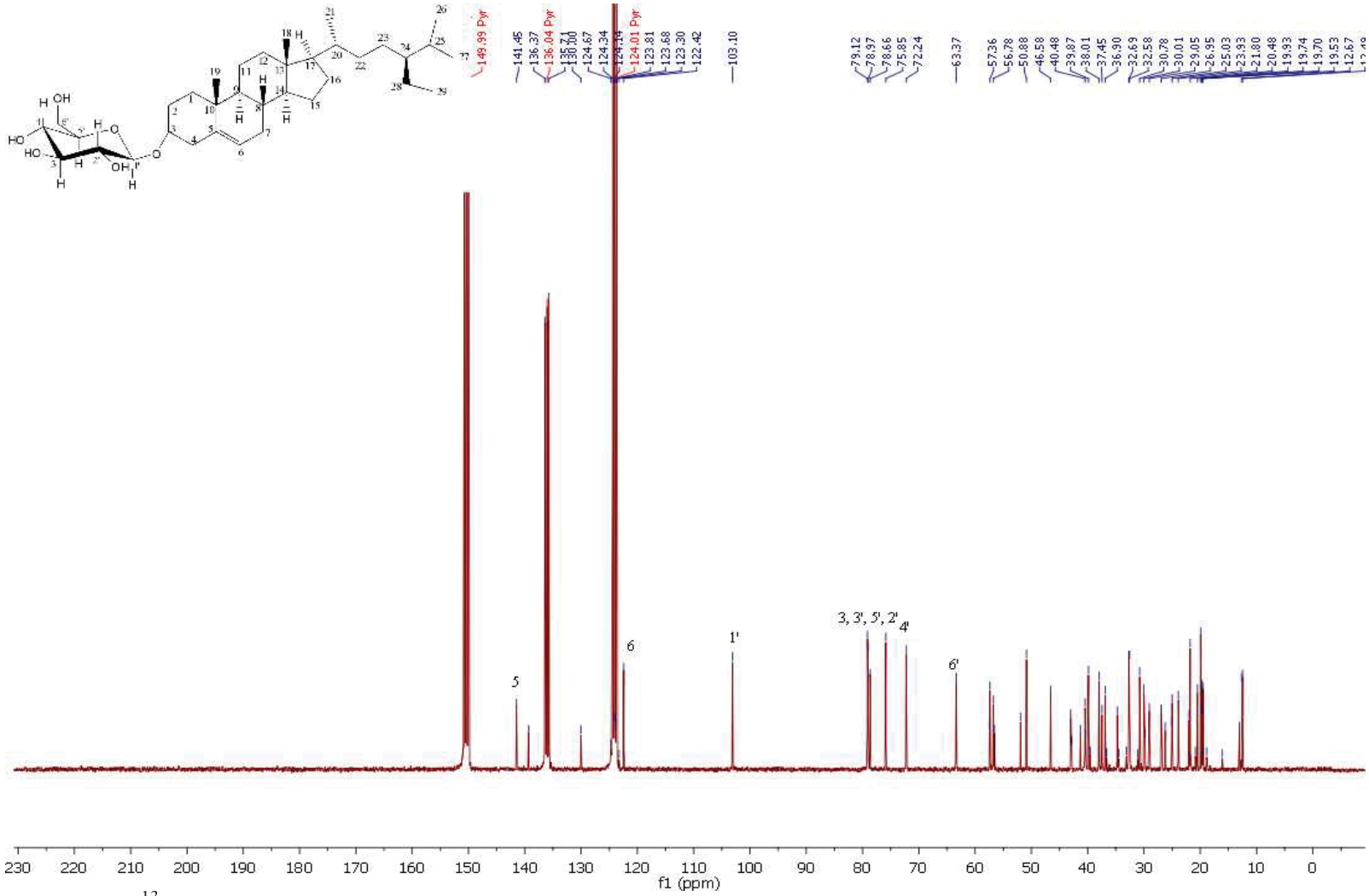

Figure 123 ^{13}C NMR (75 MHz) Spectrum of compound MEL-1 (in pyridine-d_5)

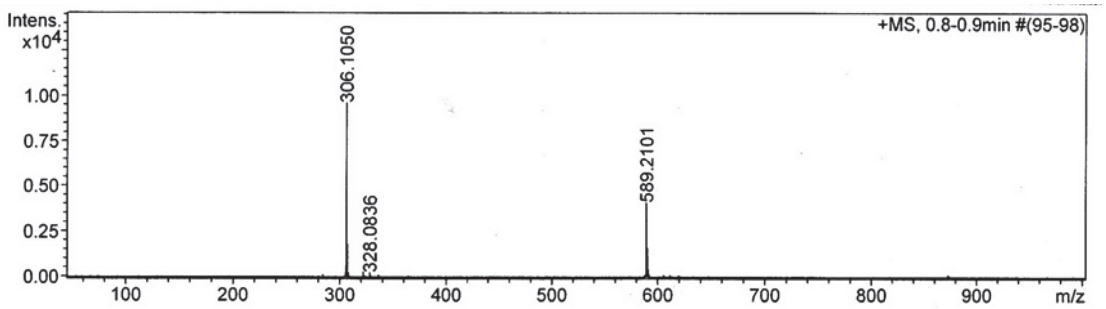

Figure 124 MS spectrum of compound MET-1

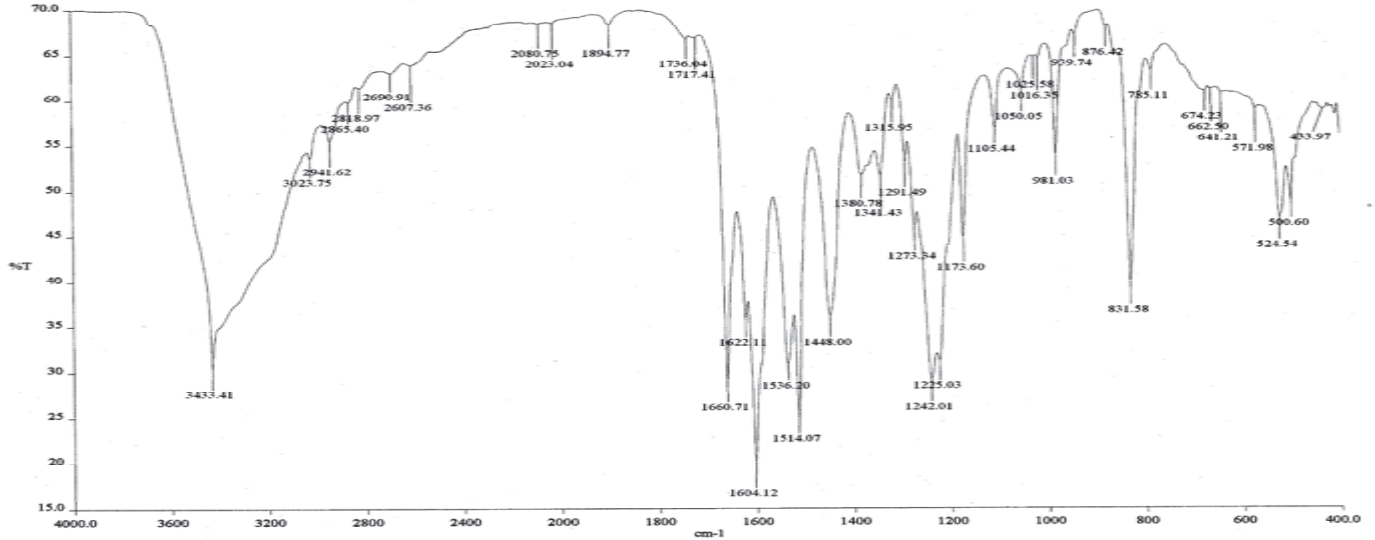

Figure 125 IR (KBr) spectrum of compound MET-1

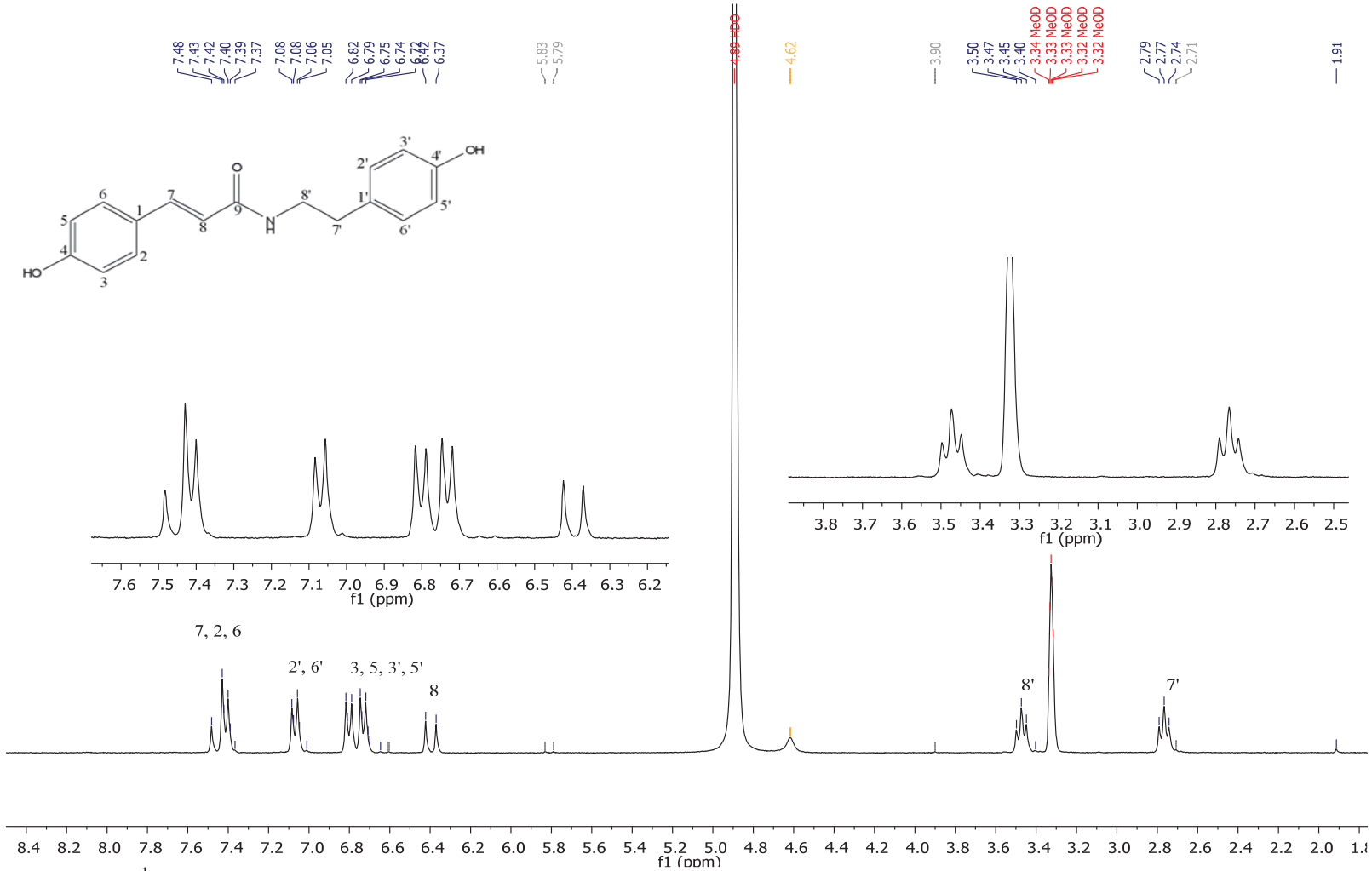

Figure 126 ^{1}H NMR (300 MHz) Spectrum of compound MET-1 (in CD_3OD)

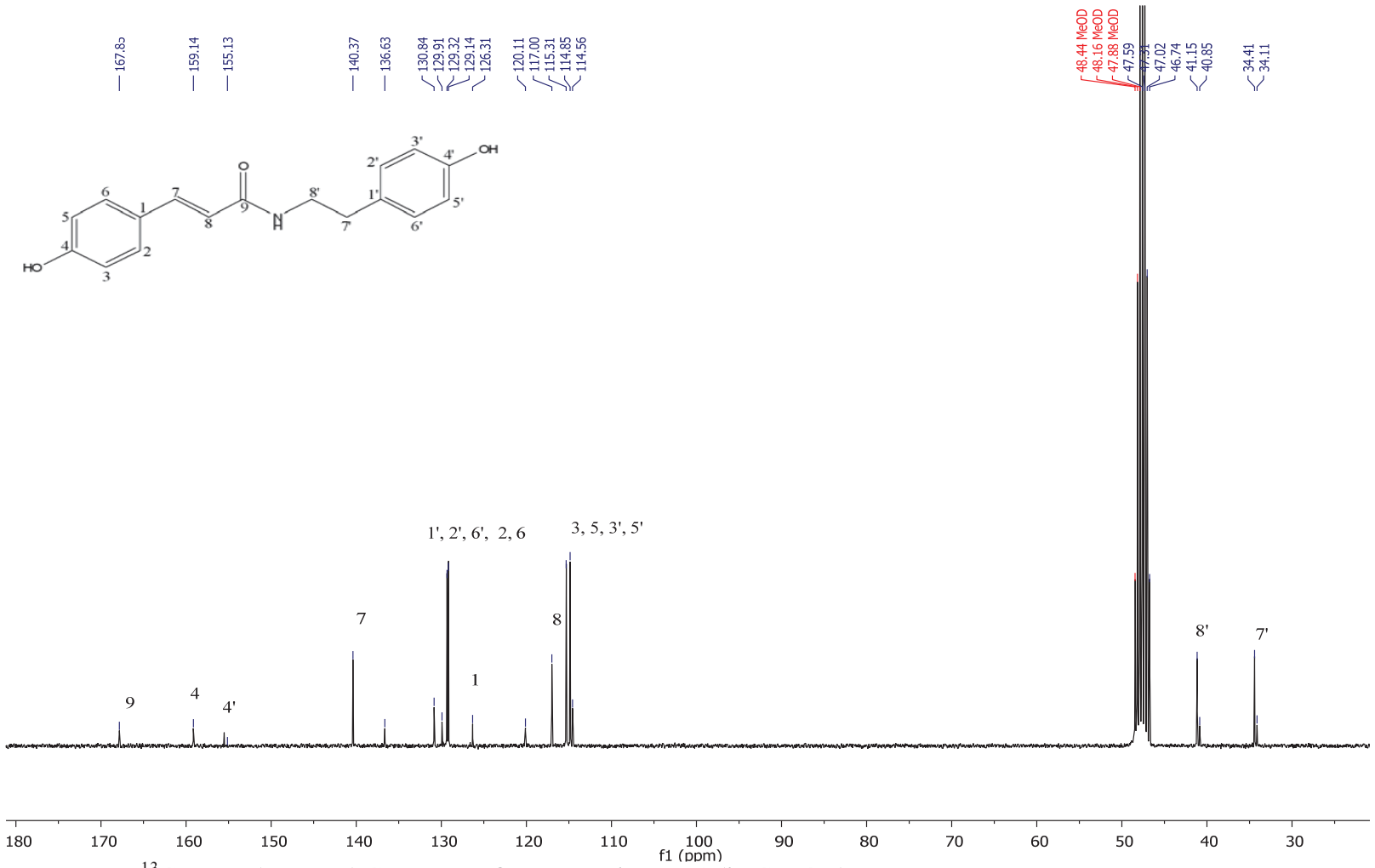

Figure 127 ^{13}C NMR (75 MHz) Spectrum of compound MET-1 (in CD_3OD)

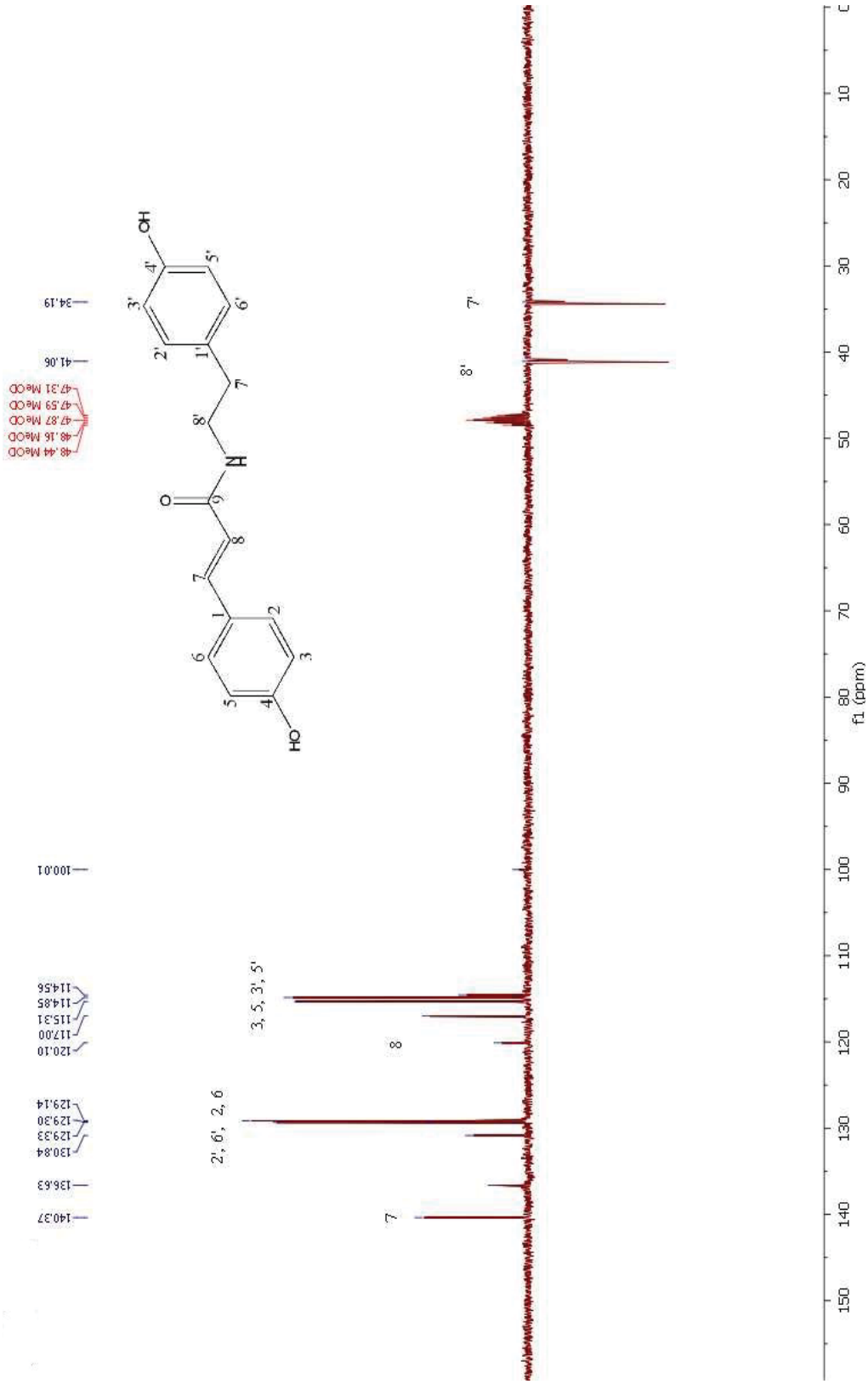

Figure 128 DEPT Spectrum of compound MET-1 (in CD_3OD)

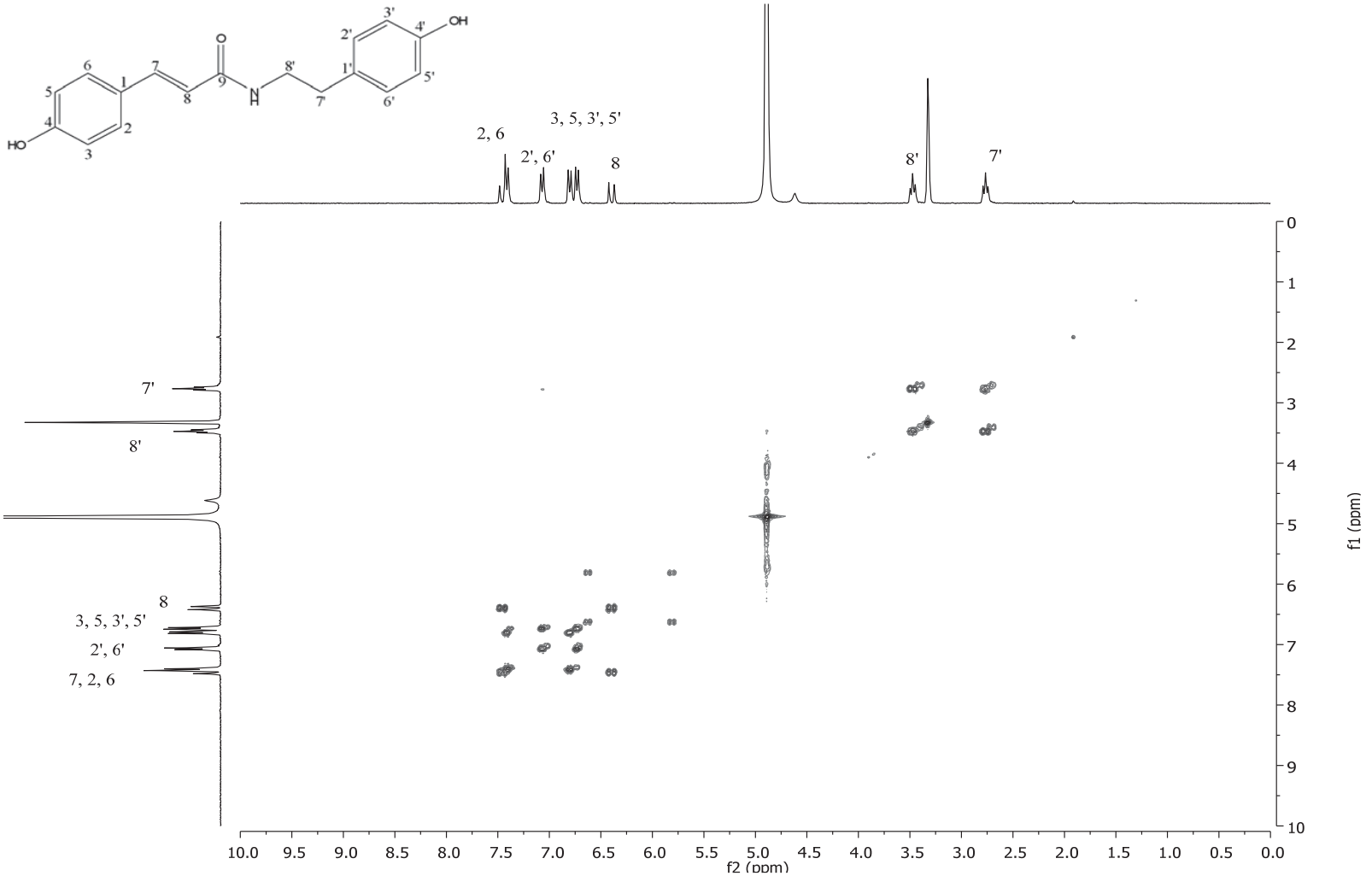

Figure 129 COSY Spectrum of compound MET-1 (in CD_3OD)

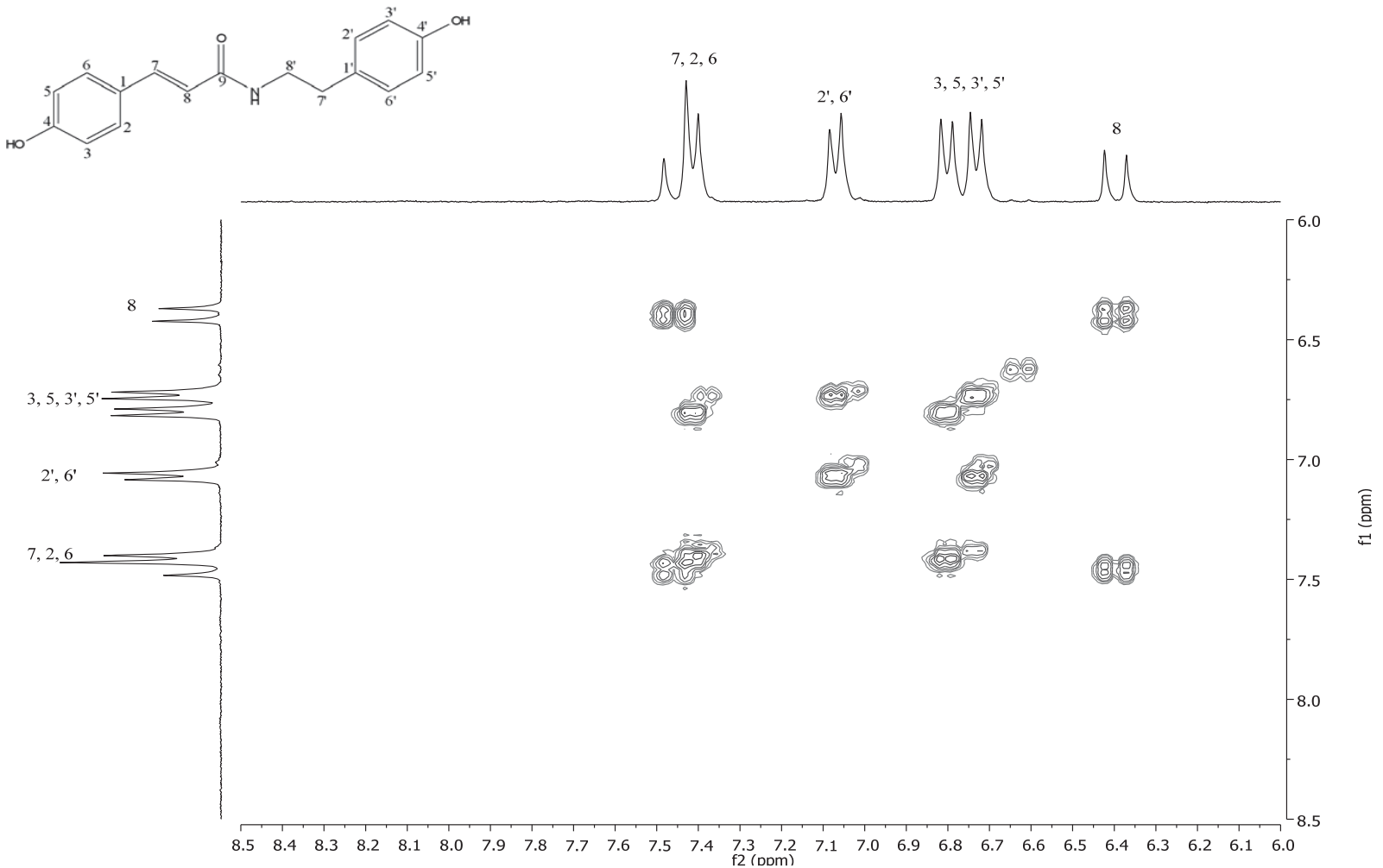

Figure 129 (Continued) COSY Spectrum of compound MET-1 (in CD_3OD)

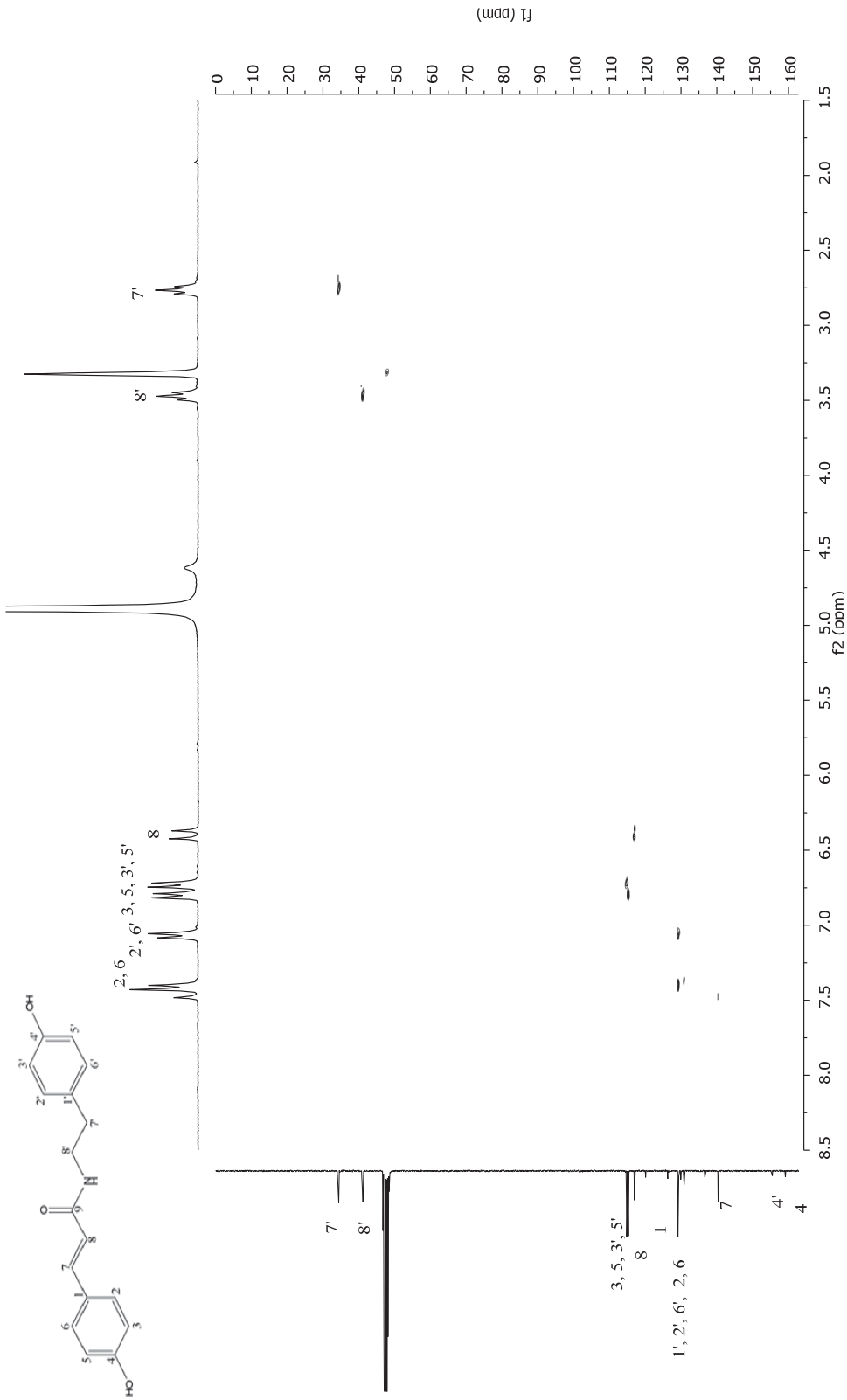

Figure 130 HMQC Spectrum of compound MET-1 (in CD_3OD)

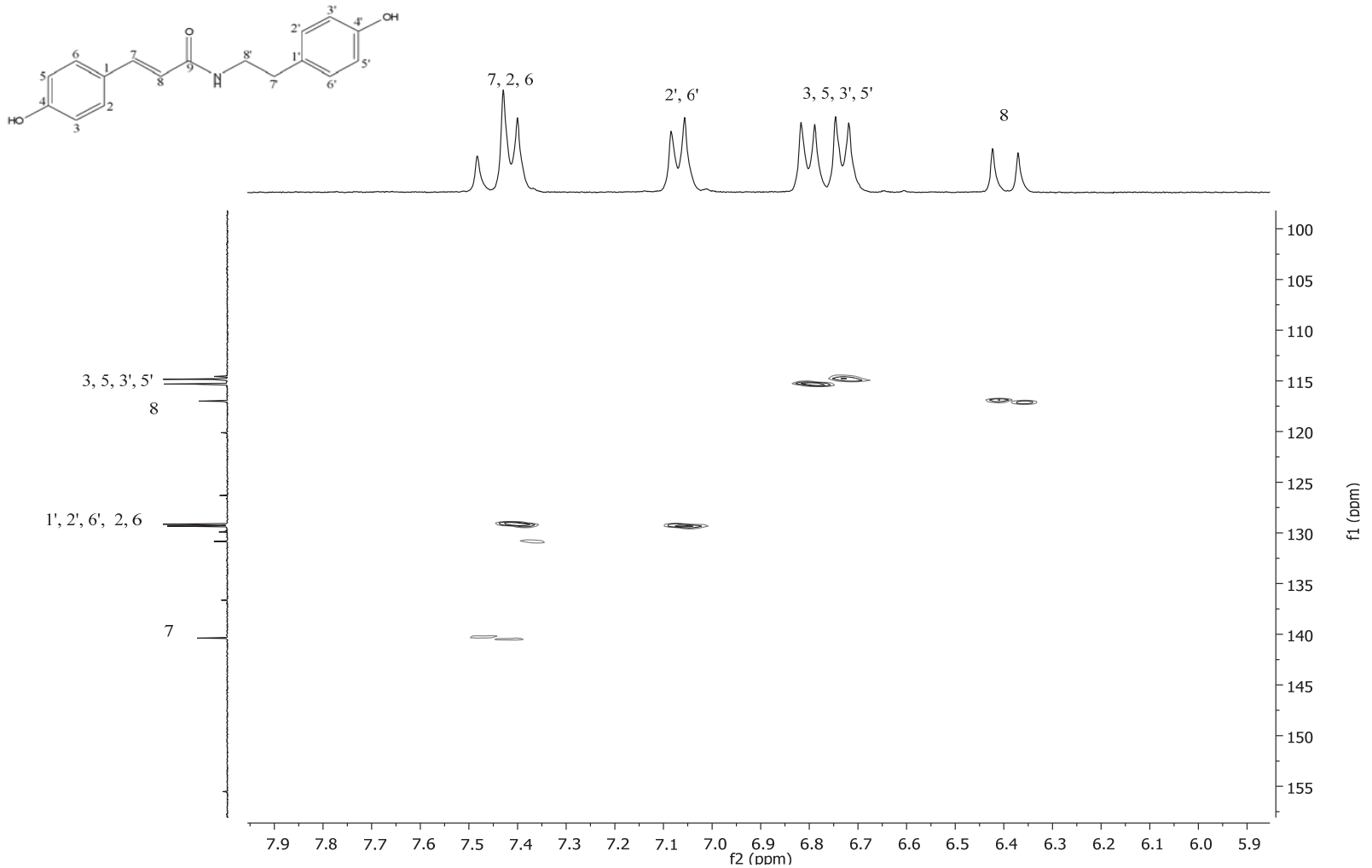

Figure 130 (Continued) HMQC Spectrum of compound MET-1 (in CD_3OD)

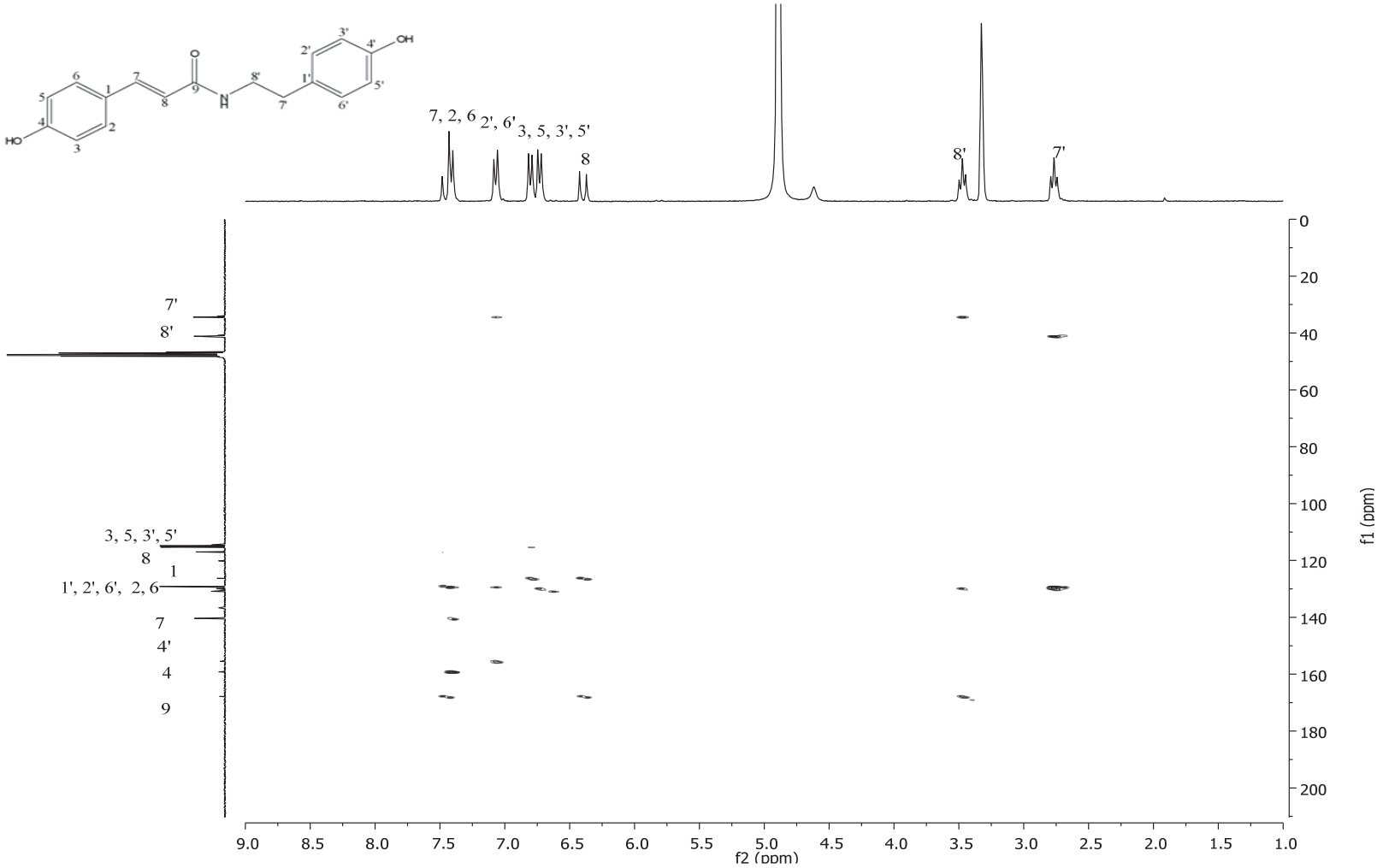

Figure 131 HMBC Spectrum of compound MET-1 (in CD_3OD)

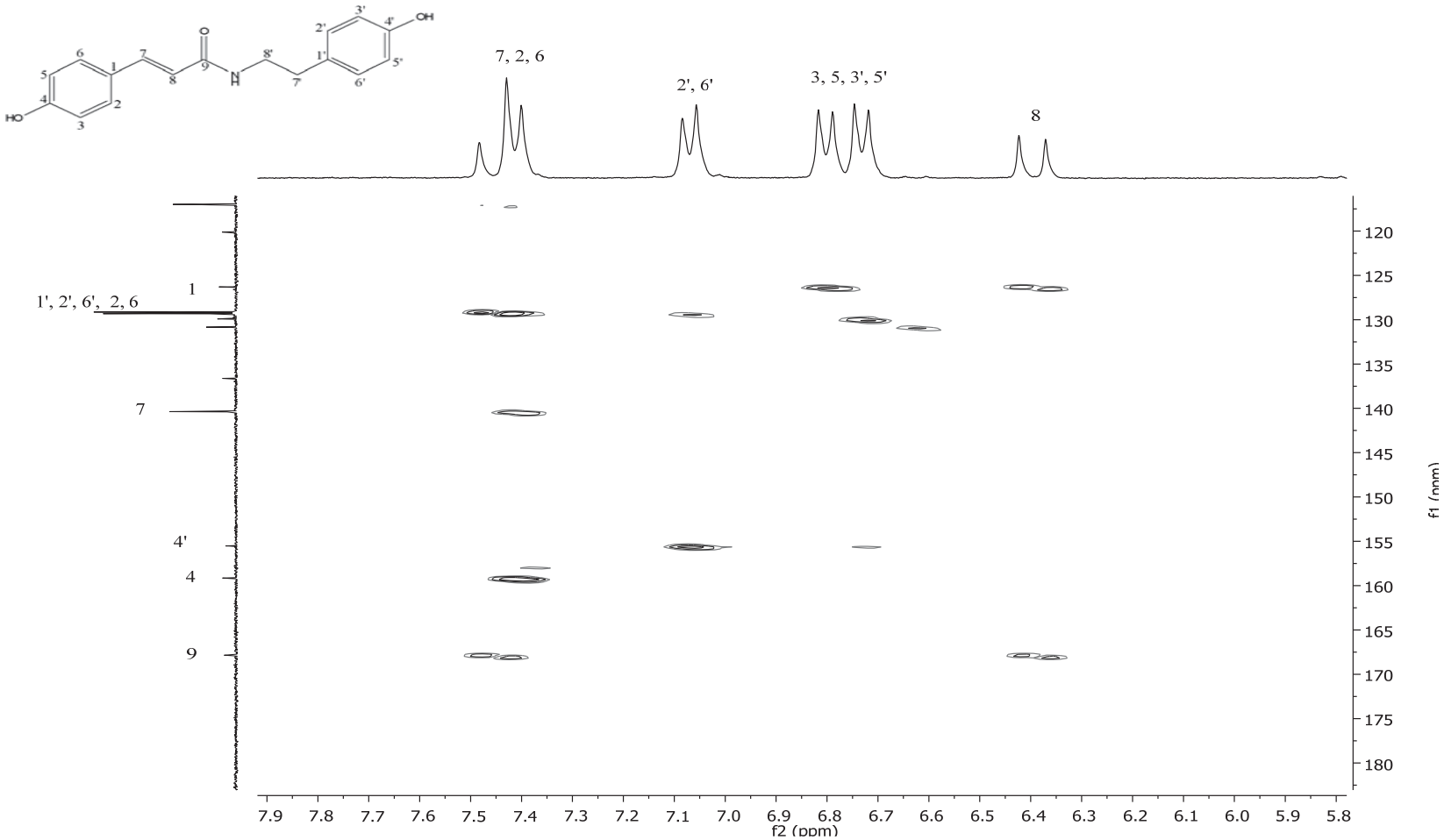

Figure 131 (Continued) HMBC Spectrum of compound MET-1 (in CD_3OD)

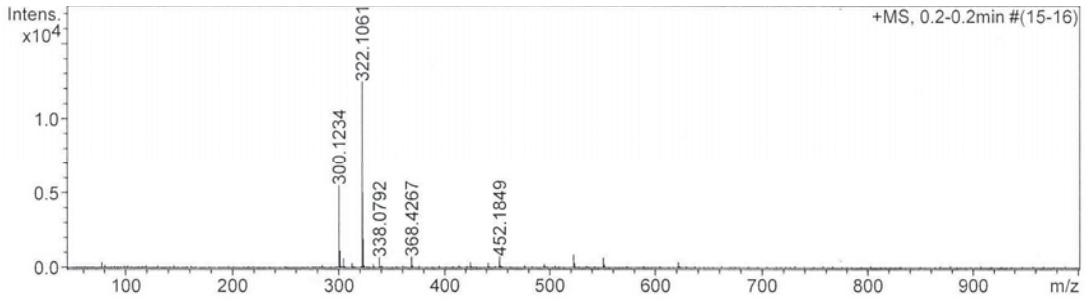

Figure 132 MS spectrum of compound MET-2

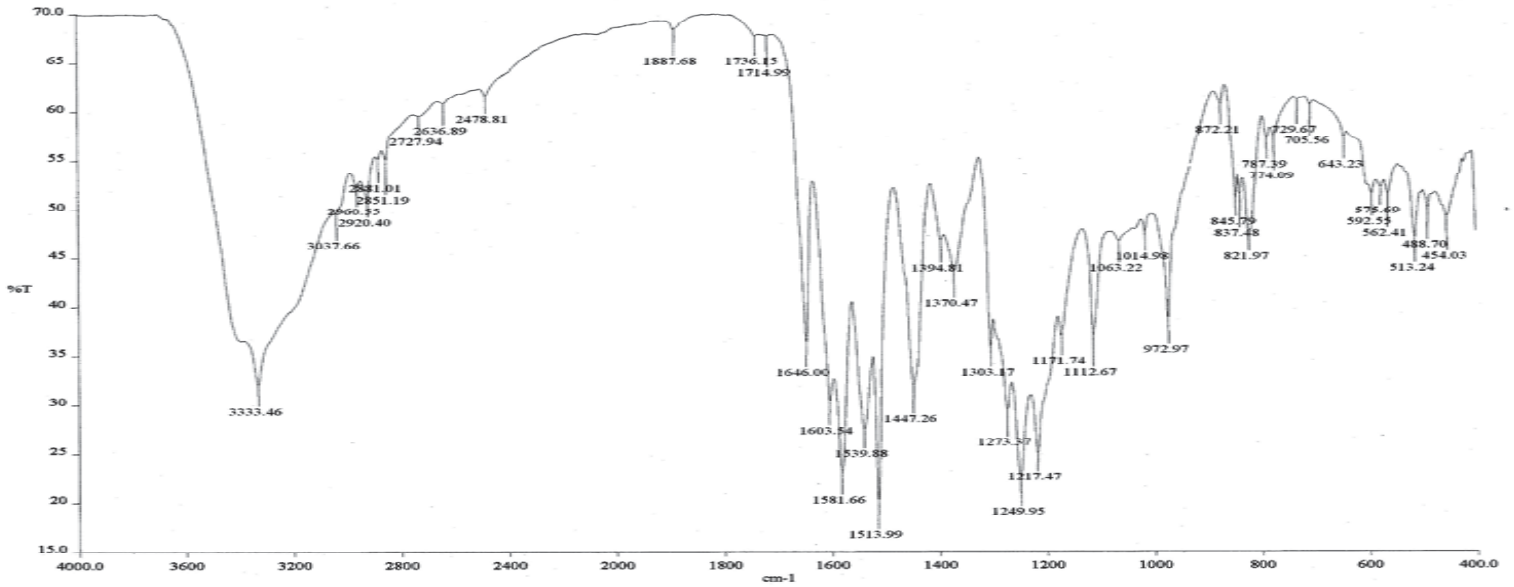

Figure 133 IR (KBr) spectrum of compound MET-2

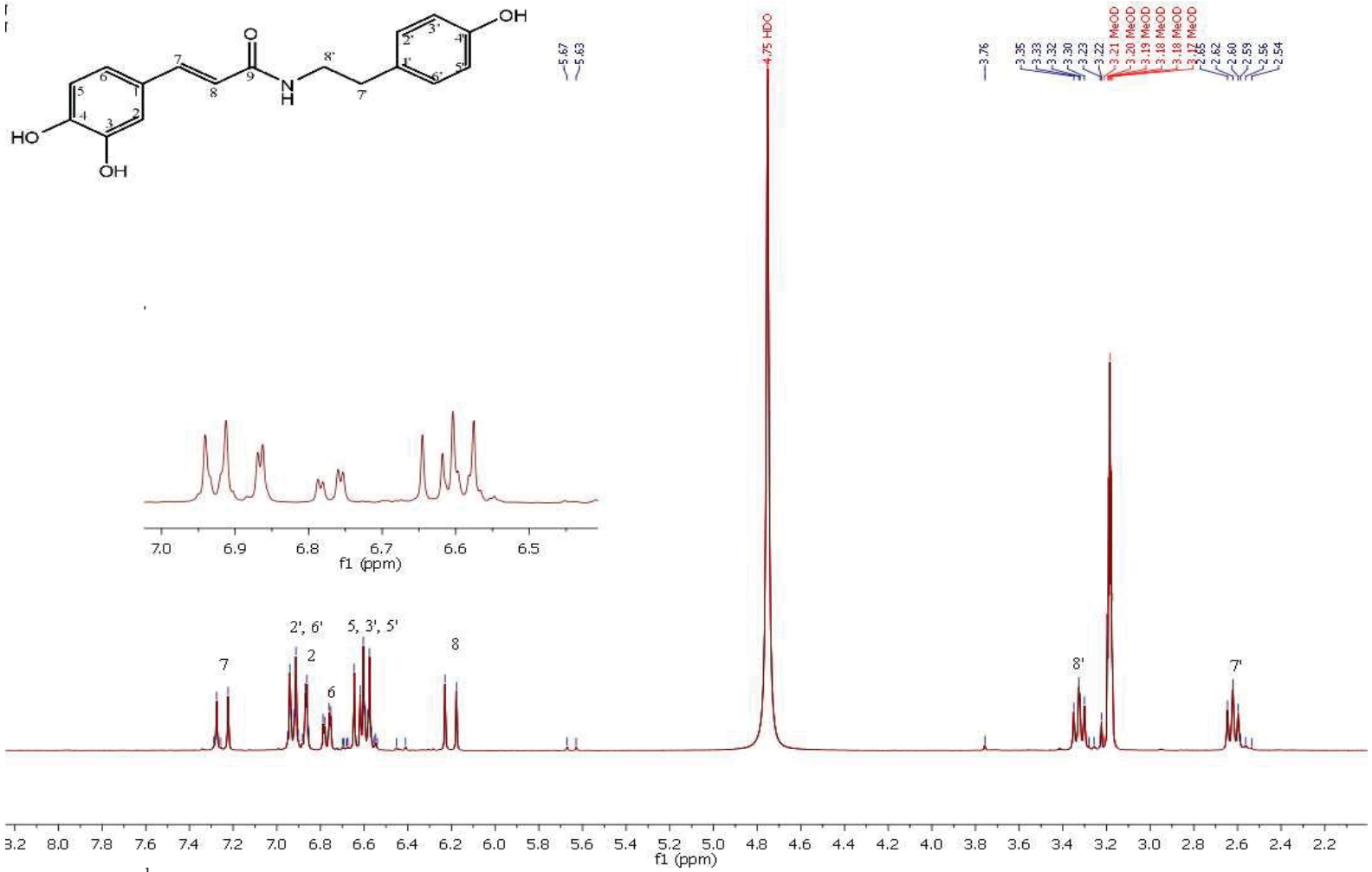

Figure 134 ^{1}H NMR (300 MHz) Spectrum of compound MET-2 (in CD_3OD)

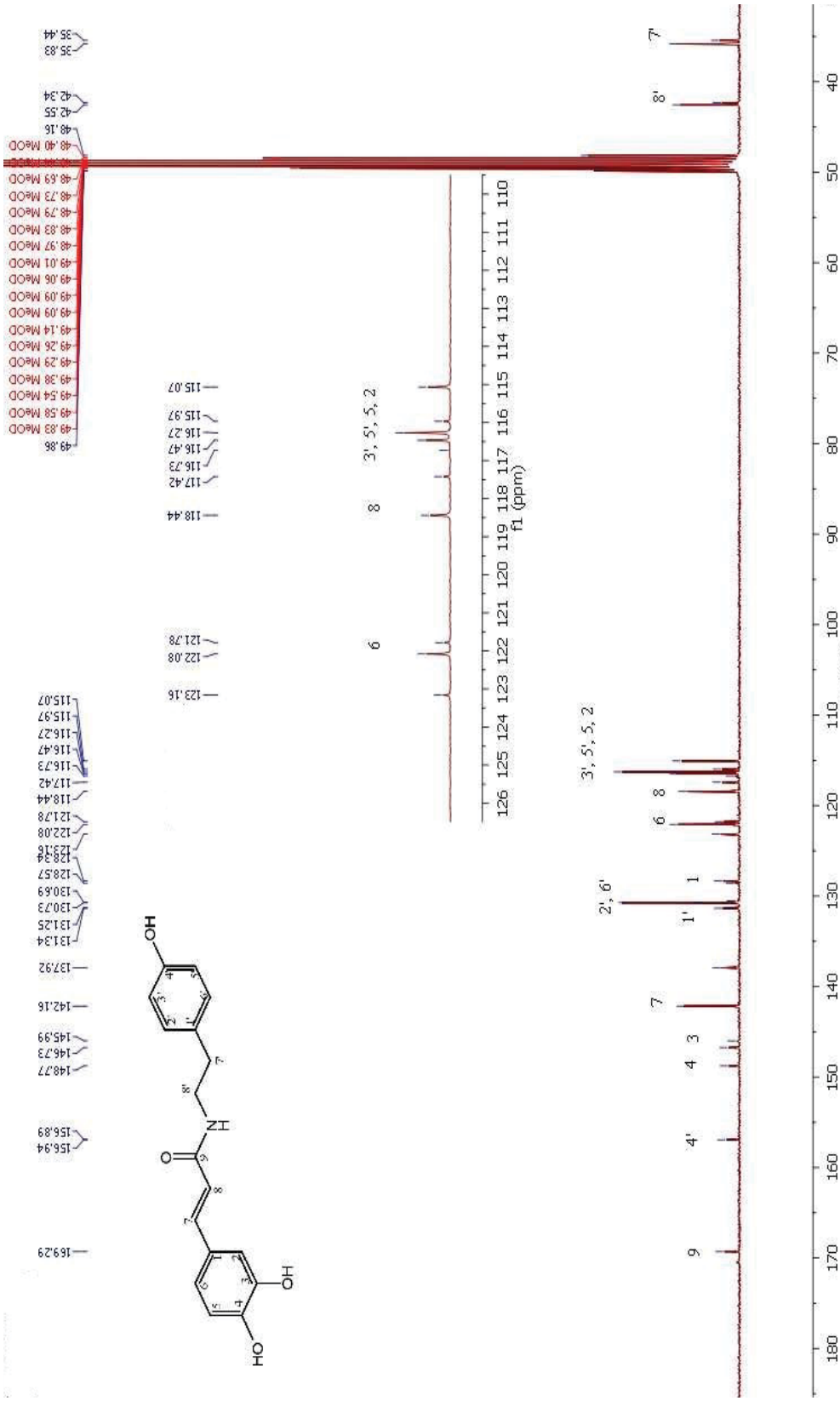

Figure 135 ^{13}C NMR (75 MHz) Spectrum of compound MET-2 (in CD_3OD)

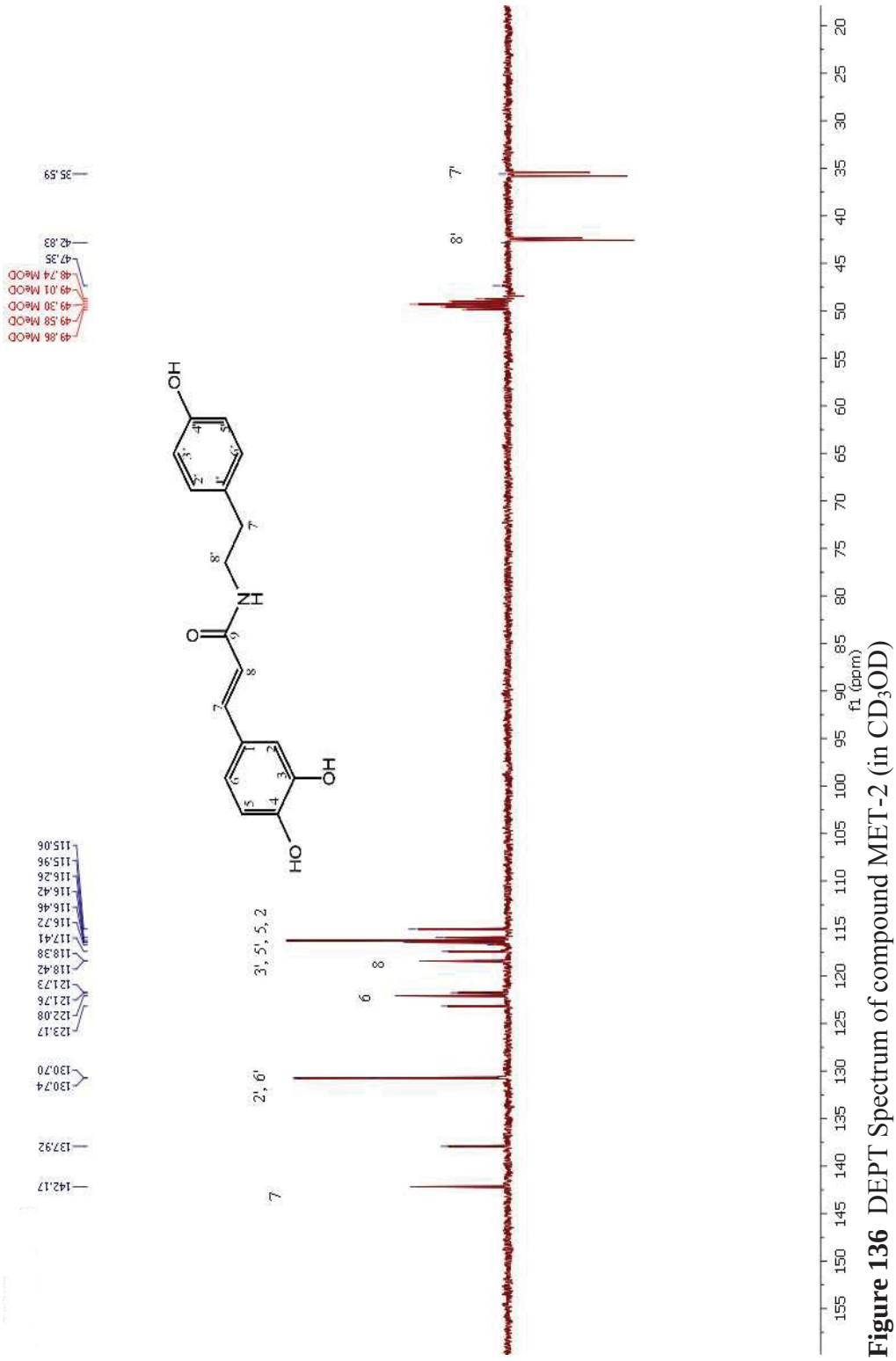

Figure 136 DEPT Spectrum of compound MET-2 (in CD_3OD)

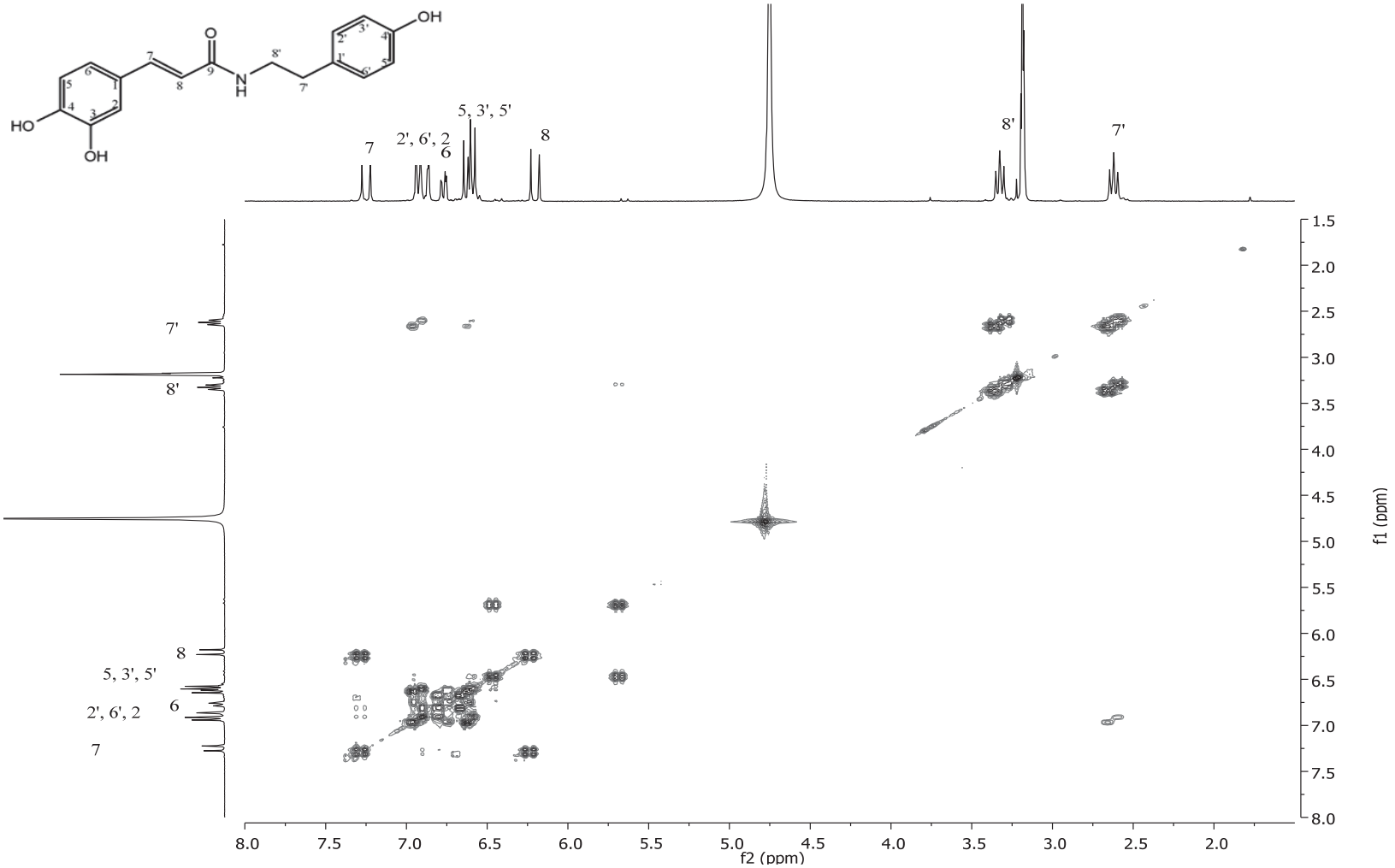

Figure 137 COSY Spectrum of compound MET-2 (in CD_3OD)

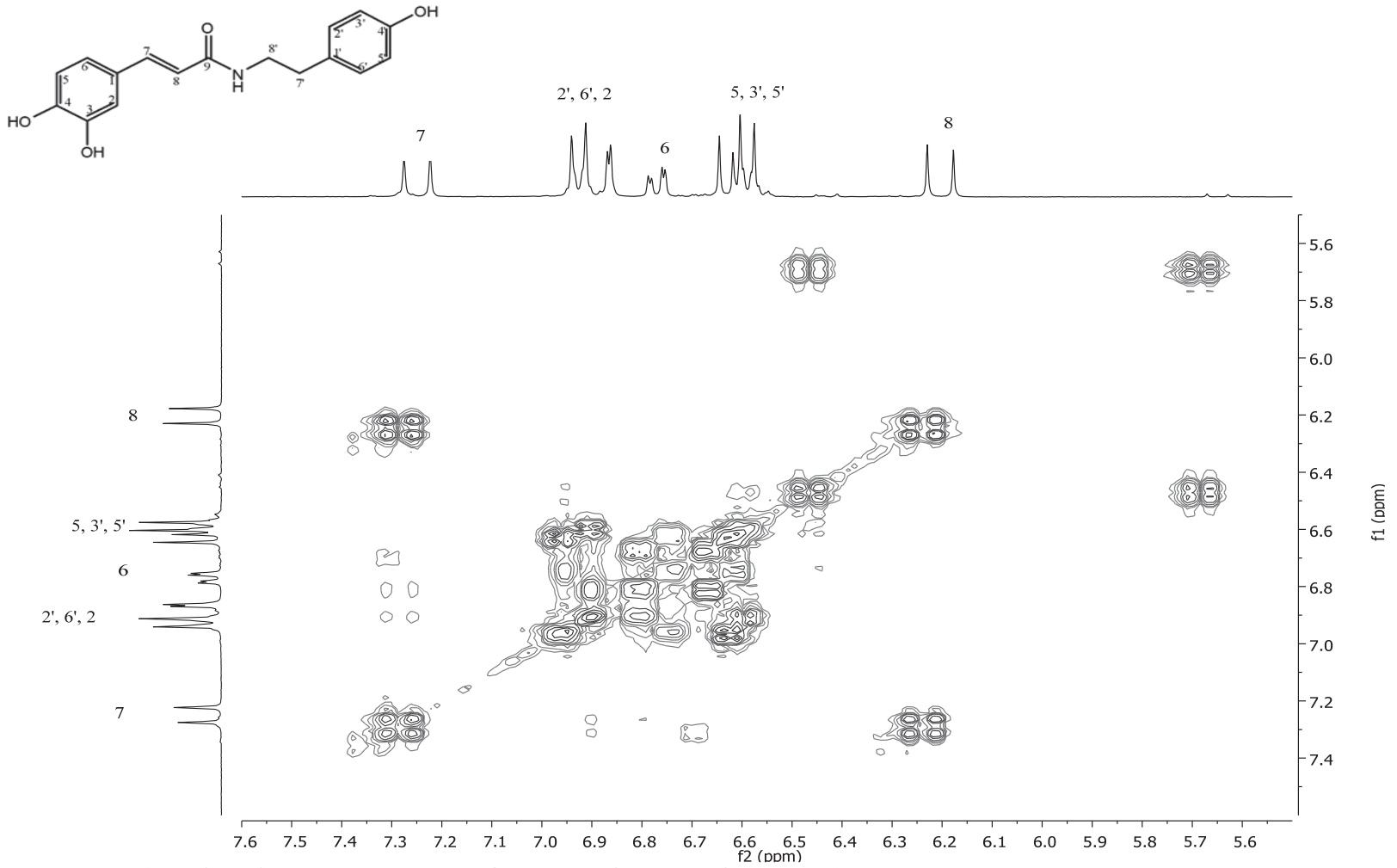

Figure 137 (Continued) COSY Spectrum of compound MET-2 (in CD_3OD)

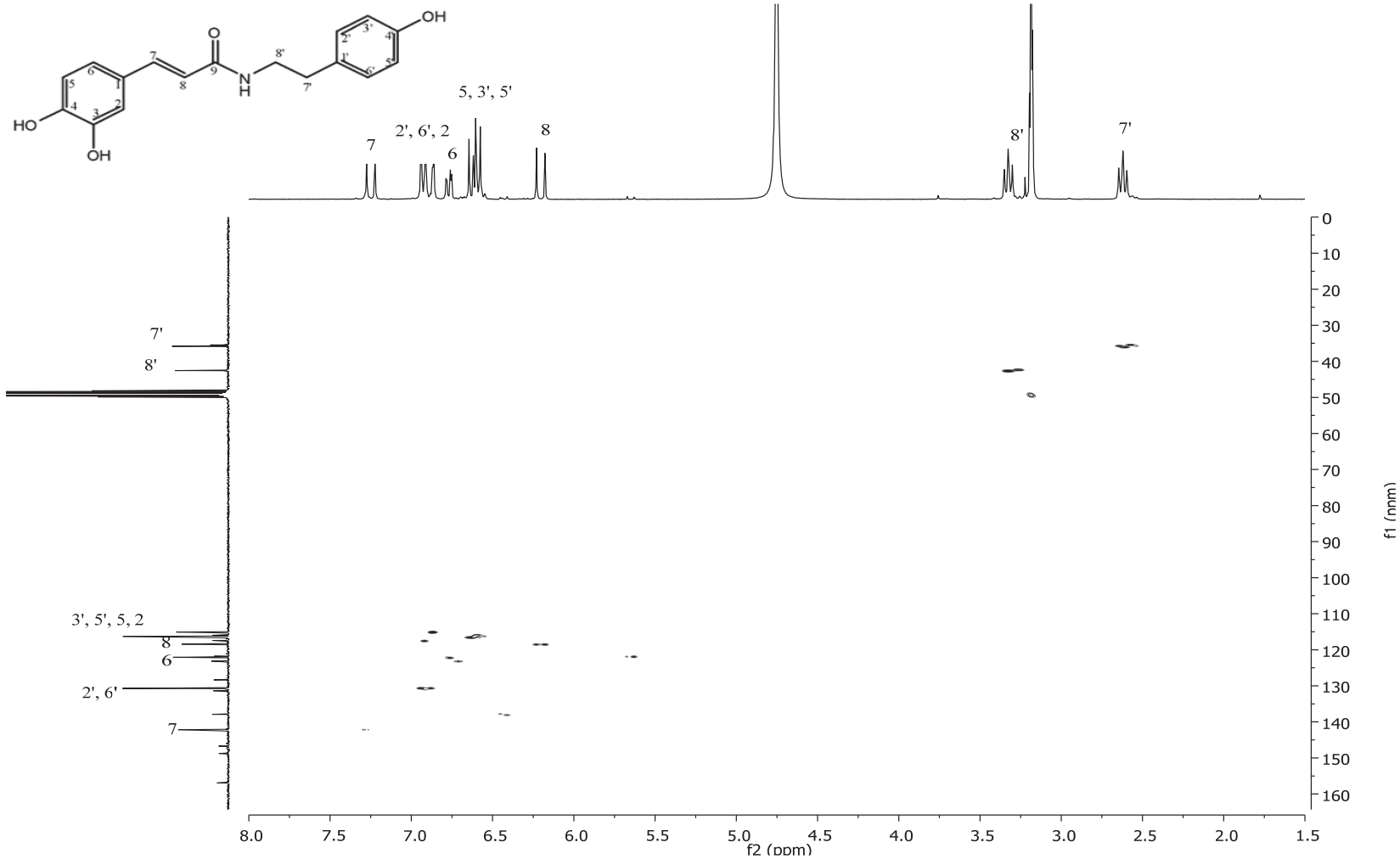

Figure 138 HMQC Spectrum of compound MET-2 (in CD_3OD)

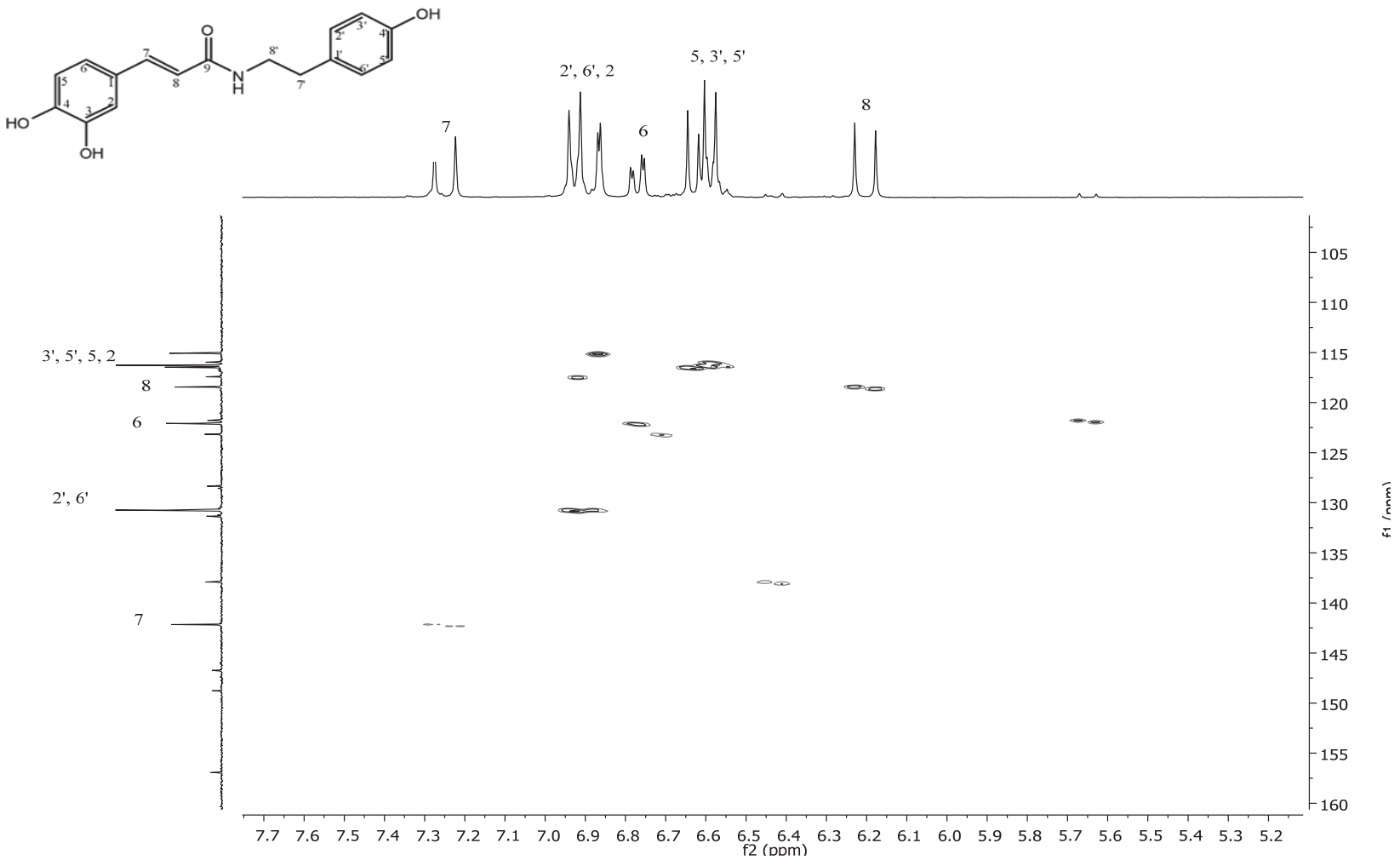

Figure 138 (Continued) HMQC Spectrum of compound MET-2 (in CD_3OD)

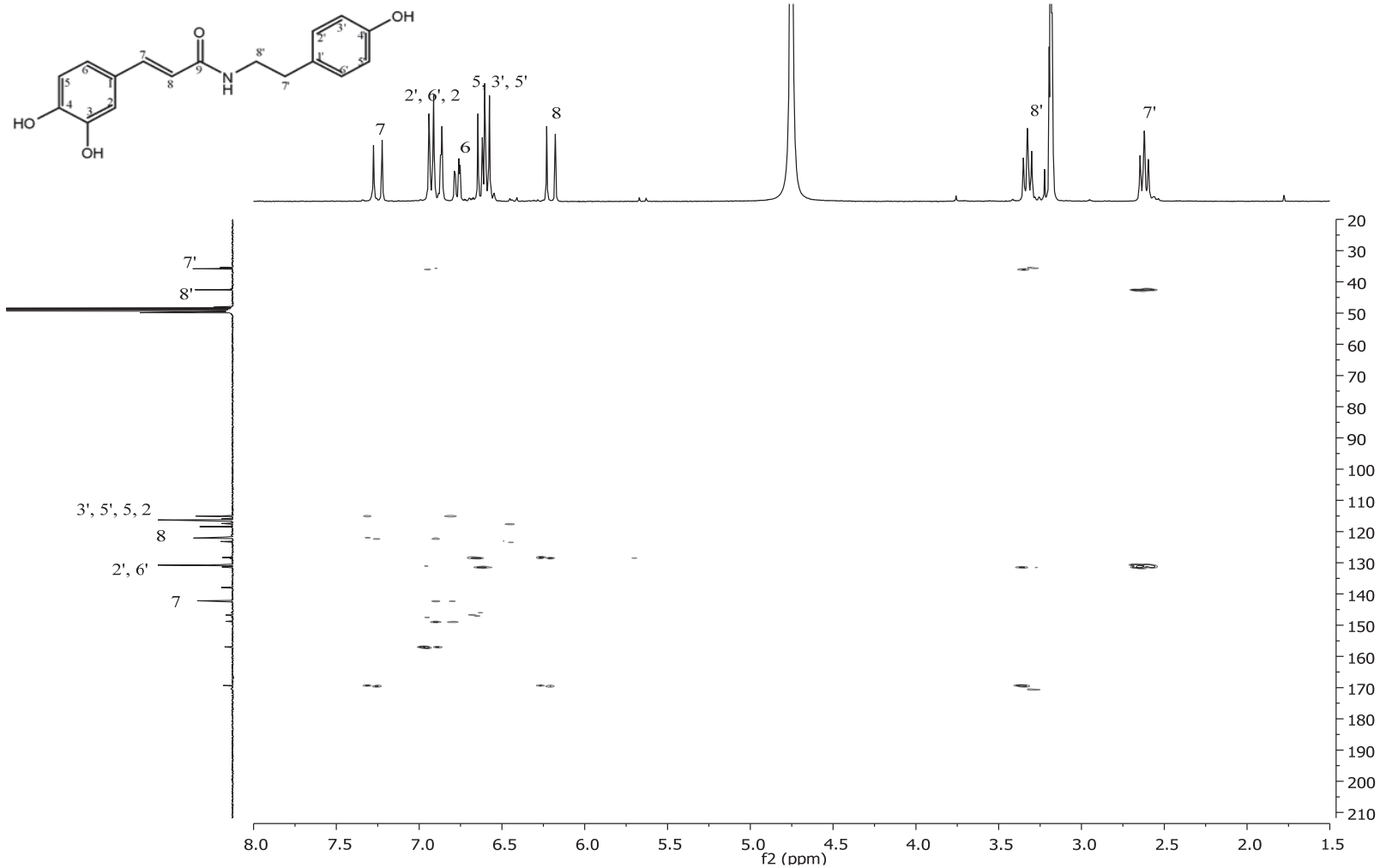

Figure 139 HMBC Spectrum of compound MET-2 (in CD_3OD)

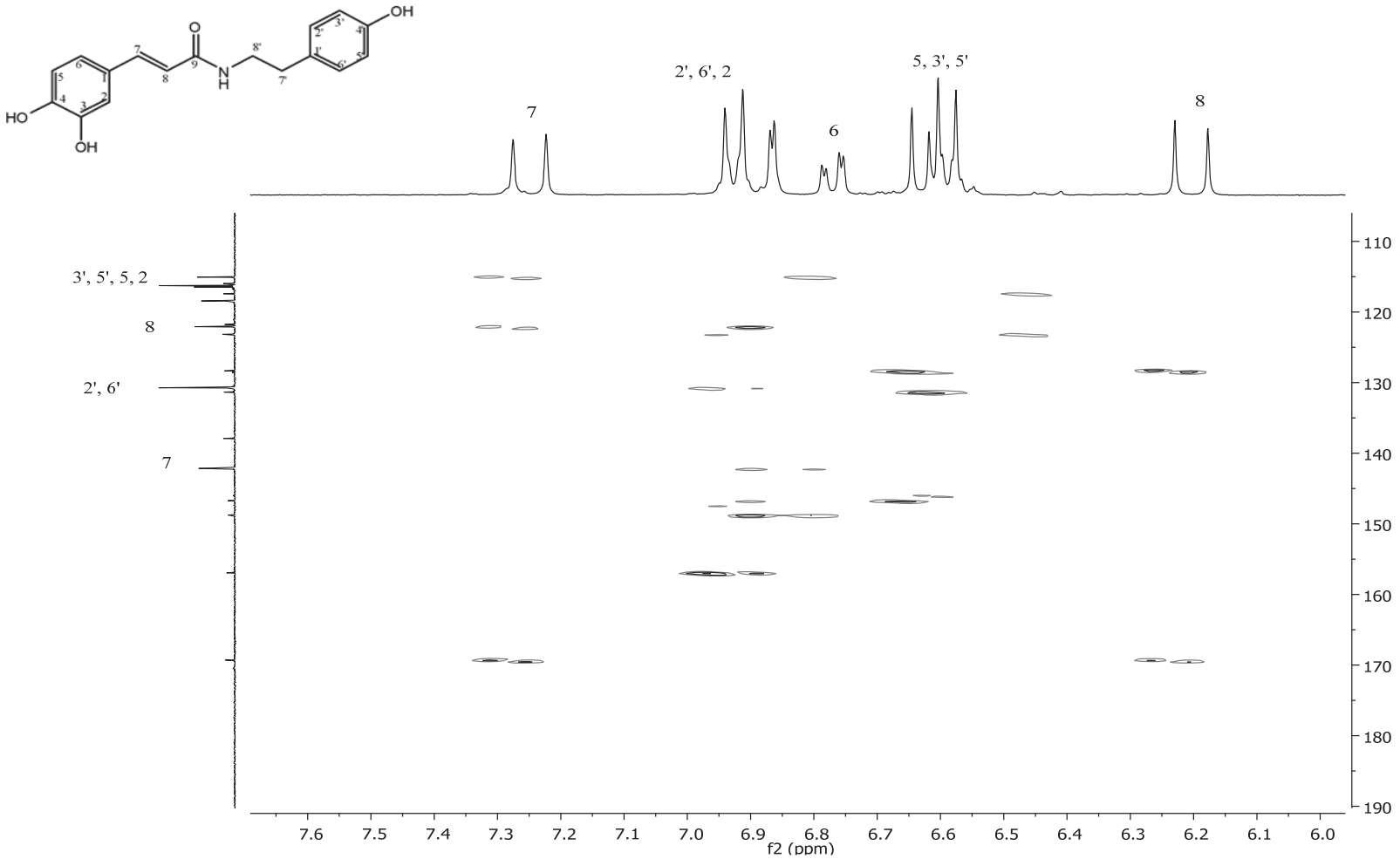

Figure 139 (Continued) HMBC Spectrum of compound MET-2 (in CD_3OD)

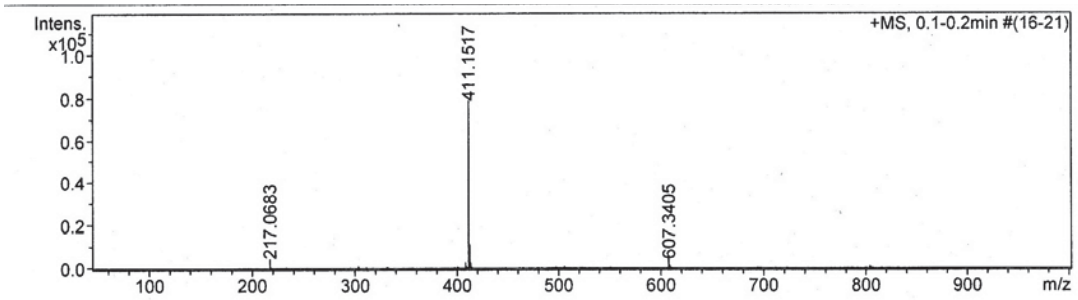

Figure 140 MS spectrum of compound MET-3

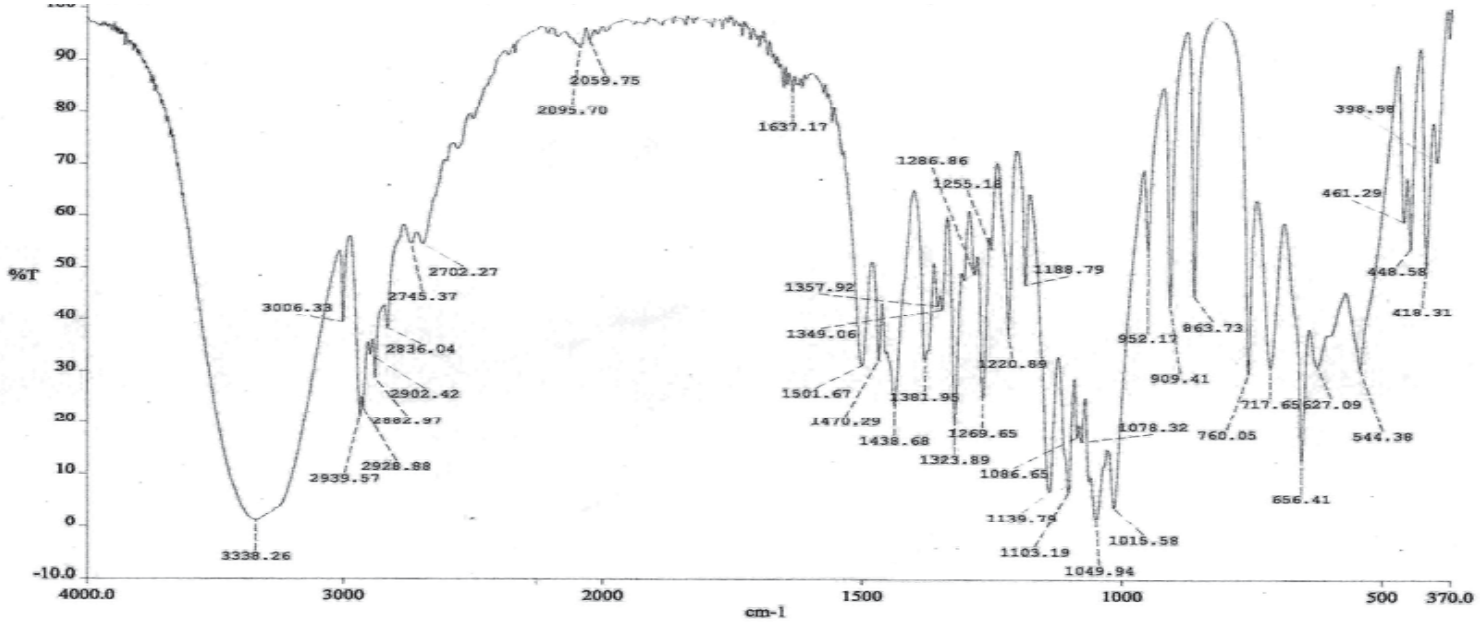

Figure 141 IR (KBr) spectrum of compound MET-3

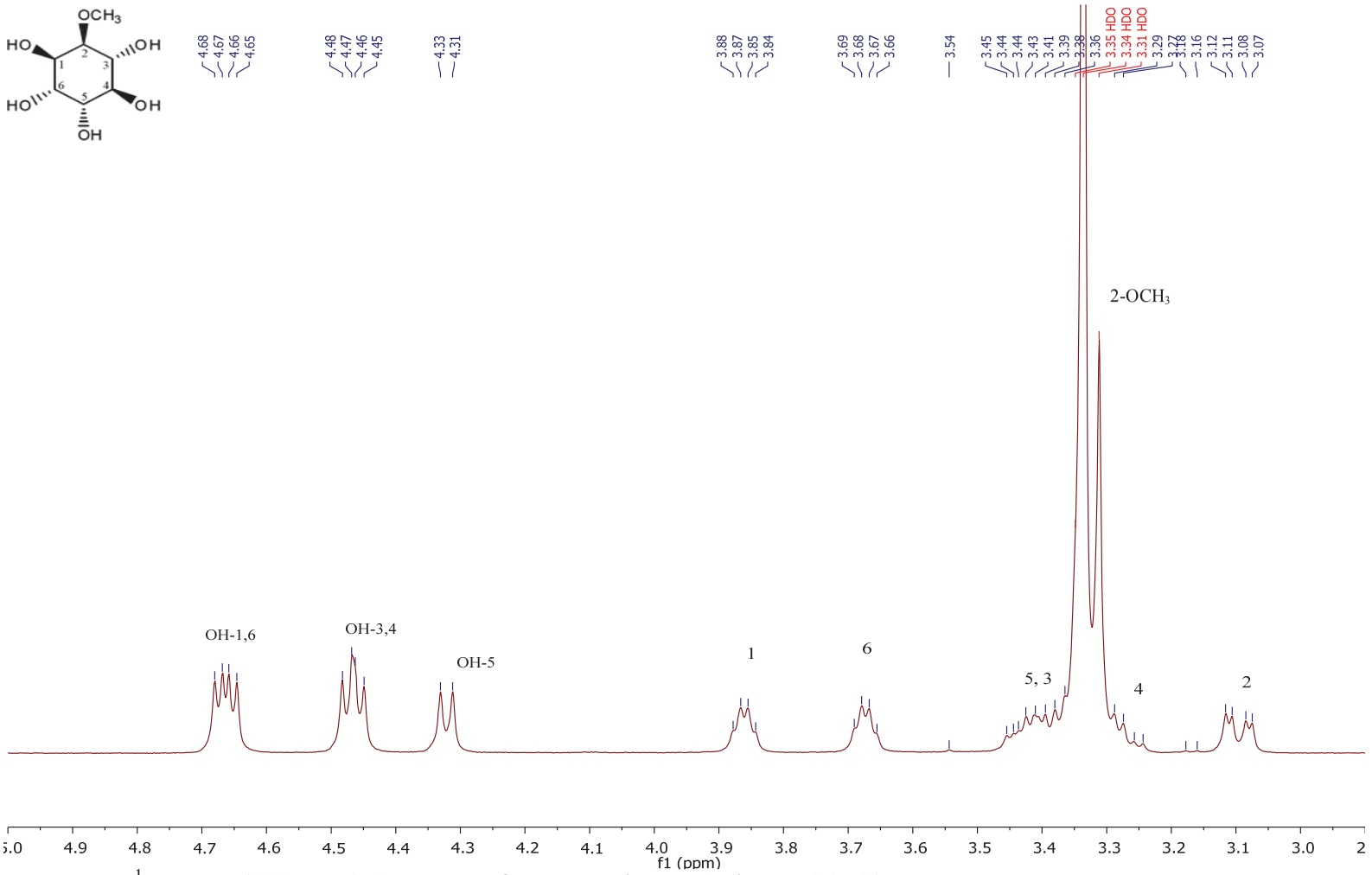

Figure 142 ^{1}H NMR (300 MHz) Spectrum of compound MET-3 (in DMSO-d_6)

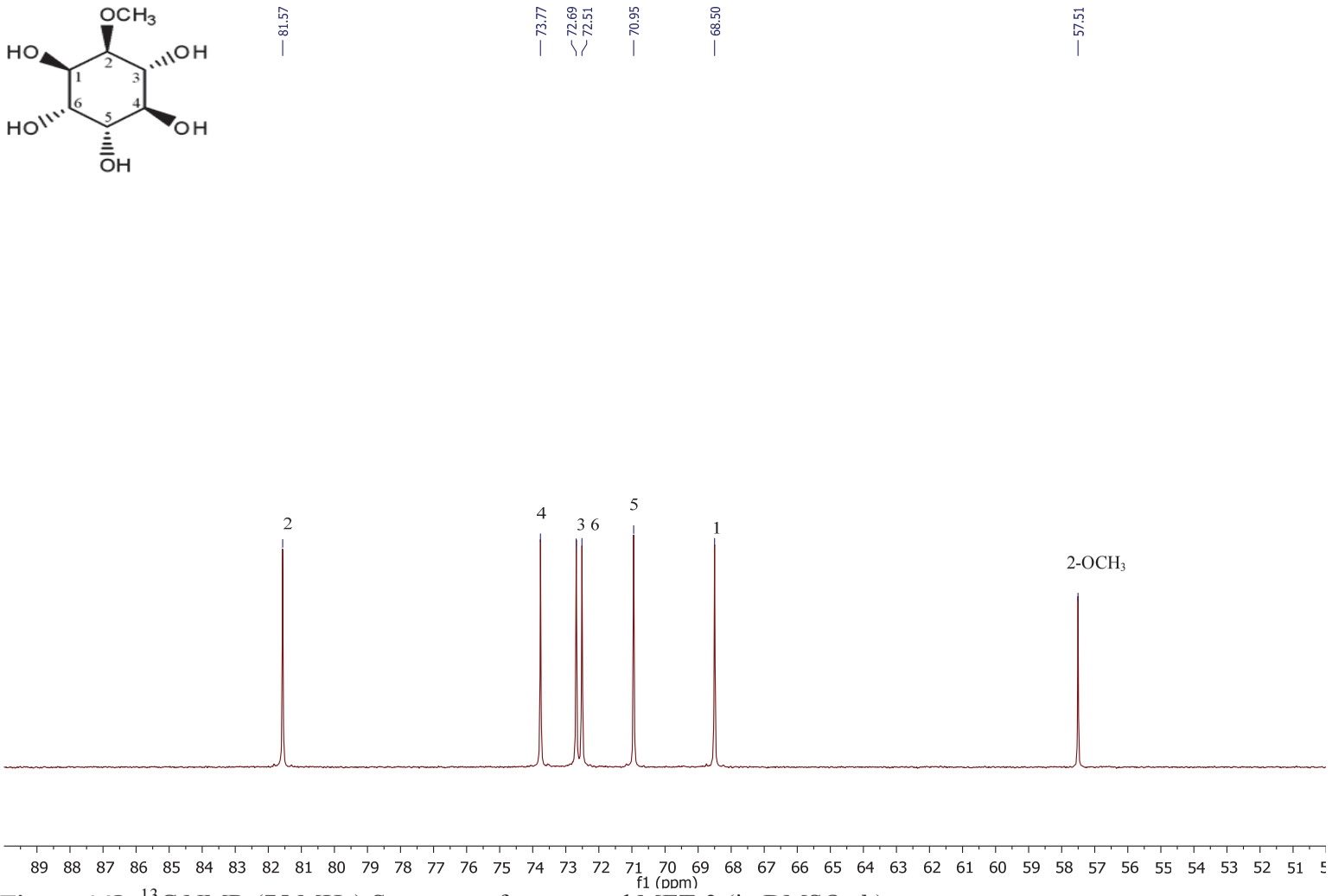

Figure 143 ^{13}C NMR (75 MHz) Spectrum of compound MET-3 (in DMSO-d_6)

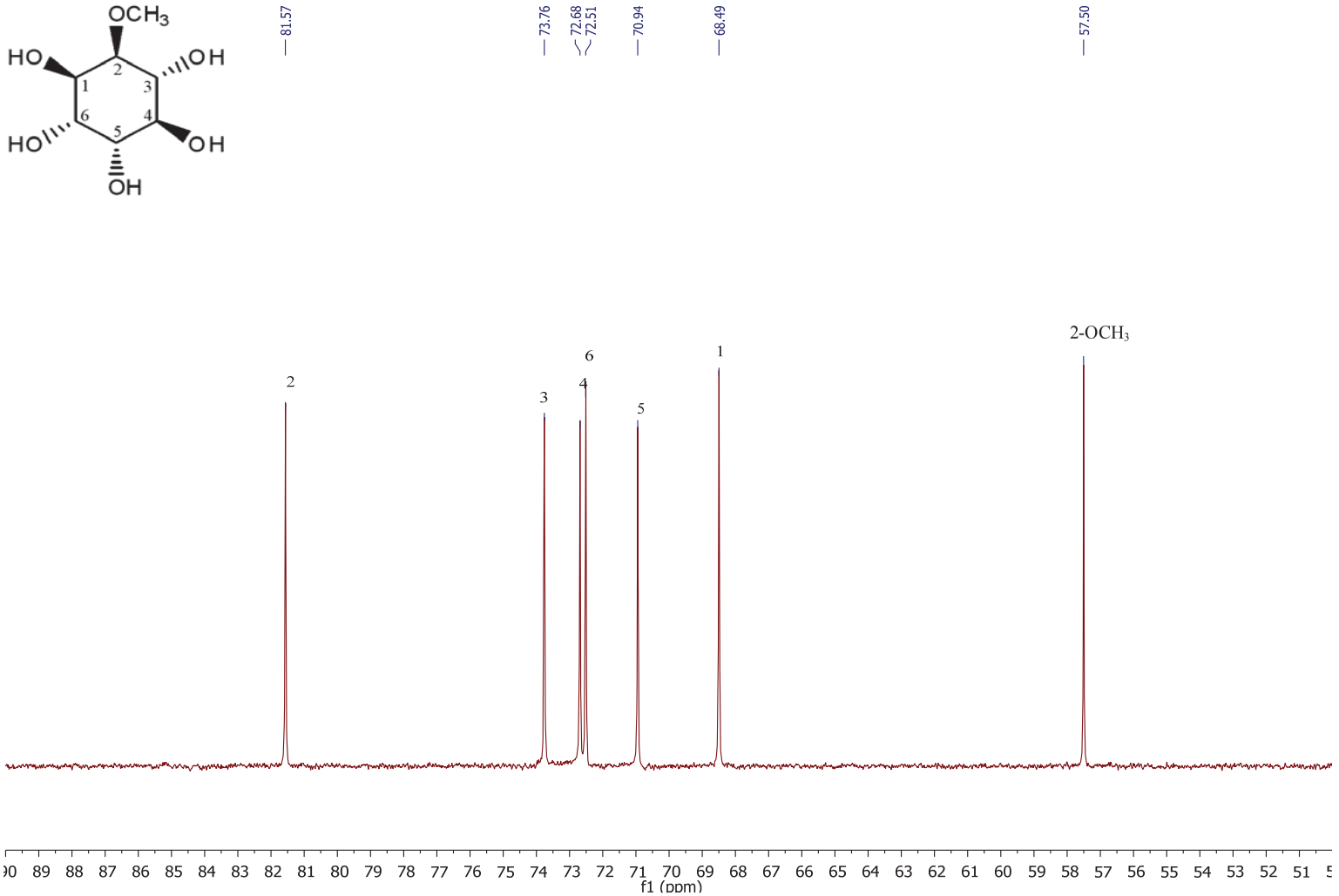

Figure 144 DEPT Spectrum of compound MET-3 (in DMSO-d_6)

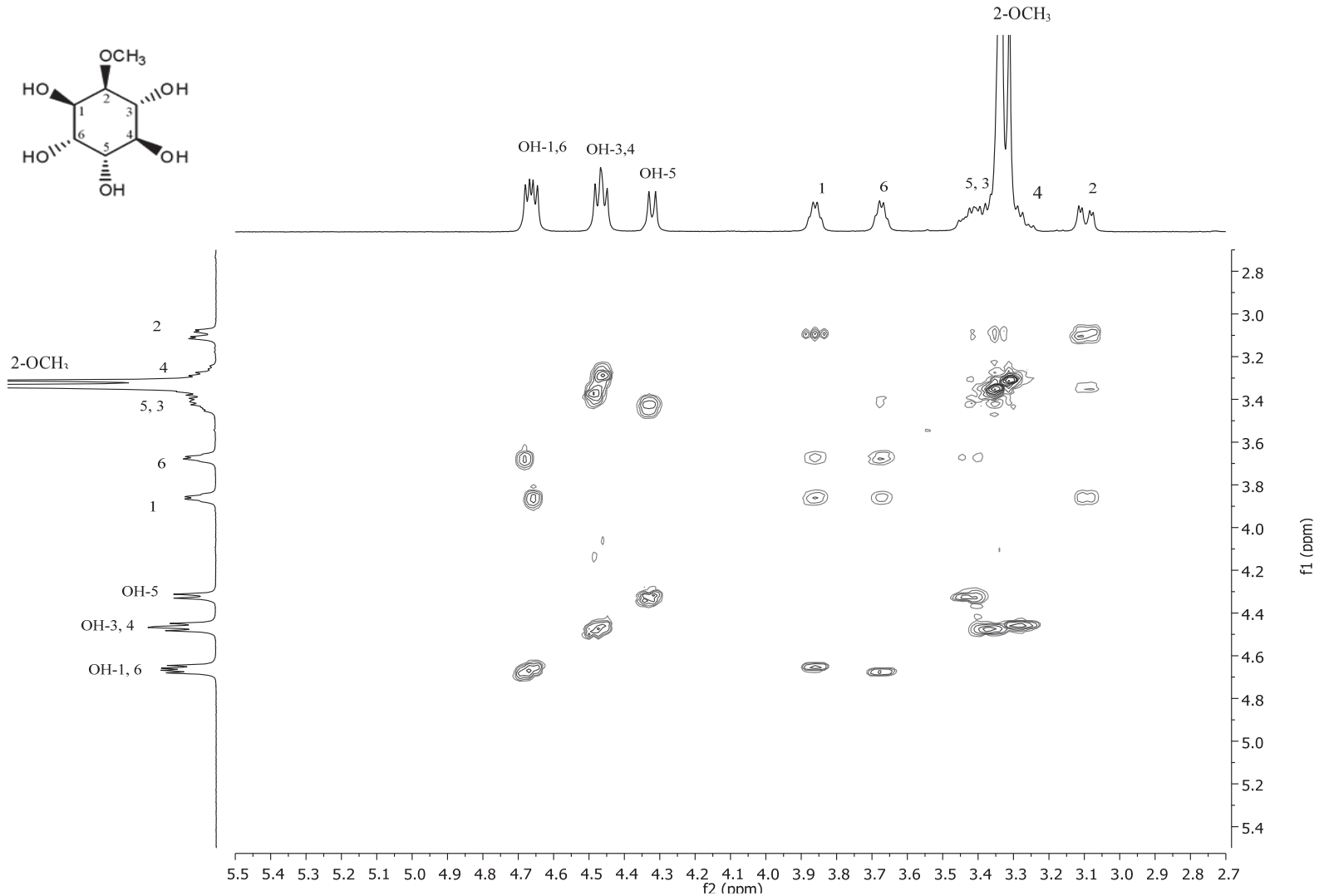

Figure 145 COSY Spectrum of compound MET-3 (in DMSO-d_6)

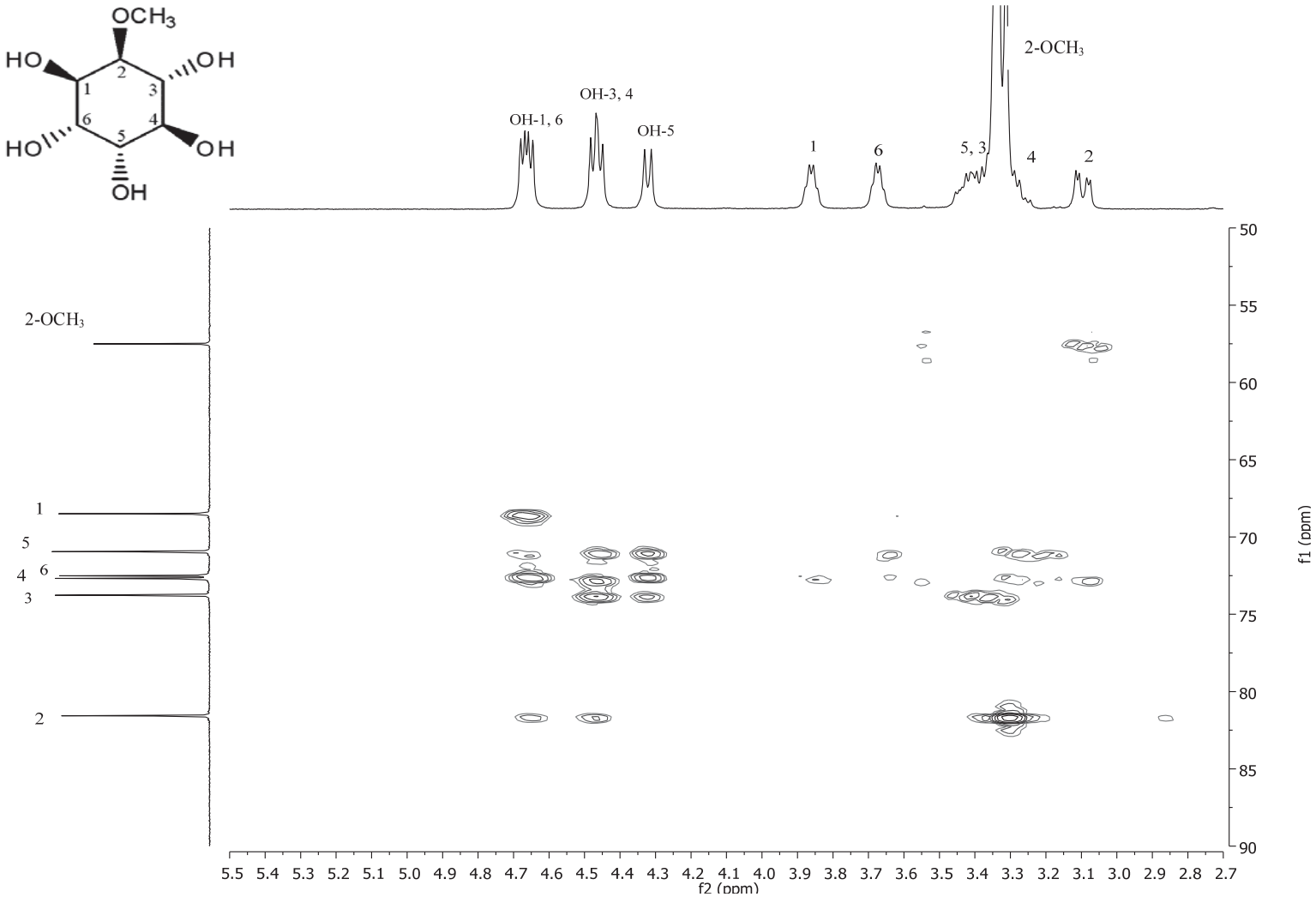

Figure 146 HMBC Spectrum of compound MET-3 (in DMSO-d_6)

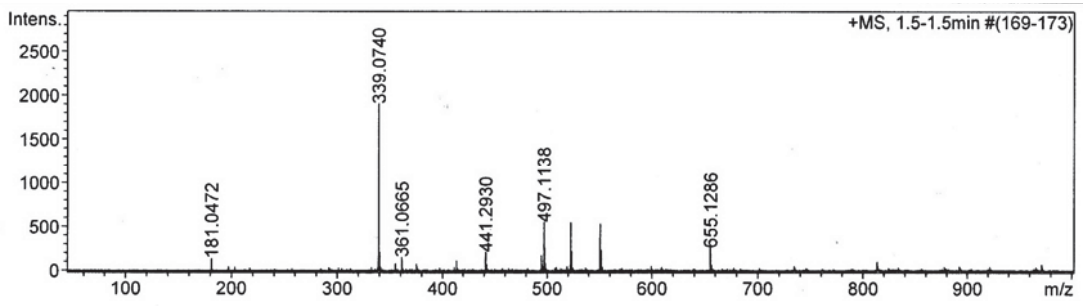

Figure 147 MS spectrum of compound MET-4

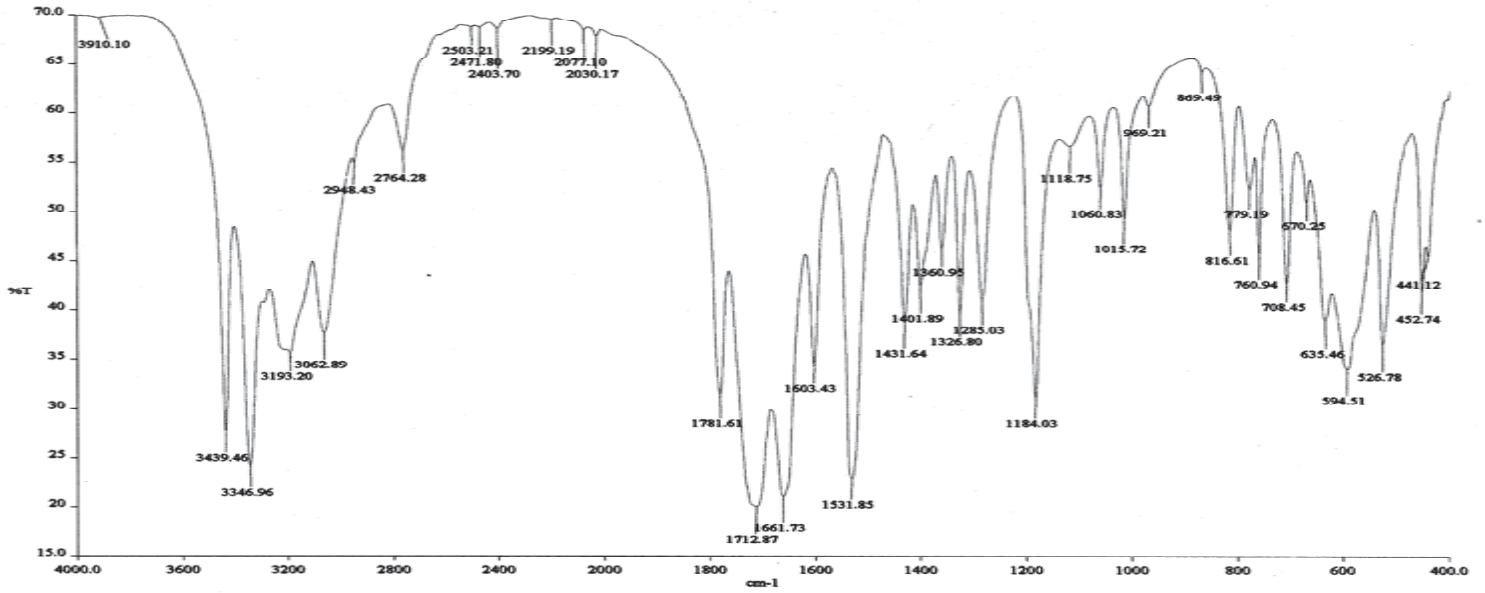

Figure 148 IR (KBr) spectrum of compound MET-4

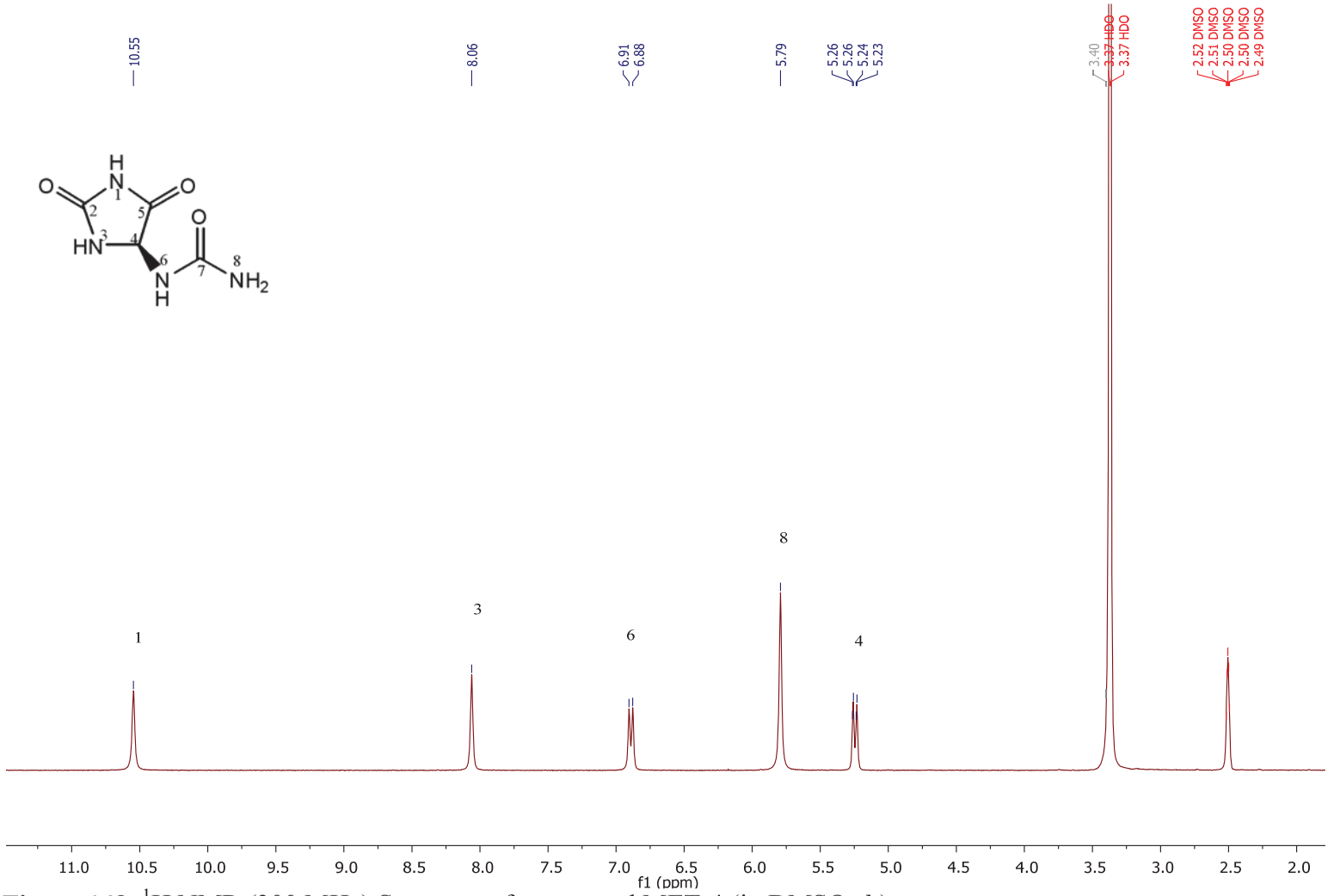

Figure 149 ^{1}H NMR (300 MHz) Spectrum of compound MET-4 (in DMSO-d_6)

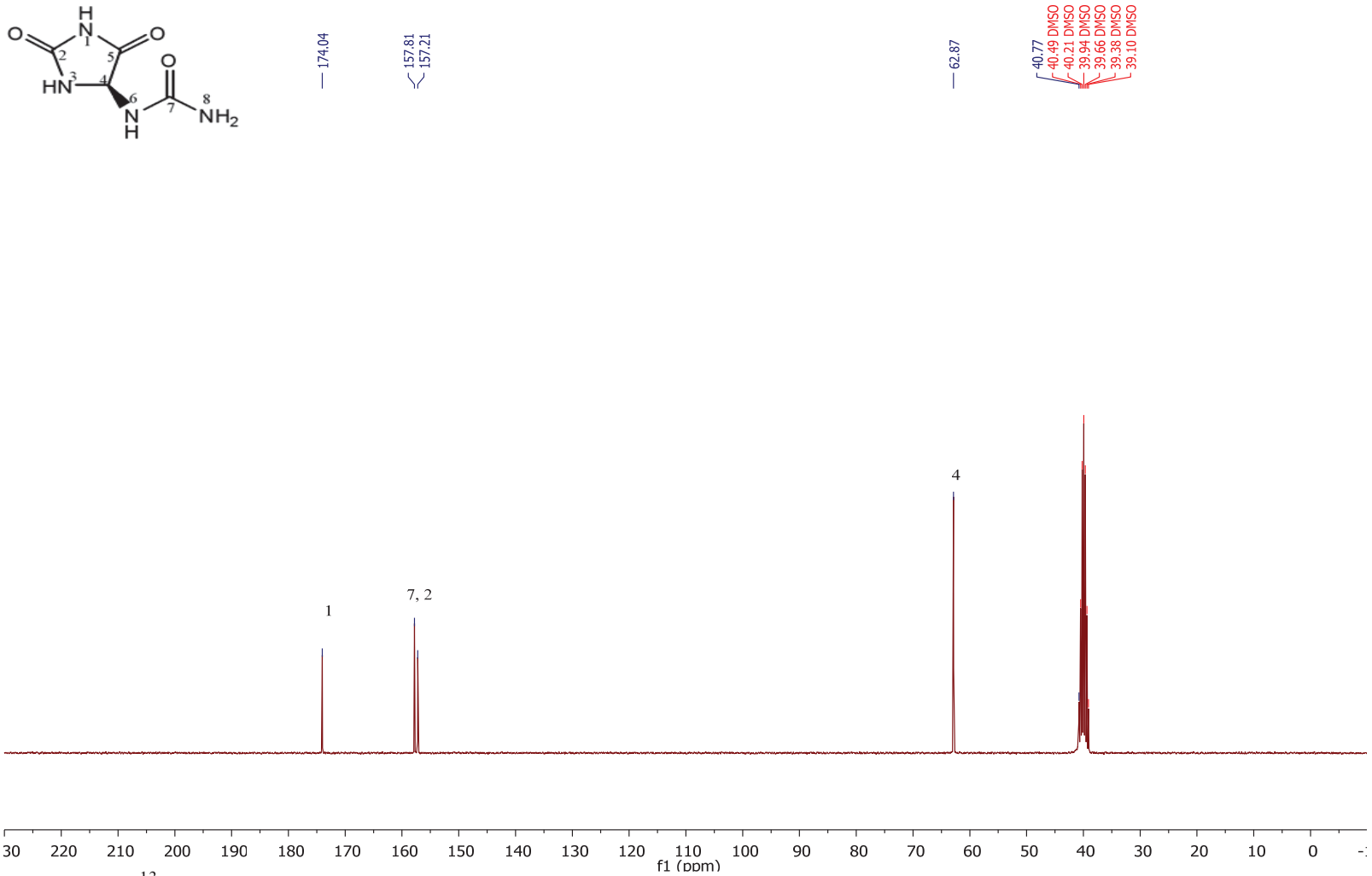

Figure 150 ^{13}C NMR (75 MHz) Spectrum of compound MET-4 (in DMSO-d_6)

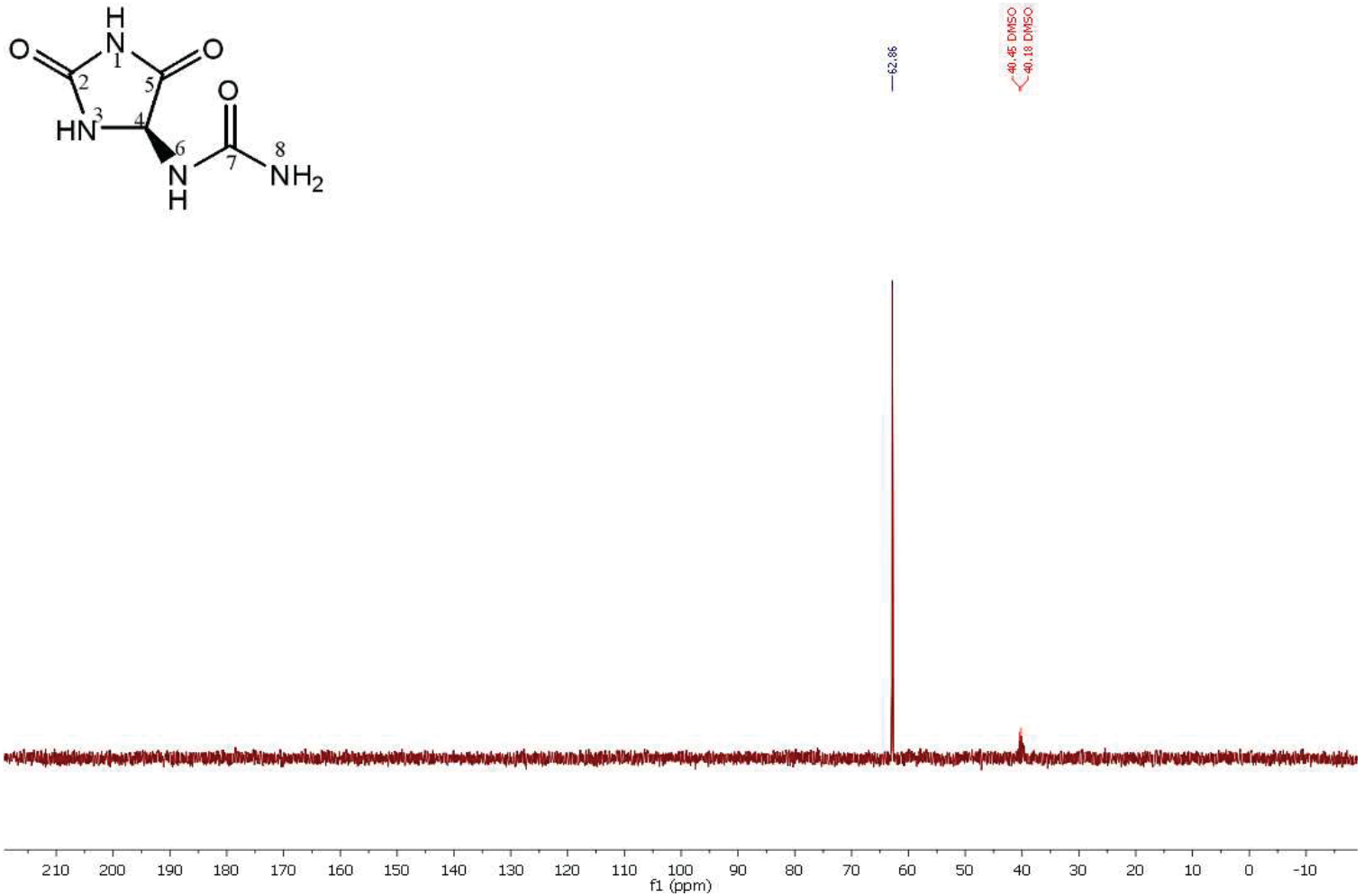

Figure 151 DEPT Spectrum of compound MET-4 (in DMSO-d_6)

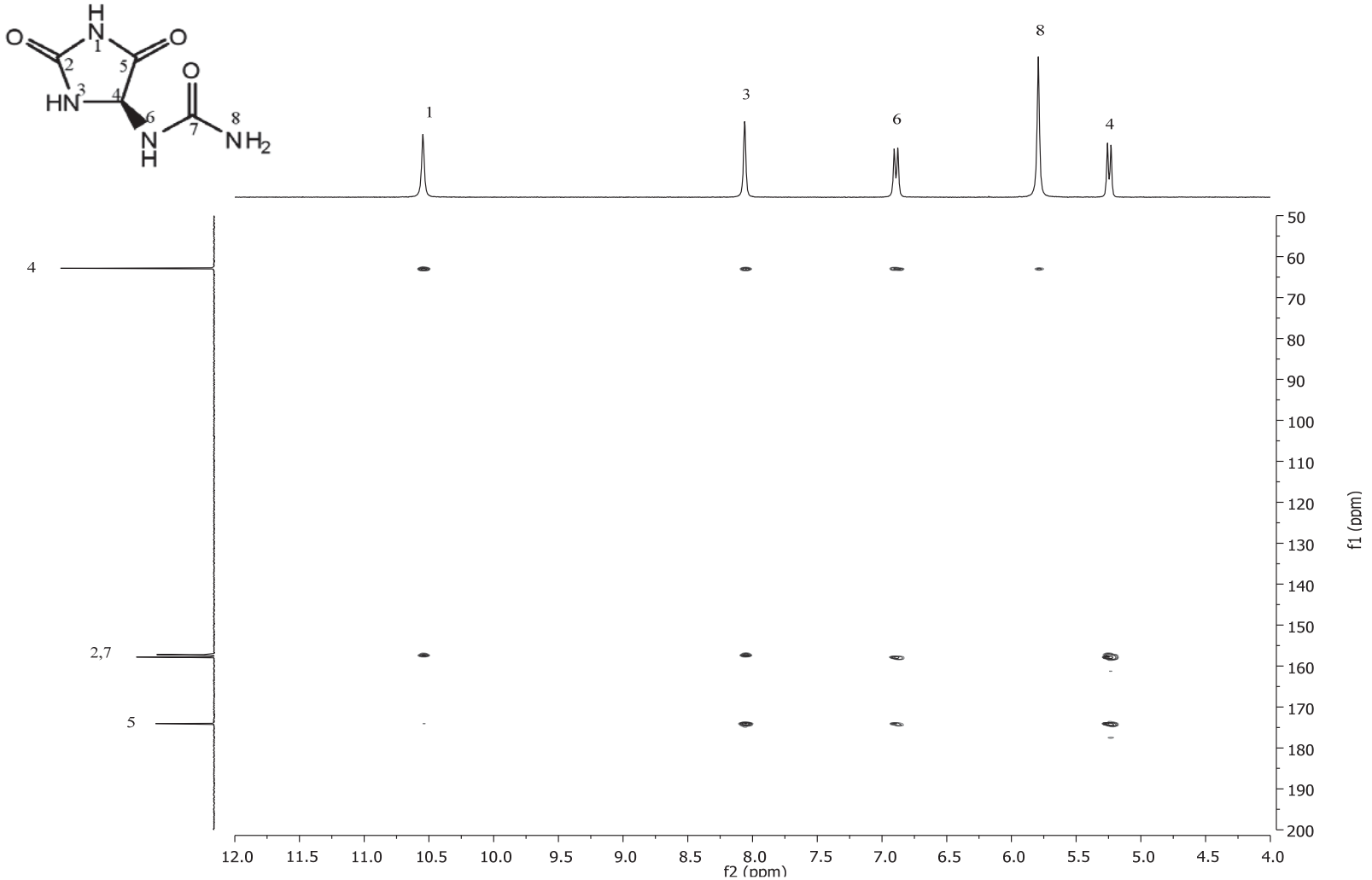

Figure 152 HMBC Spectrum of compound MET-4 (in DMSO-d_6)

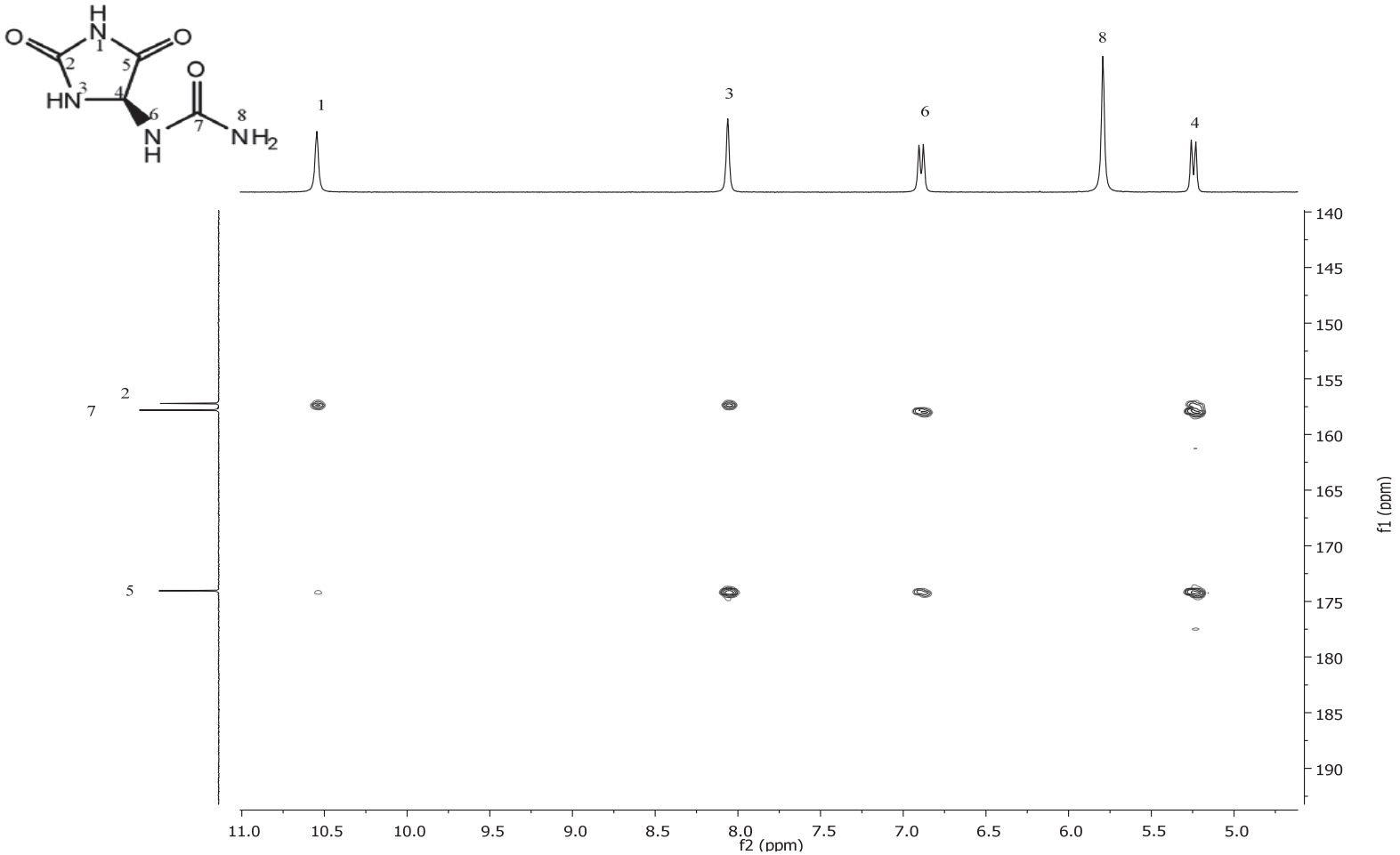

Figure 152 (Continued) HMBC Spectrum of compound MET-4 (in DMSO-d_6)

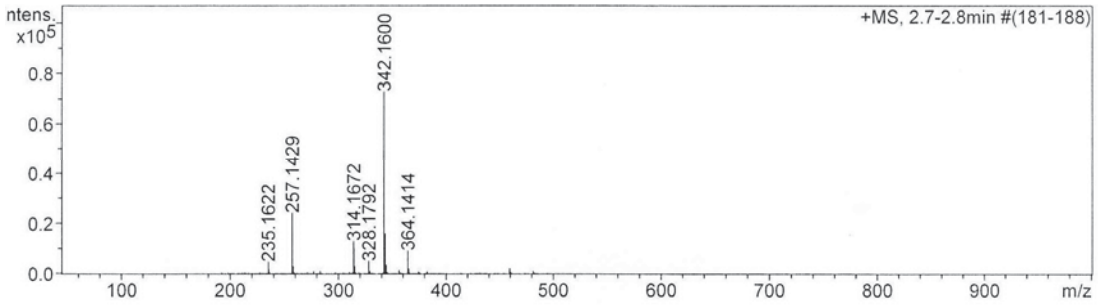

Figure 153 MS spectrum of compound MBT-1

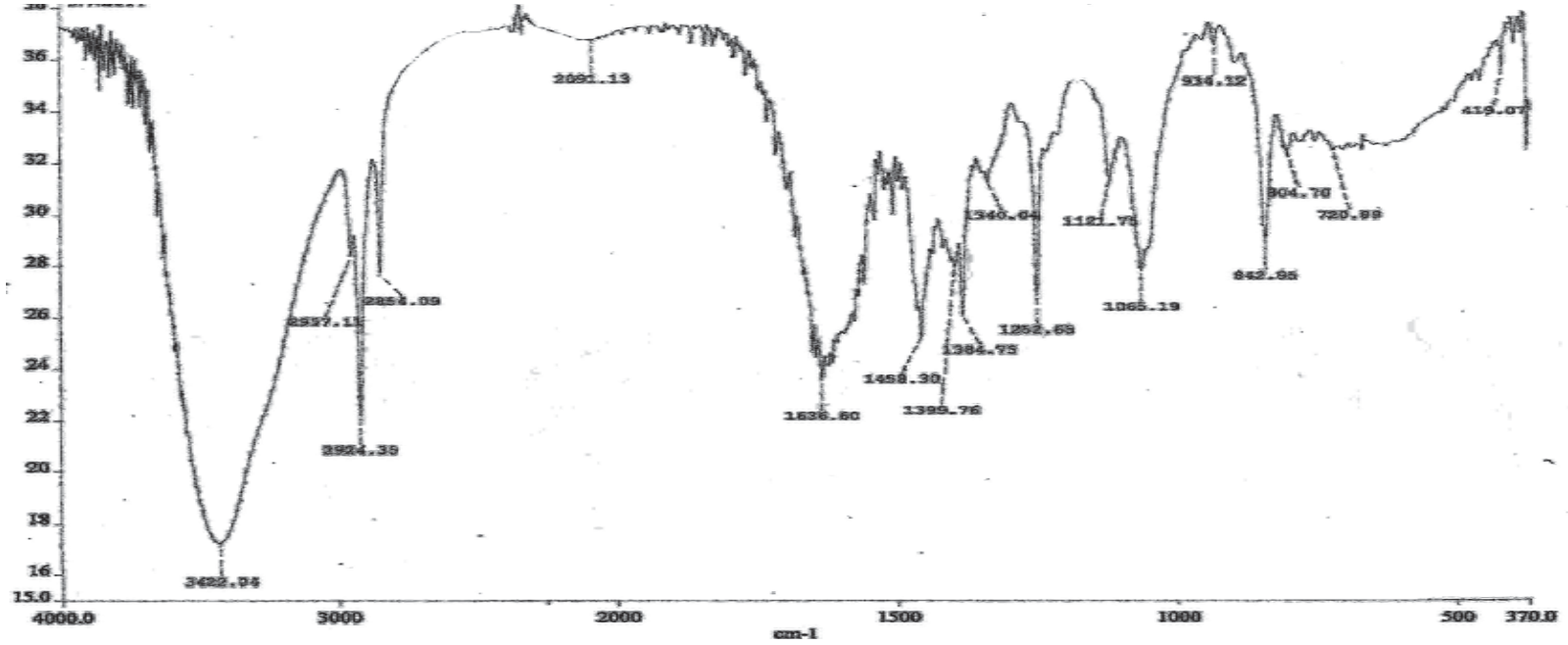

Figure 154 IR (KBr) spectrum of compound MBT-1

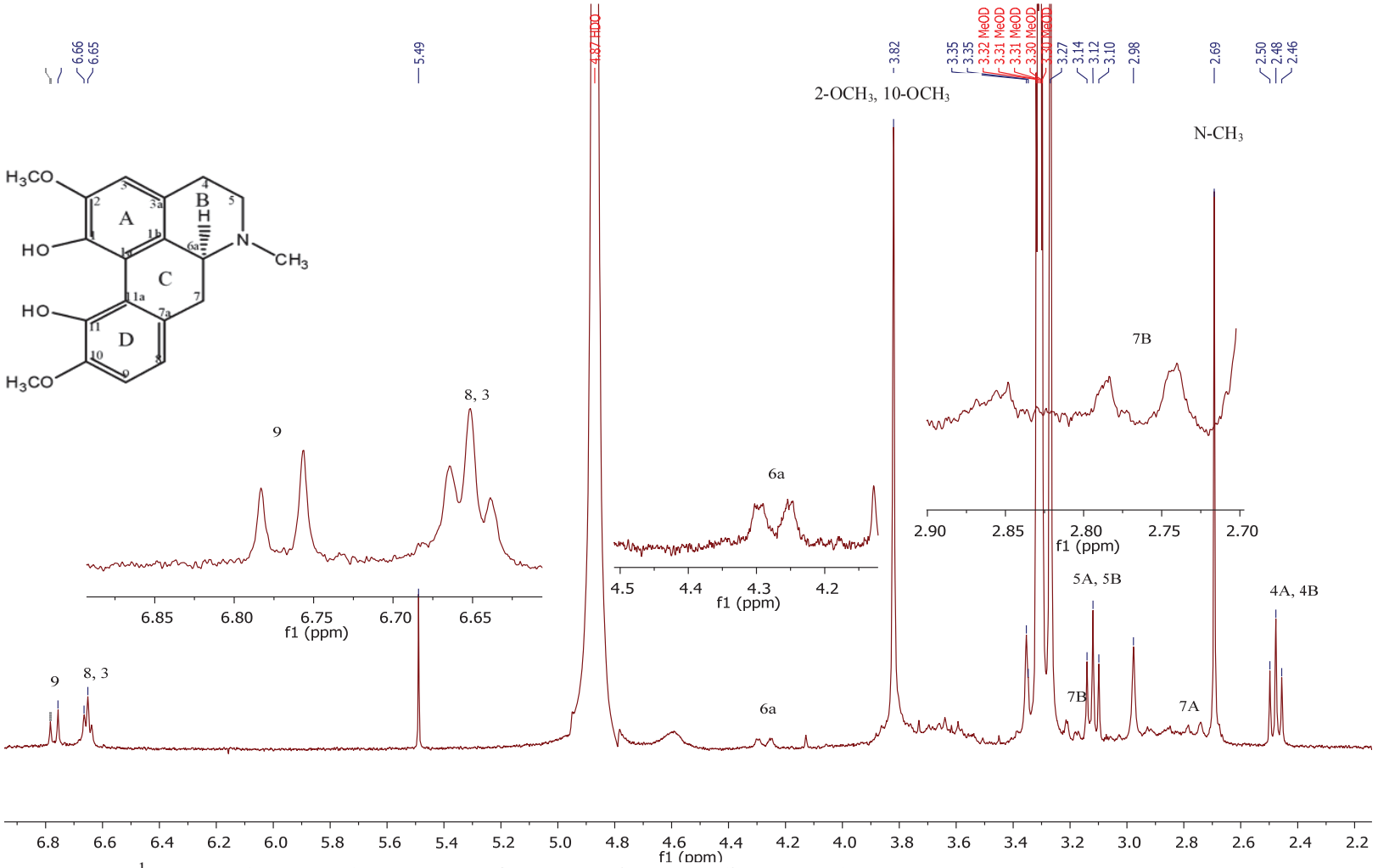

Figure 155 ^{1}H NMR (300 MHz) Spectrum of compound MBT-1 (in CD_3OD)

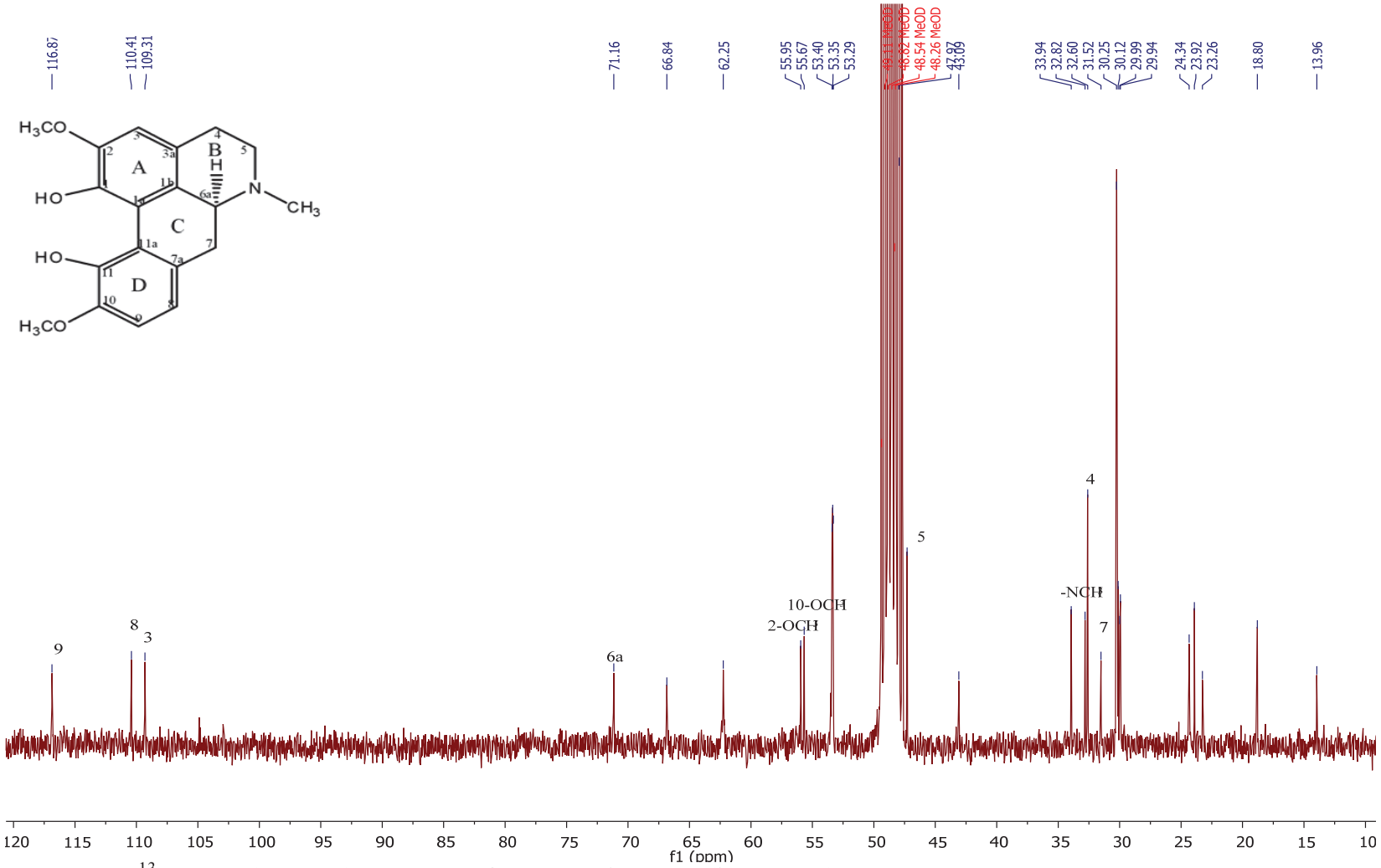

Figure 156 ^{13}C NMR (75 MHz) Spectrum of compound MBT-1 (in CD_3OD)

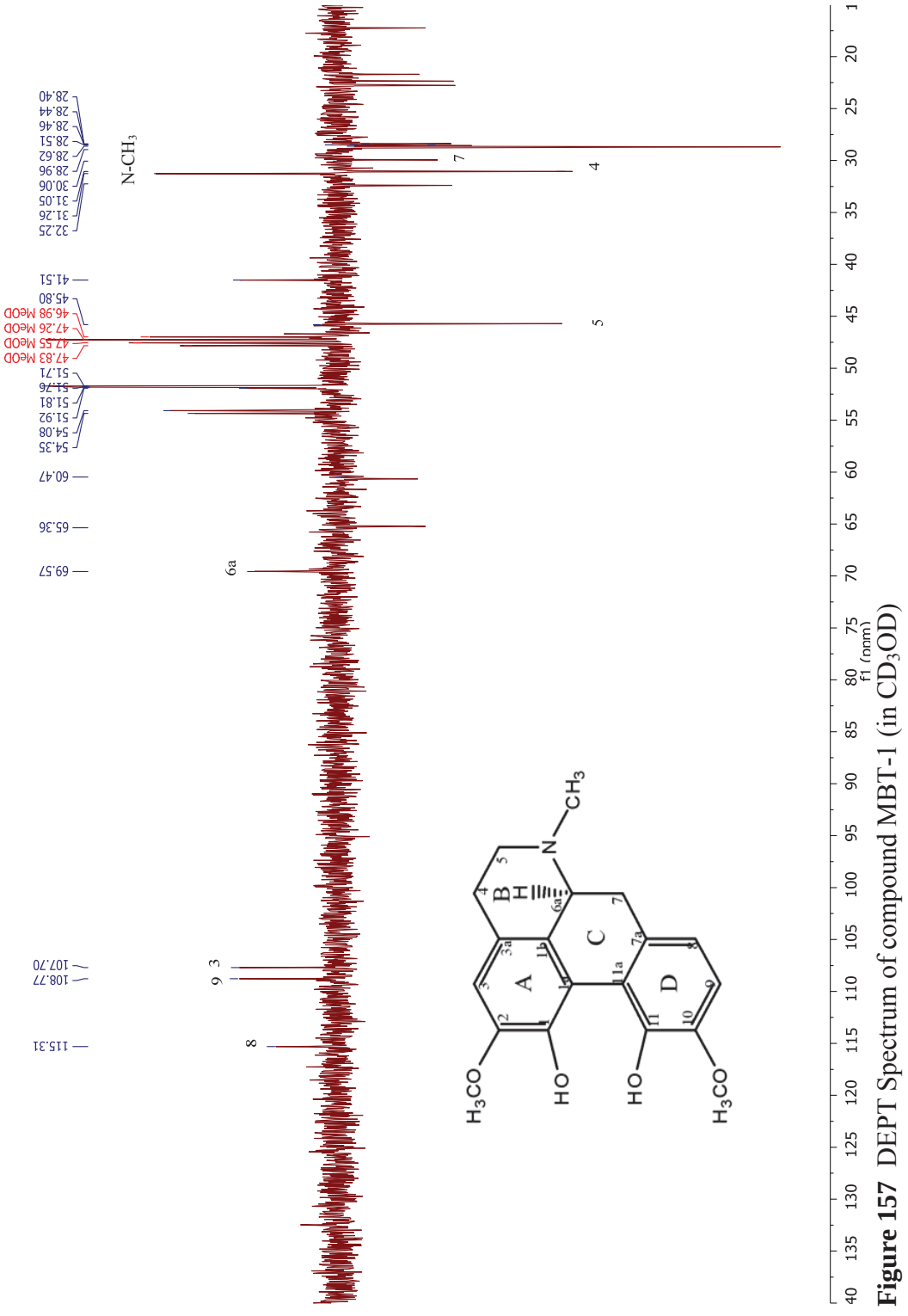

Figure 157 DEPT Spectrum of compound MBT-1 (in CD_3OD)

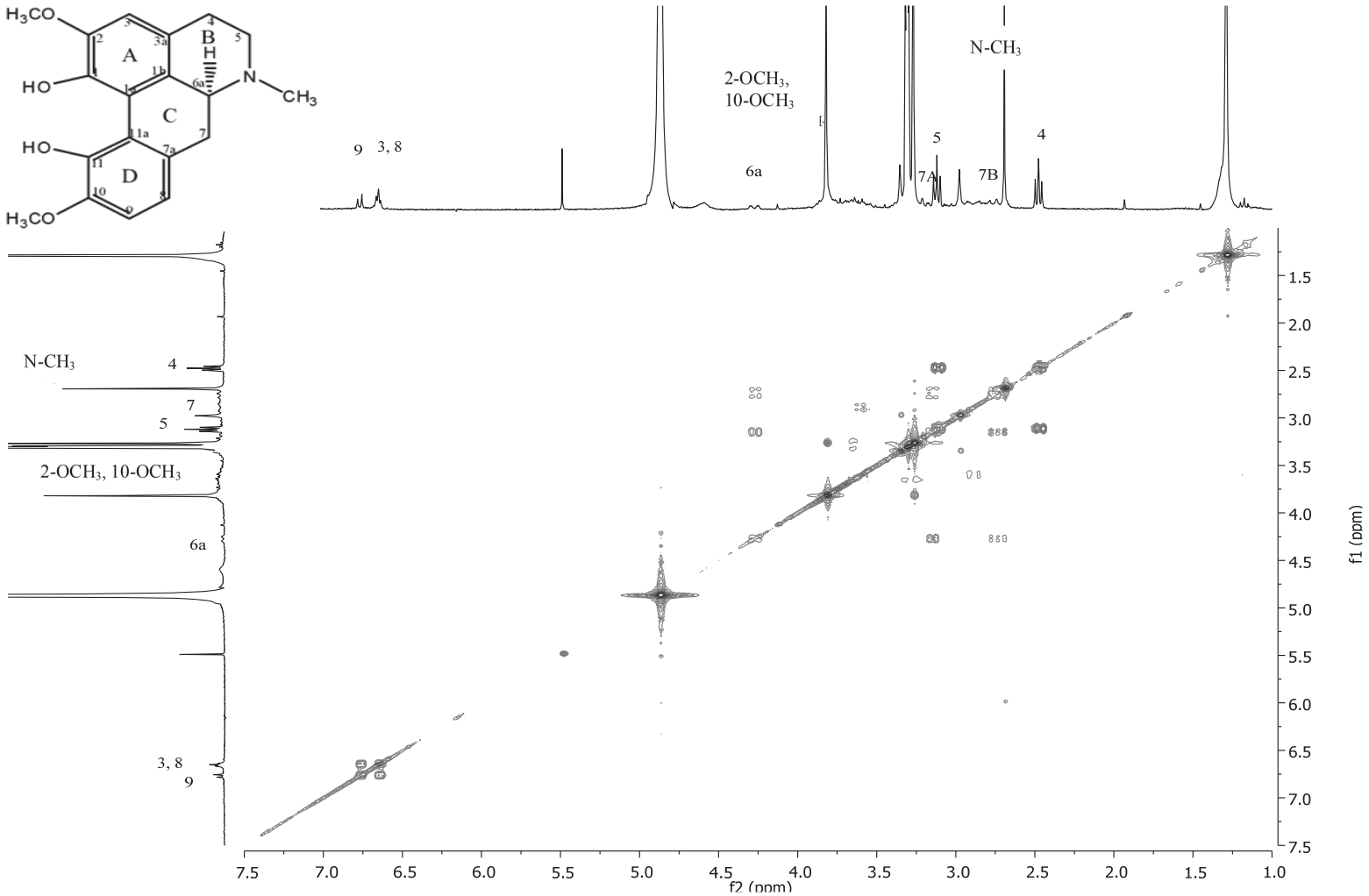

Figure 158 COSY Spectrum of compound MBT-1 (in CD_3OD)

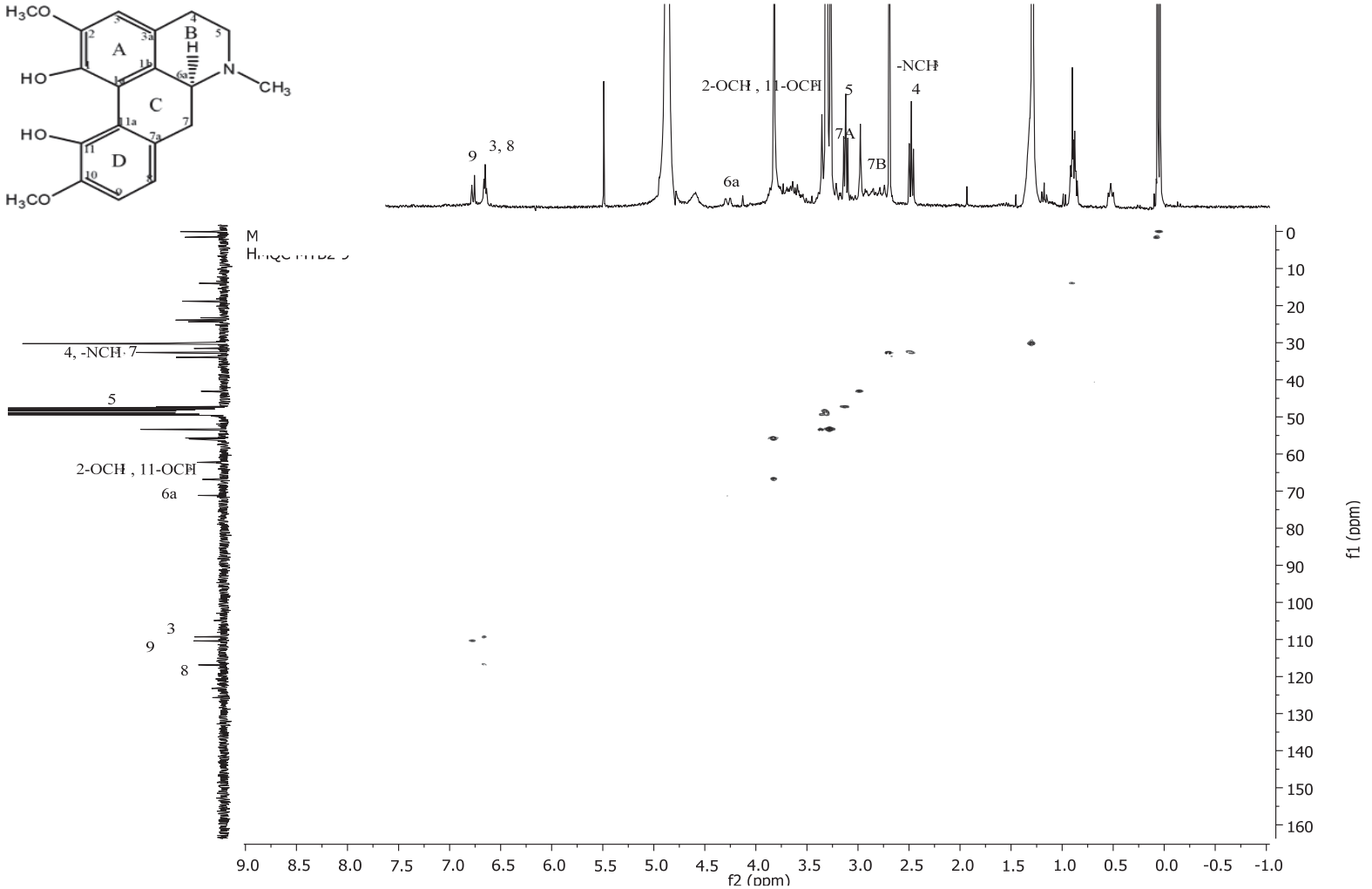

Figure 159 HMQC Spectrum of compound MBT-1 (in CD_3OD)

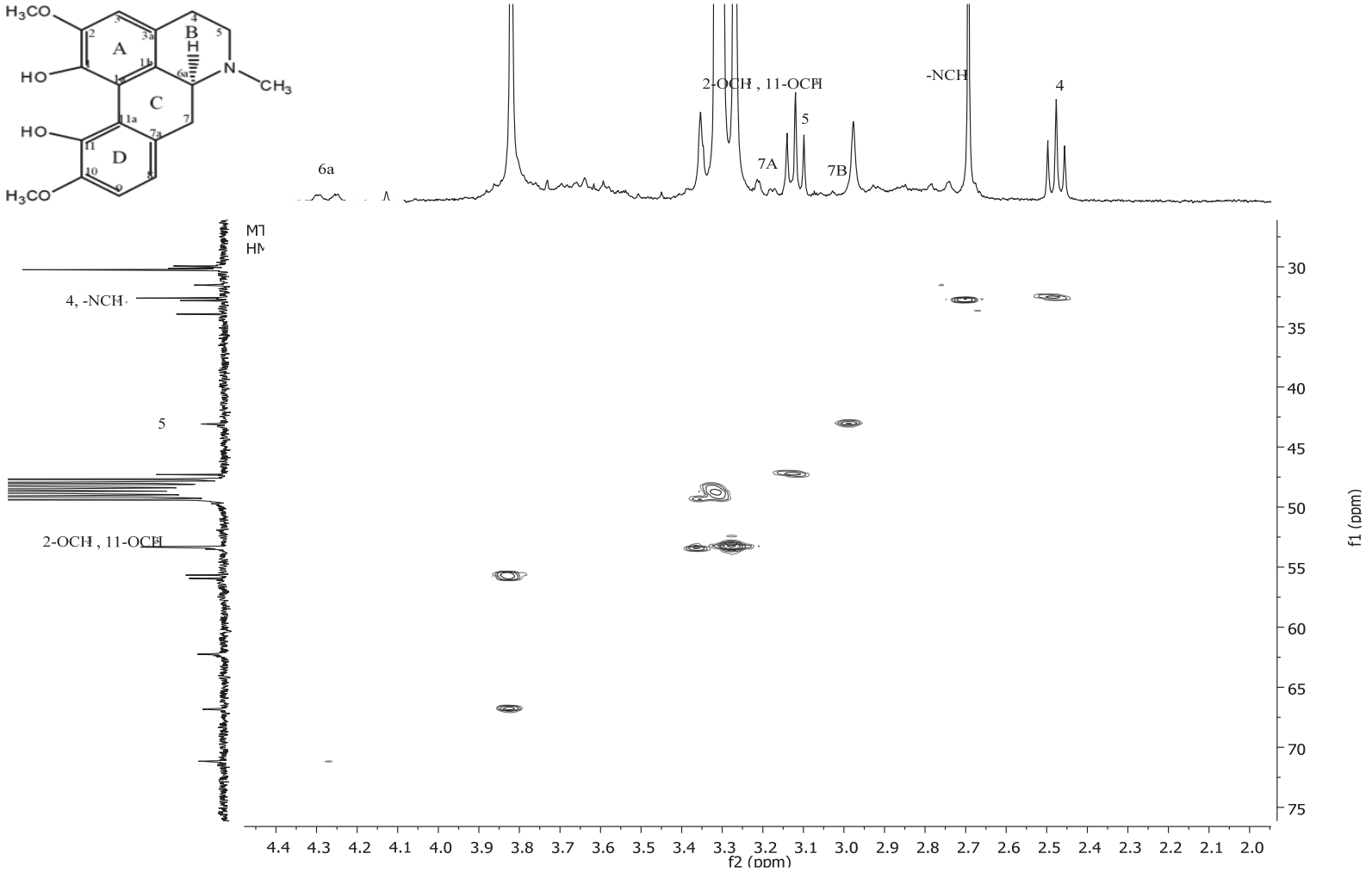

Figure 159 (Continued) HMQC Spectrum of compound MBT-1 (in CD_3OD)

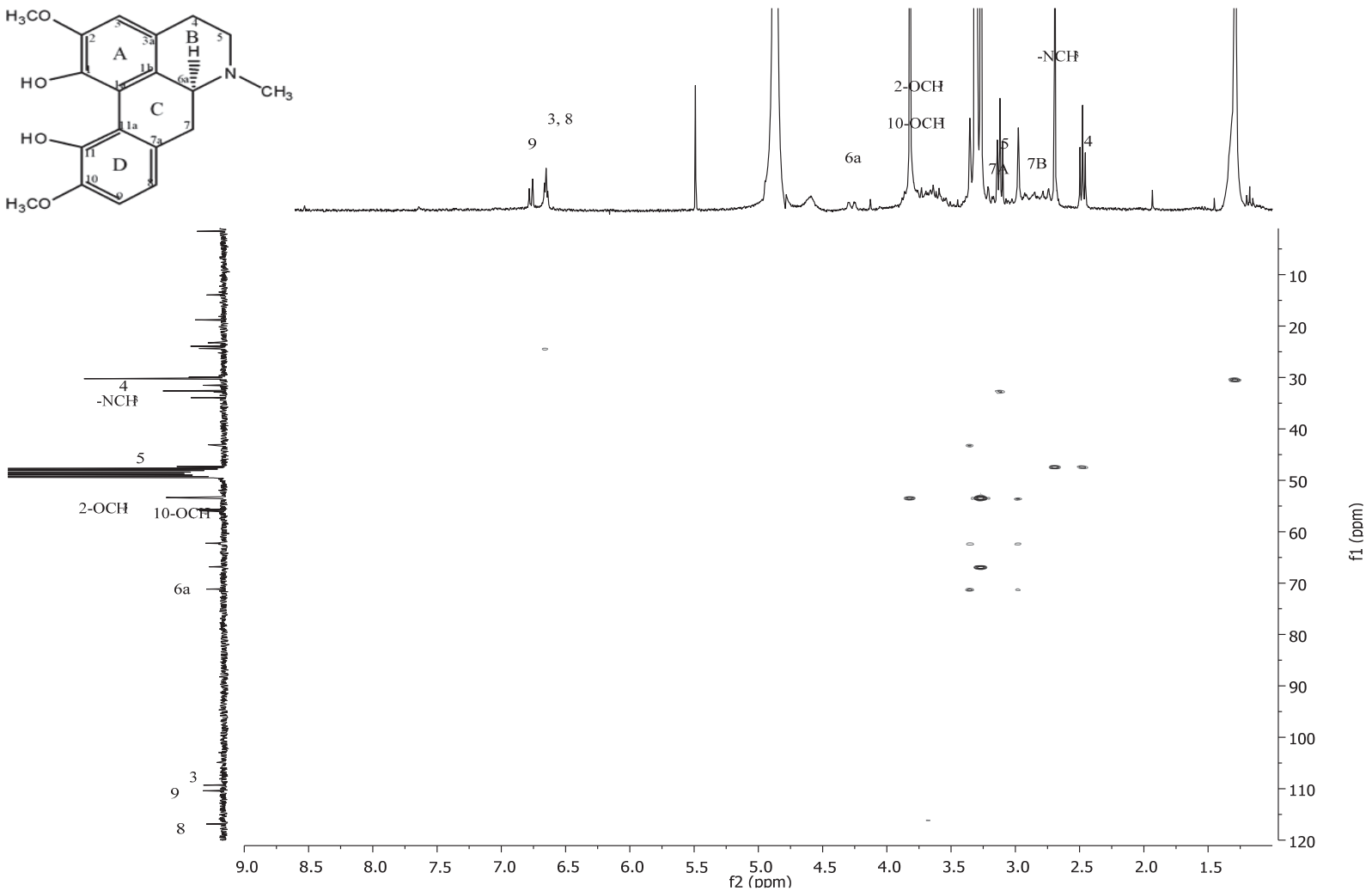

Figure 160 HMBC Spectrum of compound MBT-1 (in CD_3OD)

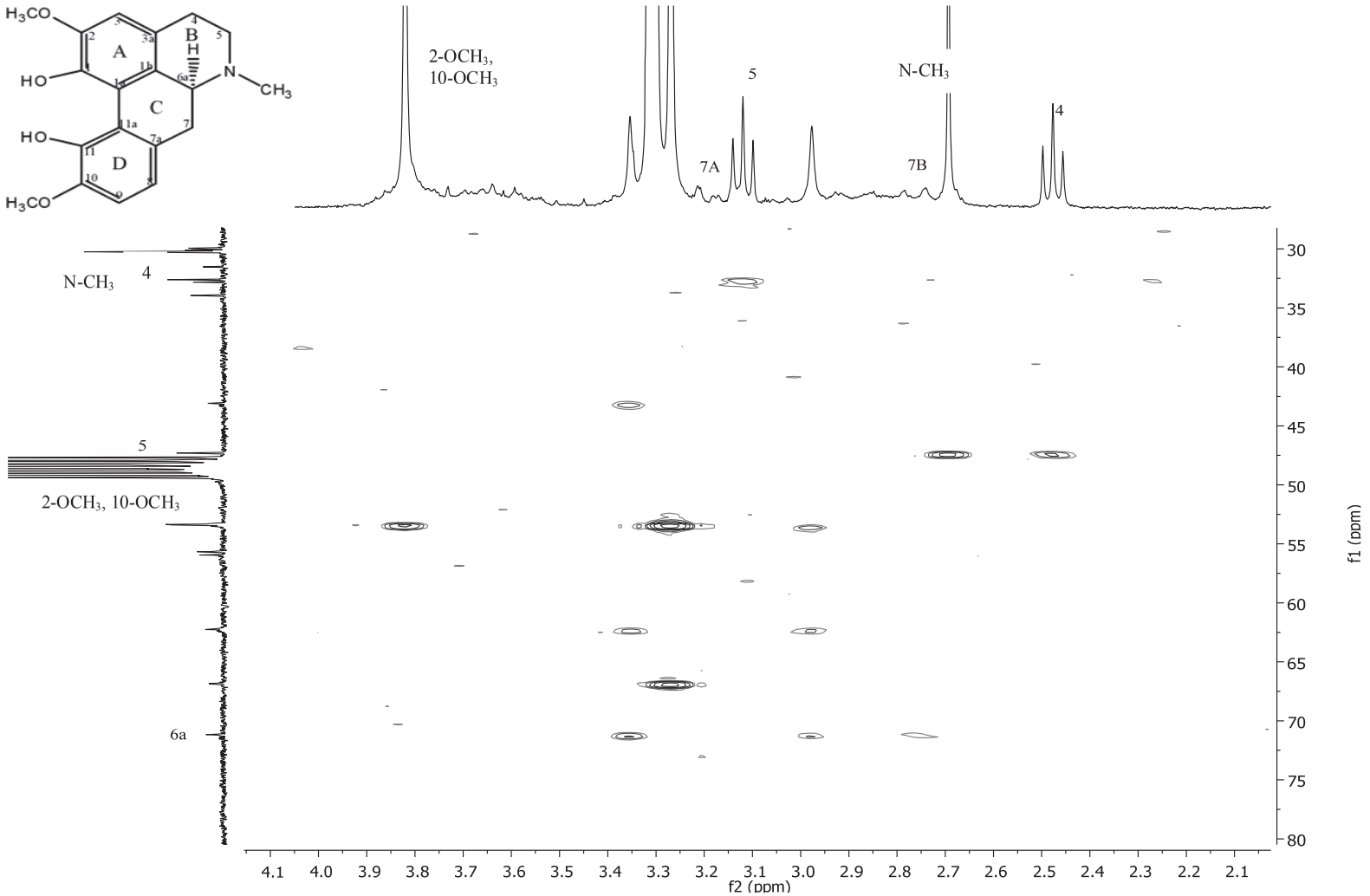

Figure 160 (Continued) HMBC Spectrum of compound MBT-1 (in CD_3OD)

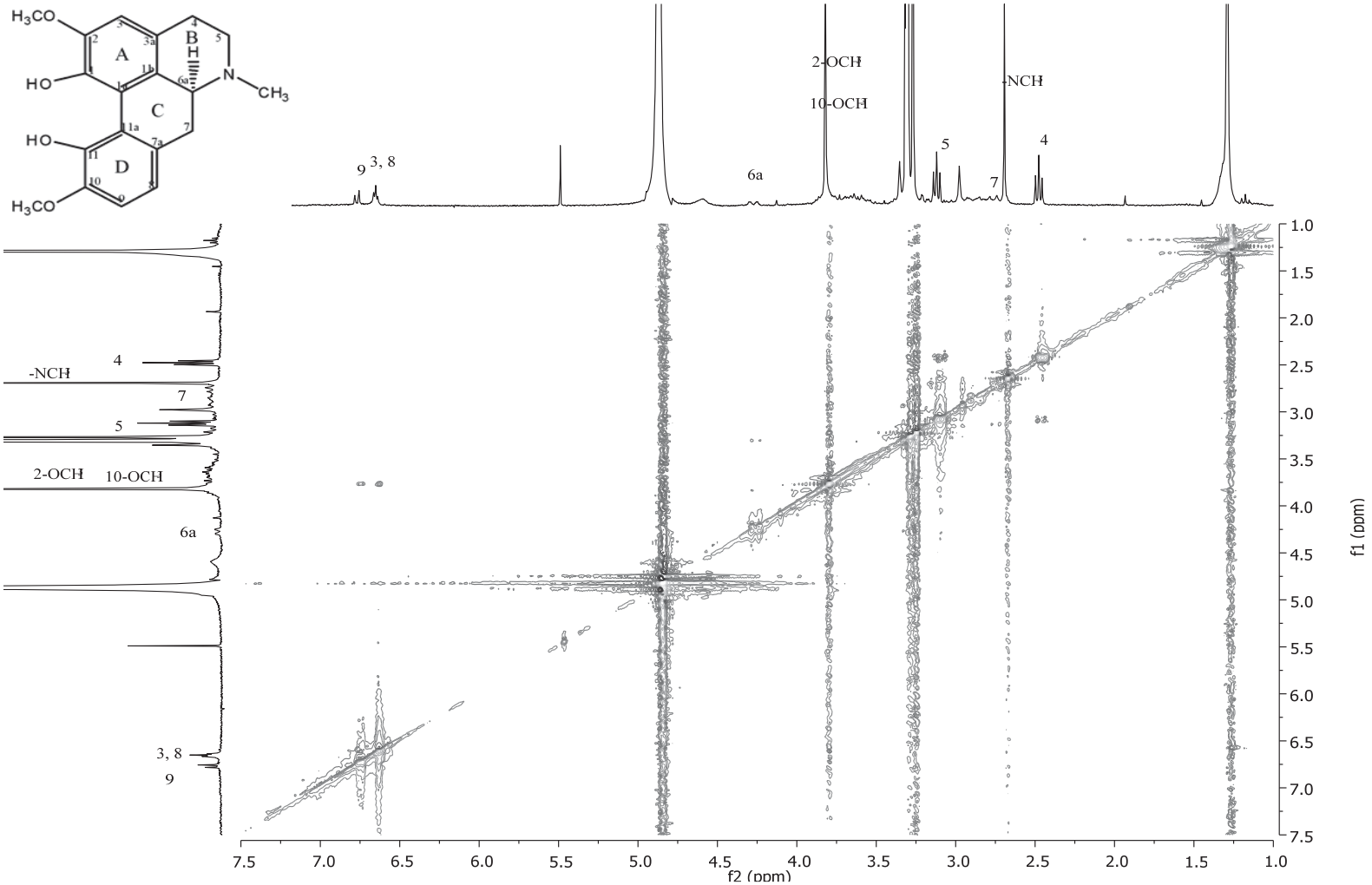

Figure 161 NOESY Spectrum of compound MBT-1 (in CD_3OD)

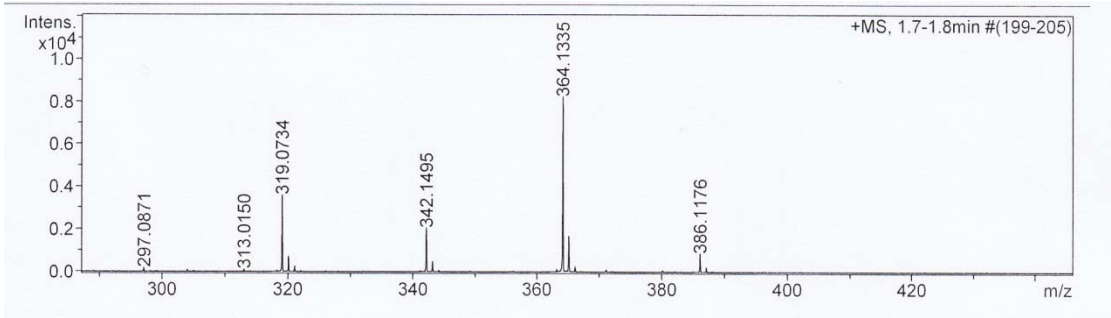

Figure 162 MS spectrum of compound MBT-2

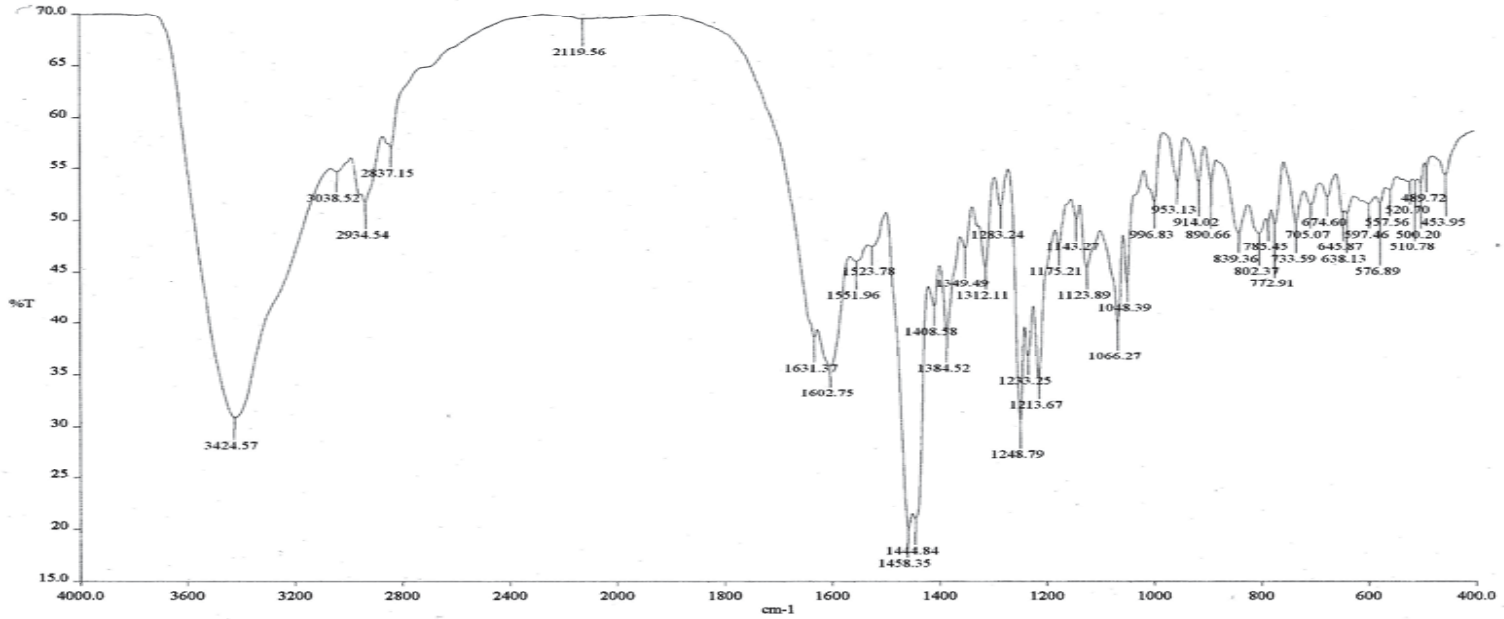

Figure 163 IR (KBr) spectrum of compound MBT-2

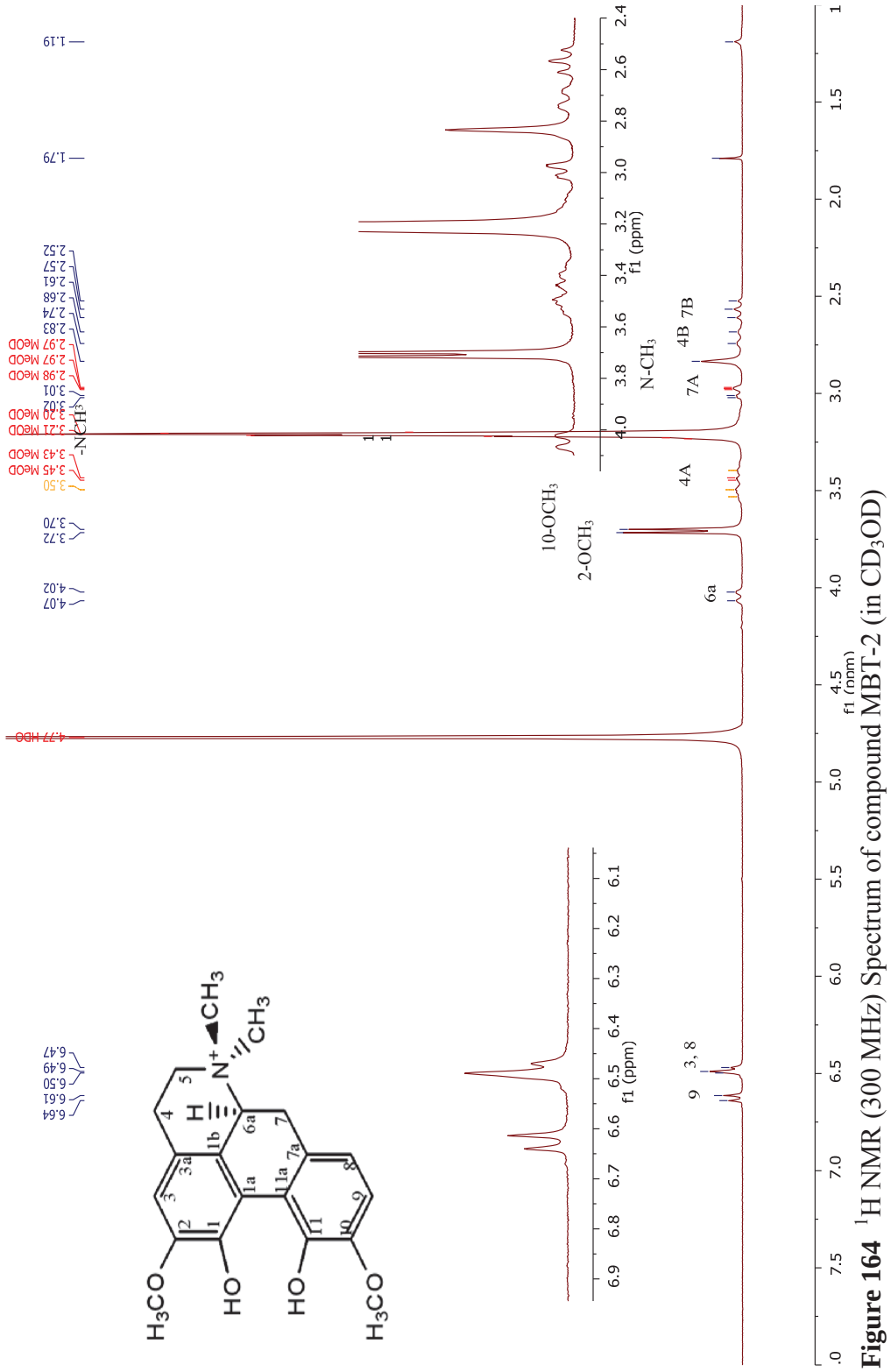

Figure 164 ^{1}H NMR (300 MHz) Spectrum of compound MBT-2 (in CD_3OD)

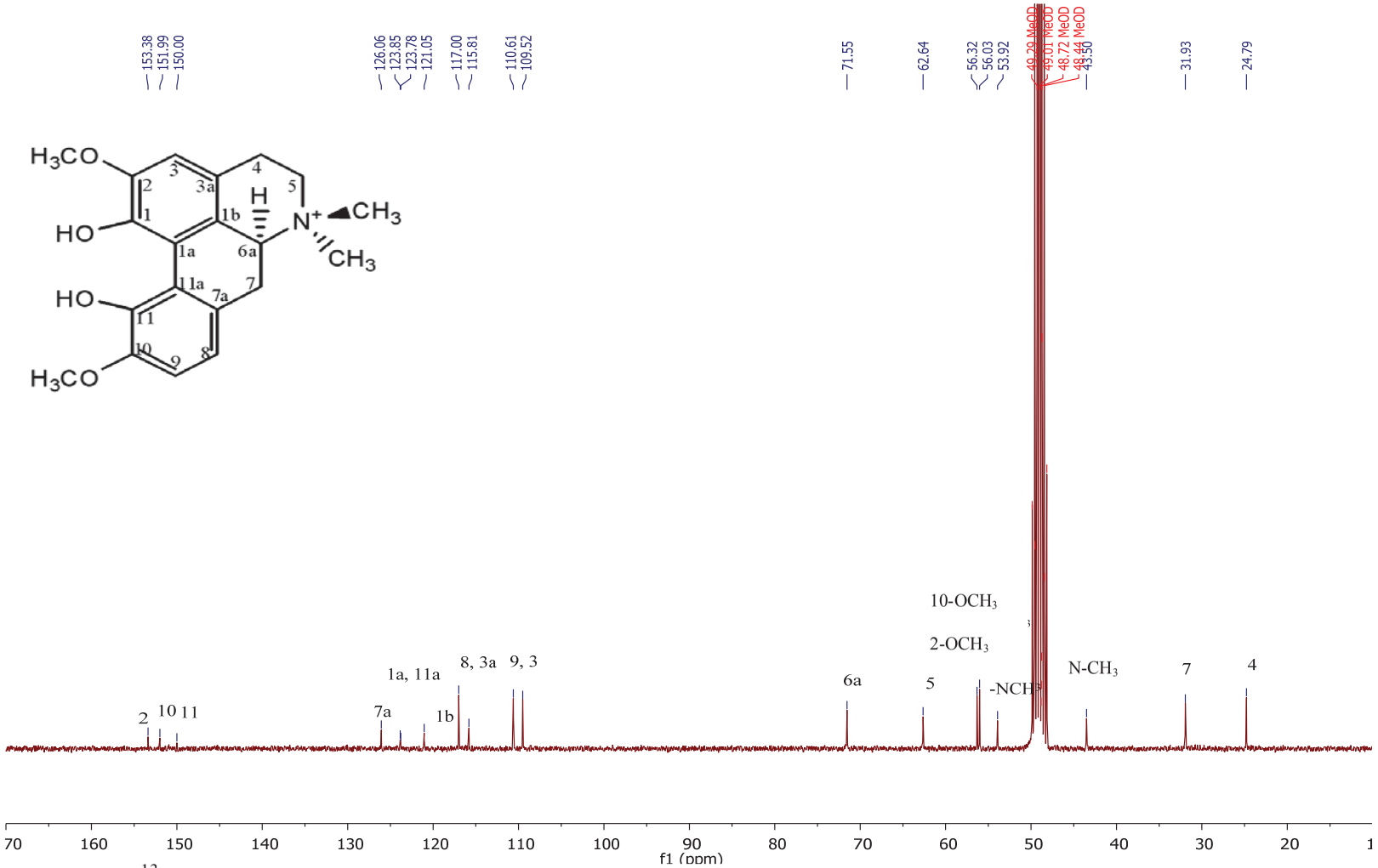

Figure 165 ^{13}C NMR (75 MHz) Spectrum of compound MBT-2 (in CD_3OD)

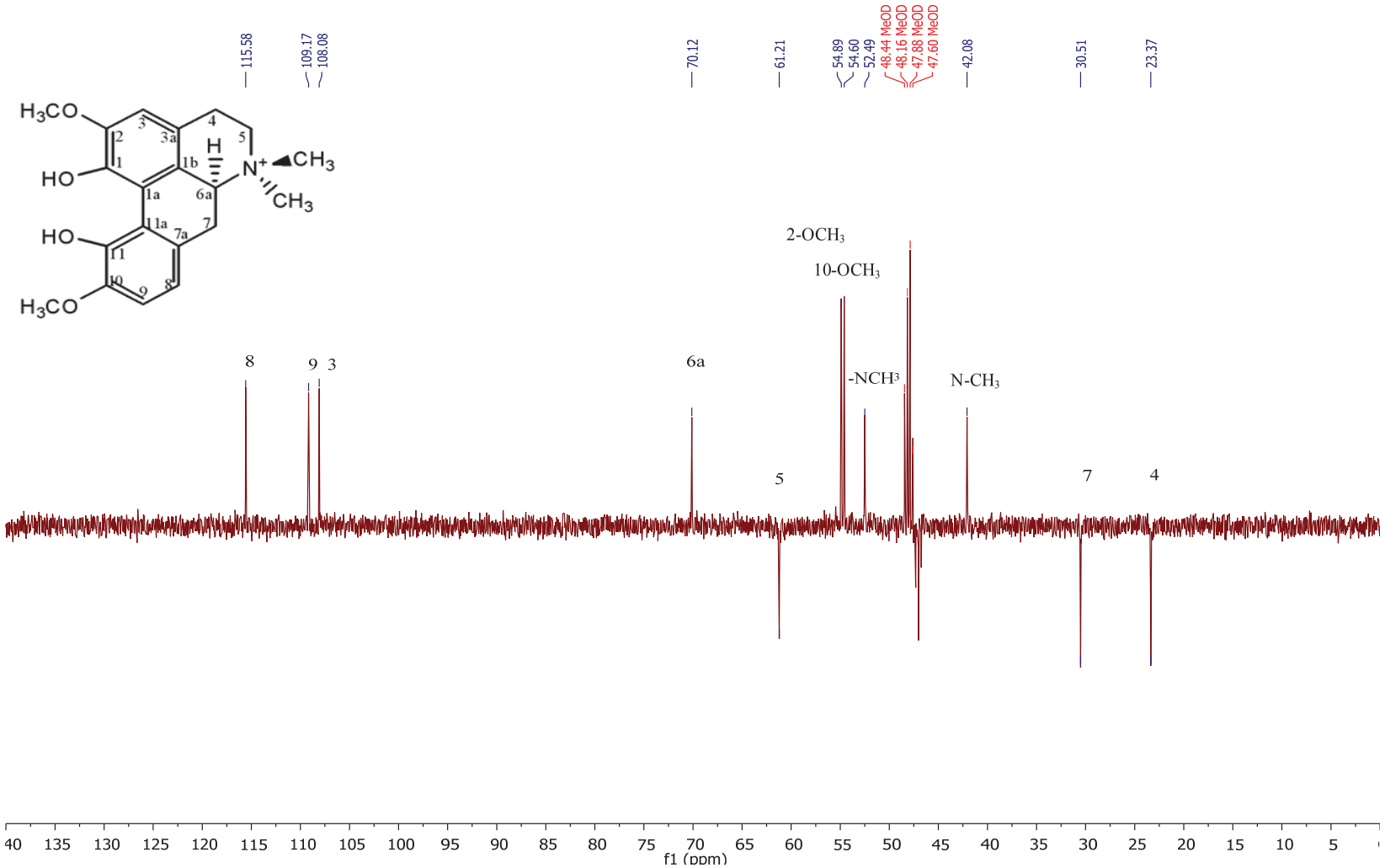

Figure 166 DEPT Spectrum of compound MBT-2 (in CD_3OD)

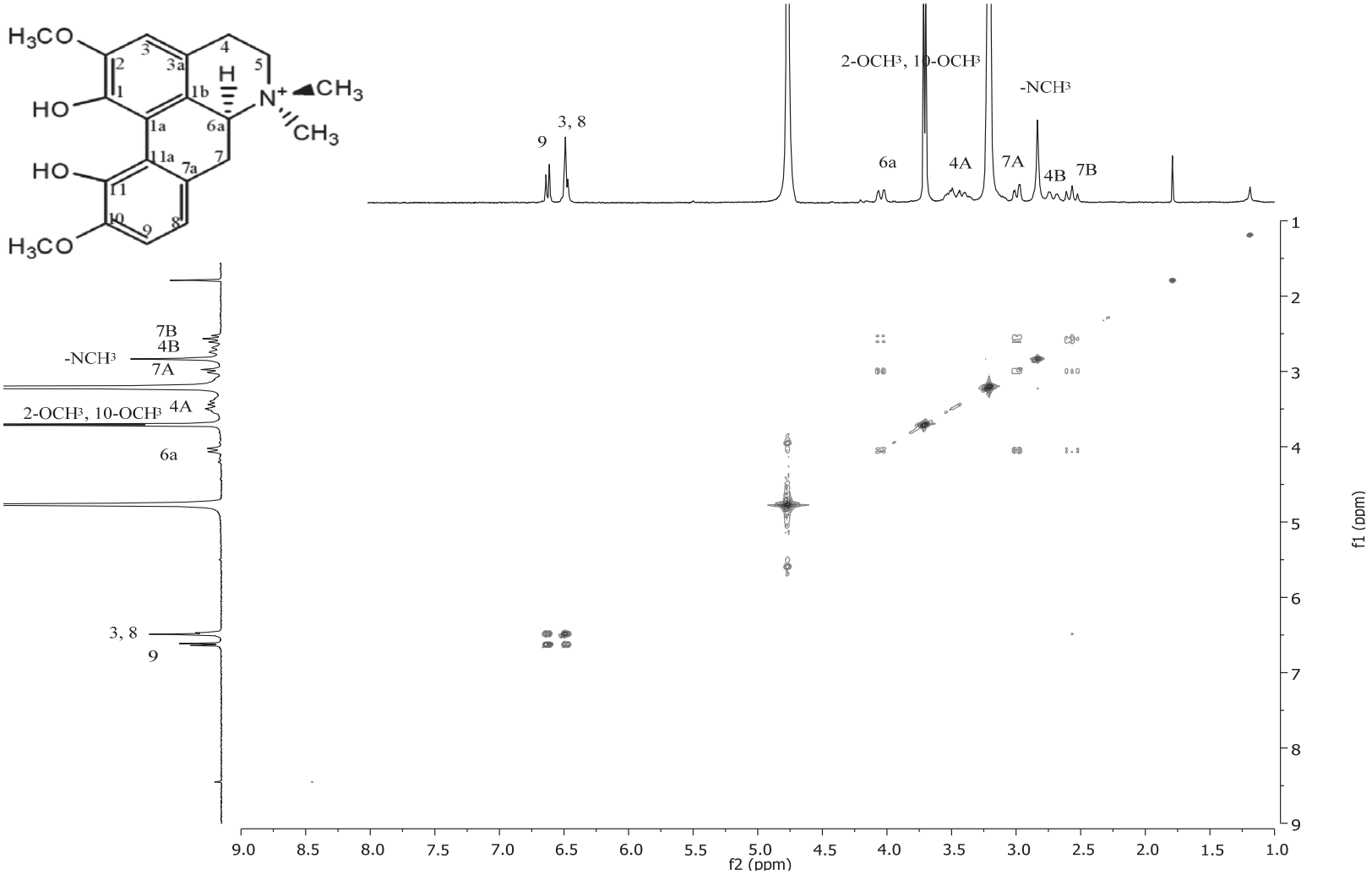

Figure 167 COSY Spectrum of compound MBT-2 (in CD_3OD)

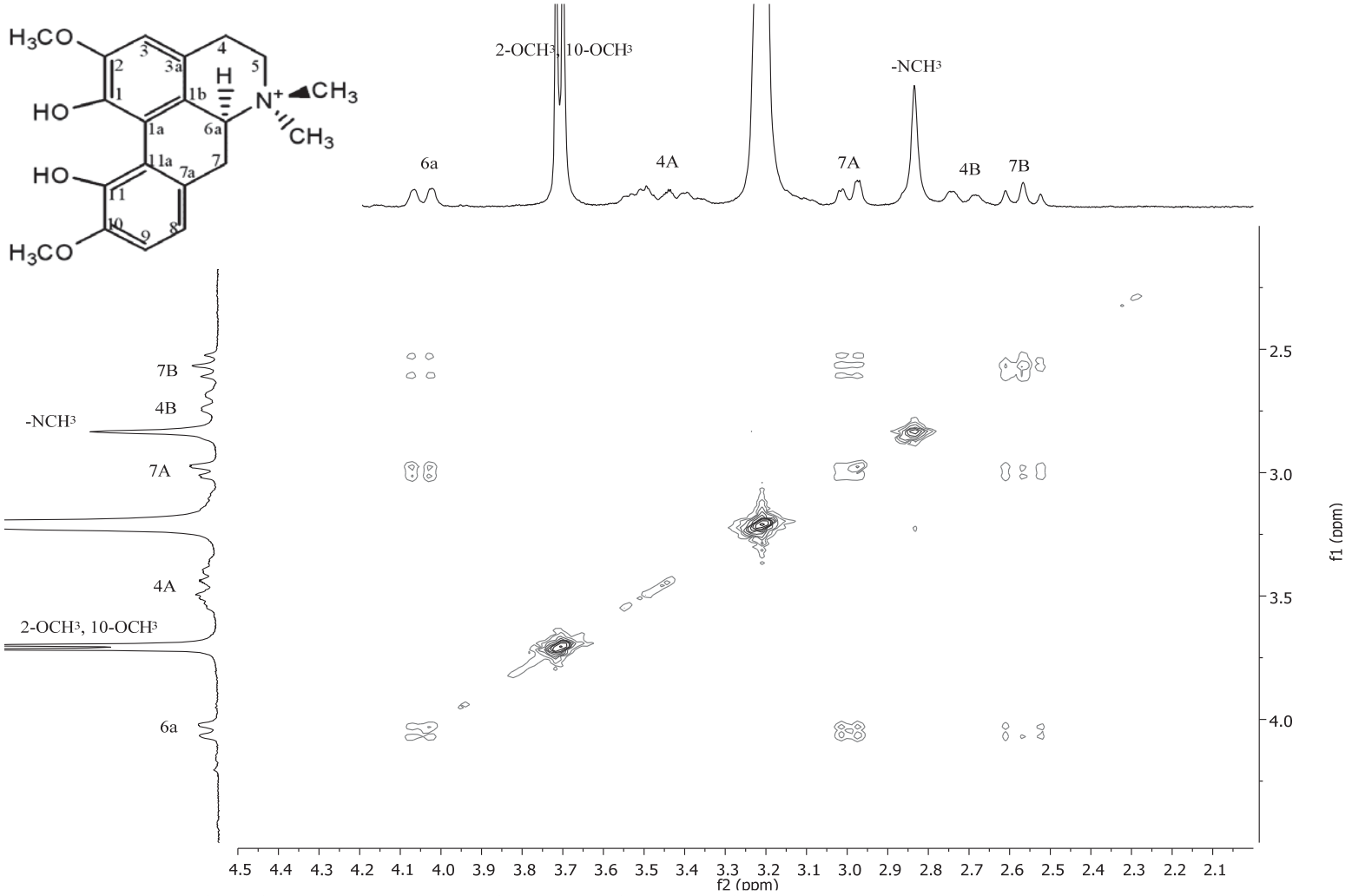

Figure 167 (Continued) COSY Spectrum of compound MBT-2 (in CD_3OD)

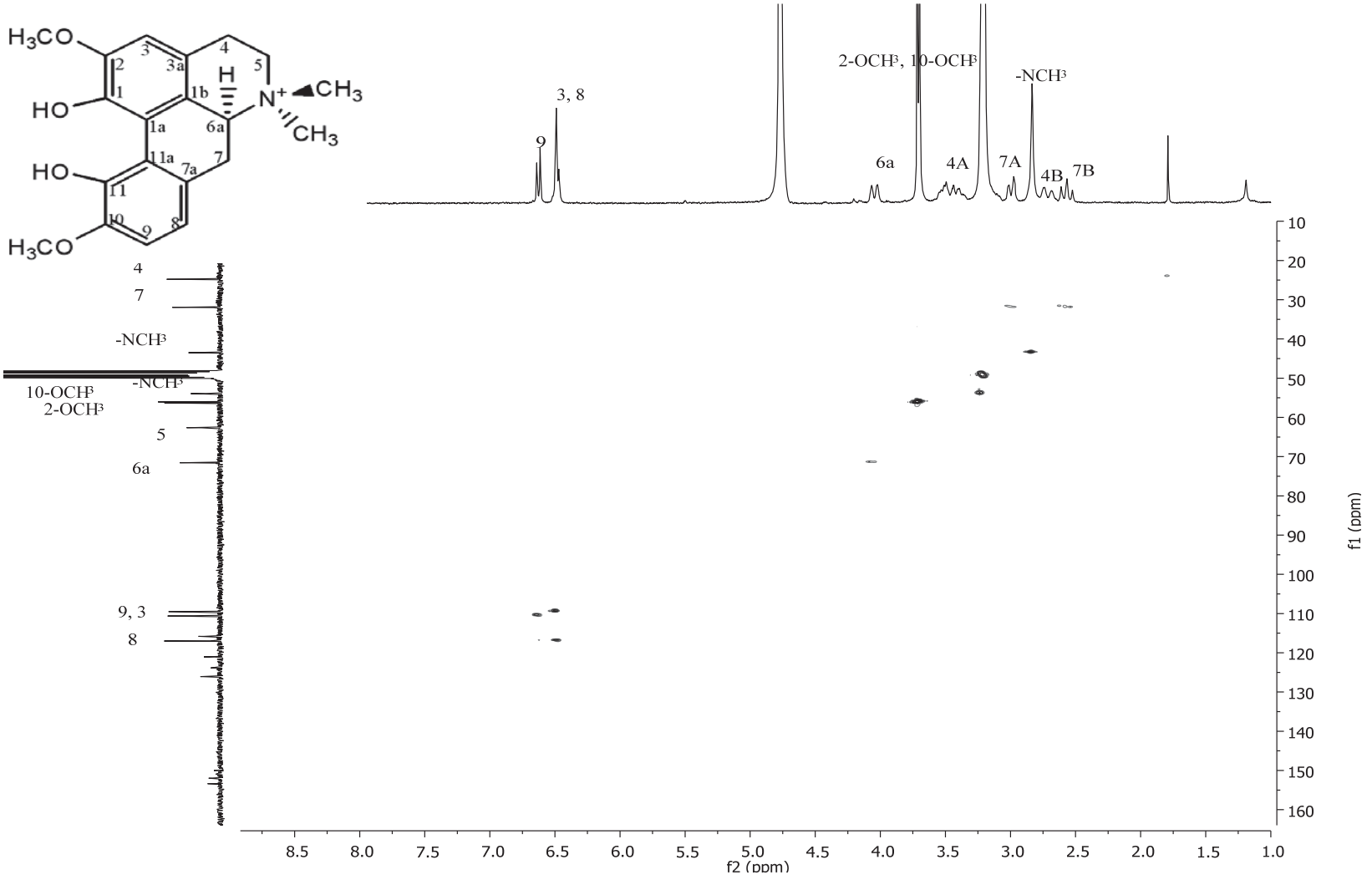

Figure 168 HMQC Spectrum of compound MBT-2 (in CD_3OD)

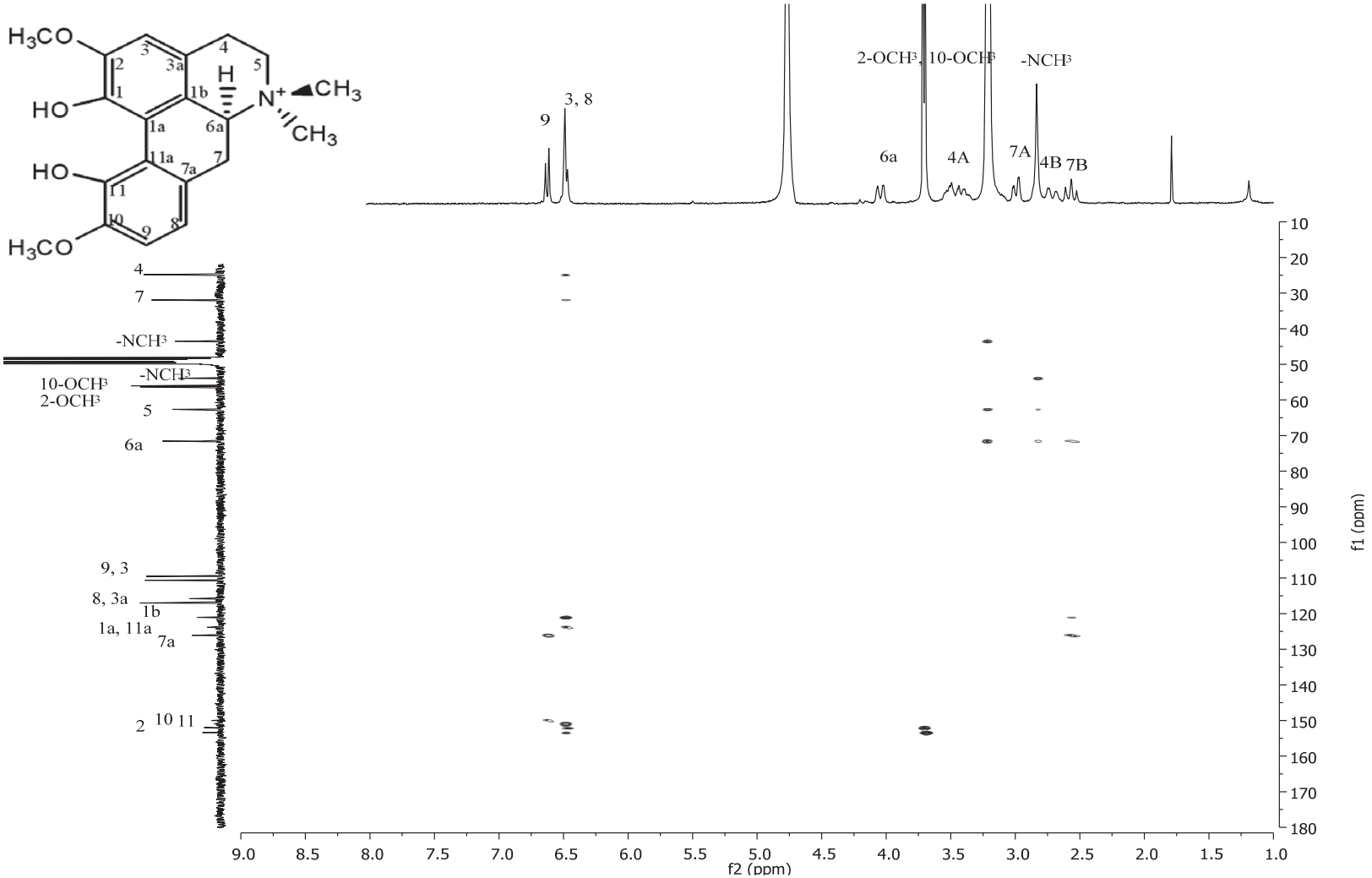

Figure 169 HMBC Spectrum of compound MBT-2 (in CD_3OD)

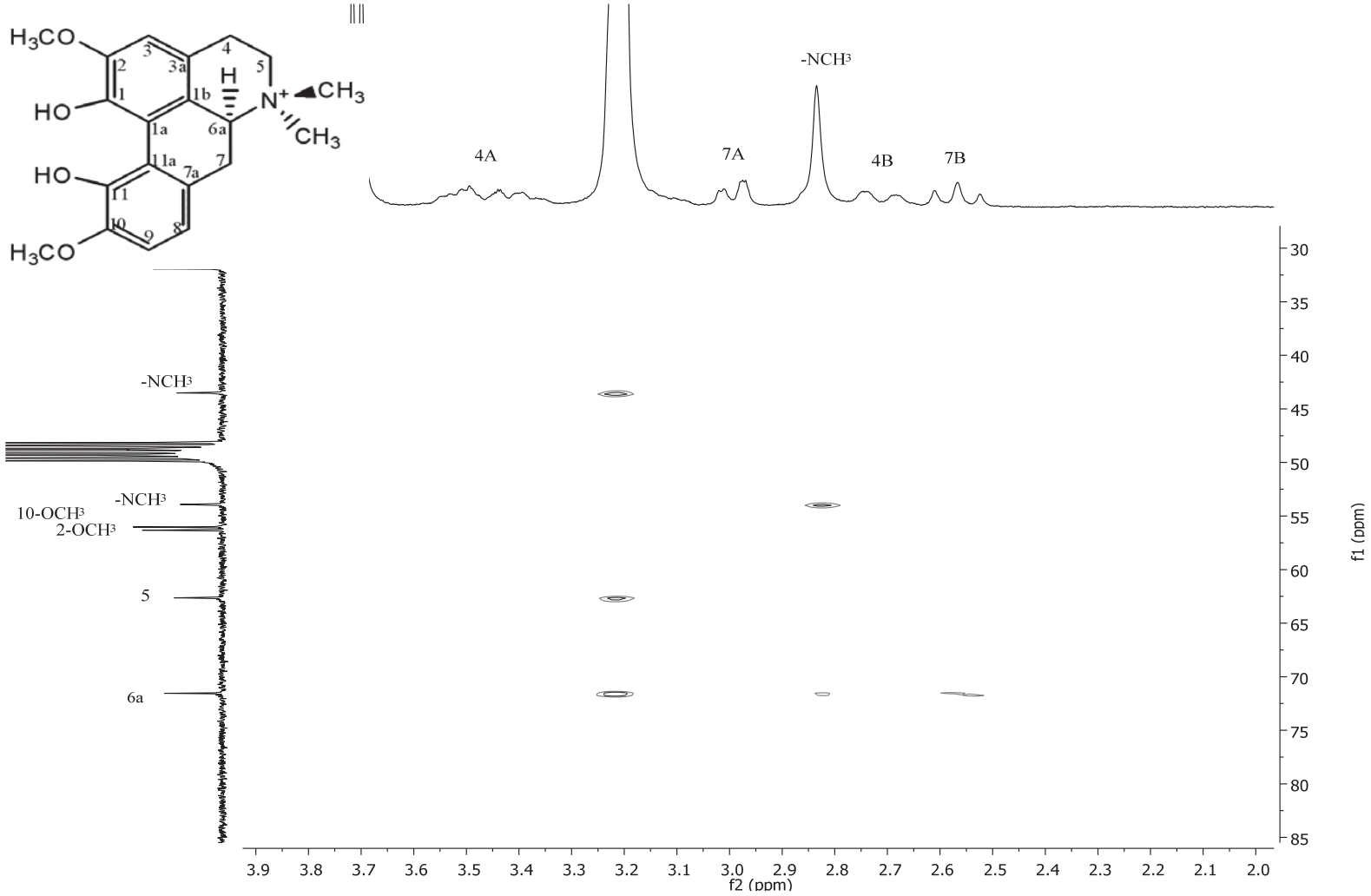

Figure 169 (Continued) HMBC Spectrum of compound MBT-2 (in CD_3OD)

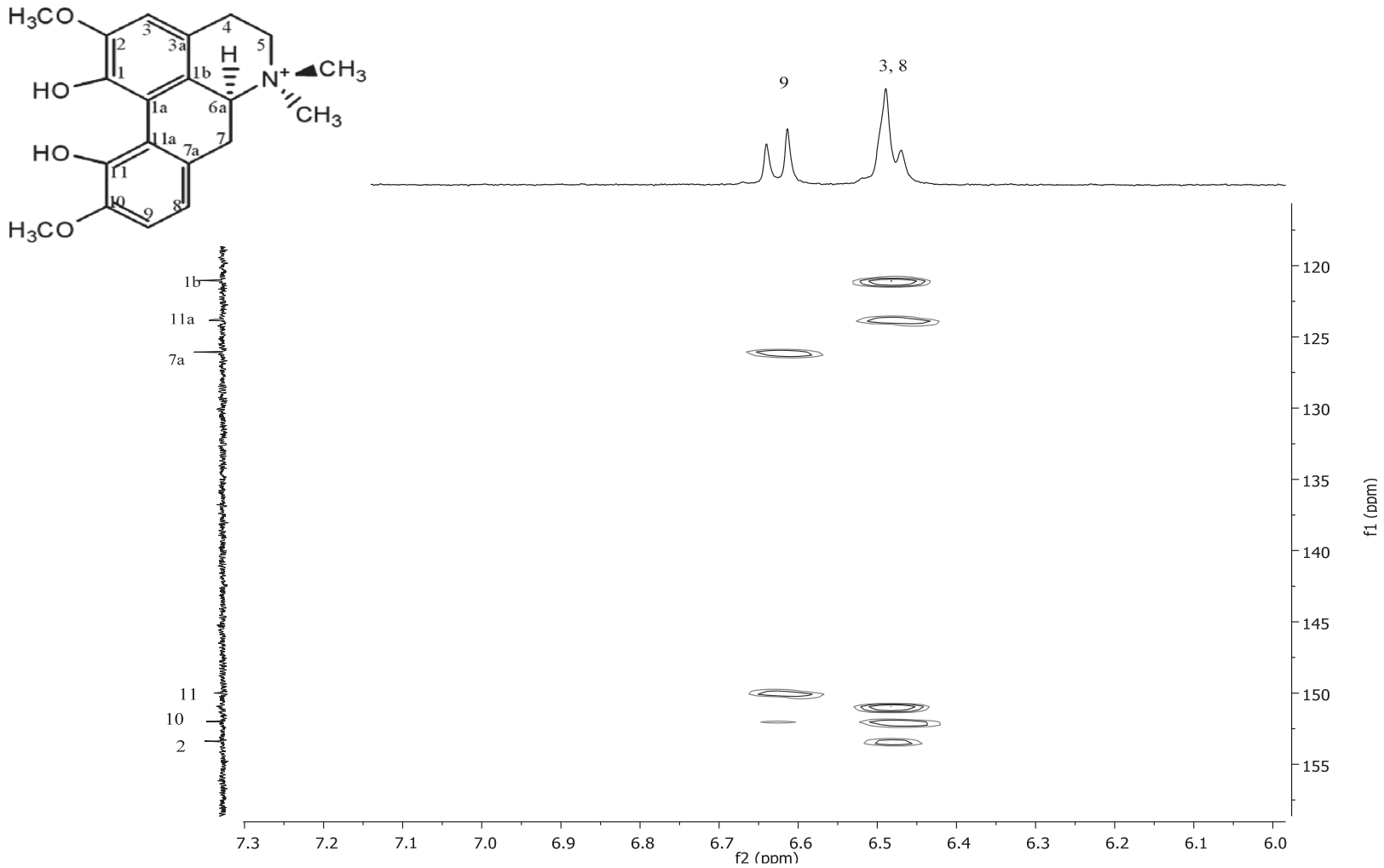

Figure 169 (Continued) HMBC Spectrum of compound MBT-2 (in CD_3OD)

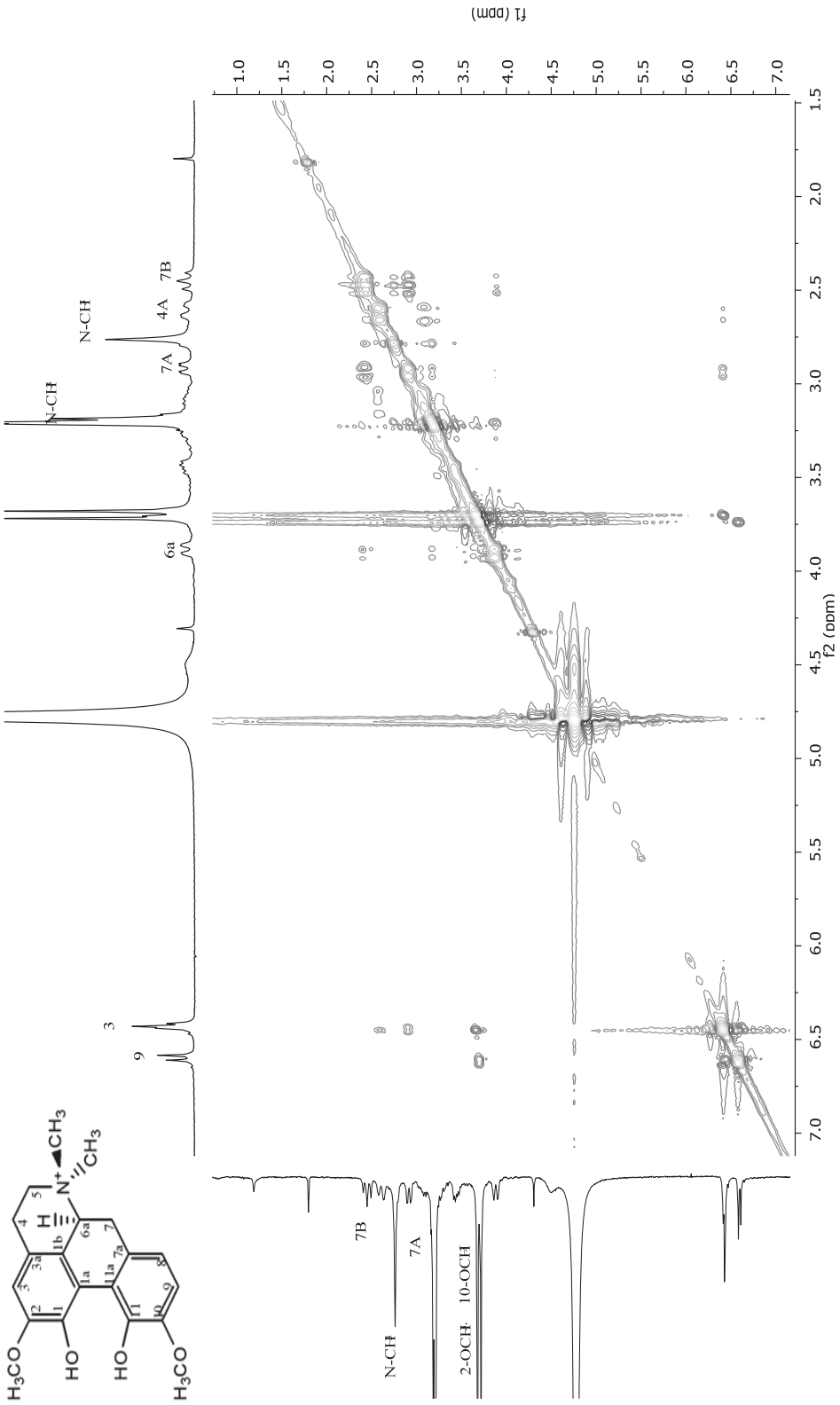

Figure 170 NOESY Spectrum of compound MBT-2 (in CD_3OD)

BIOGRAPHY

Name : Miss Patcharawan Tanamatayarat

Date of Birth : 5 February 1978

Place of Birth : Chiang Mai, Thailand

Home Address :

285 Moo. 3, Naimuang sub-district,
Phichai district, Uttaradit 53120, Thailand

Education :

2000	Bachelor of Pharmacy, Silpakorn University
2003	Master of Pharmacy in Pharmaceutical Chemistry, Chiang Mai University
2006 – 2011	Doctor of Philosophy, Ph.D. in Pharmaceutical Chemistry and Natural Products, Silpakorn University

Work :

2003-present	Lecturer, Pharmaceutical Sciences Department, School of Pharmacy, University of Phayao, Phayao 65000, Thailand

Publications :

1. Chantasitiporn, J., Chumchit, C., Tanamatayarat, P., Wongtieng, W., Yaipakdee, P. and Poobrasert, O. Biological Activity of Plant Extracts from Thai Traditional Medicinal Text for Cancer Therapy. J Multidisciplinary Res 2000; 13**:** 24-28.
2. Tanamatayarat, P., Limtrakul, P., Chunsakaow, S. and Duangrat, C. Screening of Some Rubiaceous Plants for Cytotoxic Activity Against Cervix Carcinomar (KB-3-1) Cell Line. Thai J Pharm Sci 2003, 27**:** 167-172.

3. Tanamatayarat, P. and Duangrat, C. Comparison of Chrmogenic Dyes, MTT and MTS, in Cytotoxicity Assay. Applications of Natural Materials in Pharmacy and Cosmetics. 14-15 March 2002. Chiang Mai, Thailand.
4. Tanamatayarat, P., Sotanaphun, U. and Toyama, O. (7-10 November 2008). Antioxidative Activity and Brine Shrimp lethality of 19 Thai plants from Doi Tung. *22nd Federation of Asian Pharmaceutical Associations Congress. Translational research: The approach to quality healthcare (FAPA 2008).* Singapore, p. 432.
5. Tanamatayarat, P., Sotanaphun, U. and Toyama, O. (3-4 Febauary 2009). (-)-Epicatechin from *Pterospermum grande* Craib. *The 8th NRCT-JSPS joint seminar: Innovative research in natural products for sustainable development.* Bangkok, Thailand. pp.99-100.
6. Nuntanakorn, P., Chaiyasut, C., Sittisombut, C., Tanamatayarat, P. and Toyama, O. (3-4 Febauary 2009). Antioxidant activity and total phenolic contents of *Diospyros decandra* Lour. (Ebenaceae) fruit extracts. *The 8th NRCT-JSPS joint seminar: Innovative research in natural products for sustainable development*. Bangkok, Thailand.
7. Tanamatayarat, P., Sotanaphun, U. and Poobrasert, O. 2011. Thai Plant from Doi Tung: Brine Shrimp Lethality, Antioxidative Activity, and Combination Effect with L-Ascorbic Acid. *Natural Product Research*.